



University  
of Glasgow

O'Hara, Maureen (2009) *Relating the structure of the HSV-1 UL25 DNA packaging protein to its function*. PhD thesis.

<http://theses.gla.ac.uk/1326/>

Copyright and moral rights for this thesis are retained by the author

A copy can be downloaded for personal non-commercial research or study, without prior permission or charge

This thesis cannot be reproduced or quoted extensively from without first obtaining permission in writing from the Author

The content must not be changed in any way or sold commercially in any format or medium without the formal permission of the Author

When referring to this work, full bibliographic details including the author, title, awarding institution and date of the thesis must be given

**Relating the Structure of the HSV-1 UL25 DNA  
Packaging Protein to its Function**

**by**

**Maureen O'Hara**

A thesis presented for the degree of  
Doctor of Philosophy

in

The Faculty of Biomedical and Life Sciences  
University of Glasgow

**MRC Virology Unit  
Institute of Virology  
Church Street  
Glasgow  
G11 5JR**

**September 2009**

# Table of Contents

<b>Abstract</b> .....	<b>5</b>
<b>Acknowledgements</b> .....	<b>8</b>
<b>List of tables and figures</b> .....	<b>9</b>
<b>Abbreviations</b> .....	<b>13</b>
<b>Author's declaration</b> .....	<b>19</b>
<b>1 Introduction</b> .....	<b>20</b>
1.1 Introduction to herpesviruses.....	20
1.1.1 Classification of herpesviruses .....	20
1.1.2 Human herpesviruses and disease .....	23
1.2 HSV-1 virion architecture.....	24
1.2.1 Genome.....	24
1.2.2 The capsid.....	25
1.2.3 The tegument .....	30
1.2.4 The envelope.....	31
1.2.5 L-particles.....	31
1.3 HSV-1 replication.....	32
1.3.1 Entry.....	32
1.3.2 Gene expression .....	34
1.3.3 DNA replication .....	36
1.3.4 Capsid assembly .....	38
1.3.5 DNA encapsidation.....	42
1.3.6 Egress .....	54
1.3.7 Latency.....	59
1.4 UL25 protein structure .....	60
1.4.1 The predicted functional interfaces.....	62
1.5 The binding partners of pUL25 .....	64
1.6 The aims of the study .....	66
<b>2 Materials and methods</b> .....	<b>67</b>
2.1 Materials.....	67
2.1.1 Chemicals and reagents.....	67
2.1.2 Enzymes.....	69
2.1.3 Antibiotics .....	69
2.1.4 Tissue culture cell lines .....	69
2.1.5 Tissue culture medium and growth conditions.....	70
2.1.6 HSV-1 stocks.....	70
2.1.7 Baculoviruses .....	71
2.1.8 <i>E. coli</i> strains and culture medium.....	71
2.1.9 Plasmids.....	72
2.1.10 Antibodies.....	73
2.1.11 Buffers and solutions .....	74
2.1.12 Oligonucleotides .....	76

2.1.13	Radiochemicals .....	76
2.1.14	Commercial kits .....	76
2.1.15	Computer software .....	76
2.2	Methods.....	77
2.2.1	DNA cloning and manipulation .....	77
2.2.2	Ligation of DNA fragments .....	78
2.2.3	DNA analysis and purification.....	79
2.2.4	Growth and maintenance of <i>E. coli</i> bacteria.....	81
2.2.5	Preparation and transformation of electrocompetent <i>E. coli</i> .....	81
2.2.6	Maintenance and passage of tissue culture cells .....	84
2.2.7	Complementation analysis .....	85
2.2.8	Generation of HSV-1 UL25 null mutant ( $\Delta$ UL25MO) .....	86
2.2.9	Virus plaque purification .....	90
2.2.10	Titration of HSV-1 stocks (plaque assay) .....	91
2.2.11	Large scale production of HSV-1 stocks.....	91
2.2.12	Generation of recombinant baculoviruses .....	92
2.2.13	Sterility of viral stocks .....	96
2.2.14	Detection of full length packaged viral DNA .....	96
2.2.15	Southern blots .....	98
2.2.16	Pulse field gels .....	99
2.2.17	Analysis of viral assembly in infected cells .....	100
2.2.18	Protein analysis .....	102
2.2.19	GST-fusion protein expression and GST pull-down assay .....	103
<b>3</b>	<b>Generation of the HSV-1 UL25 deletion mutant <math>\Delta</math>UL25MO... 106</b>	
3.1	Introduction.....	106
3.2	The Counter-Selection BAC Modification technique.....	106
3.2.1	Red/ET recombination.....	106
3.2.2	RpsL-neo counter-selection system .....	107
3.2.3	Generation of the rpsL-neo counter selection cassette flanked by homology arms (rpsL-neo-PCR1).....	109
3.2.4	Step 1 - insertion of rpsL-neo-PCR1 into fHSV $\Delta$ pac.....	109
3.2.5	Verification of the modified HSV-1 BAC by Southern blot analysis	110
3.2.6	Generation of the non-selectable DNA product (Non-sm) .....	111
3.2.7	Step 2 - replacing the rpsL-neo-PCR1 cassette with the non- selectable (Non-sm) DNA in fHSV $\Delta$ pac.....	112
3.3	Construction of $\Delta$ UL25MO and its marker rescuant MRUL25MO.....	113
3.3.1	$\Delta$ UL25MO.....	113
3.3.2	MRUL25MO .....	115
3.3.3	Single-step virus growth of HSV-1 viral stocks .....	116
3.4	Discussion .....	116
<b>4</b>	<b>Generation and complementation analysis of the mutant pUL25s .....</b>	<b>119</b>
4.1	Introduction.....	119
4.2	Methods used for site-directed mutagenesis .....	120
4.3	Cluster mutants .....	121
4.3.1	C1 mutant construct (pFB-UL25-C1).....	121
4.3.2	C2 mutant construct (pFB-UL25-C2).....	122
4.3.3	C3 mutant constructs (pFB-UL25-C3A and pFB-UL25-C3B) .....	123

4.3.4	C4 mutant constructs (pFB-UL25-C4A and pFB-UL25-C4B) .....	126
4.4	Loop mutants .....	127
4.4.1	L1 mutant construct (pFB-UL25-L1) .....	128
4.4.2	L2 mutant construct (pFB-UL25-L2) .....	128
4.4.3	L3 mutant construct (pFB-UL25-L3) .....	129
4.4.4	L4 mutant construct (pFB-UL25-L4) .....	129
4.4.5	L5 mutant construct (pFB-UL25-L5) .....	130
4.4.6	L6 mutant constructs (pFB-UL25-L6 and pFB-UL25-L6sub) .....	130
4.5	Combination mutant (pFB-UL25-C1L2) .....	131
4.6	Complementation assay .....	132
4.7	Discussion .....	132
<b>5</b>	<b>Ability of the mutant pUL25s to support DNA packaging ....</b>	<b>136</b>
5.1	Introduction .....	136
5.2	Generation of the baculovirus expressing the recombinant pUL25s .....	137
5.3	Viral DNA packaging assay .....	139
5.4	Pulse-field gel electrophoresis (PFGE) of encapsidated viral DNA .....	141
5.5	Discussion .....	142
<b>6</b>	<b>The effect of pUL25-L3, -L6 and -C4A on virus assembly in <math>\Delta</math>UL25MO-infected U2OS cells.....</b>	<b>144</b>
6.1	Introduction .....	144
6.2	Electron microscopic (EM) analysis .....	144
6.3	Fluorescent in-situ hybridisation (FISH) analysis .....	145
6.4	Discussion .....	146
<b>7</b>	<b>Interaction of mutant pUL25s with the capsid-binding domain of pUL36 .....</b>	<b>151</b>
7.1	Introduction .....	151
7.1.1	Construction of GST-UL36cbd expression plasmid .....	151
7.1.2	GST pull-down assay .....	152
7.2	Discussion .....	154
<b>8</b>	<b>General Discussion.....</b>	<b>157</b>
	<b>References.....</b>	<b>164</b>

## Abstract

The herpes simplex virus type 1 (HSV-1) UL25 protein (pUL25) is a minor capsid protein that is essential for packaging the full-length viral genome into preformed precursor capsid. It is also important in virus entry and recently has been implicated in the egress of the virus from the cell (Coller et al., 2007, Preston et al., 2008). The crystallographic structure of an N-terminally truncated form of pUL25 (residues 134-580) has been determined to 2.1 Å, revealing a protein with a novel fold that consists mostly of  $\alpha$ -helices and a few minor  $\beta$ -sheets (Bowman et al., 2006). An unusual feature of the protein is the presence of numerous flexible loops extending out from the stable core and its distinctive electrostatic distribution. Five of the extended loops contain unstructured regions, L1-L5, with three additional unstructured amino acids, L6, located at the carboxyl terminus of the protein (Bowman et al., 2006). Four potentially functional clusters of residues, C1-C4, were identified on the surface of the protein using evolutionary trace analysis (Lichtartge & Sowa, 2002).

To examine the function of the protein in relation to its structure, site-directed mutations were engineered into the UL25 gene in a protein expression plasmid. A series of mutant proteins was generated, each protein containing a deletion of the unstructured residues in one of the six regions, L1-L6. Another set of mutant proteins were constructed with each member containing substitutions of selected amino acids within one of the four potentially functional clusters, C1-C4, or substitutions of the three disordered amino acids in L6. The amino acid substitutions were generally to alanine, but in one case where the SIFT program predicted alanine would not affect the function of the protein an alternative residue was substituted. To determine the functional significance of the uncrystallised part of pUL25, residues 1-133, three deletion mutant proteins that spanned this region (pUL25 $\Delta$ 1-45, pUL25 $\Delta$ 1-59 and pUL25 $\Delta$ 1-133) were included in the study.

Although an existing UL25 null mutant, KUL25NS, was available at the beginning of the project for analysis of the mutant proteins, it had been made by the insertion of multiple stop codons in the UL25 ORF and as a result some UL25 sequences were still present within the virus genome. Consequently, during

complementation assays recombination between the UL25 sequences in the KUL25NS genome and the transfected expression plasmid generated low levels of wild-type (wt) progeny virus. To improve the sensitivity of the assay, a new deletion mutant,  $\Delta$ UL25MO, was created that lacked the entire UL25 gene. This mutant failed to form plaques in non-permissive Vero cells and grew well in the complementing cell line, 8-1. However, contrary to previously published work, electron microscopic (EM) analysis revealed that DNA-containing capsids as well as A- and B-capsids were present in the nuclei of both  $\Delta$ UL25MO- and KUL25NS-infected cells. As expected, none of the progeny from  $\Delta$ UL25MO-infected Vero cells expressing the wt pUL25 formed plaques on non-permissive cells. Of the 17 mutant UL25 proteins screened in the complementation assay, nine failed to complement the growth of  $\Delta$ UL25MO in Vero cells.

Three of the non-complementing mutant proteins, pUL25-C4A, pUL25-L3 and pUL25-L6, altered the phenotype of  $\Delta$ UL25MO in a transient DNA packaging assay, allowing the mutant virus to package full-length genomes in U2OS cells co-infected with  $\Delta$ UL25MO and a mammalian baculovirus vector containing the mutant UL25 gene. These results indicate that viral assembly was disrupted in these cells following DNA packaging. Five mutant proteins, pUL25-C3B, pUL25-L5, pUL25 $\Delta$ 1-45, pUL25 $\Delta$ 1-59 and pUL25 $\Delta$ 1-133 did not change the pattern of DNA encapsidation of  $\Delta$ UL25MO in this system, suggesting that C3, L5 and the N-terminal region are critical for packaging virus DNA. Since C3 and L5 regions are on different sides of pUL25, it is likely that these regions and possibly the N-terminal domain of pUL25 represent different interfaces for protein-protein interactions important for DNA packaging. To determine at which point in the virus growth cycle these post-packaging blocks occurred, EM was used to investigate the pattern of virus assembly in  $\Delta$ UL25MO-infected cells expressing pUL25-C4A, -L3 or -L6 and fluorescent in-situ hybridisation (FISH) analysis was performed to establish the distribution of virus DNA in these cells. The results showed that in  $\Delta$ UL25MO-infected cells expressing pUL25-C4A or -L3, the C-capsids failed to exit the nucleus, whereas in the cells expressing pUL25-L6 the C-capsids were seen in both the nucleus and the cytoplasm. The FISH data confirmed the EM observations, and viral DNA was detected only in the nuclei of  $\Delta$ UL25MO-infected cells expressing the C4 or L3 mutant proteins, but in the nuclei and cytoplasm of the mutant virus-infected cells expressing pUL25-L6.

These studies show that the C4 and L3 regions of pUL25 are important for egress of the C-capsids from the nuclei, whereas the L6 region is essential for virus assembly after the C-capsids are released into the cytoplasm. The C4 and L3 regions of pUL25 are situated in close proximity to each other on the surface of pUL25, with the wt residues mutated in pUL25-C4A lying along a loop adjacent to L3. The similar phenotypes of the mutant proteins generated for the C4 and L3 suggest that these two regions may represent a single functional interface of pUL25 that is critical for nuclear egress of C-capsids during HSV-1 infection. The 62 carboxyl-terminal region of the UL36 gene product (pUL36) has previously been shown to contain a capsid-binding domain (CBD) that interacts with pUL25 (Coller et al., 2007). A GST-pull down assay was used to determine whether the mutations in the post-packaging mutant proteins, pUL25-C4A, -L3, -L6, or the control packaging-competent mutant protein, pUL25-L5, disrupted the interaction of pUL25 with the CBD of pUL36. However, all of these mutant proteins and the wt pUL25 bound to the pUL36 CBD GST fusion protein.

In summary, three different classes of pUL25 mutants, each of which affect a different essential function of pUL25, have been identified, revealing that pUL25 is indeed a versatile viral protein. These mutants provide the first evidence that this DNA packaging protein is crucial for virus assembly at two different stages after DNA encapsidation, one in nuclear egress of C-capsids and the other in the assembly of the virus in the cytoplasm.

## Acknowledgements

Firstly, I would like to thank the MRC and Professor McGeoch for giving me the opportunity to undertake my PhD and for having faith that I would survive long enough to complete it. My sincere gratitude goes to Val, my supervisor, for her excellent support, guidance and patience beyond the call of duty, and her ability to calmly help me through any crisis. I would like to thank all the members of lab 201, but particularly Nigel for his advice throughout, Mary for her technical support and yummy cakes, and past member, Martin, for his friendship and help during the early years. I am indebted to Frazer Rixon for his assistance with the EM work and all the other members of staff within the unit who have helped when necessary.

On a more personal level I would like to thank all of my friends, especially Ruth for her lunchtime counselling sessions and sound advice about life and doing a PhD. To all the members of Garscube Harriers, but above all Jill, Maz and Anita for the killer races and runs we have completed and the fun nights out that have kept me sane. To my fellow students, Ash and Dan, thanks for the banter and not being too embarrassed when people thought your Mum was hanging out with you.

I would like to thank my family for their love and support, particularly Elliott my grandson for turning up just when I needed him and making me laugh, a lot. To my children, Katie and Michael, thank you for saying all the right things at just the right time and for keeping me grounded. To Mum, Dad, Billy and Pauline for always believing I could achieve anything. Finally, there is not enough space here to express how much I have appreciated my husband John's help throughout this time, but a special thank you for the amazing encouragement, for waiting patiently with those fantastic dinners, and for always being there when I needed him.

# List of tables and figures

## Chapter 1

- Table 1.1 Human herpesviruses and their classification and associated diseases (Pellet & Roizman, 2007; Davison et al., 2009)
- Table 1.2 HSV-1 genes encoding proteins involved in capsid assembly
- Table 1.3 HSV-1 glycoproteins
- Table 1.4 The residues in the extended loops (L1-L5) and the unstructured L6 region of UL25nt
- Table 1.5 The residues within the four clusters (C1-C4) of pUL25 identified in the structural analysis
- Table 1.6 UL25 protein binding partners
- Figure 1.1 Phylogenetic relationships and taxonomy of major herpesviruses
- Figure 1.2 Structure of HSV-1 virion
- Figure 1.3 HSV-1 genome structure
- Figure 1.4 Herpesvirus genome structures
- Figure 1.5 Icosahedron
- Figure 1.6 Reconstruction of the HSV-1 capsid to 8.5Å
- Figure 1.7 Surface lattice of HSV-1
- Figure 1.8 Structural organisation of the HSV-1 scaffolding genes and their protolytic products
- Figure 1.9 Alternative HSV-1 capsid forms
- Figure 1.10 Lytic replication cycle of HSV-1
- Figure 1.11 Model for HSV-1 DNA replication
- Figure 1.12 Model for HSV-1 capsid assembly
- Figure 1.13 Comparison of the HSV-1 procapsid and capsid
- Figure 1.14 HSV-1 genome and structure of the *a* sequence
- Figure 1.15 The HSV-1 portal
- Figure 1.16 Central cross-section of a cryo-EM reconstruction of the HSV-1 capsid
- Figure 1.17 HSV-1 DNA cleavage and packaging model
- Figure 1.18 Models for egress of HSV-1 from the host cell
- Figure 1.19 Molecular interactions during HSV-1 egress
- Figure 1.20 Map of the latency-associated transcript (LAT) gene
- Figure 1.21 Ribbon diagram of UL25nt

Figure 1.22 Electrostatic surface charge of UL25nt

Figure 1.23 Evolutionary trace of herpesvirus UL25 homologues

Figure 1.24 UL25nt predicted functional amino acid clusters

### Chapter 3

Table 3.1 Oligonucleotides used to generate the DNA fragments required for the Counter-Selection BAC Modification procedure

Table 3.2 Counter-Selection BAC Modification Step 1 results for DH10B and HS996 cells with modified BACs

Table 3.3 Ratio of DH10B and HS996 recombinant:non-recombinant clones obtained in step 2 of Counter-Selection BAC Modification procedure

Table 3.4 Growth of HSV-1 UL25 null viruses on non-complementing and complementing cells

Table 3.5 Complementation efficiencies of HSV-1 UL25 null viruses

Table 3.6 Yield of HSV-1 viruses from non-complementing and complementing Cells

Figure 3.1 Strategy used by McNab et al. (1998) to create a UL25 null mutant

Figure 3.2 Red/ET recombination

Figure 3.3 A schematic representation of the rpsL-neo counter-selection cassette

Figure 3.4 Map of Red/ET expression plasmid pRed/ET

Figure 3.5 Flow diagram of the experimental outline for the generation of the UL25 null HSV-1 BAC

Figure 3.6 Gel photograph showing the purified rps-neo-PCR1 PCR product

Figure 3.7 DH10B and HS966 samples generated during Step 1 of the Counter-Selection BAC modification procedure

Figure 3.8 Southern blot of BamHI digested BAC DNAs from Step 1

Figure 3.9 Comparison of the growth of wt HSV-1,  $\Delta$ UL25MO and MR $\Delta$ UL25MO in 8-1 cells

### Chapter 4

Table 4.1 DNA sequencing primers

Table 4.2 List of the pFB-UL25 constructs generated and their mutated Residues

- Table 4.3A The primers used to generate the UL25 mutant constructs listed (pFB-UL25-C1 and -C2)
- Table 4.3B The overlapping oligonucleotides and primers used to generate the UL25 mutant constructs listed (pFB-UL25-C3A, -C3B, -C4A and -C4B)
- Table 4.3C The overlapping oligonucleotides and primers used to generate the UL25 mutant constructs listed (pFB-UL25-L1, -L2, and -L3)
- Table 4.3D The overlapping oligonucleotides used to generate the UL25 mutant constructs listed (pFB-UL25-L4, -L5, -L6 and -L6sub)
- Figure 4.1 Site-directed mutagenesis by PCR
- Figure 4.2 Site-directed mutagenesis by overlap extension PCR
- Figure 4.3 Plasmid map of pFB-UL25
- Figure 4.4 pGEM-T Easy vector map
- Figure 4.5 Summary of the cloning strategies and methods used to generate the mutant UL25 constructs
- Figure 4.6 Plasmid maps of pFB-UL25-C1 and pFB-UL25-C2
- Figure 4.7 Plasmid maps of pFB-UL25-C3A and pFB-UL25-C3B
- Figure 4.8 Plasmid maps of pFB-UL25-C4A and pFB-UL25-C4B
- Figure 4.9 Plasmid maps of pFB-UL25-L1 and pFB-UL25-L2
- Figure 4.10 Plasmid maps of pFB-UL25-L3 and pFB-UL25-L4
- Figure 4.11 Plasmid map of pFB-UL25-L5
- Figure 4.12 Plasmid maps of pFB-UL25-L6 and pFB-UL25-L6sub
- Figure 4.13 Plasmid map of pFB-UL25-C1L2
- Figure 4.14 Complementation of  $\Delta$ UL25MO by mutant UL25 proteins
- Figure 4.15 Western blot analysis of pUL25 in the complementation assays
- Figure 4.16 Ribbon diagram of UL25nt

## Chapter 5

- Table 5.1 List of recombinant baculovirus
- Table 5.2 Quantification of the L and S terminal fragments encapsidated during packaging assays
- Figure 5.1 The structure of the HSV-1 genome
- Figure 5.2 Plasmid map of pFBpCI
- Figure 5.3 Experimental outline used to generate the recombinant baculovirus

- Figure 5.4 Western analysis of baculovirus-infected U2OS cell extracts for UL25 expression
- Figure 5.5 Summary of the packaging assay
- Figure 5.6 Southern blots for the packaging assays
- Figure 5.7 PFGE analysis of packaged DNA
- Figure 5.8 The C3 cleft of UL25
- Figure 5.9 Ribbon diagram of UL25nt with C3 and L5

## Chapter 6

- Table 6.1 Classes of PDZ domain-binding motifs
- Table 6.2 Potential PDZ binding domains at the C-terminus of alphaherpesvirus UL25 homologues
- Figure 6.1A Cells co-infected with  $\Delta$ UL25MO and AcWTUL25
- Figure 6.1B Cells co-infected with  $\Delta$ UL25MO and AcpCI
- Figure 6.1C Cells co-infected with  $\Delta$ UL25MO and AcUL25-C4A
- Figure 6.1D Cells co-infected with  $\Delta$ UL25MO and AcUL25-L3
- Figure 6.1E Cells co-infected with  $\Delta$ UL25MO and AcUL25-L6
- Figure 6.1F Cells co-infected with  $\Delta$ UL25MO and AcUL25-L6
- Figure 6.2 KUL25NS- and  $\Delta$ UL25MO-infected Vero cells
- Figure 6.3 Spread of viral DNA within the cell

## Chapter 7

- Table 7.1 The primers used to generate the PCR fragments encoding pUL36cbd
- Figure 7.1 Expression of GST and pGST-UL36cbd in *E. coli*
- Figure 7.2 GST pull-down assay to determine the specificity of binding of wt pUL25 to pGST-UL36cbd
- Figure 7.3 GST pull-down assay to determine the interaction of pUL25-L3, -L5, -L6 and -C4A with pGST-UL36cbd

## Chapter 8

- Table 8.1 Summary of the characteristics of the UL25 proteins

## Abbreviations

### A

Å	angstrom
aa	amino acid
Ac	<i>Autographa californica</i>
amp	ampicillin
ATP	adenosine triphosphate

### B

bp	base pair
BD II	pUL25 binding domain (UL36)
BHV-1	bovine herpesvirus type 1

### C

C-terminus	carboxyl terminus
°C	degree celsius
CBD	capsid-binding domain (UL36)
CCSC	C-capsid specific component
cm	chloramphenicol
CPE	cytopathic effect
cryo-EM	electron cryo-microscopy

### D

3D	3-dimensional
DAPI	4', 6'-diamidino-2-phenylindole
DMEM	Dulbecco's modified Eagle's medium
dH <sub>2</sub> O	distilled deionised water
DNA	deoxyribonucleic acid
DR	direct repeats
dsDNA	double stranded DNA
dNTP	2'-deoxynucleoside-5'-triphosphate

### E

E	early
EBV	Epstein-Barr virus
<i>E. coli</i>	<i>Escherichia coli</i>
EDTA	ethylenediaminetetra-acetic acid
EM	electron microscopy
ET	evolutionary trace

### F

FCS	foetal calf serum
FISH	fluorescent in-situ hybridisation
FITC	fluorescein isothiocyanate

**G**

g	gram
GAG	glycosaminoglycan
GC	G + C content of DNA
GFP	green fluorescent protein
gm	gentamicin
GST	glutathione S-transferase

**H**

h	hour
HCMV	human cytomegalovirus
HCF	host cell factor
HHV	human herpes virus
hpi	hours post infection
HSV	herpes simplex virus

**I**

IE	immediate early
INM	inner nuclear membrane
IPTG	isopropylthio- $\beta$ -D-galactoside
IR <sub>L</sub>	internal repeat long region (HSV-1 genome)
IR <sub>S</sub>	internal repeat short region (HSV-1 genome)

**K**

k	kilo ( $10^3$ )
kb	kilobase
kbp	kilobase pair
KDa	kilodalton
Km	kanamycin
KSHV	Kaposi's sarcoma-associated herpesvirus

**L**

L	late
LAT	latency associated transcript
LB	Luria broth

**M**

M	molar
m	milli ( $10^{-3}$ )
MAb	monoclonal antibody
mg	milligram
miRNA	microRNA
min	minute
ml	millilitre
mM	millimolar
MOI	multiplicity of infection
MRC	Medical Research Council
mRNA	messenger RNA

MW molecular weight

## N

nm nanometre  
 N-terminus amino terminus  
 NLS nuclear localisation signal  
 NPC nuclear pore complex  
 NPT non-permissive temperature

## O

Oct-1 octomer DNA-binding protein  
 OD optical density  
 ONM outer nuclear membrane  
*oriL* origin of replication in the long region of the HSV-1 genome  
*oriS* origin of replication in the short region of the HSV-1 genome  
 ORF open reading frame

## P

PCR polymerase chain reaction  
 pen penicillin  
 PFU plaque forming units  
 PrV pseudorabies virus  
 PT permissive temperature

## R

REN restriction endonuclease  
 RNA ribonucleic acid  
 rpm rotations per minute  
 RSB reticulocyte standard buffer  
 RT room temperature

## S

SDS-PAGE sodium dodecyl sulphate polyacrylamide gel electrophoresis  
 Sf *Spodoptera frugiperda*  
 ss single stranded  
 stp streptomycin

## T

TEMED N,N,N',N',-tetramethylethylene  
 tet tetracycline  
 Tris tris (hydroxymethyl) aminoethane  
 TR<sub>L</sub> terminal repeat long region (HSV-1 genome)  
 TR<sub>S</sub> terminal repeat short region (HSV-1 genome)  
 ts temperature-sensitive

**U**

u	unit
μ	micro (10 <sup>-6</sup> )
μg	micrograms
μl	microlitre
U <sub>L</sub>	unique long (HSV-1 genome)
μm	micrometre
U <sub>S</sub>	unique short (HSV-1 genome)
UV	ultraviolet

**V**

vhs	virion host shutoff protein
V	volts
v/v	volume to volume ratio
VZV	varicella-zoster virus

**W**

wt	wild-type
w/v	weight to volume ratio

**X**

X-gal	5-bromo-4-chloro-3-indolyl-β-D-galactosidase
-------	--

**Amino acid abbreviations**

<u>Amino Acid</u>	<u>Three letter code</u>	<u>One letter code</u>	<u>Properties</u>
Alanine	Ala	A	Non-polar (hydrophobic)
Arginine	Arg	R	Basic
Asparagine	Asn	N	Polar (neutral)
Aspartic acid	Asp	D	Acidic
Cysteine	Cys	C	Polar (neutral)
Glutamine	Gln	Q	Polar (neutral)
Glutamic acid	Glu	E	Acidic
Glycine	Gly	G	Polar (neutral)
Histidine	His	H	Basic
Isoleucine	Ile	I	Non-polar (hydrophobic)
Leucine	Leu	L	Non-polar (hydrophobic)
Lysine	Lys	K	Basic
Methionine	Met	M	Non-polar (hydrophobic)
Phenylalanine	Phe	F	Non-polar (hydrophobic)
Proline	Pro	P	Non-polar (hydrophobic)
Serine	Ser	S	Polar (neutral)
Threonine	Thr	T	Polar (neutral)
Tryptophan	Trp	W	Non-polar (hydrophobic)
Tyrosine	Tyr	Y	Polar (neutral)
Valine	Val	V	Non-polar (hydrophobic)

**Nucleotide abbreviations**

Base	One letter code
Adenine (Purine)	A
Cytosine (Pyrimidine)	C
Guanine (Purine)	G
Thymidine (Pyrimidine)	T
Uracil (Pyrimidine)	U

## **Author's declaration**

I declare that all the work presented in this thesis was obtained by my own efforts unless stated otherwise.

# 1 Introduction

## 1.1 Introduction to herpesviruses

### 1.1.1 Classification of herpesviruses

Herpesviruses are a large diverse group of double-stranded DNA (dsDNA) viruses with a wide range of host species, including most vertebrate and at least one invertebrate. Few herpesviruses naturally infect more than one species and it is likely that the 200 herpesviruses identified so far only reflects a small proportion of the probable number in existence (Pellet & Roizman, 2007). Historically, members of the herpesvirus family were identified by their virion morphology, which consists of four distinct layers (Section 1.2) (Davison, 2002, Pellet & Roizman, 2007). In addition to virion structure, members of the family exhibit the following common biological characteristics:

- They all encode a large range of enzymes and proteins involved in nucleic acid metabolism, DNA synthesis and the processing of proteins.
- Viral DNA replication, capsid assembly and encapsidation of viral DNA occur in the nucleus, while further viral maturation takes place in the cytoplasm of the infected cell.
- The production of infectious viral progeny invariably leads to destruction of the infected cell.
- They all share the ability to maintain a dormant or latent persistent infection throughout the lifetime of the host. Latent viruses express only a subset of viral genes and retain the capacity to replicate and cause disease on reactivation.

Although family members share these features, different herpesviruses also display considerable variation with respect to other biological properties: they differ in the clinical manifestations of the diseases they cause, their host cell

range *in vitro* and the length of their replicative cycle. In addition, the specific cell type in which the different herpesviruses remain latent varies.

Since the advent of DNA sequencing technology, the traditional approach for classifying family members on biological criteria has been replaced by classification based primarily on DNA sequence homology and genome organisation (Davison, 2002, McGeoch et al., 2006). On this basis a new order has been established, *Herpesvirales*, which has divided the former *Herpesviridae* family into three distinct lineages (Davison et al., 2009). The revised *Herpesviridae* family retains the herpesviruses that infect mammals, birds and reptiles, while the new family *Alloherpesviridae* comprises viruses with fish or amphibian hosts and the other new family *Malacoherpesviridae* currently includes a single virus that infects marine bivalves (Davison et al., 2005, McGeoch et al., 2006). The family *Herpesviridae* has been further classified into the subfamilies *Alphaherpesvirinae*, *Betaherpesvirinae* and *Gammaherpesvirinae*. Eight distinct human herpesviruses have been identified so far and there are representatives from each of the three subfamilies (Table 1.1).

Currently there is an extensive catalogue of sequence data for herpesvirus genomes, which range in size from 124-241 kilo base pairs (kbp) with an estimated one gene per 1.5-2 kbp of herpesvirus genome (Davison et al., 2003, McGeoch et al., 2006). The DNA sequence information allowed the reassessment of herpesvirus classification on the basis of gene conservation, positioning and arrangement of gene clusters relative to one another, the arrangement of terminal sequences or the presence of nucleotides subject to methylation (McGeoch et al., 2006, McGeoch et al., 2005, Pellet & Roizman, 2007). In the light of these data the original system proved to be remarkably accurate, since only a few viruses had to be re-classified. Two human herpesviruses, HHV-6 and HHV-7, were reassigned to the *Betaherpesvirinae* subfamily following amino acid and DNA sequence comparisons. In addition, DNA sequence information enabled the construction of a phylogenetic tree illustrating the common ancestral origin of the herpesvirus family (Figure 1.1).

Virus	Common Name	Abbreviation	Subfamily	Genera	Genome Size (kb)	Disease
HHV-1	Herpes simplex virus type 1	HSV-1	<i>Alphaherpesvirinae</i>	<i>Simplexvirus</i>	152	Cold sores
HHV-2	Herpes simplex virus type 2	HSV-2	<i>Alphaherpesvirinae</i>	<i>Simplexvirus</i>	152	Genital ulcers
HHV-3	Varicella-zoster virus	VZV	<i>Alphaherpesvirinae</i>	<i>Varicellovirus</i>	125	Chicken pox, shingles
HHV-4	Epstein-Barr virus	EBV	<i>Gammaherpesvirinae</i>	<i>Lymphocryptovirus</i>	172	Infectious mononucleosis, Burkitt's lymphoma, Hodgkin's disease.
HHV-5	Human cytomegalovirus	HCMV	<i>Betaherpesvirinae</i>	<i>Cytomegalovirus</i>	236	Disseminated disease in neonates and in immunocompromised individuals
HHV-6	Human herpesvirus 6	HHV-6	<i>Betaherpesvirinae</i>	<i>Roseolovirus</i>	160	<i>Exanthema subitum</i> (Infant rash)
HHV-7	Human herpesvirus 7	HHV-7	<i>Betaherpesvirinae</i>	<i>Roseolovirus</i>	145	<i>Exanthema subitum</i> (Infant rash)
HHV-8	Kaposi's sarcoma-associated herpesvirus	KSHV	<i>Gammaherpesvirinae</i>	<i>Rhadinovirus</i>	170	Associated with Kaposi's sarcoma

**Table 1.1 Human herpesviruses and their classification and associated diseases (Pellet & Roizman, 2007; Davison et al., 2009)**

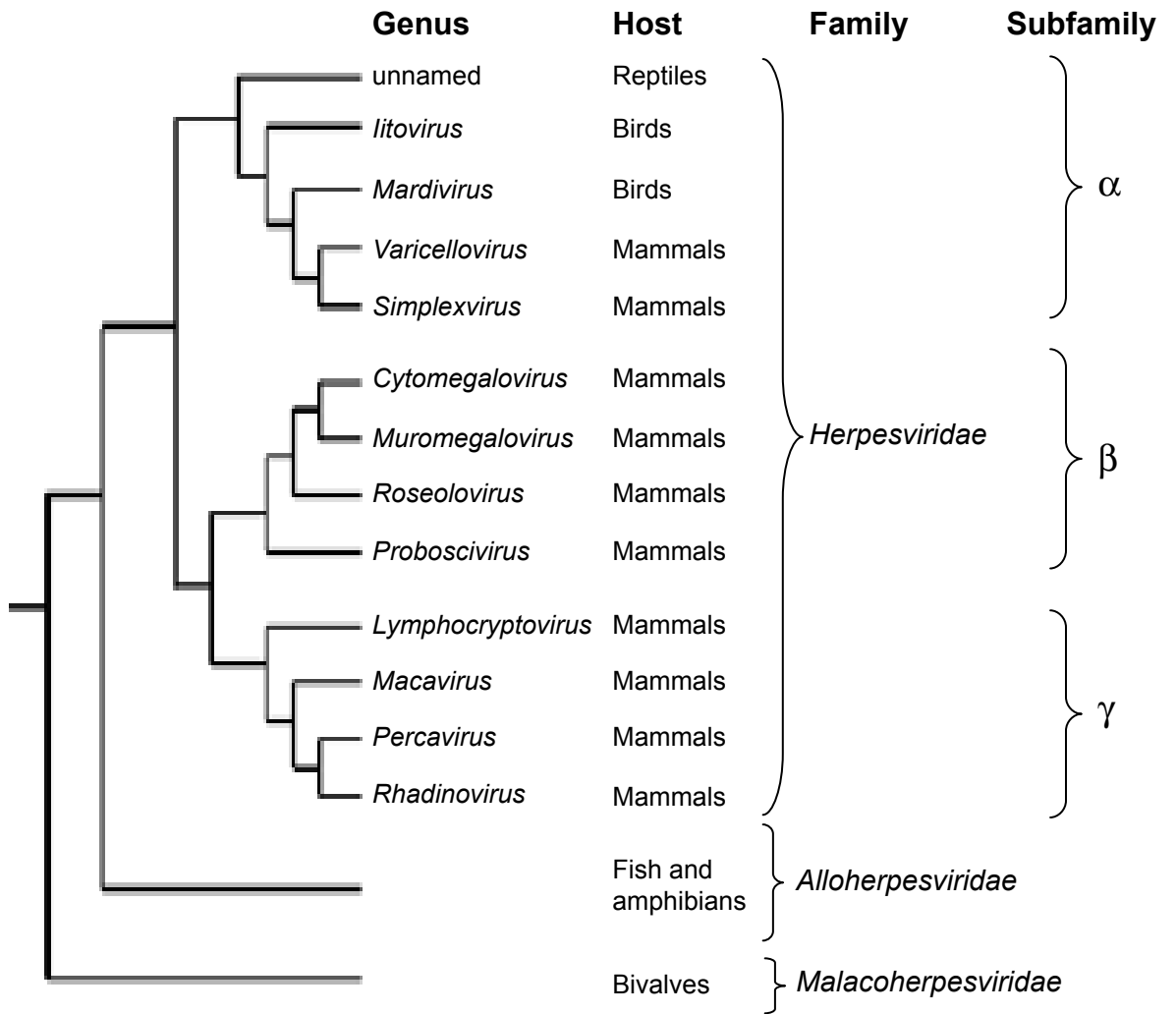


**Figure 1.1 Phylogenetic relationships and taxonomy of major herpesviruses**

The diagram shows branching patterns and not evolutionary relationships (adapted from Pellet & Roizman 2007).

### 1.1.1.1 *Alphaherpesvirinae*

The main features for members of this subfamily are: they display a variable host range *in vitro*, with the ability to infect a variety of cell lines in culture; they have a relatively short replicative cycle of less than 24 hours (h); spread rapidly in tissue culture; show a strong cytopathic effect (CPE) in infected cells and establish latency primarily in sensory ganglia. The subfamily is further divided into the four genera: *Simplexvirus*, which includes herpes simplex virus type 1 (HSV-1) and type 2 (HSV-2); *Varicellovirus*, which includes varicella-zoster virus (VZV); *Mardivirus* and *Iltovirus*, members of which infect avian hosts (Pellet & Roizman, 2007).

### 1.1.1.2 *Betaherpesvirinae*

Members of this subfamily have a restrictive host range *in vitro* and *in vivo*. The reproductive cycle is long, infection progresses slowly in culture and infected cells often become enlarged (cytomegalia). Carrier cultures can be readily established in which cells survive following infection. In the natural host the virus is maintained in the latent form in a wide range of cell types including secretory glands, lymphoreticular cells, kidneys and other tissues. This subfamily contains the genus *Cytomegalovirus*, which includes human cytomegalovirus (HCMV) and the genus *Roseoloviruses*, which include human herpesvirus type 6 (HHV-6) and type 7 (HHV-7) (Pellet & Roizman, 2007).

### 1.1.1.3 *Gammaherpesvirinae*

Herpesviruses within this subfamily are characterised by a limited experimental host range, restricted to the family or order to which the natural host belongs. In culture all members replicate in lymphoblastoid cells and are usually specific for either T or B lymphocytes. Latent infections also occur frequently within lymphoblastoid tissue. However, some viruses in this group produce a productive or lytic infection in other cell types, such as epithelioid and fibroblastic cells. Two genera in this subfamily have viruses that infect humans. The Epstein-Barr virus (EBV) as a member of *Lymphocryptovirus*, whereas *Rhadinovirus* includes human herpesvirus type 8 (HHV-8), also known as Kaposi's sarcoma-associated herpesvirus (KSHV). Recent evidence indicates that

members of the genus *Lymphocryptovirus* consist of two major lineages that have coevolved with their hosts: viruses of the Old World (humans, chimpanzees) and New World (marmosets) primates (Gerner et al., 2004, McGeoch et al., 2005, Pellet & Roizman, 2007).

### **1.1.2 Human herpesviruses and disease**

So far eight human herpesviruses have been identified and characterised (Table 1.1). Generally symptoms in infected individuals are asymptomatic and consequently lead to widespread transmission of the virus in early life. Exceptions to these are infections with VZV, which is the causative agent of chicken pox, or HSV-2 causing neonatal, disseminated herpes infections. In most other cases symptoms are largely the consequences of the re-emerging latent virus. The most extensively studied herpesvirus is HSV-1, and in populations that have been analysed usually 50-90% of individuals are infected. Primary infection by HSV-1 can occur at a number of sites, but the classic route is through mucosal membranes of the mouth and nose, leading to latent infection of the trigeminal ganglia. Reactivation of the latent virus is often associated with stress, exposure to UV light, fever, tissue damage or immuno-suppression, resulting in the appearance of the characteristic cold sore lesions at, or close to, the site of primary infection (Roizman et al., 2007). In some cases the reactivated virus can cause more severe conditions such as HSV-1 encephalitis, which can be fatal, or keratoconjunctivitis that can result in blindness. In the case of latent VZV infections, reactivation is restricted to a single nerve tract where it causes the painful condition referred to as shingles. Immuno-compromised individuals, such as transplant or AIDS patients, are particularly at risk from infections due to reactivated virus, including life-threatening conditions from reactivated HCMV. In addition, two gammaherpesviruses, EBV and KSHV, have been linked to neoplastic transformations that include Burkitt's lymphoma (EBV) and Kaposi's sarcoma (KSHV) (Pellet & Roizman, 2007). Since the work carried out in this thesis relates to the prototypical herpesvirus, HSV-1, the following discussions will focus predominately on this virus.

## 1.2 HSV-1 virion architecture

The mature or infectious virion consists of four morphologically distinct structural components. The central core comprises the linear dsDNA genome, which is enclosed within a protective icosahedral capsid that together form the nucleocapsid. The capsid in turn is embedded in a protein matrix known as the tegument and, finally, the tegument is surrounded by a lipid bilayer or envelope containing several viral glycoproteins (Roizman et al., 2007, Wildy et al., 1960). A generalised representation and a detailed electron micrograph of the herpesvirus structure are shown in Figure 1.2.

### 1.2.1 Genome

The HSV-1 genome consists of a single linear dsDNA molecule, which is approximately 152 kbp in length, has a GC content of 68% and contains at least 75 open reading frames (ORFs) (McGeoch et al., 1993). The viral genome consists of two covalently linked regions designated long (L) and short (S), which each contain unique sequences, termed  $U_L$  and  $U_S$ , respectively. The  $U_L$  region is 107.9 kbp and the  $U_S$  region is 13 kbp long, and both regions are bordered by inverted repeat sequences. The terminal and internal repeats flanking  $U_L$  are referred to as  $TR_L$  and  $IR_L$ , respectively, whilst those flanking  $U_S$  are known as  $TR_S$  and  $IR_S$ , respectively. Genes in the unique and repeated sequences have prefixes  $U_L$ ,  $U_S$ ,  $R_L$  or  $R_S$  and are numbered according to their relative position in the genome (Roizman et al., 2007). Each of the inverted repeats flanking the  $U_L$  or  $U_S$  regions are composed of various combinations of repeat elements termed  $a$ ,  $b$  and  $c$ . The  $a$  and  $b$  repeats are found in  $TR_L$  and their inversions ( $a'$  and  $b'$ ) in  $IR_L$ , and the  $a$  and  $c$  elements are found in  $TR_S$  and their inversions ( $a'$  and  $c'$ ) in  $IR_S$ . Multiple  $a$  sequences are frequently found in  $TR_L$  and also at the junction of  $IR_L$  and  $IR_S$ , but in the opposite orientation to the terminal  $a$  sequences (McGeoch et al., 1988). Thus the HSV-1 genome can be written as  $a_n b - U_L - b' a'_m c' - U_S - c a$ , where  $n$  and  $m$  represent variable copies of the  $a$  sequence (Roizman et al., 2007). An illustrated version of the HSV-1 genome is shown in Figure 1.3. As a consequence of the inverted repeats at either end of the  $U_L$  and  $U_S$  recombination can occur during viral replication, resulting in the inversion of one region relative to the other and the formation of four genome isomers

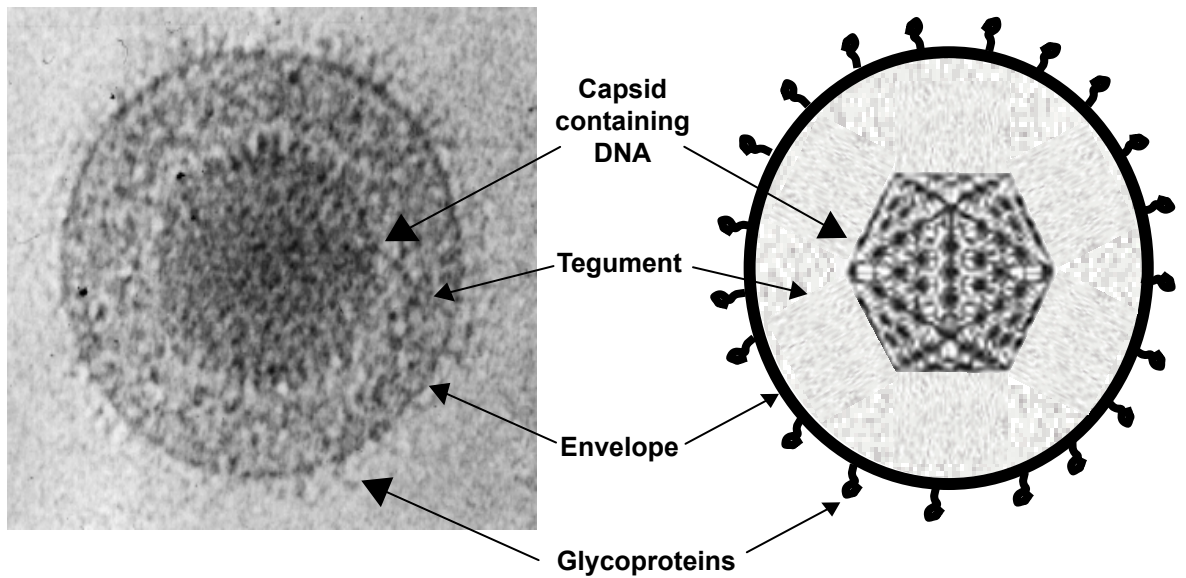


**Figure 1.2 Structure of the HSV-1 virion**

The HSV-1 virion is composed of four structural elements. The double-stranded DNA genome is packaged into the icosahedral capsid. The tegument surrounds the capsid and consists of a collection of proteins that are organised into at least two layers, one which interacts with the envelope proteins and one that is closely associated with the capsid. The envelope is a lipid bilayer infused with viral glycoproteins and encloses both the tegument and the DNA containing capsid.

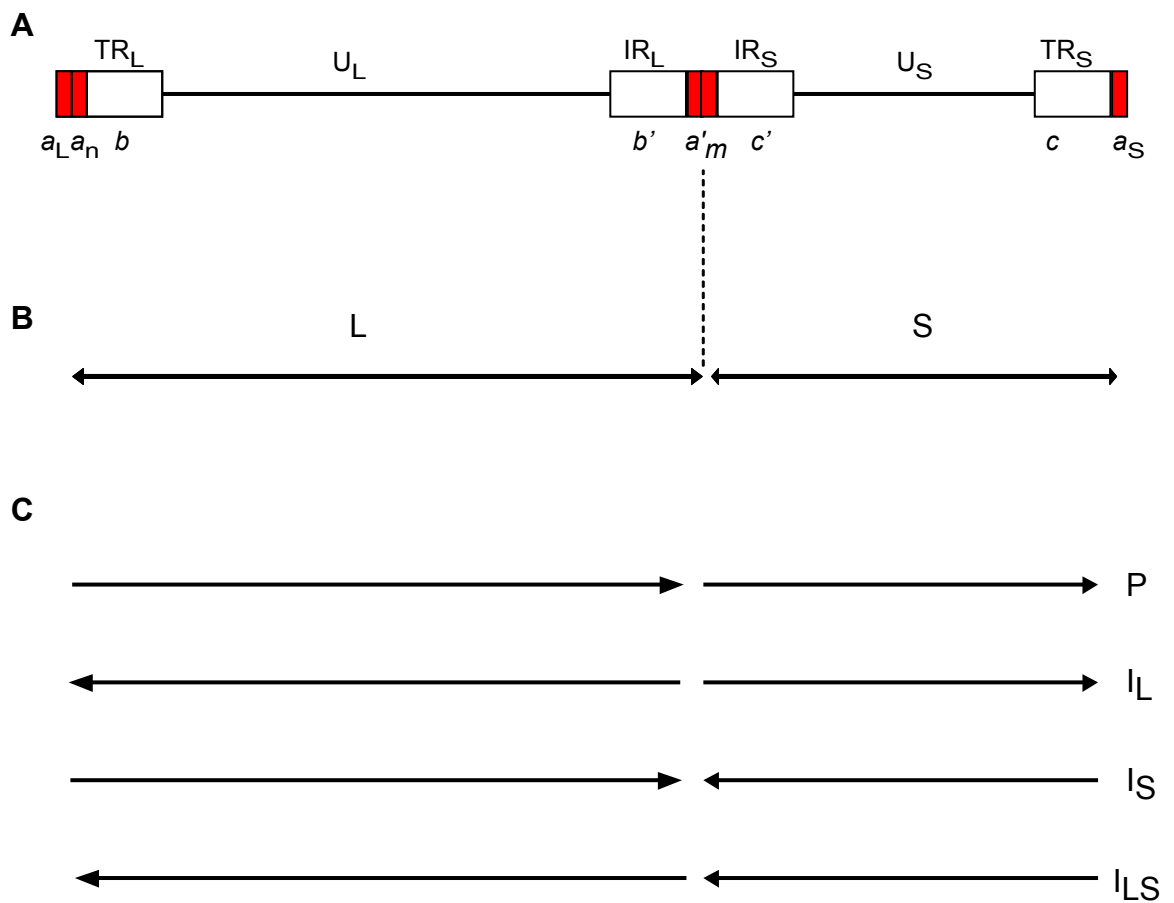


**Figure 1.3 The HSV-1 genome structure**

The HSV-1 genome (A) consists of the L and S domains, shown in (B). The L and S domains each contains a unique sequence,  $U_L$  and  $U_S$ , respectively, which is flanked by inverted repeats ( $TR_L/IR_L$  and  $TR_S/IR_S$ ). The genome contains the *a* sequence at the end of each terminal repeat ( $a_L$  and  $a_S$ ) and this sequence is also present at the L-S junction in an inverted orientation ( $a'$ ). The  $TR_L$  has a variable number of *a* sequences ( $a_n$ ) and there is also a variable number at the L-S junction ( $a'_m$ ). The *b* sequence is only present in  $TR_L$  and in an inverted position in  $IR_L$ . Similarly, the *c* sequence is only found in  $TR_S$  and in an inverted orientation in  $IR_S$ . (C) The arrows indicate the relative orientation of the four possible genomic isomers of HSV-1 that result from inversion of the L and S domains during DNA replication. P indicates the prototype and no inversion of either L or S domains,  $I_L$  indicates inversion of the L region and  $I_S$  indicates inversion of the S region, while  $I_{LS}$  signifies that both L and S domains are inverted.

(Figure 1.3), which exist in equimolar amounts in HSV-1 populations. The role of the various genome isomers during viral replication is unknown, since HSV-1 mutants with specific repeat sequences removed and their genomes frozen in any given isomeric form still remained viable in culture (Roizman et al., 2007). Herpesvirus genomes in general can be divided into seven groups on the basis of the overall arrangement of their repeat sequences and unique regions, and the HSV-1 genome is typical member of group 6 (Davison & McGeoch, 1995). An illustration of the various genome structures found in herpesvirus and a summary of their salient features are shown in Figure 1.4.

### 1.2.2 The capsid

The virus genome is packaged into an icosahedral capsid, consisting of protein subunits that self-assemble around a scaffold core in the nuclei of infected cells. The proteins required for capsid formation are conserved within the *Herpesviridae* and a list of the genes that encode them in HSV-1 are shown in Table 1.2 (Steven et al., 2005).

Gene	Protein	MW (kDa)	Description
UL18	VP23	34	Structural component of triplexes
UL19	VP5	15	Structural component of hexons and pentons
UL26	VP21	40	Minor scaffolding protein
UL26	VP24	26.5	Maturation protease
UL26.5	VP22a	34	Major scaffolding protein
UL35	VP26	12	Accessory protein located on hexon tips
UL38	VP19C	50	Structural component of triplexes

**Table 1.2 HSV-1 genes encoding proteins involved in capsid assembly**

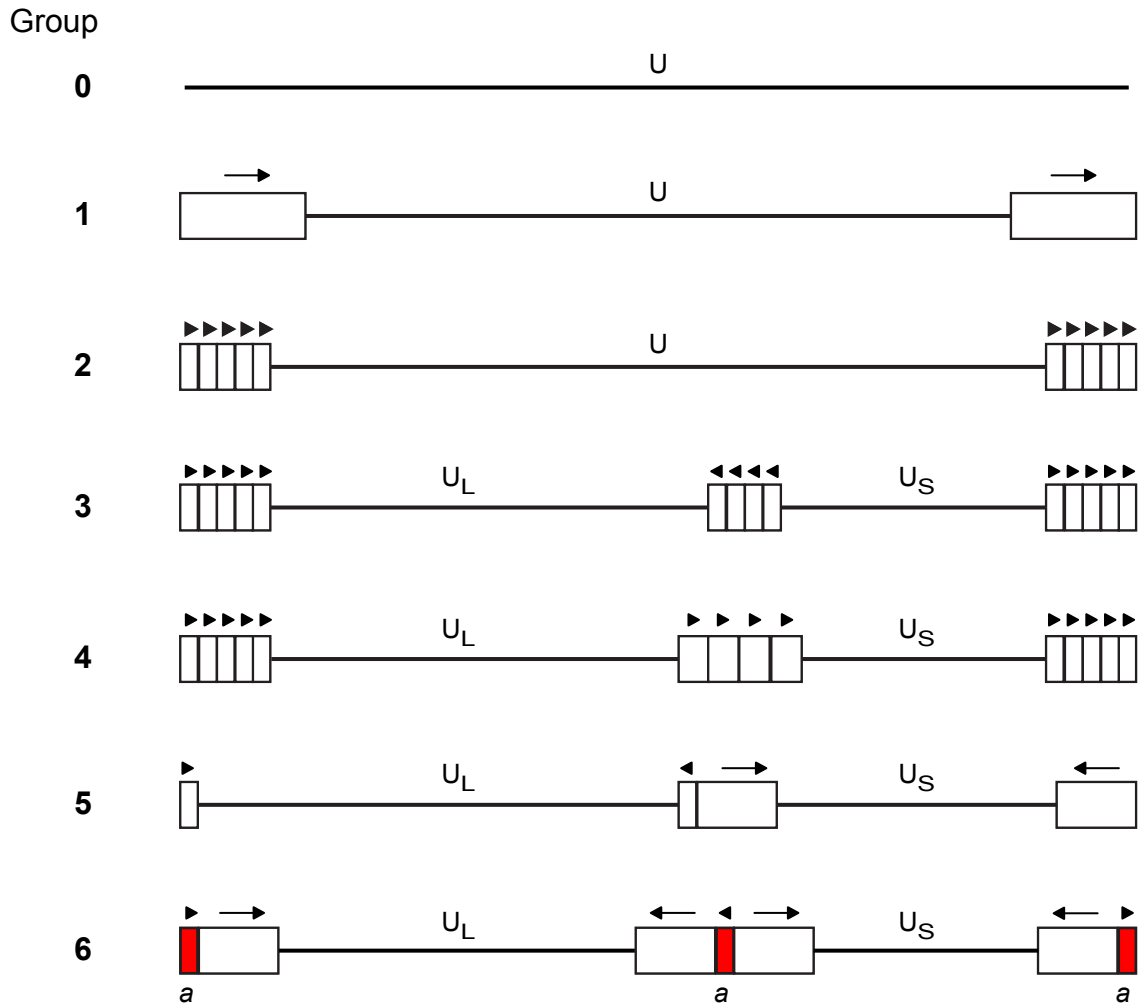


**Figure 1.4 Herpesvirus genome structures**

The genome structures of herpesviruses, defined by Roizman (1992) and Davison & McGeoch (1995), are illustrated. The unique regions are indicated by the letter U, with the long and short unique regions denoted as UL and US, respectively. The repeat units are depicted by boxes and their orientation is indicated by the arrowheads. Group 0 genomes each consists of a single unique coding region and no repeat units. An example is tree shrew herpesvirus (Koch et al., 1985). The group 1 genomes each consists of a single unique region and single direct repeat sequences at each terminus. An example being channel catfish virus (Davison, 1992). Each group 2 genome also contains a single unique region, but has multiple copies of repeat units at each terminus. An example is herpesvirus saimiri (Albrecht et al., 1992). The group 3 genomes each has multiple repeat units located at each terminus and an internal repeat unit in the opposite orientation at the junction of the UL and US domains. An example is the cottontail rabbit herpesvirus (Cebrian et al., 1989). Group 4 genomes are similar to group 3 genomes, but the internal repeats show no similarity to the end terminal repeats and the gammaherpesvirus EBV has a genome with this arrangement (Baer et al., 1984). Group 5 genomes each has two unrelated inverted repeats flanking the UL and US regions respectively, however, the ones at either end of the UL domain are much smaller than those at each end of the US domain. An example of this group is VZV (Davison & Scott, 1986). Group 6 genomes are similar to group 5 genomes, but they contain additional repeat units termed a sequences that are located at each terminus of the genome and at the junction of the UL and US region in the opposite orientation. In addition, the inverted repeats flanking the UL domain are much larger than those contained in group 5 genomes. Both HSV-1 and HSV-2 have genomes of this type (Roizman, 1979).

### 1.2.2.1 Icosahedral symmetry

Crick & Watson (1956) were the first to point out that due to the limited coding capacity of the viral genome, it was economical to construct capsids from a small number of protein subunits. In the case of the spherical viruses, a closed shell could be achieved by using the symmetry of Platonic polyhedra, for example tetrahedron, octahedron or icosahedron. So far only examples of icosahedral capsids have been found, perhaps because the most economical way to build a symmetric shell, of maximal internal volume using nonsymmetric protein molecules, is to arrange the proteins in identical equilateral triangular structures that can be joined to form an icosahedron. An icosahedron has 20 triangular faces and 12 vertices related by two-, three- and fivefold axes of rotational symmetry (Figure 1.5). In the simplest packing arrangement, each triangular face of the capsid comprises three identically placed proteins ( $\times 20$  faces = 60), with each of the 60 subunits (asymmetric units) interacting with their neighbour in an identical (equivalent) environment. Consequently, although the volume in such a capsid depends on the size of the protein, it is still quite small and can only package a small genome. Larger genomes, such as HSV-1, require larger capsids and therefore must contain more than 60 protein subunits. The apparent contradiction of the structural properties of larger particles was accounted for by the theory of quasi-equivalence developed by Caspar & Klug (1962). They proposed that when a capsid contained more than 60 subunits, each subunit occupied a quasi-equivalent position, where the bonding properties of subunits in different structural environments are similar, but not identical as in the case of the 60-subunit structure. In a larger structure, such as the HSV-1 capsid, five subunits make fivefold symmetric contact at each of the 12 vertices, forming the pentons. The additional subunits are interposed between the pentons and arranged with six-fold symmetry, forming the hexons. The addition of the hexons allows the size of the shell to increase without disrupting the basic geometry of the icosahedral capsid. In such a structure, each subunit can be present in one of three different structural environments. Nevertheless, all subunits bond to their neighbours in similar ways. Another important concept introduced by Caspar & Klug (1962) was the triangulation number,  $T$ , a mathematical means used to describe the number of

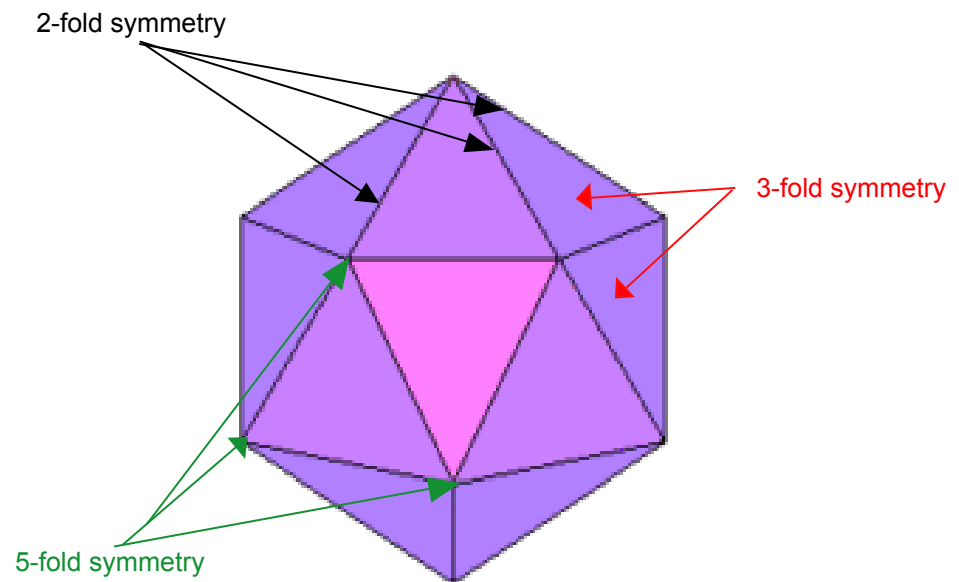


**Figure 1.5 Icosahedron**

An icosahedron has 20 equilateral triangular faces and 12 vertices related by 2-, 3- and 5-fold symmetry.

structural units required per triangular face that would be needed to assemble an icosahedron in a given structure.

### 1.2.2.2 Capsid structure

A reconstruction of the HSV-1 capsid has been determined to a resolution of 8.5 Å and is illustrated in Figure 1.6 (Zhou et al., 2000). The capsid has a diameter of 125 nm and is approximately 15 nm thick. The genes encoding the major proteins of the capsid are summarised in Table 1.2. Three viral proteins, VP5, VP23 and VP19C, are essential for HSV-1 capsid formation. The major capsid protein, VP5, assembles into 161 subunits or capsomers, which are connected to each other at the innermost layer of the shell cavity to form the capsid floor (Baker et al., 1990). Capsomers can be subdivided into two populations of 150 hexons and 11 pentons, which form the structural units of the T=16 icosahedral capsid (Wildy et al., 1960). Eleven of the 12 vertices of the HSV-1 capsid are occupied by pentons, each comprising identical populations of five VP5 molecules. The twelfth capsid vertex is occupied by a cylindrical portal made up of 12 molecules of UL6, forming a channel through which viral DNA is packaged into the capsid and possibly released (Chang et al., 2007, Deng et al., 2007, Homa & Brown, 1997, Newcomb et al., 2001, Valpuesta & Carrascosa, 1994). The hexons, composed of six VP5 molecules, form the edges and faces of the icosahedron and are decorated by the small non-essential protein VP26 (Zhou et al., 1994). In contrast to pentons, there are three quasi-equivalent populations of hexons (Figure 1.7). The hexons lying adjacent to the pentons are known as peripentonal or P hexons, while those located on the faces of the icosahedron are termed C hexons and ones situated on the edges are referred to as E hexons. The hexons and pentons are interconnected by a heterotrimeric complex of proteins known as the triplex, composed of two copies of VP23 and one copy of VP19C, which form their connections by interacting with the middle and floor domains of the surrounding capsomers (Newcomb et al., 1993, Trus et al., 1995). Triplexes, like hexons, can be divided into quasi-equivalent populations (termed Ta, Tb, Tc, Td, Te and Tf) based on their location within the icosahedral lattice (Zhou et al., 1994). The positions of the quasi-equivalent hexons and triplexes on the surface lattice of the capsid are illustrated in Figure 1.7.

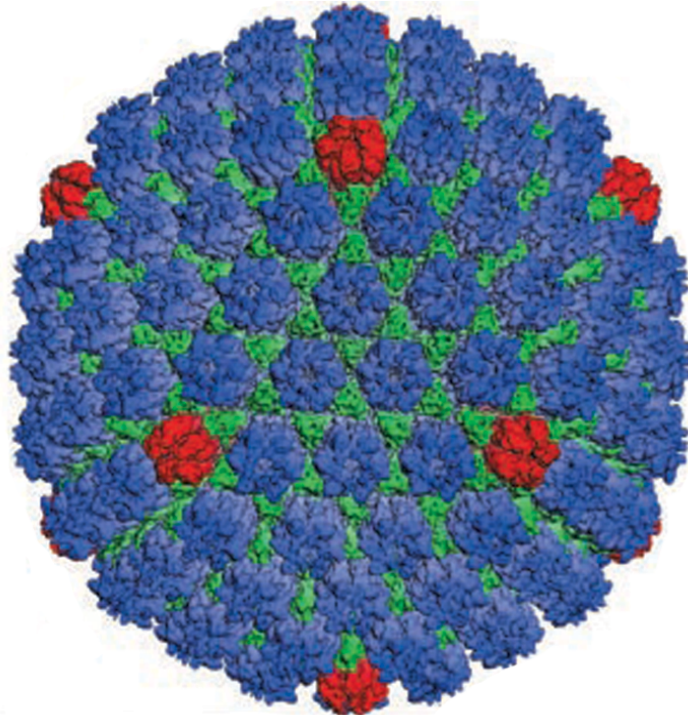


**Figure 1.6 Reconstruction of the HSV-1 capsid to 8.5 Å**

Shaded surface view of the T=16 HSV-1 capsid, which has a diameter of 1250 Å and is 150 Å thick. The capsid shell consists of 161 capsomers, with 150 hexons (blue) forming the faces and edges, 11 pentons (red) forming the vertices, and 320 triplexes (green) lying between adjacent capsomers (adapted from Zhou et al., 2000).

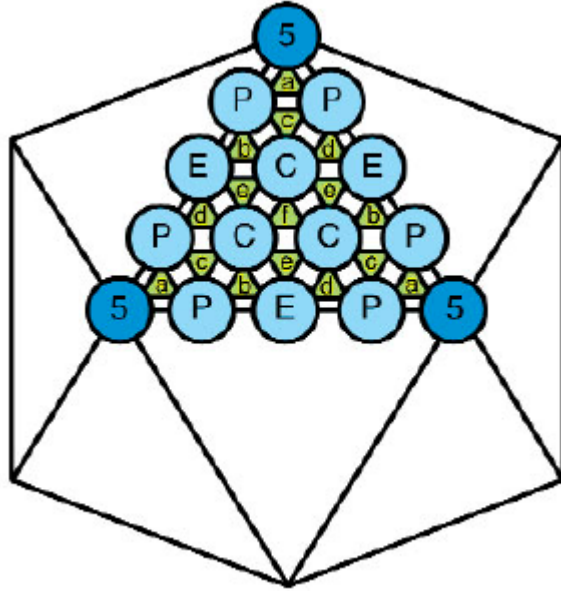


**Figure 1.7 Surface lattice of HSV-1**

The position of the quasi-equivalent capsomers and triplexes. The peripentonal, edge and central hexons (pale blue circles) are denoted by the letters P, E and C, respectively. The pentons are positioned at the vertices and are indicated by the dark blue circles and the number 5. The six triplexes Ta-Tf (green triangles) are denoted a-f (adapted from Heyman et al., 2003).

### 1.2.2.3 Capsid scaffold

Assembly of the HSV-1 capsid requires not only the structural proteins VP5, VP19C and VP23, but involves the participation of the scaffolding proteins, VP22a and VP21, which form the scaffold, or core, and the maturational protease, VP24. The scaffolding proteins direct the fidelity of the maturing capsid's assembly, with the structural proteins co-assembling with and around the core, which interacts directly with VP5 (Hong et al., 1996, Thomsen et al., 1995). In contrast to the other capsid proteins, which are encoded in separate transcriptional units, the scaffolding proteins are encoded by two in-frame overlapping genes, UL26 and UL26.5 (Liu & Roizman, 1991), the arrangement of which is illustrated in Figure 1.8. As a consequence of their gene organisation, the UL26.5 gene product preVP22a (the major scaffolding protein) has an identical sequence to the C-terminal 329 amino acids of the UL26 precursor protein, preVP21/VP24 (Figure 1.8). The 635 amino acid preVP21/24 has an N-terminal protease fragment (VP24), several oligomerisation domains, and a VP5 binding site located at the C-terminus (Deckman et al., 1992, Hong et al., 1996, Liu & Roizman, 1992). During capsid assembly, the UL26 protein is incorporated into the structure and the intrinsic protease activity (VP24) it contains cleaves either autoproteolytically or in *trans* (Liu & Roizman, 1993, Preston et al., 1983). Cleavage at the R site (A247-S248) of the UL26 precursor molecule releases two products, the N-terminally located functional protease, VP24 (M1-S247), and the C-terminal encoded scaffolding protein preVP21 (S248-R635). A second cleavage event is initiated by the maturational protease at the maturation or M site (A610-S611) present in the C-terminal portion of the scaffolding proteins, preVP21 and preVP22a, which are attached to the inner capsid shell via the VP5 binding domains located in each protein at the C-terminus (Hong et al., 1996, Robertson et al., 1996). Although the scaffolding proteins participate in capsid assembly, they are removed during capsid maturation by cleavage at the M site of preVP21 and preVP22 to release VP21 (S348-A610) and VP22 (M307-A610), respectively, while the protease (VP24) remains in the capsid shell (Figure 1.8) (Homa & Brown, 1997, Roizman et al., 2007). Activity of the protease, VP24, is required for the assembly of DNA-containing capsids (Preston et al., 1983; Gao et al., 1994).

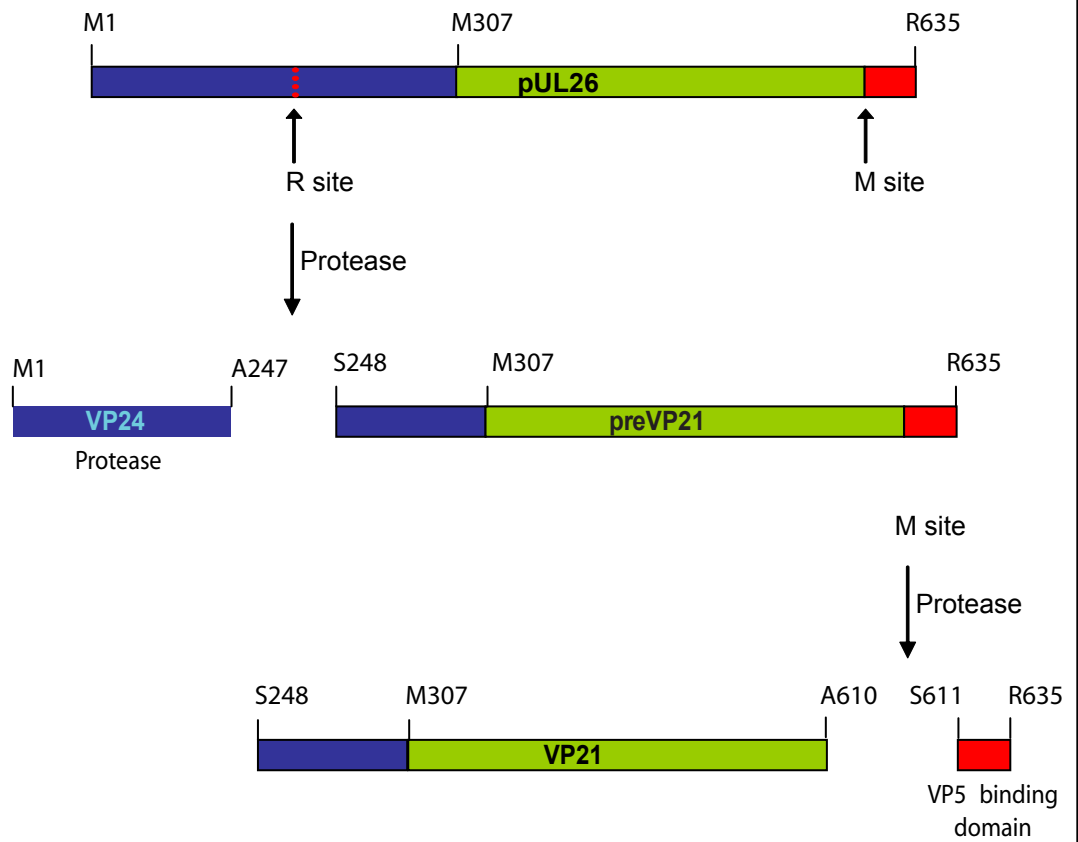
**Figure 1.8 Structural organisation of the HSV-1 scaffolding genes and their proteolytic products**

(A) The scaffolding proteins are encoded by two overlapping genes, UL26 and UL26.5. As a consequence of their gene organisation, the UL26.5 gene product, pre-VP22a, has an identical sequence to the C-terminal 329 amino acids of the UL26 encoded protein (M307-R635). For convenience these residues are also labelled as M307-R635 in the UL26.5 illustration and are highlighted in both scaffolding proteins in green and red. The red portion indicates the VP5 binding domain. (B) During capsid maturation the UL26 encoded protein is cleaved at the R site to release the VP24 maturational protease (residues M1-A247) and preVP21 (S248-R610). Cleavage of preVP21 at the M site results in removal of the VP5 binding domain (S611-R635) and releases the minor scaffolding protein VP21 (S248-A610) from the capsid. (C) Cleavage of preVP22a at the M site removes the VP5 binding domain (S611 – R635) and releases the major scaffolding protein VP22a (M307-A610) from the capsid.

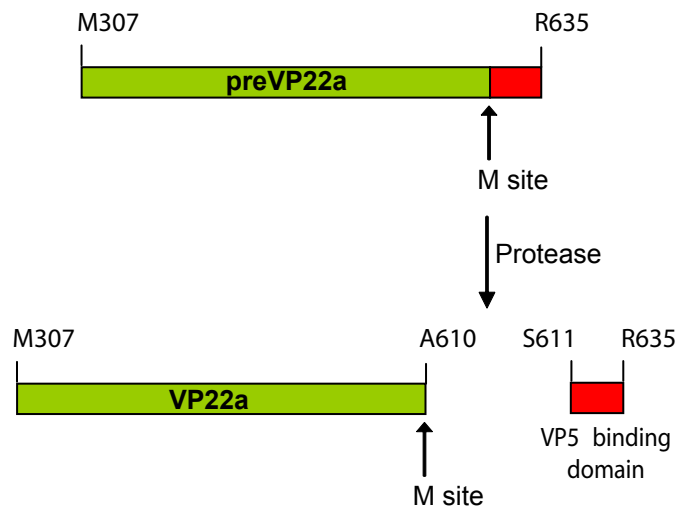
**A** The UL26 and UL26.5 gene products



**B** Proteolysis of the UL26 gene product



**C** Proteolysis of the UL26.5 gene product



#### **1.2.2.4 Capsid forms**

In the nuclei of infected cells, electron microscopic studies have identified three forms of angularised HSV-1 capsids, which have been classified as A-, B- and C-capsids (Gibson & Roizman, 1972). Although the capsids have the same basic icosahedral structure that was described previously, they can be separated by sucrose density gradient ultracentrifugation. The differences in density and morphology between the three capsid forms are due to the material contained in the cavity of their shells. C-capsids, which contain the virus genomes, are the successful end product of DNA packaging that will eventually form part of the infectious virion. A- and B-capsids are considered the abortive or dead-end products of failed DNA packaging events. A-capsids are empty shells that lack DNA and scaffolding proteins, while B-capsids also lack DNA but are filled with a core of cleaved scaffolding proteins, primarily VP22a (Homa & Brown, 1997, Newcomb et al., 1996, Rixon & McNab, 1999, Sherman & Bachenheimer, 1988, Trus et al., 1996). An additional capsid form has been identified, the procapsid, which is the precursor of the other three types and will be discussed in detail in Section 1.3.4. An illustration of all four capsid forms is shown in Figure 1.9

#### **1.2.2.5 Accessory capsid proteins**

Maturation of the procapsid to the angularised capsid involves large cooperative conformational changes (Section 1.3.4). In addition to providing increased stability, these changes create new binding sites that are required for downstream reactions and optimal infectivity. Reconfiguration of the hexons during maturation generates new binding sites on the outer surface of the mature capsid shell that VP26 interacts with. The precise role of this protein is unclear, since it is dispensable and does not appear to confer additional stability to the assembling capsid. However, its absence does reduce infectious virion production (Desai et al., 1998, Newcomb et al., 1993). In addition to the structural and scaffolding proteins, a number of viral proteins have been identified as minor components of the HSV-1 capsid. Most of these minor capsid constituents are involved in DNA packaging and include the proteins encoded by the UL6, UL15, UL17, UL28, UL25 and UL33 genes, which will be discussed further in Section 1.3.5.2.

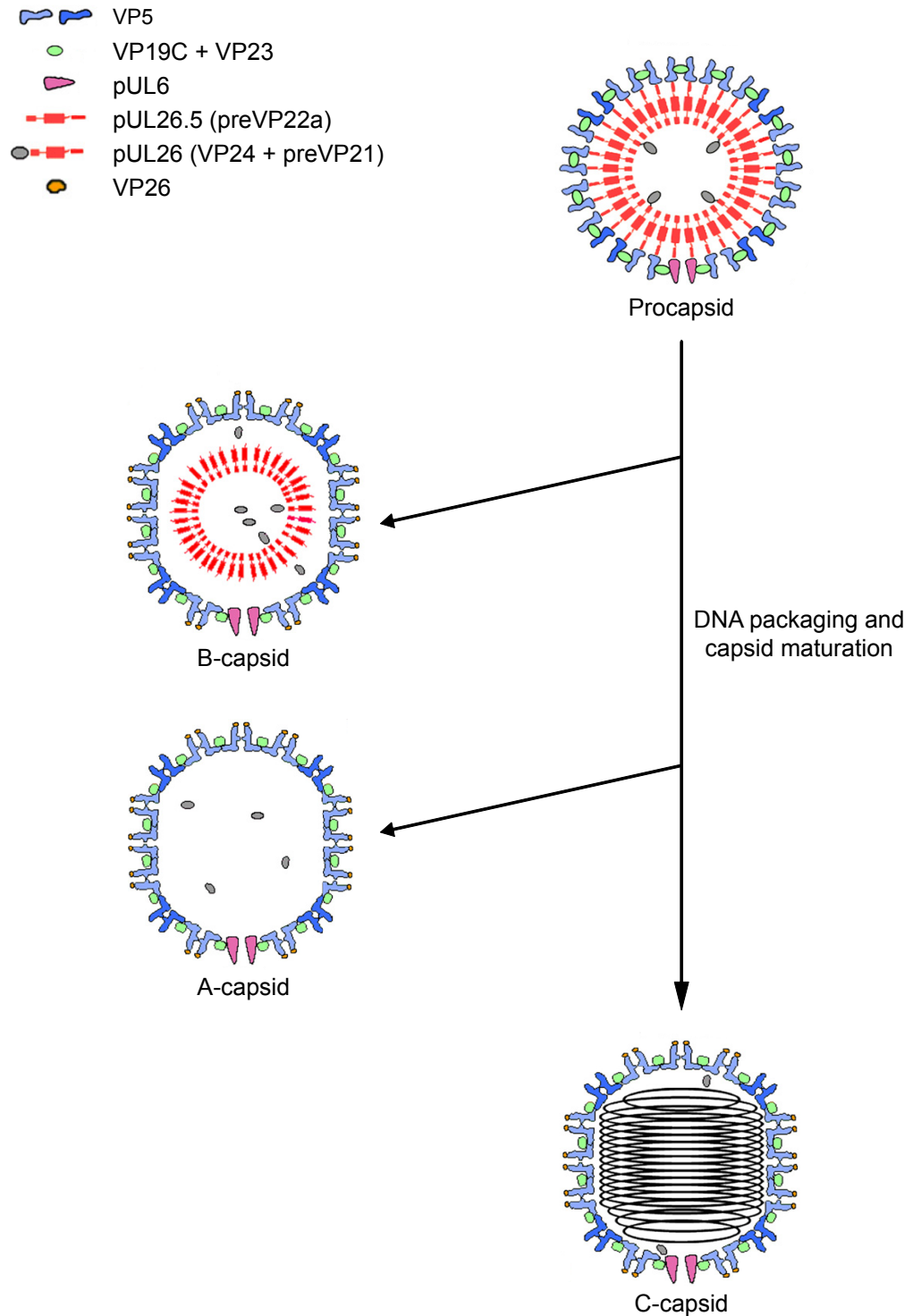


**Figure 1.9 Alternative HSV-1 capsid forms**

The procapsid is the immature spherical form that during viral DNA packaging and maturation switches to the more angularised capsid. C-capsids are the successful end product of DNA encapsidation. B-capsids are dead-end products that lack DNA but are filled with a core of cleaved scaffolding proteins. A-capsids are empty shells that lack DNA and scaffolding proteins and are considered the abortive products of failed DNA packaging events. The hexons on the procapsid shell, highlighted in light blue, and the pentons (mid-blue) are coordinated by the triplexes made up of heterotrimers of VP19C and VP23 (green). The inner shell of the procapsid is composed of the scaffolding proteins pUL26.5 (red) and pUL26 (red and grey). During maturation, the protease is released by autoproteolysis from pUL26 and processes the C termini of the scaffolding proteins attached to the inner capsid shell wall. The conformational switch in capsid morphology creates binding sites for VP26, which are located at the tips of hexons (yellow). The UL6 gene product is arranged as a single dodecamer at the portal (pink) and is the channel where viral DNA is inserted into the capsid during encapsidation (adapted from Trus et al., 2007).

### 1.2.3 The tegument

In contrast to the symmetrical uniformity of the capsid, the tegument is a largely unstructured proteinaceous layer that is located between the capsid and outer envelope (Figure 1.2). More than 15 viral proteins are present in the tegument and there is some evidence that cellular components are also incorporated (Del Rio et al., 2005, Grünewald et al., 2003). Many of the tegument proteins share no sequence homology between alpha-, beta- and gammaherpesviruses and their origin and evolution remains unclear. Indeed, many can be deleted without obviously affecting virion structure (Homa & Brown, 1997, Mettenleiter, 2002, Steven & Spear, 1997). An important function of the tegument is to carry with it an assortment of already synthesised viral proteins that following infection can assist the virus in managing the host environment. These proteins include, the UL41 encoded virion host shut off protein (vhs) that acts by shutting off host cell protein synthesis, and VP16, which is encoded by UL48 and that stimulates expression of HSV-1 immediate-early genes (Cambell et al., 1984, Pellet & Roizman, 2007).

Information from cryo-EM and 3D reconstructions have revealed that the tegument, although regarded as largely amorphous, is composed of at least two distinct layers referred to as the inner and outer tegument layers. The outer layer is asymmetrically organised, heterogeneous and interacts with the cytoplasmic domains of viral membrane proteins, while the inner layer is tightly associated with the vertices of the capsid and displays a more ordered icosahedral morphology (Gibson & Roizman, 1972, Zhou et al., 1999). One of the constituents of the inner tegument layer is the UL36 encoded protein (pUL36), which is highly conserved among the herpesviruses and is essential for viral morphogenesis (Desai, 2000, Klupp et al., 2002). Since pUL36 has been demonstrated to be tightly associated with the capsid at the pentons and also directly interacts with VP5, the protein was suggested as a good candidate for the icosahedrally ordered tegument observed in cryo-EM reconstructions (Gibson & Roizman, 1972, Zhou et al., 1999). Subsequently, a functionally conserved capsid-binding domain (CBD), located in the last 62 amino acids of HSV-1 and PrV pUL36, was identified, which specifically bound to the minor capsid protein pUL25 that is predicted to be situated adjacent to the capsid vertices (Coller et

al., 2007, Trus et al., 2007). More recently this interaction was confirmed, and a second domain in pUL36 (residues 2037-2353) that interacts with pUL25 has also been identified (Pasdeloup et al., 2009). Indications that these interactions may act as the link that binds the capsid to the tegument in the infectious virion has been provided using an HSV-1 UL36 null mutant (Roberts et al., 2009), since in cells infected with the pUL36 deletion mutant, C-capsids lacking tegument accumulated in the cytoplasm and no enveloped capsids were observed in the cytosol.

#### **1.2.4 The envelope**

The outer boundary of the virion is formed by the envelope (Figure 1.2), a lipid bilayer that is created from host cell membranes during viral assembly, and which is thought to originate at the trans-Golgi network (Mettenleiter, 2002). The envelope contains numerous protrusions of virally encoded glycoproteins that function during viral entry, egress and cell-to-cell spread (Beitia Ortiz de Zarate et al., 2004, Farnsworth & Johnson, 2006, Farnsworth et al., 2007). HSV-1 encodes at least 11 glycoproteins (Table 1.3) and the total copy number of these proteins can exceed 1,000 per virion (Pellet & Roizman, 2007).

#### **1.2.5 L-particles**

L-particles resemble virions in size and shape, but are simply enveloped tegument structures that lack capsids (Szilágyi & Cunningham, 1991). They have been detected in all alphaherpesviruses examined for their presence and their existence indicates that tegument proteins have an intrinsic ability to self-assemble in the absence of capsids (McLauchlan & Rixon, 1992). L-particles are formed in productive infections and in instances where virus assembly is blocked and can be easily purified (Rixon et al., 1992). Since they have an envelope, L-particles retain the capacity to penetrate cells and have proved to be a useful experimental tool for analysing the viral constituents of the tegument. Their existence in nature has been hypothesised to facilitate HSV-1 infections, for example, by acting as decoys during the host's immune response, by complementing partially defective co-infecting virions, or by enhancing reactivation of latent virus (Dargan et al., 1995, McLauchlan et al., 1992).

Gene	Protein	Function of protein
UL1	gL	Interacts with gH and is required for membrane fusion and viral entry.
UL10	gM	Forms a complex with UL49A and is present in cellular and virion membranes. It is thought to be involved in secondary envelopment.
UL22	gH	Interacts with gL and is required for membrane fusion and viral entry. It is also thought to play a role during egress and cell-to-cell spread.
UL27	gB	Forms dimers and is required for membrane fusion and the initial attachment of the virus via heparan sulphate.
UL44	gC	Involved in the initial attachment of the virus to the cell membrane via heparan sulphate.
UL53	gK	Involved in cell fusion and required for efficient virus exocytosis.
US4	gG	Involved in egress and cell-to-cell spread.
US5	gJ	Non-essential for virus replication in cell culture.
US6	gD	Involved in cell receptor binding, cell fusion and viral entry.
US7	gL	Involved in the acquisition of the viral envelope during secondary envelopment and forms a complex with gE.
US8	gE	Involved in the acquisition of the viral envelope during secondary envelopment and forms a complex with gL.

**Table 1.3 HSV-1 glycoproteins**

## 1.3 HSV-1 replication

Productive infection by HSV-1 can be divided into several stages, which are described below and are summarised in Figure 1.10. In permissive tissue culture cells, from initial infection to the release of infectious progeny, HSV-1 replication takes approximately 18-20 h.

### 1.3.1 Entry

#### 1.3.1.1 Cell binding and fusion

HSV-1 can enter cells in two ways. The primary pathway involves fusion of the envelope with the plasma membrane and transport of released capsids to the nuclear pore. The secondary pathway involves endocytosis of the enveloped capsid and although this auxiliary pathway has been defined experimentally in a few cell lines, its role in natural infections is unclear (Roizman et al., 2007). However, both routes of entry share an initial and reversible attachment of the virion to the cell surface that is mediated by the viral glycoproteins. HSV-1 first attaches to the cells by the interaction of gC, and to a lesser extent gB, to cell-surface glycosaminoglycans (GAGs) such as heparan sulphate (Herold et al., 1991, Shieh et al., 1992, WuDunn & Spear, 1989). HSV-1 gD then binds to specific cell receptors to stabilise the virion-cell interaction. At least three different types of receptors have been identified. These are nectins, herpes virus entry mediator (HVEM), and a selected form of 3-O-sulphated heparan sulphate, none of which act as co-receptors during entry. Finally, gD together with gB, gH and gL, enable the viral envelope to fuse with the cellular plasma membrane to allow penetration of the viral capsid and tegument into the cell (Cai et al., 1988, Campadelli-Fiume et al., 2000, Forrester et al., 1991, Ligas & Johnson, 1988, Spear & Longnecker, 2003, Turner et al., 1998). Binding and fusion appear to be distinct events, since binding has been demonstrated to be reversible and viruses eluted from the cell surface are still infectious (Bender et al., 2005).

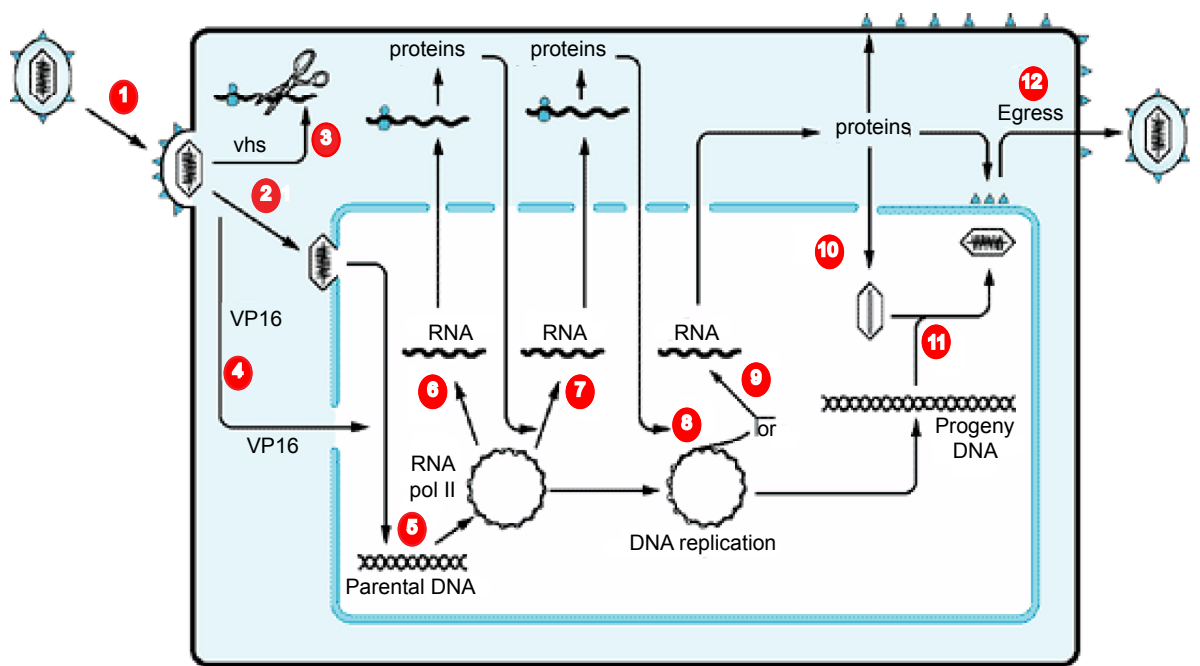


**Figure 1.10 Lytic replication cycle of HSV-1**

(1) The virion binds to the host cell membrane via specific interactions between the viral glycoproteins and the plasma membrane. The viral envelope then fuses with the host cell membrane releasing the capsid and tegument proteins into the cytoplasm. (2) The capsid containing the inner tegument proteins is transported via microtubules to the nucleus where the capsid binds to the nuclear pore complex and releases the viral DNA into the nuclear compartment. (3) The outer tegument is released into the cytoplasm and virion host shut-off (vhs) protein causes degradation of host messenger RNA (mRNA). (4) Another component of the outer tegument, VP16, localises to the nucleus where it activates HSV-1 gene expression and where viral genes are expressed in a tightly regulated cascade. (5) Viral DNA circularises in the nucleus prior to replication and gene expression. (6) The viral DNA is transcribed by host RNA polymerase II to give first the IE gene transcripts ( $\alpha$  mRNA), a process which is stimulated by VP16. The viral mRNAs are exported to the cytoplasm for translation on cellular ribosomes and five of the six IE or  $\alpha$  proteins act to regulate viral gene expression in the nucleus. (7) The IE proteins transactivate the E ( $\beta$ ) gene products. (8) The E proteins are involved in replicating the viral DNA molecule, with the vast majority of progeny DNA genomes forming concatemers. (9) Viral DNA synthesis stimulates L ( $\gamma$ ) gene expression. (10) The L proteins are mainly structural proteins involved in assembling the procapsid in the nucleus. (11) The concatemeric progeny DNA is cleaved into monomeric unit-length genomes that are packaged into the preformed procapsids. During DNA encapsidation the procapsid undergoes extensive conformational remodelling to form the mature angularised DNA-containing C-capsid. (12) The C-capsid exits the nucleus by budding into the perinuclear space and then fuses with the outer nuclear membrane and is released into the cytoplasm. Tegument is assembled around the capsid and is initiated by an interaction of the UL36 protein with the capsid vertices. The tegumented capsids subsequently acquire an envelope by budding into the trans-golgi network, a process that involves the interaction of the tegument with the cytoplasmic tails of the viral glycoproteins gD, gE/gI and gM. The enveloped virion finally exits the cell via the secretory pathway, a stage that is thought to involve the viral glycoprotein gK (adapted from Roizman et al., 2007).

### 1.3.1.2 Capsid translocation to the nucleus

Following penetration, the outer layer of tegument proteins quickly dissociates from the capsid and the tegument proteins involved in host-cell management are transported to the appropriate cellular compartments (Luxton et al., 2005). Vhs localises in the cytoplasm, while VP16 makes its way to the nucleus independently of the capsid (Batterson & Roizman, 1983, Taddeo et al., 2006). The capsid, containing the residual inner layer of tegument proteins comprising pUL36 and pUL37, is transported along microtubules from the periphery of the cell to the nuclear pore complex (NPC). This process is mediated by an interaction between as yet unknown capsid-associated protein and the cellular motor protein dynein, together with the co-factor dynactin (Dohner et al., 2002, Sodeik et al., 1997). Sodeik et al. (1997) reported that the microtubules interact with the pentons on incoming capsids. Several HSV-1 proteins have been proposed as the interaction sites for dynein, but the prime candidates are likely to be the inner tegument or outer capsid proteins. Strong contenders are the large tegument protein, pUL36 and the minor capsid protein encoded by UL25 (pUL25) that is located on the external shell (Newcomb et al., 2006, Thurlow et al., 2006, Trus et al., 2007). In PrV, pUL36, pUL37 and pUL25 remain linked with the capsid during its transport across the cytoplasm to the NPC (Granzow et al., 2005, Kaelin et al., 2000, Luxton et al., 2005).

Once the capsid arrives at the nucleus it docks at the NPC. The component proteins of the NPC are termed nucleoporins and these multiprotein structures selectively control the passage of material through the nuclear envelope (reviewed in Lim & Fahrenkrog, 2006). The first evidence that virus DNA is uncoated at the nuclear pores came from studies with a temperature-sensitive (*ts*) mutant of UL36, *tsB7*. At the non-permissive temperature (NPT), cells infected with *tsB7* accumulate capsids containing DNA at the NPC. When the infected cells are shifted to the permissive temperature (PT), DNA is released from the capsids and virus gene expression follows (Batterson et al., 1983, Knipe et al., 1981). Subsequently, proteolytic cleavage of pUL36 has been demonstrated to be required for release of the HSV-1 DNA into the nucleus (Jovasevic et al., 2008). A second HSV-1 *ts* mutant, *ts1249*, which has a mutation in the essential DNA packaging gene UL25, has a phenotype similar to that of *tsB7*, suggesting that pUL25 is required for uncoating the genome

(Preston et al., 2008). Recently, Pasdouloup et al. (2009) identified the nucleoporin CAN/Nup214 as the nuclear receptor for incoming HSV-1 capsids in infected cells and showed, using an immunoprecipitation assay, that pUL25 interacted directly with the protein. In addition, they demonstrated binding of pUL25 to the large tegument protein pUL36 and the portal protein pUL6, both of which have key roles in virus DNA release (Batterson et al., 1983, Jovasevic et al., 2008, Newcomb et al., 2007). Taken together these results suggest that pUL25 is the interface on the capsid that binds incoming capsids to the NPC and triggers the release of virus DNA into the nucleus. It is in the infected cell nucleus that HSV-1 gene expression, DNA replication, capsid assembly, DNA packaging and egress takes place (Shahin et al., 2006, Strang & Stow, 2005, Strang & Stow, 2007).

### **1.3.2 Gene expression**

Upon entering the nucleus the linear HSV-1 genome rapidly circularises with the help of cellular factors and virus gene expression is initiated. During the lytic cycle of infection a molecular hallmark of herpesviruses is the temporally ordered sequence of RNA polymerase II-directed gene transcription (reviewed in Roizman et al., 2007). The virus genes can be divided into three classes, named immediate early (IE or  $\alpha$ ), early (E or  $\beta$ ) and late (L or  $\gamma$ ), depending on their pattern of transcription. Although the precise kinetics of viral gene expression is dependent on the cell type infected and the MOI, in general the initiation of expression of the IE genes starts approximately 30 minutes post-infection (hpi) at 37°C. The IE proteins produced are responsible for propelling the transcription cascade forward by activating expression of the next set of virus genes. There are six IE proteins, designated ICP0, ICP4, ICP22, ICP27, ICP47 and US1.5. The ICP0, ICP4, ICP22 and ICP27 products each play important regulatory roles in viral gene expression of E and L gene products, but IE proteins are also involved in modulating the host antiviral defence system or exploiting the cell's machinery for productive virus infection. Transcription of IE genes does not require prior viral protein synthesis, since their promoters are recognised by host transcription factors and RNA polymerase II. The HSV-1 protein VP16, however, has an important role in expression of IE genes following its interaction with two host cell proteins. On its release from the incoming capsids, VP16 binds to a

cellular protein called host cell factor (HCF) and is transported to the nucleus. Within the infected cell nucleus, the VP16-HCF complex binds to a cellular transcription factor, Oct-1 (octamer DNA-binding protein), and the stable interaction of VP16 with Oct-1 promotes Oct-1 binding to viral DNA (Hughes et al., 1999). Oct-1 binds to the octamer core sequence present in the promoters of all IE genes, while VP16 binds to Oct-1 and the adjacent HSV-1 sequences, forming an activator complex (Gaffney et al., 1985, O'Hare et al., 1988). ICP0 is a transcriptional activator that stimulates viral gene expression and viral infection, which has been proposed to be involved in controlling the balance between lytic and latent HSV-1 infection, such that in its absence the latent state is favoured (Hagglund & Roizman, 2004, Preston & Nicholl, 1997, Samaniego et al., 1998). There is accumulating evidence to suggest that blocks the infected cell's repression of viral transcription by disrupting nuclear substructures known as ND10 domains. The disruption of ND10 sites during HSV-1 infection is caused by the  $\gamma$ -induced degradation of cellular proteins, which are important components of ND10 sites, by interacting with the ubiquitin-proteasome pathway (Everett et al., 2007, Everett et al., 2006).

Expression of the E genes requires the IE transactivator, ICP4, and in its absence the synthesis of E and L virus gene transcripts is blocked (DeLuca et al., 1985). The mechanism that ICP4 uses to activate E and L gene transcription is unclear, although it does contain a DNA binding site that is essential for its transactivation function (DeLuca & Schaffer, 1988). In addition, evidence suggests it functions by enhancing the assembly of transcription complexes onto the viral promoters (Grondin & DeLuca, 2000). If unrestrained, IE transcription would be expected to compete with E gene expression during viral replication and overwhelm the initiation of E mRNA translation. Three mechanisms are thought to play a role in shutting off of IE gene expression. First, ICP4 represses its own transcription by binding to specific sequences located across its own transcription initiation site (Faber & Wilcox, 1986). Second, during the productive infection, E gene products down-regulate IE expression, and finally, one of the functions of vhs is to synchronise sequential viral gene expression.

Expression of E genes reaches a peak at approximately 4-8 hpi and the products generated are required during DNA replication and nucleotide metabolism. Two groups of E proteins,  $\beta_1$  and  $\beta_2$ , have been identified. The  $\beta_1$  proteins are

expressed a short time after the onset of IE protein synthesis, while the  $\beta_2$  proteins are transcribed later and include DNA polymerase. Since the  $\beta_2$  proteins require ICP27 for their activation, this may explain their expression kinetics (McCarthy et al., 1989). ICP27 is a multifunctional IE regulatory protein that not only initiates viral gene expression but also represses it in the presence of ICP4 (Panagiotidis et al., 1997). In addition, it contributes to the shut-off of host protein synthesis during productive infection by preventing mRNA splicing of host gene transcripts and has a role in promoting nuclear export of viral mRNA (reviewed in Roizman et al., 2007).

L genes are also activated by IE proteins, but it is only after DNA replication that their expression reaches its peak at approximately 8-10 hpi, with their gene products being required for virion assembly, DNA packaging and egress. Similar to E genes, the L genes can be divided into two groups termed  $\gamma_1$  (leaky/late) and  $\gamma_2$  (true late) genes. The  $\gamma_1$  proteins are expressed prior to viral DNA synthesis, while the onset of viral DNA replication is required prior to the expression of the proteins encoded by the true late genes. The ultimate goal of L gene expression is to express large amounts of structural proteins for the assembly of progeny viral particles. The relatively abundant major capsid protein, VP5, is a product of both  $\gamma_1$  and  $\gamma_2$  L gene transcripts during infection, while the tegument protein pUL36 is expressed by a true late gene (Roizman et al., 2007).

### 1.3.3 DNA replication

DNA replication initiates on the circular viral DNA molecules that accumulate in the infected cell nucleus in specialised structures known as replication compartments, which are located next to sub-nuclear structures termed ND10 domains (Qinlan et al., 1984). New ND10 domains also assemble around incoming viral genomes and these are thought to play an essential part in the cell's defence mechanism against viral infection (Everett, 2006, Everett & Murray, 2005, Everett et al., 2006). However, as infection progresses the ND10 structures are degraded by a mechanism involving the IE viral protein . In addition to the E gene products required during DNA synthesis, replication compartments also contain the HSV-1 proteins necessary for capsid assembly and

DNA packaging and as a consequence are thought to be the sites of viral DNA cleavage and encapsidation (de Bruyn Kops et al., 1998, Lamberti & Weller, 1998).

Herpesvirus genomes contain three origins of replication that consist of two copies of *oriS*, located in the IR<sub>S</sub> and TR<sub>S</sub> regions of the viral genome, and one *oriL* that is situated in the centre of the U<sub>L</sub> region. The apparent reason(s) for these three potential origins of replication in the viral genome is currently unclear, since mutant viruses lacking *oriL* or both copies of *oriS* are still viable (Polvino-Bodnar et al., 1987, Roizman et al., 2007). In addition to the cis-acting origins of replication, seven trans-acting proteins are required during viral DNA replication. Three of these proteins, encoded by UL5, UL8 and UL52, are components of the heterotrimeric helicase-primase complex. Two of the proteins form a heterodimeric DNA polymerase complex, comprising the catalytic subunit encoded by UL30 and its processivity factor encoded by UL42. The remaining two trans-acting replication proteins are the single-stranded DNA binding protein expressed by UL29, also referred to as ICP8, and the origin-binding protein encoded by UL9 (pUL9).

A model based on the current information available for HSV-1 DNA replication has been proposed and is illustrated in Figure 1.11. After the viral DNA molecules have entered the cell nucleus, the circular genomes generated serve as templates for DNA synthesis. Binding of pUL9 in association with ICP8 to the origin sequences initiates the preliminary theta (bi-directional) mode of replication that quickly switches to a sigma or rolling-circle form by an unknown mechanism. Evidence that replication is initially bi-directional comes from observations that viral DNA accumulates with nonlinear kinetics during early DNA synthesis and that cellular topoisomerase II is also required at this stage, suggesting a need for decatenation of circular progeny molecules (Hammarsten et al., 1996). Following binding, the ATP-dependent helicase activity of pUL9 is stimulated by its interaction with ICP8, inducing a distortion in the DNA and the formation of a single-stranded stem loop structure that is subsequently coated with ICP8. Separation of the two DNA strands then permits access of the helicase-primase complex, which is recruited to the origin by its interaction with pUL9, ICP8 or both, and the DNA polymerase complex to establish a replication

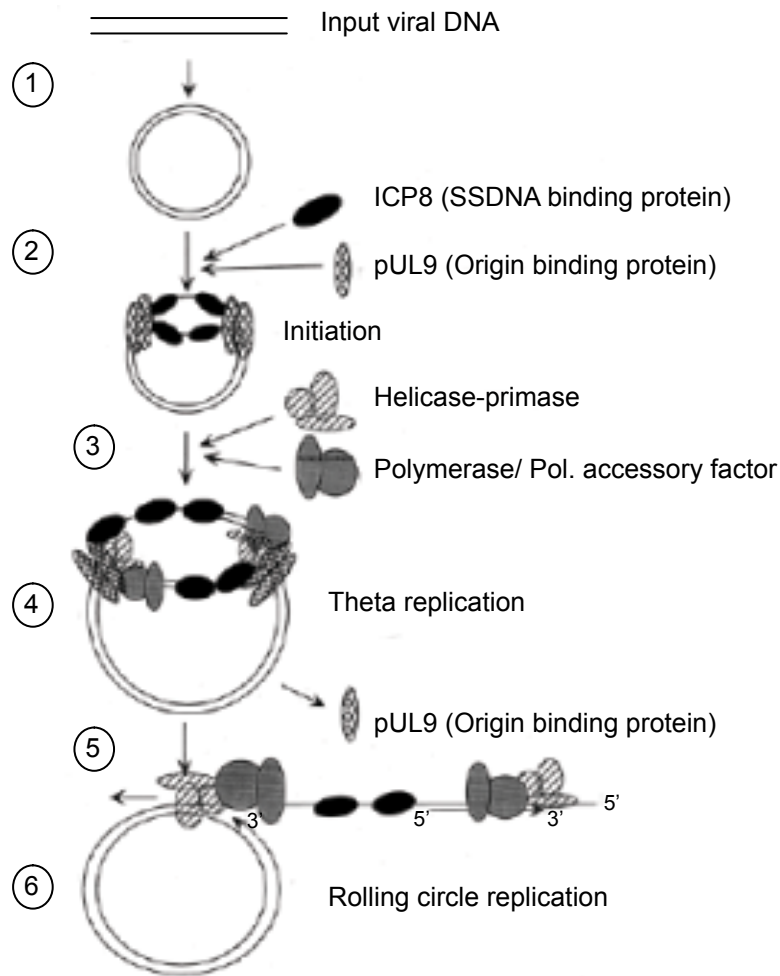


**Figure 1.11 Model for HSV-1 DNA replication**

(1) Input DNA is circularised on entry into the nucleus. (2) pUL9, the origin binding protein, initially binds to specific elements in the origin (either *oriL* or *oriS*) and begins to unwind the DNA. pUL9 then recruits ICP8, the ssDNA binding protein, to the unwound ssDNA. (3) pUL9 and ICP8 recruit the five remaining viral DNA replication proteins to the replication fork. (4) The helicase-primase proteins and the viral polymerase complex assemble at each replication fork for initial rounds of theta form replication. (5) Replication switches to the rolling circle mode by an unknown mechanism. pUL9 is not necessary for rolling circle replication, because this process is origin independent. (6) Rolling circle DNA replication produces long head-to-tail concatemers of viral DNA, which are the substrates for DNA cleavage and packaging (adapted from Roizman et al., 2007).

fork (reviewed in Lehman & Boehmer, 1999 and Roizman et al., 2007). However, once DNA replication is initiated the origin binding protein is no longer required (Schildgen et al., 2005). The origin-dependent theta replication switches to an origin-independent rolling-circle and/or recombination-mediated replication mechanism that produces progeny DNA in the form of head-to-tail concatemers (Jacob et al., 1979).

### **1.3.4 Capsid assembly**

A feature of herpesviruses is that DNA replication, capsid assembly and DNA encapsidation all occur in the nucleus of the infected cell. Therefore, prior to capsid assembly the structural and scaffolding proteins that are translated in the cytoplasm must be transported to the nucleus. However, only VP19C and preVP22a can localise to the nucleus independently, which suggests that these proteins contain a nuclear localisation signal (NLS). The other structural proteins, VP5, VP23 and VP26, are transported to the nuclear compartment via direct or indirect interactions with either or both VP19C and preVP22a (Desai & Person, 1996, Nicholson et al., 1994, Rixon et al., 1996). The distribution of the capsid proteins in the nucleus during virus infection has been studied using confocal microscopy techniques (de Bruyn Kops et al., 1998, Ward et al., 1996). This has revealed that capsid proteins accumulate at punctate foci within nucleus known as replication compartments.

A possible common ancestry between herpesviruses and dsDNA bacteriophages, such as T4, P22 and  $\lambda$ , has been revealed by similarities in their capsid structure and in the way capsids are formed (Baker et al., 2005, Booy et al., 1991, Davison, 1992, Trus et al., 2004). Since the process of capsid assembly and DNA encapsidation has been extensively studied and is well defined in the large dsDNA bacteriophages (Baker et al., 2005, Hendrix, 2005, Johnson & Chiu, 2007, Rixon, 2008, Steven et al., 2005), this information has provided a framework for studying these processes in HSV-1. In its basic features the pathway for capsid assembly and DNA packaging in HSV-1 resembles that in the large dsDNA bacteriophage. In both systems the capsid proteins and internal scaffolding proteins co-assemble to form a spherical and mechanically fragile intermediate empty shell, termed the procapsid. Following DNA replication, the

concatemeric viral DNA molecules formed are cleaved into unit-length genomes. The sequence of events that yield progeny virions proceeds through the overlapping events of capsid maturation, DNA packaging and the release of cleaved scaffolding proteins from the maturing capsid. The procapsid is the key site of maturation and its surface shell undergoes a morphological transition into the mature capsid, which stabilises the particle and enables it to withstand the increasingly high pressure that is imposed on it as the viral genome is inserted during encapsidation.

#### **1.3.4.1 Procapsid assembly**

An understanding of the mechanism of how the structural and scaffolding components of the capsid assemble advanced significantly with the development of the baculovirus expression system. Baculoviruses naturally infect arthropods and baculovirus vectors that express foreign genes at high levels in cultured insect cells, such as *Spodoptera frugiperda* (Sf cells) have been developed. By analysing the structures formed in Sf cells infected with various combinations of baculoviruses expressing the capsid shell proteins and the products of the scaffolding genes, the essential viral proteins required during capsid assembly were identified (Tatman et al., 1994, Thomsen et al., 1994). Closed icosahedral capsids were detected in insect cells co-infected with baculoviruses expressing the capsid shell proteins VP5, VP19C, VP23 and the scaffolding proteins encoded by either UL26 or UL26.5. These experiments revealed that the expression of UL35 (encoding VP26) was not essential for capsid formation. Omission of the UL26 gene product from the system resulted in a high number closed icosahedral capsids with large internal cores, due to the presence of intact preVP22a, which was not cleaved in the absence of the maturational protease. In cells expressing preVP22a alone, a large number of core-like structures formed indicating that this scaffolding protein could self-assemble in the absence of other capsid proteins, a property not observed when preVP21 was expressed on its own (Preston et al., 1994). In the absence of preVP22a, fewer capsids were detected in the baculovirus expression system and no distinct core was apparent. Nevertheless, in mammalian cells infected with an HSV-1 mutant that did not express preVP22a, infectious virions were still produced but at significantly reduced yields relative to the wt virus (Gao et al., 1994). These results suggested that although the UL26 polypeptide could still serve as a scaffold

during capsid formation, it formed a less effective one than those containing preVP22a. However, no intact capsids were formed when both UL26 and UL26.5 gene products were absent, indicating that the presence of a scaffolding protein was required for the assembly of a closed icosahedral capsid (Gao et al., 1994, Preston et al., 1994, Tatman et al., 1994, Thomsen et al., 1994).

The baculovirus expression system and analysis of the capsid protein interactions from recombinant baculovirus-infected cell extracts led to the development of an *in vitro* based model for capsid assembly (Desai & Person, 1996, Newcomb et al., 1999, Newcomb et al., 1994, Preston, 2002, Rixon et al., 1996). In the *in vitro* system, closed angularised icosahedral capsids formed in samples of mixed cell extracts containing capsid shell proteins and the scaffolding proteins incubated at 27°C for 12 h (Newcomb et al., 1994). The requirements for cell-free assembly, in terms of input viral gene products, were the same as for assembly in insect cells co-infected with multiple baculovirus vectors expressing HSV-1 structural proteins. Optimal assembly required the major capsid protein, the triplex proteins and the major scaffolding protein. By immunoprecipitating the complexes formed in the *in vitro* assembly reaction mixtures and analysing them under the electron microscope, several intermediate capsid forms were identified (Newcomb et al., 1996). During progressively longer periods of incubation, partial capsids, followed by closed spherical capsids, termed procapsids, and finally angularised icosahedral capsids were observed. While the various capsid structures all contained VP5, VP19C, VP23 and the scaffolding proteins preVP22a and VP21, procapsids were found to be more labile at low temperatures than the angular capsids formed. In addition, upon continued incubation of purified procapsids *in vitro* they underwent an energy-independent conformational change and spontaneously formed angularised capsids. These observations, which were consistent with the prohead maturation events reported in dsDNA bacteriophages, led Newcomb et al. (1996) to propose a model for HSV-1 capsid assembly. The capsid assembly model is illustrated in Figure 1.12 and begins with formation of the partial capsid that consists of angular segments of the closed structure, and then proceeds through the more fragile and closed spherical procapsid intermediate to the stable and mature icosahedral capsid.

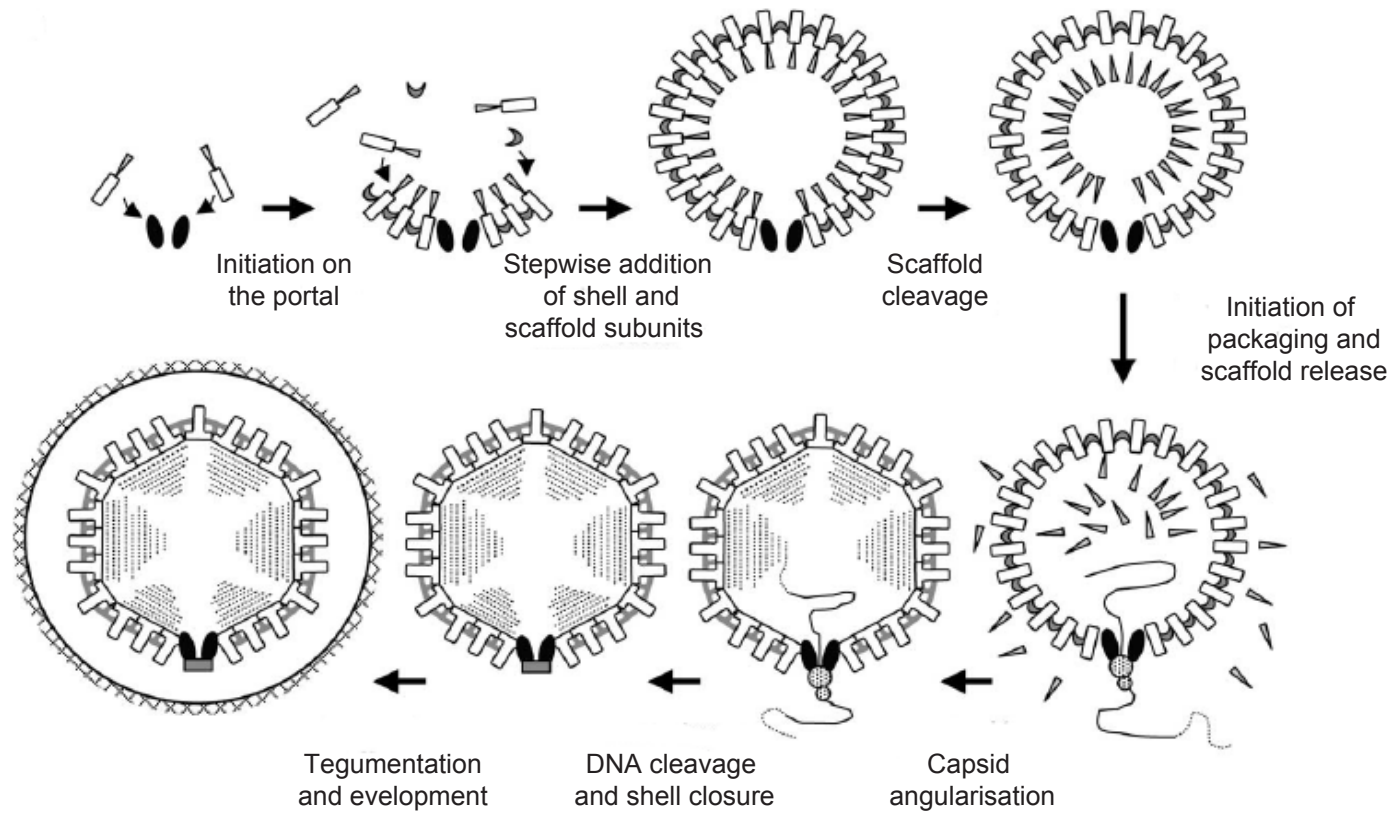


**Figure 1.12 Model for HS-1 capsid assembly**

The major events in HSV-1 viral assembly are illustrated and show the relationship between capsid assembly, maturation and DNA packaging. The open boxes represent the major capsid protein (VP5) that makes up the hexons and pentons, the triplexes are denoted by crescents and the scaffolding proteins by triangles. Similar to bacteriophage systems, HSV-1 capsids contain a portal vertex, which is known to associate with scaffold. These observations have prompted the suggestion that the capsid assembly in HSV-1 is initiated through an interaction between the portal complex and the major scaffolding protein, UL26.5 (Newcomb et al., 2003). Although not precisely defined, the cleavage and release of the scaffolding proteins is concomitant with DNA packaging. On completion of DNA encapsidation the portal channel is sealed by an unknown mechanism, followed by the final stages of viral assembly (adapted from Rixon and Chiu, 2003).

### 1.3.4.2 Procapsid structure and maturation

The procapsids identified in the cell free capsid assembly system were confirmed as intermediates in HSV-1 capsid assembly by characterising capsids formed in cells infected with the HSV-1 temperature-sensitive (ts) protease mutant, ts1201 (Rixon & McNab, 1999). Cryo-EM analysis and image reconstruction techniques showed that procapsids were spherical with a T=16 icosahedral symmetry and had a looser architecture than the more angularised mature HSV-1 capsid (Figure 1.13) (Heymann et al., 2003, Newcomb et al., 1999, Newcomb et al., 2000, Trus et al., 1996). In the procapsid there is little interaction between the neighbouring VP5 hexon and penton subunits, with contact between the capsomers being coordinated exclusively by the surrounding triplexes. Within a given capsomer the main intersubunit contacts take place in the innermost layer of the capsid cavity, where the VP5 subunit floor domains form rings. The result is that the trans-hexonal channel, which is a small circular opening in the mature capsid, is considerably wider in the procapsid. The more porous and fragile architecture of the procapsid is a consequence of this loose association between its components (Newcomb et al., 1996, Newcomb et al., 2000). As the procapsid matures, the conformational changes that take place results in enhanced interactions between the floor domains of neighbouring capsomers. These contacts are reinforced by the triplexes, which transform into molecular clamps overlying the trigonal points at which three capsomers come together in the floor domains. In addition, the highly asymmetric hexons present in the procapsid are transformed into the symmetric configurations detected in the mature capsid (Heymann et al., 2003). The precise kinetics of capsid maturation *in vivo* is unknown, but thin sections of infected cells do not reveal procapsids except when the protease is inactivated, implying that they mature shortly after assembly (Rixon et al., 1988).

Capsid maturation overlaps with viral DNA packaging and is initiated by the protease clipping the terminal peptide at the M site in the assembled scaffolding proteins, disrupting their interaction with the outer shell (Section 1.2.2.3). The successful end product of procapsid maturation is the mature angularised nucleocapsid, which has lost its internal scaffold and contains a viral genome. Although the link between DNA packaging and loss of the scaffold has been shown, the prompt that initiates scaffold cleavage and expulsion is still unclear

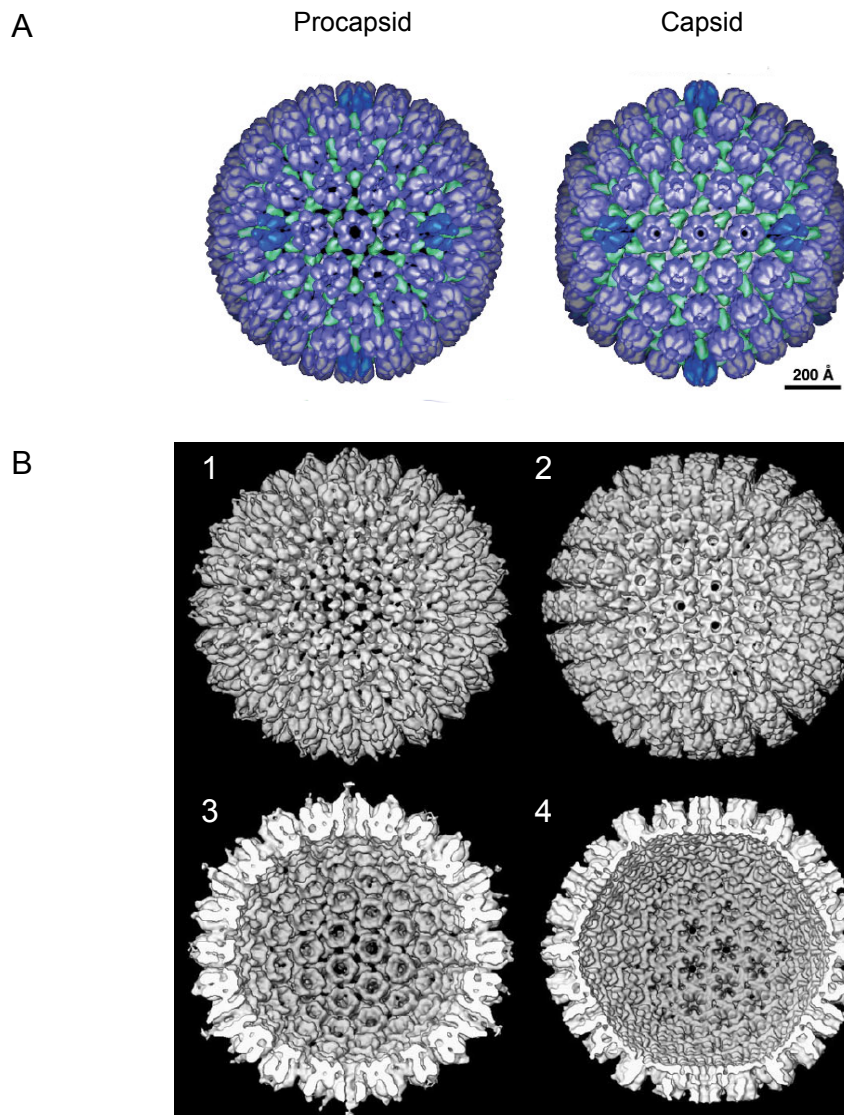


**Figure 1.13 Comparison of the HSV-1 procapsid and capsid**

(A) The colour illustration show the difference in shape between the spherical procapsid and the more angularised capsid. The capsomers are highlighted in blue and the triplexes in green. (B) Outside (1 and 2) and inside (3 and 4) views of reconstructions of the HSV-1 procapsid (1 and 3) and capsid (2 and 4). All views are shown looking along a 3-fold icosahedral axis. The procapsid retains some icosahedral symmetry, which is apparent by the hexagonal arrangement of the capsomers seen in the internal view (3). The procapsid subunits are less clearly defined than those of the capsid. In addition, the contacts between the individual subunits are looser and the continuous floor is absent, since there is no contact at the bases of the capsomers in the procapsid.

(Church & Wilson, 1997, Dasgupta & Wilson, 1999, Preston et al., 1983, Rixon & McNab, 1999). In bacteriophage systems the transformation from procapsid to mature capsid is promoted by the electrostatic repulsive forces exerted by packaged DNA on the inner capsid surface (Conway et al., 2001). In the HSV-1 system, it has been suggested that these forces alter the ionic environment within the capsid cavity, triggering the dissociation of the scaffold from the shell (McClelland et al., 2002). In addition, the physical force exerted on the capsid shell as more DNA is packaged during encapsidation would be expected to facilitate changes in procapsid maturation.

### 1.3.5 DNA encapsidation

DNA encapsidation requires two linked events, cleavage of the replicated head-to-tail concatemeric viral DNA into unit-length genomes and packaging of these DNA molecules into capsids (Ladin et al., 1980, Ladin et al., 1982). As well as the maturational protease, seven *trans*-acting virus-encoded proteins, UL6, UL15, UL17, UL25, UL28, UL32 and UL33 are essential during the process (reviewed in Baines & Weller, 2005). When cells are infected with HSV-1 mutants lacking the function of any of these genes, apart from UL25, capsid formation and DNA replication takes place, but no DNA packaging occurs. By analogy to the extensively studied bacteriophage system, it is presumed that HSV-1 encodes a multicomponent enzyme, the terminase, which links the DNA to the procapsid and cleaves the DNA precisely into unit-length genomes. After the initial cleavage of the concatemeric viral DNA, the cleaved DNA is inserted through the unique vertex, or portal, and is driven into the maturing capsid by the terminase complex and ATP hydrolysis, with concomitant loss of the internal scaffold. A second cleavage event occurs to release a monomeric viral genome that is stably encapsidated as a consequence of the interaction of viral gene products with the maturing capsid, resulting in the successful production of the precursor of the infectious virion (reviewed in Baines & Weller, 2005).

#### 1.3.5.1 Cleavage and packaging signals

In addition to the essential *trans*-acting viral proteins that direct the site-specific DNA cleavage and packaging process, *cis*-acting viral DNA sequences termed Pac1 and Pac2 are also involved and have been mapped to the *U<sub>b</sub>* and *U<sub>c</sub>*

domains of the *a* sequences, respectively (Varmuza & Smiley, 1985). In various herpesvirus strains the sequences within the *a* region consist of a series of direct repeat units (DR) and unique regions (Uc or Ub), arranged as DR1-Uc-DR4<sub>m</sub>-DR2<sub>n</sub>-Ub-DR1, where *m* and *n* designate variable numbers of repeats (Figure 1.14). The size of these components and the type of direct repeat units (DR1, DR2 or DR4) present can vary between strains, but are thought to be consistent within a strain. In HSV-1 strain 17 syn<sup>+</sup> the *a* sequence encompasses a region of approximately 400 base pairs (bp) in length, containing only the DR1 and DR2 direct repeat units (Figure 1.14). A single *a* sequence is flanked by DR1, while junctions containing more than one *a* sequence share a single intervening DR1 (Davison & Wilkie, 1981, Mocarski & Roizman, 1981, Mocarski & Roizman, 1982). Lying internally to the DR1 repeats are two unique regions, Ub and Uc, which contain highly conserved packaging elements termed Pac1 and Pac2, respectively (Deiss et al., 1986, Nasserri & Mocarski, 1988).

Upon entry, the linear viral genomes fuse at their terminal sequences and generate the circular DNA molecules that are the substrate for viral DNA replication. Fusion at the terminal *a* sequences creates a Uc-DR1-Ub junction (Figure 1.14) that has been demonstrated to be the minimal packaging signal required during DNA encapsidation (Hodge & Stow, 2001, Nasserri & Mocarski, 1988, Stow, 2001). Cleavage of the concatemeric viral DNA occurs within the DR1 repeat, although the actual sequence of DR1 is not important. The cleaved concatemeric end consists of a truncated DR1 with 18 of its 20 bp plus a single-nucleotide 3' overhang and in HSV-1 strain 17 syn<sup>+</sup> this is followed by Uc (Pac2), DR2, Ub (Pac1), DR1 and U<sub>L</sub> sequences (Mocarski & Roizman, 1982). After association of the cleaved DNA termini with the capsid portal the viral genome is inserted into the capsid shell in the direction of the U<sub>L</sub> to U<sub>S</sub> region. The second cleavage is dependent on the Pac1 motif and occurs in such a way that the DNA being packaged is terminated by a single bp of DR1 with a 3' nucleotide overhang. Consequently, the terminus of the unpackaged cleaved concatemeric DNA is identical to the terminus generated following the first cleavage event and as a result would be expected to initiate the next round of DNA packaging (Stow, 2001).

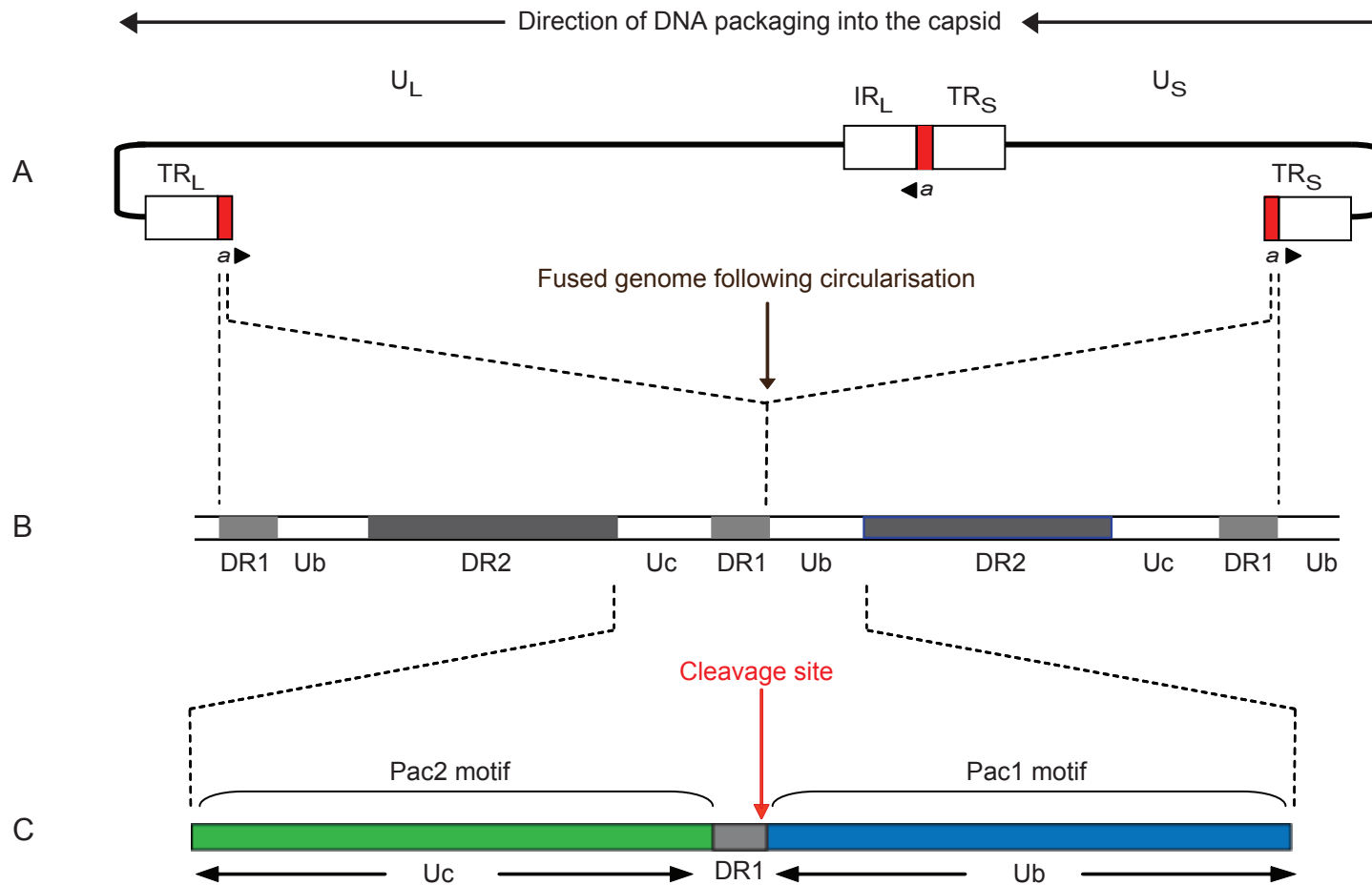


**Figure 1.14 HSV-1 genome and structure of the a sequences**

(A) The positions of the a sequences in the HSV-1 genome are highlighted in red and their relative orientations are indicated by the arrowheads. For simplicity only a single a sequence is shown at the L terminus and L/S junction. (B) Generation of the minimal cleavage/packaging signal Uc-DR1-Ub upon fusion of a sequences. (C) The cleavage site in concatemeric DNA is situated close to one end of the DR1 sequence as indicated.

### 1.3.5.2 Components of the packaging machinery

Mutational analysis of the seven essential packaging genes, UL6, UL15, UL17, UL25, UL28, UL32 and UL33, provided evidence that, although DNA cleavage and DNA packaging were linked, they were distinct events in the process of DNA encapsidation. In cells infected with null mutants of UL6, UL15, UL17, UL28, UL32 or UL33 the concatemeric DNA produced is neither cleaved or packaged into capsids, resulting in an accumulation of B-capsids that contain processed scaffolding proteins (Lamberti & Weller, 1996, Lamberti & Weller, 1998, Patel et al., 1996, Reynolds et al., 2000, Salmon & Baines, 1998, Yu et al., 1997). In contrast in cells infected with a UL25 null mutant, DNA cleavage occurs and DNA packaging is initiated but less than unit-length viral genomes are stably encapsidated and there is an overrepresentation of empty A-capsids (Stow, 2001).

#### 1.3.5.2.1 *The portal vertex (UL6)*

In the dsDNA bacteriophages, such as  $\Phi$ 29, T4, P22 and epsilon15, the portal complex is located at a unique vertex on the icosahedral capsid shell and consists of a dodecameric ring of portal protein (Chang et al., 2006, Jiang et al., 2006, Lander et al., 2006). Evidence has accumulated that indicates the UL6 gene product (pUL6) forms the portal or channel through which viral DNA is inserted into the capsid and presumably is released during HSV-1 entry. The protein is a component not only of the procapsid, but also of the angularised A-, B- and C-capsid forms and the mature virion, which suggests that pUL6 is an integral part of the capsid shell and its association is unaffected by capsid maturation or DNA packaging (Patel et al., 1996, Sheaffer et al., 2001). Subsequently, immunogold-labelling experiments revealed that HSV-1 pUL6 was present at one of the twelve vertices of B-capsids from HSV-1 infected cells (Newcomb et al., 2001). To determine if pUL6 could actually form ring-like structures that resembled portals, soluble pUL6 was purified from insect cells infected with recombinant baculovirus expressing the protein (Newcomb et al., 2001). The samples were examined by EM and revealed a uniform population of rings with an internal diameter of 5 nm and external diameter of 16.4 nm. The dimensions of the ring-like structures corresponded closely to the diameters

observed of the portal complexes of the dsDNA bacteriophages, which range in size from 14.5 nm - 17.5 nm externally and 2.5 nm - 4.5 nm internally (Bazinet & King, 1985, Valpuesta & Carrascosa, 1994). Further analysis to determine the mass of the individual pUL6 rings using dark-field scanning electron microscopy, revealed a homogenous population with an oligomeric state that equalled 12, the same number determined for bacteriophage dodecameric portal complexes (Bazinet & King, 1985, Valpuesta & Carrascosa, 1994). Similar to the portal proteins of the bacteriophage T4, pUL6 associates with the scaffolding proteins. Newcomb et al. (2005) used an *in vitro* capsid assembly assay to demonstrate that pUL6's interaction with the scaffold protein was essential for incorporation of the portal into the capsid. However, from the data discussed in Section 1.3.4.1 it is clear that capsid assembly can occur in the absence of pUL6. Newcomb et al. (2005) also showed that capsids containing portals only formed when portals were present at the initiation of capsid assembly, any delay in the availability of portals at this stage resulted in the formation of capsids lacking portals.

The mass of a single portal subunit in HSV-1 is 74 kDa, making the entire mass of the portal approximately 888 kDa, which is similar in size to the 747 kDa penton (Newcomb et al., 2001, Zhou et al., 2000). The equivalent size of the vertices has presented a challenge in determining the location and structure of the portal in the HSV-1 capsid using electron microscopy coupled with 3-dimensional (3D) reconstruction. A recent study used electron cryotomography to reveal the organisation of the HSV-1 portal in B-capsids treated with 6 M urea, which does not remove the portal protein but selectively removes proteins associated with the other 11 vertices (Chang et al., 2007). The portal in HSV-1 appears to be organised in a similar manner to those observed in some of the dsDNA bacteriophage capsids, specifically P22 and Epsilon15. In these systems the majority of the portal extends inwards into the interior of the capsid shell, while the remainder of the structure does not extend far but lies predominately flat against the external capsid shell (Figure 1.15). Since the structure is lodged deep within the shell, this may explain the difficulties that have been encountered until recently in detecting the HSV-1 portal.

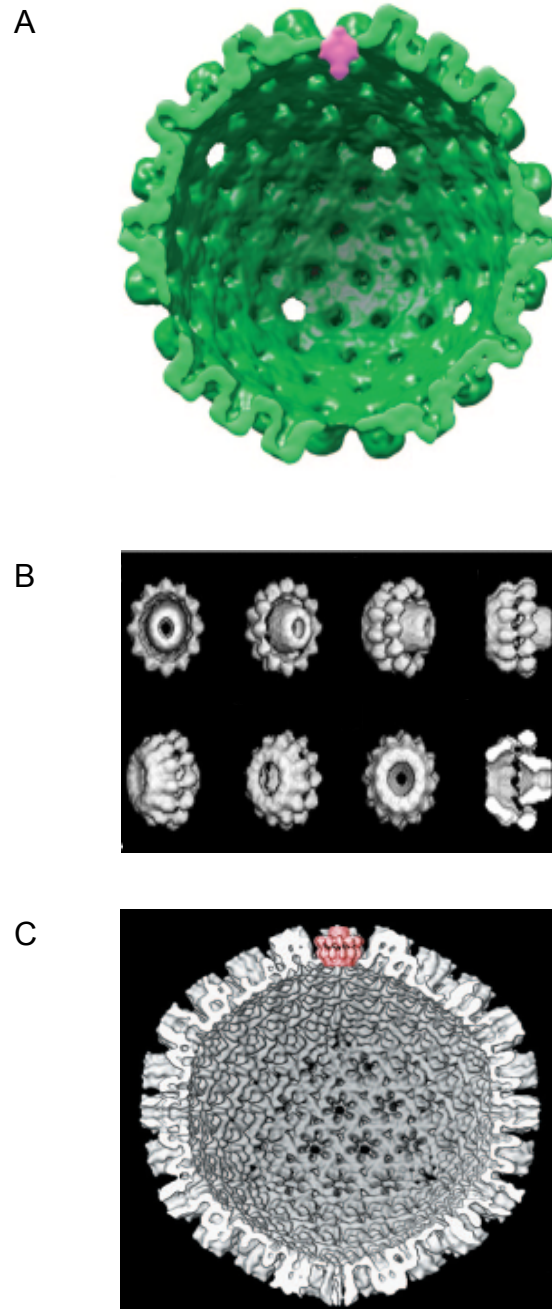


**Figure 1.15 The HSV-1 portal**

(A) The HSV-1 portal structure (magenta) is shown in the context of the icosahedral averaged tomographic map of the capsid shell (green). The density represented by magenta is 14 nm tall and 11 nm wide. (B) Various views of a 3D reconstruction of the 12 mer HSV-1 portal at 16 Å resolution. (C) Interior view of a capsid model at 18 Å resolution. A penton of VP5, the major capsid protein, was computationally excised and replaced by the portal shown in magenta (adapted from Trus et al., 2004 and Chang et al., 2007).

### **1.3.5.2.2 Putative terminase complex (pUL15, pUL28 and pUL33)**

By analogy with the multicomponent terminases of the bacteriophage systems, the HSV-1 terminase would be predicted to specifically recognise DNA ends within the viral genomes, and have the ability to cleave and link these DNA molecules to the capsid at the portal. Since the encapsidation of DNA requires energy, the putative HSV-1 terminase would also be expected to mediate the DNA packaging process by translocating the DNA into the capsid cavity by ATP hydrolysis (Dasgupta & Wilson, 1999). The first indication that the UL15 gene product (pUL15) was involved in DNA packaging and may form part of the HSV-1 terminase complex came from observations that the gene shared sequence homology with the ATP binding motif of the bacteriophage T4 terminase subunit, gp17 (Davison, 1992, Davison et al., 1992). Confirmation that the UL15 gene product was essential during DNA encapsidation was provided by analysis of two UL15 null viruses, in which the UL15 gene was either truncated or replaced by a LacZ insertion (Baines et al., 1997, Yu et al., 1997). These studies revealed that in non-permissive cells infected with the mutant virus, viral DNA cleavage or packaging did not occur. The idea that the UL15 gene product formed the ATPase subunit of the HSV-1 terminase was reinforced when a mutant pUL15, encoding a mutation in the putative ATP binding domain, failed to support DNA encapsidation when expressed in HSV-1 UL15 null mutant-infected non-permissive cells (Yu & Weller, 1998b). More recent evidence that UL15 encodes a terminase function has been provided by mutational analysis of the conserved UL15 sequences shared with the ATPase subunits of phage terminase, which revealed that DNA encapsidation was impaired in cells infected with HSV-1 mutant viruses expressing pUL15 with a point mutation in one of the four conserved regions (Przech et al., 2003). Since the mutated pUL15s associated with capsids localised to replication compartments, these residues are likely to be directly required for cleavage and packaging of viral DNA.

The components of the putative HSV-1 terminase have been identified by protein interaction studies, which have established that pUL15 interacts with two other essential DNA packaging proteins encoded by UL28 (pUL28) and UL33 (pUL33) (Abbotts et al., 2000, Beard et al., 2002, Koslowski et al., 1999, Yu & Weller, 1998b). These observations led to the suggestion that in contrast to the two subunit bacteriophage terminases, the putative HSV-1 terminase is a

heterotrimeric complex of pUL15, pUL28 and pUL33. Direct binding between pUL15 and pUL28 was originally demonstrated when HSV-1 pUL15 was shown to relocate PrV pUL28 to the nucleus when the proteins were transiently expressed together in un-infected cells (Koslowski et al., 1997). A study using co-immunoprecipitation assays subsequently showed pUL33 also formed a complex with pUL15 and pUL28 in virus-infected cells (Beard et al., 2002). A further study using immunoprecipitation assays demonstrated that pUL28 was required for the interaction of pUL15 with pUL33, while the presence of pUL33 enhanced the binding of pUL15 to pUL28 (Yang & Baines, 2006). An indirect interaction between pUL15 and pUL33 was confirmed by co-immunoprecipitation analysis on HSV-1 UL28 null mutant-infected cells (Jacobson et al., 2006). In addition, experiments have revealed that the putative heterotrimeric terminase of HSV-1 was assembled in the cytoplasm of infected cells, and that a nuclear localisation signal present in pUL15 was necessary for the import of the complex into the nucleus (Yang et al., 2007).

A potential terminase complex would be predicted to interact with capsids and indeed components of the putative HSV-1 terminase have been found to associate with the different capsid forms. Both pUL15 and pUL28 have been detected on procapsids, the capsid substrate required during the DNA cleavage and packaging process, and on A-, B- and C-capsids (Sheaffer et al., 2001). In addition, pUL33 has been observed on all three forms of angularised capsid, but its association with capsids is independent of that of pUL15 or pUL28 (Beard & Baines, 2004). Although the location of the pUL15 and pUL28 on the HSV-1 capsid is not known, both proteins have been shown to interact with the UL6 portal protein, an observation that supports the suggestion that pUL15 and pUL28 form part of the terminase complex (White et al., 2003). Studies have shown that as the capsid matures in infected cells, decreasing concentrations of pUL15, pUL28 and pUL33 are detected, suggesting that the putative terminase's association with the capsid may be transient (Beard et al., 2004, Salmon et al., 1998, Sheaffer et al., 2000, Sheaffer et al., 2001, Taus et al., 1998, Yu & Weller, 1998a). Approximately about the time of the first cleavage event during DNA encapsidation, epitopes encoded by the first 35 aa of pUL15 are proteolytically removed (Salmon et al., 1999). Sequence analysis of this portion of UL15 has revealed that it has a potential coiled-coil motif that may mediate protein-

protein interactions, removal of this segment during DNA encapsidation could release the protein and mediate the terminase activity (Baines & Weller, 2005, McGeoch et al., 1988).

An *in vitro* DNA binding activity for the putative pUL28 terminase subunit was suggested, when the purified protein bound to a novel ssDNA structure formed by the HSV-1 DNA Pac1 cleavage signal. In addition, pU28 also bound to the DNA structures induced by the Pac1 motif of HCMV with only slightly less affinity, and mutations in sequence elements within the HCMV Pac1 motif eliminated DNA cleavage and packaging and prevented DNA binding by HSV-1 pUL28 (Adelman et al., 2001). Consequently, it was claimed that this provided indirect evidence that HSV-1 pUL28 recognises Pac1 sequences *in vivo*. However, the DNA binding activity associated with pUL28 has not been confirmed, and these experiments could not be repeated (Dr N. Stow, personal communication). In addition, since the Pac1 sequence is required for the second cleavage event and the correct production of S-termini during HSV-1 DNA encapsidation, the observations suggested that Pac1 DNA binding by pUL28 occurs later during cleavage and packaging (Hodge & Stow, 2001). However, there is evidence that pUL28 may also be required during the early stages of encapsidation, since mutants lacking UL28 demonstrate defects in the initiation of the DNA cleavage and packaging reaction (Addison et al., 1990, Tengelsen et al., 1993). No *in vitro* DNA packaging system exists to verify that pUL15, pUL28 and pUL33 comprise the HSV-1 terminase. Nevertheless, a substantial body of evidence does exist to suggest these proteins possess the predicted functional profiles of the constituents of such a complex.

### **1.3.5.2.3 UL32**

Characterisation of two UL32 mutants, tsN20 and *hr64*, confirmed that the gene was essential for HSV-1 cleavage and packaging (Lamberti & Weller, 1998, Schaffer et al., 1973). The UL32 protein (pUL32) is a cysteine rich, zinc-binding protein, which although required for encapsidation has an indirect role during DNA cleavage and packaging, since it is not directly associated with capsids (Al-Kobaisi et al., 1991, Chang et al., 1996, Lamberti & Weller, 1998, Reynolds et al., 2000). In the absence of pUL32, capsids did not appear to accumulate in replication compartments and this observation led to suggestions that the

protein functioned during capsid transport (Lamberti & Weller, 1998). However, subsequent experiments in our laboratory do not support this suggestion (Dr V. Preston, personal communication).

#### **1.3.5.2.4 UL17**

UL17 was first recognised as an essential HSV-1 DNA cleavage and packaging protein following analysis and characterisation of a UL17 null mutant. In contrast to wt virus-infected cells where B-capsids are dispersed within the nucleus, in the HSV-1 UL17 null-infected cells the B-capsids accumulated in large aggregates around the periphery of the nuclei (Roizman et al., 2007, Salmon & Baines, 1998, Taus et al., 1998). On the basis of these observations it was suggested that the UL17 protein (pUL17) was involved in pathways that either directly transported capsids through the nucleus or produce capsids competent for intranuclear transport. Initially, it was proposed that pUL17 was a component of the tegument since it was readily detected L-particles (Section 1.2.5) and virions, and this finding was later confirmed using a more potent anti-pUL17 antibody in Western blot analysis of virions and related particles (Salmon et al., 1998, Thurlow et al., 2005). Subsequently pUL17 was identified as a minor component of the procapsid and the angularised A-, B- and C-capsids (Goshima et al., 2000, Thurlow et al., 2005). Thus, it appears that UL17 is present in two different structural components of the mature virus particle, the capsid and the tegument. A recent report demonstrated that pUL17 was present at higher concentrations on C-capsids compared to B-capsids and that its presence on capsids was required for efficient binding of the DNA packaging protein encoded by UL25 (Thurlow et al., 2006). Additional viral proteins have been implicated in delaying the transformation of the spherical procapsid to the angularised capsid in infected cells, since *in vitro* procapsids formed from the capsid shell and major scaffolding proteins angularise more readily than *in vivo* procapsids (Newcomb et al., 1999, Newcomb et al., 2000, Rixon & McNab, 1999). In addition, in virus-infected cells and in the absence of DNA packaging, the HSV-1 procapsid spontaneously angularises. Given that UL17 is an essential DNA packaging gene and appears to be required at an earlier stage of DNA encapsidation than pUL25, Thurlow et al. (2006) suggested that pUL17 was a strong candidate for preventing premature angularisation by stabilising the procapsid during DNA encapsidation.

### **1.3.5.2.5 UL25**

The HSV-1 UL25 gene product is a minor capsid protein that, in contrast to the other essential DNA packaging genes, functions during the later stages of the process. UL25 was initially classified as an essential DNA encapsidation gene following characterisation of two ts mutants, ts1204 and ts1208 (Addison et al., 1984). One mutant, ts1208, failed to produce C-capsids at the NPT, while ts1204 had two defects, a reversible defect during the initial stages of infection and another that was evident during DNA packaging. Because ts1204 contained two ts lesions, one of which lay outside the UL25 ORF, the UL25 ts mutation was transferred into wt virus and the mutant ts1249 was isolated. Indirect immunofluorescence assays and in-situ hybridisation analysis of virus-infected cells revealed that ts1249 was not impaired in penetration of the host cell but had an uncoating defect at the NPT. When ts1249-infected cells were initially grown at the PT to allow uncoating of the viral genome and subsequently transferred to the restrictive temperature, a DNA packaging defect was observed, suggesting that pUL25 was involved not only during viral entry but also during DNA encapsidation (Preston et al., 2008).

Confirmation that UL25, unlike the other essential cleavage/packaging genes, was involved in DNA encapsidation during the later stages came from studies involving the UL25 null mutant, KUL25NS (McNab et al., 1998, Stow, 2001). In virus-infected cells lacking the UL25 protein (pUL25), B-capsids were present and an accumulation of A-capsids were observed, which are the by-products of failed DNA packaging events (McNab et al., 1998). In addition, considerably more genomic L termini were generated than S terminal sequences in KUL25NS-infected cells. Since the direction of packaging is generally regarded to be in the direction of the L to S termini, the results suggested that packaging was initiated but failed to go to completion and was aborted prior to the second cleavage event (Stow, 2001, Varmuza & Smiley, 1985). Although, DNA-containing capsids were not observed in KUL25NS-infected Vero cells characterised by McNab et al. (1998) packaged viral DNA, shorter than unit-length, was subsequently detected in the mutant-infected cells by Stow (2001). This work led Stow (2001) to suggest that HSV-1 pUL25 is critical for the retention of full-length viral DNA in capsids.

When large amounts of DNA are tightly packaged into the confines of the capsid shell the packaging rate decreases as the immature capsid is filled, indicating that a large internal energy is generated that creates an increased potential force for DNA exit (Smith et al., 2001). Stow (2001) proposed that by binding to capsids pUL25 could stabilise the capsid against the internal forces generated as increasing amounts of DNA are packaged. However, alternative mechanisms have been suggested to explain the means that pUL25 uses to retain full-length viral genomes in C-capsids. Ogasawara et al. (2001) carried out experiments which indicated that pUL25 bound to the *a* sequence of the HSV-1 genome. They proposed that pUL25 functioned by physically plugging the portal, thereby retaining the packaged DNA in C-capsids. However, to date no DNA binding activity has been confirmed for pUL25. Indeed, experiments carried out within our lab failed to detect binding of purified pUL25 to DNA (Dr N. Stow, personal communication). It has also been suggested that pUL25 enhances the activity of the packaging machinery by stabilising the terminase complex that drives the DNA into the capsid shell. Nevertheless in support of Stow's (2001) hypothesis, conformational changes do occur on the maturing capsids that create or expose new binding sites, such as the VP26 binding sites on hexons following procapsid maturation. It is therefore conceivable that new pUL25 binding sites also become available during capsid maturation, which allows the protein to stabilise the structure thereby overcoming the expected tendency of the DNA to exit the shell. Consistent with this idea is the observation that increasing concentrations of the protein are observed in the maturing capsid forms. Very little pUL25 is detected on procapsids, greater amounts are observed on B-capsids and DNA-containing C-capsids contain the highest levels (Ogasawara et al., 2001, Sheaffer et al., 2000, Sheaffer et al., 2001). In the light of these results, Sheaffer et al. (2001) proposed that the recruitment of pUL25 was inversely related to level of scaffold protein present in the maturing capsid. While procapsids contain a full complement of unprocessed scaffolding proteins, B-capsids have a cleaved scaffolding core and mature C-capsids contain no scaffold. Thus, this latter model predicts that the sequential addition of pUL25 to the maturing capsid, with concomitant loss of the scaffolding proteins during DNA packaging, stabilises the structure enabling the mature C-capsid to retain its full DNA cargo. This system is not unprecedented and is analogous to the functions of the head stabilising proteins of bacteriophage  $\lambda$ , gpW and gpD (Maxwell et al., 2000,

Perucchetti et al., 1988). During DNA packaging of phage  $\lambda$  the head expands by approximately 20%, exposing binding sites that gpD interacts with on the surface lattice of the icosahedral shell (Imber et al., 1980). Once packaging is complete, gpW also interacts with the DNA-filled heads to stabilise them. Similar to pUL25, both gpD and gpW are dispensable for procapsid assembly but are essential for stable encapsidation of the viral genome and, like pUL25, the requirement for gpD is redundant if less than unit-length genomes are packaged (Perucchetti et al., 1988, Sternberg & Weisberg, 1977a, Sternberg & Weisberg, 1977b). Although there is no head expansion in HSV-1, like gpD and gpW, pUL25 has been predicted to bind to different regions on the icosahedral capsid shell (Trus et al., 2007).

The UL25 protein is not only involved in DNA packaging but is also important during DNA entry and has been implicated in egress (Coller et al., 2007, Padeloup et al., 2009, Preston et al., 2008). The binding partners that interact with the multifunctional pUL25 together with crystallographic structure for the protein are discussed in Section 1.4.

### 1.3.5.3 Packaged state of viral DNA

In the HSV-1 virion the encapsidated DNA is so densely packed within the capsid shell that it exists in a liquid-crystalline state (Booy et al., 1991). It is a remarkable achievement that viral DNA is packaged to a near-crystalline state, since entropic, electrostatic and bending energies of the DNA must be overcome. A study using optical tweezers to pull on single DNA molecules as they are packaged into the phage heads of  $\Phi$ 29 allowed a quantitative estimate of the build-up of the internal force that the prohead experiences as it is filled (Smith et al., 2001). The force on the prohead starts to build only after approximately half of the  $\Phi$ 29 genome is already packaged. However, the estimated pressure transmitted to the phage head on completion of the packaging of the viral genome suggests that the capsid must have a tensile strength that is similar to a typical aluminium alloy (Smith et al., 2001).

Packaged DNA inside HSV-1 virions is organised into concentric layers (Figure 1.16), a configuration that has been compared to the 'spooling' model of DNA

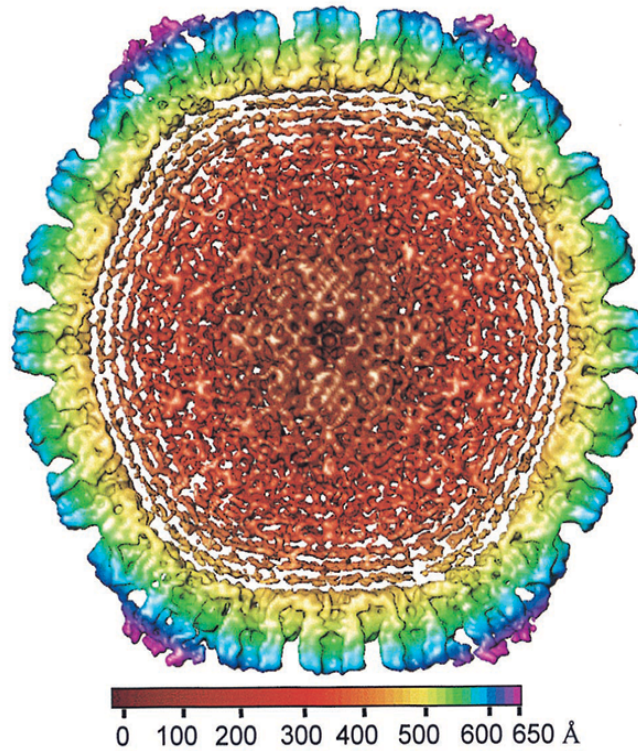


**Figure 1.16 Central cross-section of a cryo-EM reconstruction of HSV-1**

The resolution of the virion reconstruction is 20 Å. The central cross-section (100 Å thick) through the structure is viewed along the two-fold axis, and is coloured radially as indicated on the colour bar below the virion. The packaged viral DNA (red) is seen as concentric shells of density inside the capsid shell, with the spacing between the layers being 26 Å. The capsid floor is shown in yellow and the triplexes and middle domains of the capsomers are indicated in green. The outer domains of the capsomers together with the tegument densities associated with pentons are coloured blue and purple, respectively (adapted from Zhou et al., 1999).

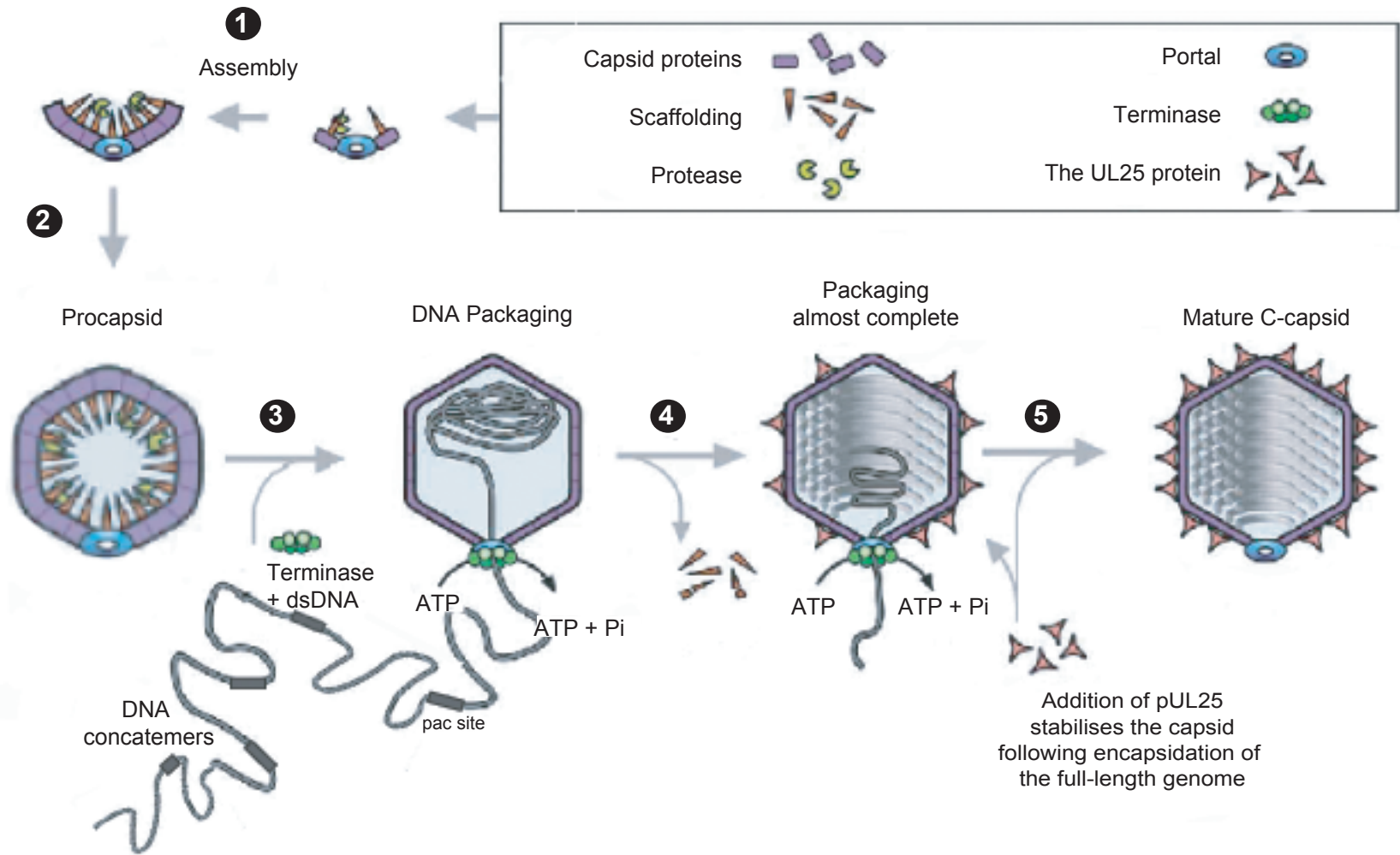
packaging proposed for bacteriophage T7 where the strands are packaged in a hexagonal lattice (Cerritelli et al., 1997, Zhou et al., 1999). This arrangement suggests that once the DNA has been inserted through the portal, it is packaged into the confines of the capsid cavity by wrapping around the inner surface of the shell and organising itself layer upon layer. However, as the DNA is progressively packaged the layers become less ordered the further they are from the outer shell (Harrison, 1983). Although the DNA appears to be closely associated with the inner shell, the structure of the packaged DNA shows no icosahedral symmetry that would indicate it specifically interacts with the capsid proteins (Zhou et al., 1999). In the bacteriophage HK97 the inner floor of the capsid shell is highly charged (Wikoff et al., 2000). Therefore, it has been suggested that in viral capsids the energy of the encapsidated negatively charged DNA may be lowered by its close association with the positively charged inner capsid floor (Tzlil et al., 2003). However, to date there is no information on the charge present in the inner floor of the HSV-1 capsid.

#### **1.3.5.4 Model of HSV-1 DNA encapsidation**

Based on the current information outlined above, a model for HSV-1 packaging has been proposed and is illustrated in Figure 1.17 (Baines & Weller, 2005). In addition to the concatemeric viral genomes generated following DNA replication, two other substrates, procapsids and the terminase are required for DNA encapsidation. The procapsids, which contain the unprocessed scaffolding proteins preVP21 and preVP22a, are assembled within the nucleus close to or within replication compartments. The putative terminase consists of pUL15, pUL28 and pUL33 and binds to the viral DNA concatemers via the pUL28 subunit. The terminase/DNA complex then binds to the capsid predominately through an interaction with the portal protein, pUL6. The terminase scans the DNA for the appropriate Pac2 cleavage signal and at fixed distance from this site an initial cleavage event releases an L terminal genomic end. The cleaved S terminal end that is not bound to the capsid is degraded. The DNA cleavage and packaging reactions are initiated by protease activation and scaffold cleavage and the processed products VP21 and VP22a are released, while the protease (VP24) remains in the capsid. Concurrently, the L-terminal viral DNA is inserted through the portal and translocation of the L/S junction followed by the S-terminal end of the viral genome into the capsid is achieved by the energy

### **Figure 1.17 HSV-1 DNA cleavage and packaging model**

(1) The immature capsid is assembled in the nucleus. (2) The procapsid is delivered to the replication compartment, the site of DNA encapsidation. (3) The putative terminase, which consists of a heterotrimeric complex of the UL15, UL28 and UL33 gene products, binds the viral DNA concatemers via the UL28 protein subunit, and the DNA/terminase complex docks with the capsid at the portal. The DNA is scanned by the terminase and the DNA concatemer is cleaved at the Pac2 signal. A genomic L terminal end from the cleaved DNA concatemer is then inserted into the cavity of the capsid via the portal channel, and DNA packaging commences with the hydrolysis of ATP. (4) Concomitantly as the DNA is packaged into the capsid, the cleaved scaffolding proteins, VP21 and VP22a, are released. (5) The UL28 protein cleaves the DNA concatemer again, this time at the Pac1 motif, leaving a unpackaged L terminus and an encapsidated unit-length viral genome. During the final stages of DNA encapsidation, the structure is stabilised by the association of the UL25 protein to the binding sites that are exposed during capsid maturation (adapted from Steven et al., 2005).



1

Assembly

2

Procapsid

DNA Packaging

4

Packaging almost complete

5

Mature C-capsid

Capsid proteins

Scaffolding

Protease

Portal

Terminase

The UL25 protein

3

Terminase + dsDNA

ATP

ATP + Pi

DNA concatemers

pac site

ATP

ATP + Pi

Addition of pUL25 stabilises the capsid following encapsidation of the full-length genome

supplied through ATP hydrolysis, which is mediated by the terminase associated pUL15. As the procapsid matures, pUL17 is added to prevent premature angularisation, which would inhibit DNA packaging. In addition, pUL28 cleaves the viral DNA again, on this occasion using the Pac1 cleavage signal, generating the packaged 5'-terminus of the full-length viral genome. At the same time the internal scaffold is lost and pUL25 is added to the outer shell through its interaction with pUL17, stabilising the structure and resulting in the production of the mature C-capsid.

### **1.3.6 Egress**

Once DNA encapsidation is complete, unit length DNA-containing C-capsids must cross the nuclear membrane to complete the assembly of the infectious virus particle in the cytoplasm. The nuclear envelope consists of an inner and an outer nuclear membrane (INM and ONM, respectively) that are traversed by multiple nuclear pore complexes (NPCs) and lined by a meshwork of intermediate filaments comprising the nuclear lamina. Three proteins, encoded by US3, UL31 and UL34, allow the C-capsid to escape the egress barrier presented by the nuclear membrane. Following the release of the naked C-capsid into the cytoplasm, tegument proteins bind to the capsid and direct the transport of the particle to the site of secondary envelopment, where further tegument proteins are added prior to envelopment and the release of mature virions from the cell by exocytosis (reviewed in Mettenleiter, 2006, Roizman et al., 2007).

#### **1.3.6.1 Nuclear egress and primary envelopment**

Three different models have been proposed for nuclear egress of C-capsids, which have been designated the 'envelopment/de-envelopment', the 'luminal' and the 'nuclear pore' pathways, each of which are illustrated in Figure 1.18 (Johnson & Spear, 1982, Roizman et al., 2007, Skepper et al., 2001, Wild et al., 2005). A prerequisite for capsid egress is the engagement of the C-capsid with INM. Two of the proposed pathways, the envelopment/de-envelopment and the luminal model, involve budding of the capsid at the INM and result in enveloped capsids within the perinuclear space. In the luminal or single envelopment model, the primary envelope retains its integrity and the enveloped virus

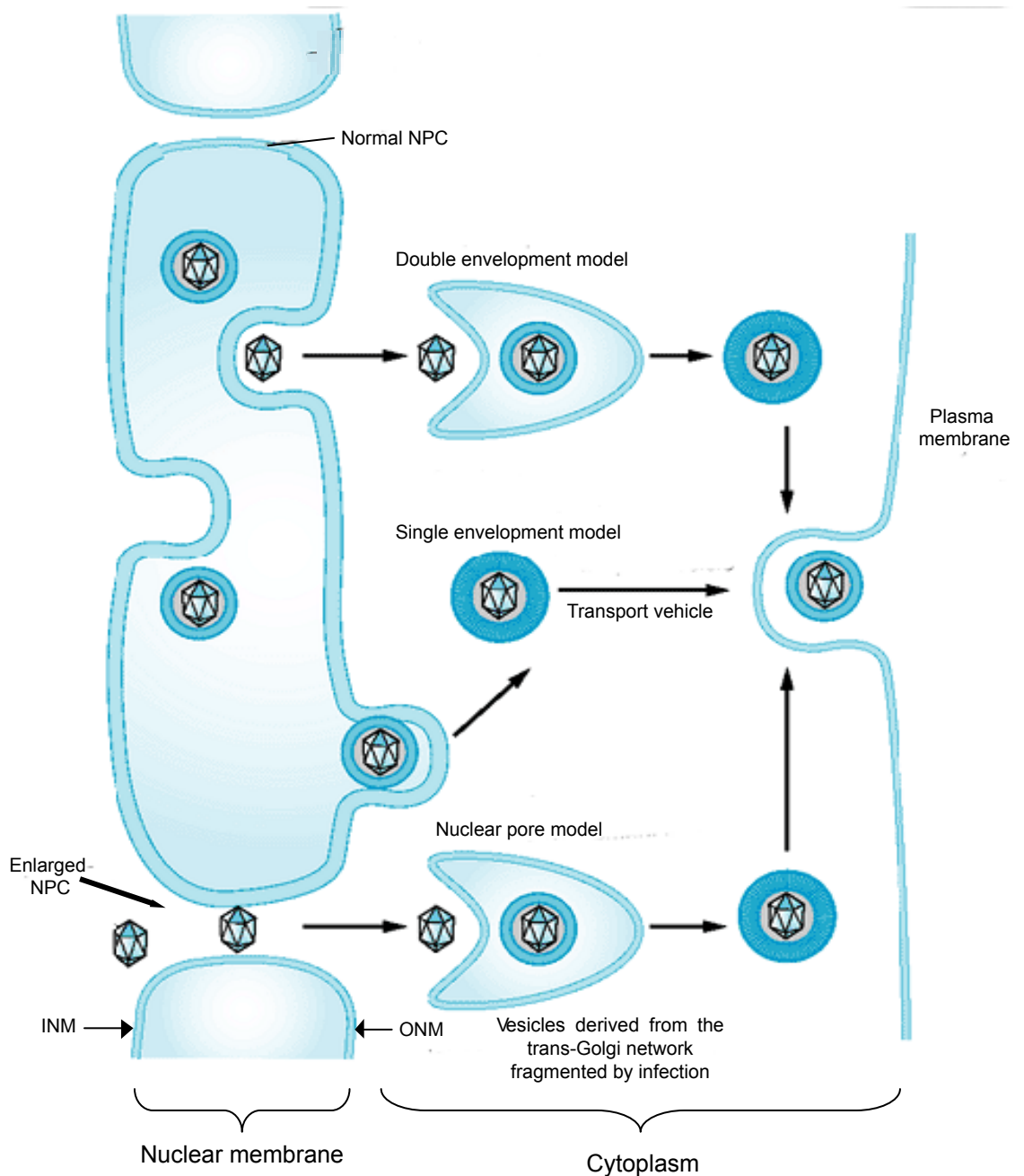


**Figure 1.18 Models for egress of HSV-1 from the host cell**

The proposed pathways for maturation of filled capsids from the nucleus to the exterior of the infected cell are illustrated. In the double envelopment pathway, C-capsids undergo primary envelopment at the inner nuclear membrane (INM), then de-envelopment at the outer nuclear membrane (ONM), followed by secondary envelopment at cytoplasmic membranes. The enveloped viral particles are then transported in vesicles to the plasma membrane. Fusion of the vesicle with the plasma membrane releases the virion into the extracellular space. In the single envelopment model, the C-capsid is enveloped at the INM, enters a vesicle at the ONM and is then transported to the plasma membrane where the virion is released. In the nuclear pore model, C-capsids exit the nucleus through enlarged nuclear pores and become enveloped by budding into cytoplasmic vesicles, which are transported to the plasma membrane where the virion is released (adapted from Roizman et al., 2007).

particle is transported via the secretory pathway to the extracellular space (Roizman et al., 2007). In the envelopment/de-envelopment or double envelopment model the primary envelope is subsequently lost by fusion with the ONM, resulting in de-envelopment and release of 'naked' capsids into the cytosol, followed by subsequent secondary envelopment at the trans-Golgi network (Stackpole, 1969).

A third pathway, the nuclear pore model, for nuclear capsid egress was suggested following analysis of bovine herpesvirus type 1-infected cells using high pressure freeze-fracturing (Wild et al., 2005). In these studies the nuclear pores appeared enlarged, with nuclear material including capsids, protruding into the cytoplasm of the infected cells. These observations led to the proposal that capsids escape the nucleus via dilated NPC (Figure 1.18). Such a pathway suggests that the general integrity of the NPC is violated in order to accommodate this process (Leuzinger et al., 2005). However, subsequent findings have indicated that NPC morphology is unaffected and that their gating function remained intact until late infection (Hofemeister & O'Hare, 2008, Mettenleiter et al., 2006). In support for these studies, nuclear capsid egress does not appear to be conditional on the alterations to the NPC that occur late during infection (Nagel et al., 2008). In the single envelopment pathway all the components of the primary enveloped particle must be part of the mature virion, equally, all the constituents of the mature particle would be expected to be components of the primary enveloped particle. Inconsistent with this idea is the observation that neither of the two major components of primary enveloped capsids, pUL31 and pUL34, have been detected on mature virions (Fuchs et al., 2002a, Klupp et al., 2000, Reynolds et al., 2002). Conversely, other tegument and envelope proteins that are constituents of mature virions have not been detected on primary enveloped viral particles (Granzow et al., 2004). Further support for a double envelopment mechanism of capsid egress is demonstrated not only by the difference in the protein composition between primary enveloped and mature virions but also in differences observed between their lipid envelope. Unlike the nuclear membrane seen in perinuclear virions, in mature virions the lipid membrane resembles those observed in Golgi-derived vesicles (Van Genderen et al., 1994).

Translocation of naked or enveloped capsids into the cytoplasm requires at least three viral proteins encoded by UL34, UL31 and US3 (Poon et al., 2006, Reynolds et al., 2004, Reynolds et al., 2001, Reynolds et al., 2002). The proteins encoded by UL31 (pUL31) and UL34 (pUL34) are essential for primary envelopment and in the absence of either, intranuclear capsids do not access the INM. Both UL31 and UL34 are structurally and functionally conserved throughout *Herpesviridae*, UL34 encodes a type II transmembrane protein that is present in nuclear membranes and in primary envelopes, and physically interacts with pUL31 (Fuchs et al., 2002a, Lake & Hutt-Fletcher, 2004, Reynolds et al., 2002, Sanchez & Spector, 2002). Since the passage of C-capsids through the INM is obstructed by the nuclear lamina network, the pUL34/pUL31 complex is required for conformational alterations to the nuclear lamins (Mou et al., 2008, Reynolds et al., 2004, Simpson-Holley et al., 2005). The network of nuclear lamins is loosened by phosphorylation, predominately by pUL31/pUL34 recruitment of the cellular protein kinase C and the HSV-1 kinase encoded by US3 (pUS3) (Mou et al., 2008, Muranyi et al., 2002, Park & Baines, 2006). EM studies have shown that, in the absence of HSV-1 or PRV pUS3, enveloped particles accumulate in the perinuclear space, indicating that primary envelopment takes place but de-envelopment is impaired (Reynolds et al., 2002, Wagenaar et al., 1995). It appears that expression of pUS3 in infected cells promotes but is not essential for nuclear egress, since in cultured epithelial cells the absence of pUS3 only mildly reduces the titre of extracellular virions (Klupp et al., 2007).

### **1.3.6.2 Tegumentation and secondary envelopment**

Following nuclear egress, the C-capsid acquires its full complement of tegument proteins and the final or secondary envelope. By conventional EM analysis cytosolic capsids appear 'naked', however, immunolabelling studies have revealed that pUL36 and pUL37 are closely associated with cytoplasmic C-capsids (Fuchs et al., 2002a). Whether these proteins are added during primary envelopment and remain associated with the translocated capsid, or whether they are recruited after nuclear egress remains unclear. However, structural analysis of HSV-1 has indicated that there is a clear distinction between the envelope-associated amorphous outer tegument layer and the icosahedrally arranged capsid-associated inner tegument layer (Zhou et al., 1999). In addition, the stoichiometric proportions of the inner tegument proteins are

relatively constant, whereas the outer tegument proteins can show considerable variation (Del Rio et al., 2005, Michael et al., 2006).

Studies have indicated that in the absence of pUL36 in PrV, the movement of virus particles to the site of secondary envelopment is blocked during egress (Luxton et al., 2006). Since PrV and HSV-1 pUL36 appear to be functionally conserved, the results suggest that pUL36 may be linked to cytoplasmic capsid transport, which is dependent on microtubules in virus-infected cells (Coller et al., 2007). This possible role for pUL36 during exit is supported by observations that during entry a few tegument proteins, including pUL36 and pUL37, remain associated with incoming capsids during their transport along microtubules to the NPC (Antinone & Smith, 2006, Granzow et al., 2005, Luxton et al., 2005). While both pUL36 and pUL37 are essential for virion morphogenesis (Section 1.2.3), pUL37 is dispensable during entry but may play an accessory role in pUL36 function, for example, by increasing the mobility of the capsid along the microtubule network (Krautwald et al., 2009, Leege et al., 2009, Roberts et al., 2009). Herpesvirus capsids are connected to the envelope via the outer tegument proteins. The UL36 protein appears to play a pivotal role during viral assembly by acting as the link between the capsid and tegument components, since the capsid-tegument interaction is suggested to be mediated through an association between pUL36 and capsid-associated pUL25 (Section 1.2.3).

Cytoplasmic structures termed 'assembly compartments' have been defined as the sites of secondary envelopment for several herpesviruses, in particular for HCMV (Das et al., 2007, Sanchez et al., 2000). How partially tegumented capsids are directed to the assembly compartments for secondary envelopment is unclear. It is apparent, however, that subsequent layers of outer tegument are added to the viral particle in an ordered manner not only during nucleocapsid transport through the cytoplasm but also at the site of secondary envelopment (reviewed in Mettenleiter, 2006). Interestingly, the production of L-particles within infected cells where tegumentation of cytoplasmic C-capsids is impaired suggests that secondary envelopment is not dependent on the presence of nucleocapsids (McLauchlan & Rixon, 1992). Whereas entry requires dynein-mediated minus-end microtubule-directed transport, egress is dependent on kinesin-mediated plus-end directed movement (reviewed in Lyman & Enquist,

2009). The difference in tegument composition between the incoming and outgoing viral particles has been suggested to influence the direction of capsid transport (Luxton et al., 2005).

The final stage in viral assembly is the acquisition of the secondary envelope, followed by transport of vesicles containing the enveloped particle to the plasma membrane and the subsequent budding of these structures at the plasma membrane to release the virus to the extracellular matrix. The tegumented capsids in the cytoplasm of the infected cell gain their final envelope from vesicles that are derived from the trans-Golgi network and where the viral glycoproteins are acquired (Harley et al., 2001, Mettenleiter, 2004). A complex network of protein-protein interactions, which are summarised in Figure 1.19, drives primary envelopment, de-envelopment, tegumentation and secondary envelopment by budding at the trans-Golgi network. The conservation of the complex interactions between tegument proteins across the alphaherpesviruses is highlighted by the observation that HSV-1 pUL11 interacts with HSV-1 and PrV UL16 encoded proteins (pUL16), and PrV pUL16 in turn complexes with PrV UL21 encoded protein (pUL21), which suggests the formation of a tripartite complex (Klupp et al., 2005, Loomis et al., 2003, Yeh et al., 2008). The HSV-1 UL11 encoded tegument protein plays an important role during viral exit, since a deletion mutant of pUL11 has been shown to be deficient in egress (Baines & Roizman, 1992). In addition, pUL11 has been suggested to direct tegument proteins to the secondary envelopment site (Baines & Roizman, 1992, Fulmer et al., 2007). Indeed, the protein appears to show intrinsic targeting properties, since a fusion protein of HSV-1 pUL11 and HIV-1 gag was found to be directed to the Golgi apparatus instead of the plasma membrane, while the protein itself has been demonstrated to localise to a cytoplasmic site overlapping the ER-Golgi intermediate compartment (Bowzard et al., 2000, Sanchez et al., 2000). It has been proposed that pUL11 binds to membranes via N-terminal myristoyl and palmitoyl lipid side chains attached to the protein at conserved sites, which are essential for efficient packaging of the protein into virions (Baird et al., 2008, Koshizuka et al., 2007, Loomis et al., 2006).

As mentioned above, viral glycoproteins are present on trans-Golgi derived vesicles prior to secondary envelopment, since they are transported to this compartment to undergo post-translational modifications following translation

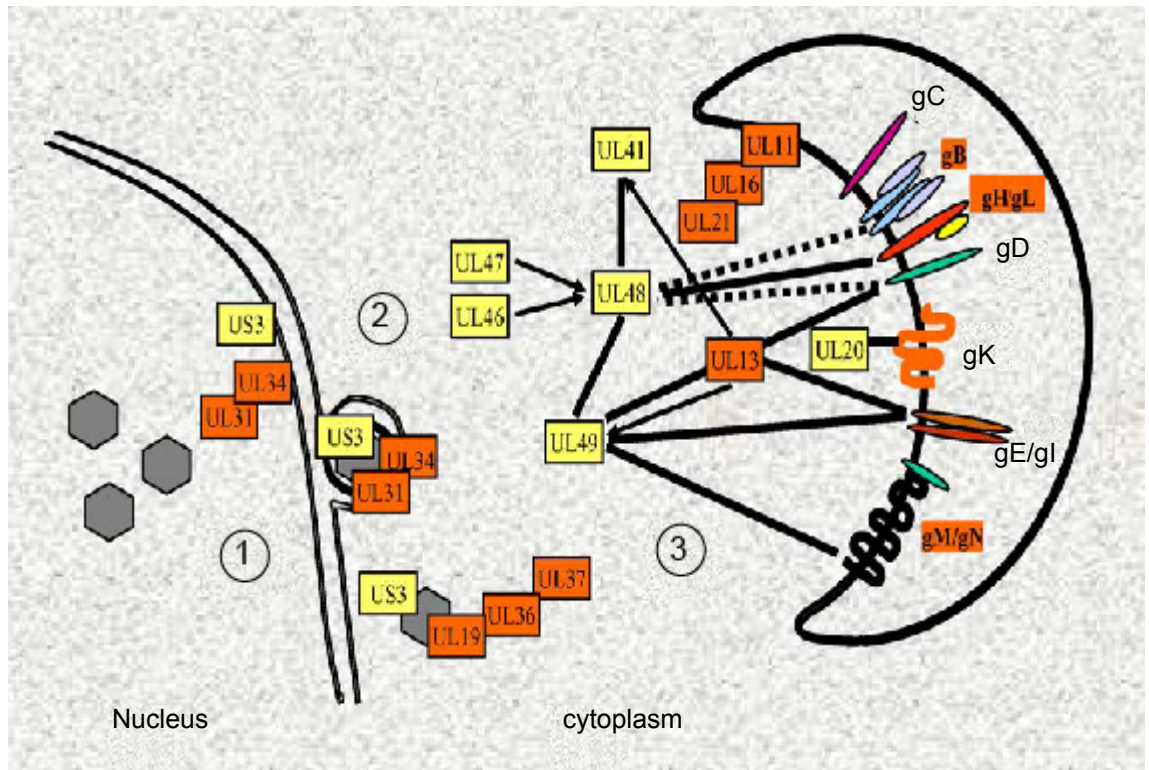


**Figure 1.19 Molecular interactions during HSV-1 egress**

The numbers indicate primary envelopment (1), de-envelopment (2), and secondary envelopment (3). The rectangles represent the designated gene and solid lines or direct contacts between them denote physical interactions, whereas arrows indicate functional effects. Dotted lines indicate suggested but not firmly established interactions. In the case of glycoproteins only direct contacts resulting in complex formation are depicted. Proteins that are conserved in all three herpesvirus subfamilies are marked in orange (adapted from Mettenleiter, 2006).

on the ribosomes of the endoplasmic reticulum. Nucleocapsids are connected to the envelope by the tegument through interactions between tegument proteins and the cytoplasmic tails of the envelope glycoproteins. In PrV the UL49 encoded outer tegument protein, pUL49, binds to the cytoplasmic domains of gE and gM. Deletion of both these glycoproteins genes results in the accumulation of cytoplasmic C-capsids embedded in tegument and the inhibition of secondary envelopment (Brack et al., 1999, Fuchs et al., 2002a). In addition, this interaction is required for the inclusion of pUL49 into mature virions. In HSV-1, pUL49 also binds to gE and gM, although only the interaction with gE is essential during virion morphogenesis. HSV-1 pUL49 also interacts with another tegument protein, VP16 expressed by UL48, which in turn binds to the cytoplasmic tail of gH and gD. VP16 has been proposed as the protein that links the inner and outer layers of tegument during virion morphogenesis through its interaction with pUL36 (Fuchs et al., 2002b, Kamen et al., 2005, Mossman et al., 2000). Nevertheless, the link between inner and outer tegument proteins may involve multiple proteins, since there is a significant degree of redundancy found between the networks of interactions that occur among tegument proteins and between tegument and envelope proteins (reviewed in Mettenleiter, 2006).

### **1.3.7 Latency**

One of the defining features of herpesviruses is their ability to establish a life-long latent infection in the host. Unlike the persistent lytic infection, no viral progeny are produced during latent infections and only very limited amounts of gene transcription can be detected in infected cells. Latency can be divided into three stages; establishment, maintenance and reactivation (Rock, 1993). Following primary infection, HSV-1 enters sensory neurons in the dorsal root ganglia by fusion at the axonal termini and is transported via retrograde axonal transport to the nucleus of the neuronal cell body. Once in the neuron, the viral DNA persists in the nucleus in a circular episomal form for the lifetime of the host. Periodic reactivation of infectious virus can occur in the neurons harbouring latent HSV-1 in response to external stimuli. The virus then passes down the axons by anterograde axonal transport to replicate near the site of the initial infection (reviewed by Roizman et al., 2007).

Although lytic gene expression has been detected at very low levels in latently infected cells, the only abundant viral mRNAs transcribed during latency are the latency associated transcripts (LATs) (Wagner et al., 1995). Despite extensive research, the precise role of LATs during latency is controversial and remains unclear. Expression of the LAT gene transcription unit (Figure 1.20) is controlled by a latency specific promoter (LAP) and splicing of its primary 8.3 kb transcript yields several RNA species. The 8.3 kb transcript accumulates at low levels in latently infected neurons, while the 2.0 kb and 1.5 kb introns derived from the primary transcript are abundant and stable (Wagner et al., 1988). However, since no LAT-encoded protein has been conclusively demonstrated to exist, one recent investigation has focused on the idea that the LAT might function as a primary microRNA (miRNA) transcript (Drolet et al., 1997, Umbach et al., 2008). These miRNA molecules are single-stranded non-coding RNA structures, which vary in length from between 21-23 nucleotides and are partially complementary to mRNA, while their main function is to regulate gene expression. Umbach et al. (2008) demonstrated that the LAT transcript encodes four distinct miRNAs in HSV-1 infected cells, one of which is transcribed in an antisense orientation to ICP0, the virus IE transcriptional activator that is important for productive HSV-1 replication and is thought to have a role in reactivation from latency (Everett, 2000). They found the miRNA associated with ICP0 was able to reduce the protein's expression, thereby increasing the possibility that the virus in infected neurons entered and maintained latency. In addition, they identified another HSV-1 encoded miRNA that showed partial complementarity to ICP4 mRNA and reduced the expression of the gene (Umbach et al., 2008). Similar to ICP0, ICP4 can also promote the reactivation of HSV-1 from latency, thus the presence of at least two primary HSV-1 miRNA may assist the establishment and maintenance of the latent state in infected neurons (Halford et al., 2001, Umbach et al., 2008).

## 1.4 UL25 protein structure

HSV-1 pUL25 is a 580 residue, 62.7 kDa minor capsid protein, and the crystallographic structure of an N-terminally truncated form of the protein (UL25nt), corresponding to the residues 134-580, has been determined to 2.1 Å (Bowman et al., 2006). Large quantities of soluble protein are required as a starting material for crystallographic studies. However, initial attempts to

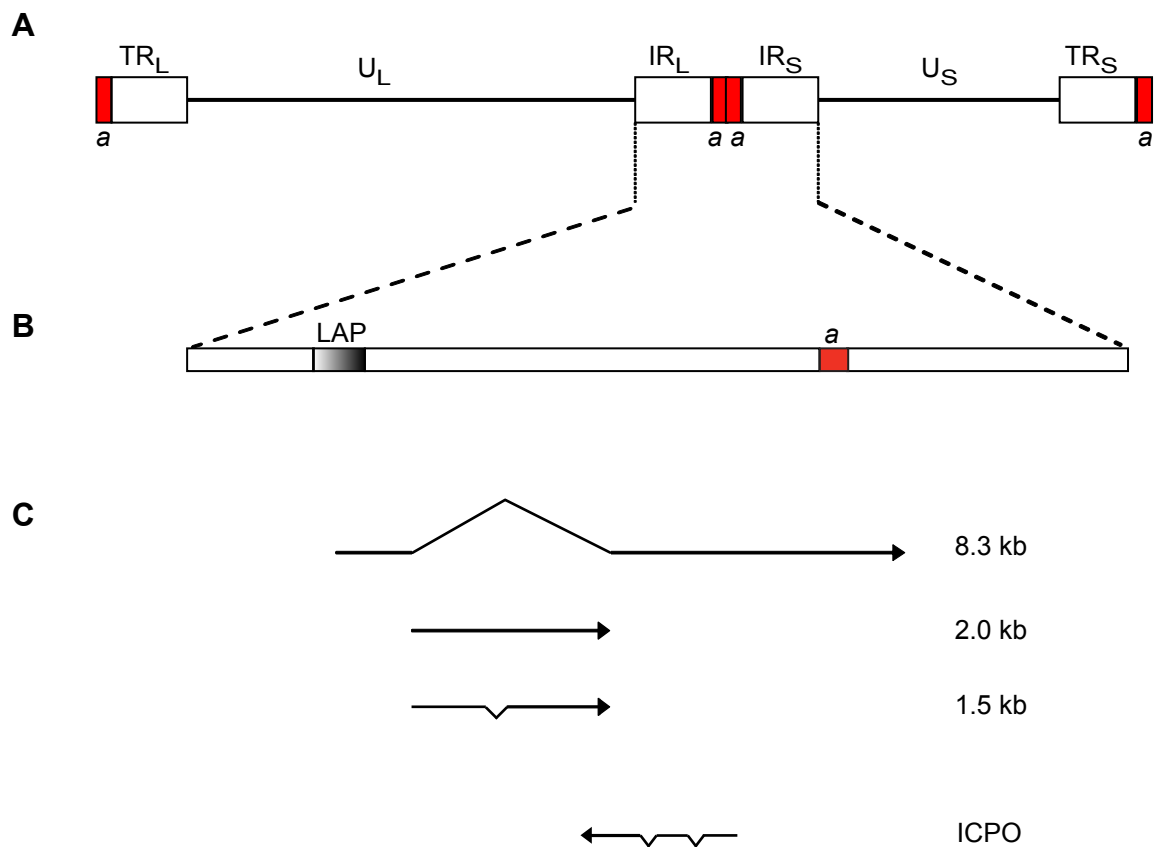


**Figure 1.20 Map of the latency-associated transcript (LAT) gene**

(A) The HSV-1 genome structure is shown. The  $U_L$  and  $U_S$  denote the unique sequences of the long (L) and short (S) components of the genome, respectively. The unique regions are flanked by the inverted repeats ( $TR_L/TR_S$  and  $IR_L/IR_S$ ). The 'a' sequences are highlighted in red. (B) Expanded view of L and S junction showing the relative position of the LAT promoter (LAP). (C) Locations and orientations of transcripts of the L-S junction region are denoted by arrows. These include the LAT primary transcript at 8.3 kb and the two transcripts, 2.0 kb and 1.5 kb, which are stable intron transcripts derived from the full-length 8.3 kb RNA. The LATs are transcribed antisense and at least partially complementary to the gene encoding ICPO (adapted from Roizman et al., 2007).

express and purify the full-length pUL25 as a GST fusion protein in sufficient quantities necessary for crystallography were unsuccessful. Secondary-structure analysis predicted the presence of a long unstructured loop in the N-terminal region of pUL25. When sequences encoding this loop were removed from the construct, the resulting GST-fusion protein containing the pUL25 residues R45-V580 was soluble and expressed to high levels in *E. coli*. During the purification of this fusion protein, removal of the GST tag by protease digestion resulted in a secondary cleavage event that released a stable fragment of 48 KDa, referred to as UL25nt, which formed crystals that diffracted. To date, the structure of UL25nt is the only herpesvirus DNA packaging protein that has been solved. It exists as a monomer in the crystal, and the first ordered N-terminal residue is A134. UL25nt has a novel fold that consists of a box-shaped core comprised mostly of  $\alpha$ -helices, with a few minor  $\beta$ -sheets, and a striking feature of the molecule is the presence of numerous loops that emanate from the core of the protein, some of which extend for some distance (Figure 1.21).

Interestingly, five of the extended loops (L1-L5) in the UL25nt crystal contain disordered residues, with an additional unstructured region, containing three amino acids (L6) situated at carboxyl terminus of the protein (Figure 1.21). Regions that are referred to as disordered or unstructured are areas of the crystallised protein that are missing from the resulting electron density maps determined by X-ray crystallographic studies. For successful crystallography experiments, the corresponding atoms in the different protein molecules must be uniformly spaced throughout the crystallised protein, which leads to a regular diffraction pattern from these atoms. If a region is dynamically flexible or adopts different structures in different molecules in the crystal, then the atoms in the same region are not uniformly spaced and therefore fail to diffract. The unstructured residues contained in the regions L1-L6 are shown in Table 1.4. The crystal structure of UL25nt does not include the N-terminal 133 residues of pUL25. The secondary-structure prediction for this region suggests it is composed of a long  $\alpha$ -helix (residues 48-110), preceded by a 45-residue unstructured N-terminal loop (Bowman et al., 2006). Analysis of the electrostatic surface potential of UL25nt revealed an interesting distribution of surface charges, with one face of the protein being essentially electropositive while the opposing face is essentially electronegative (Figure 1.22). The

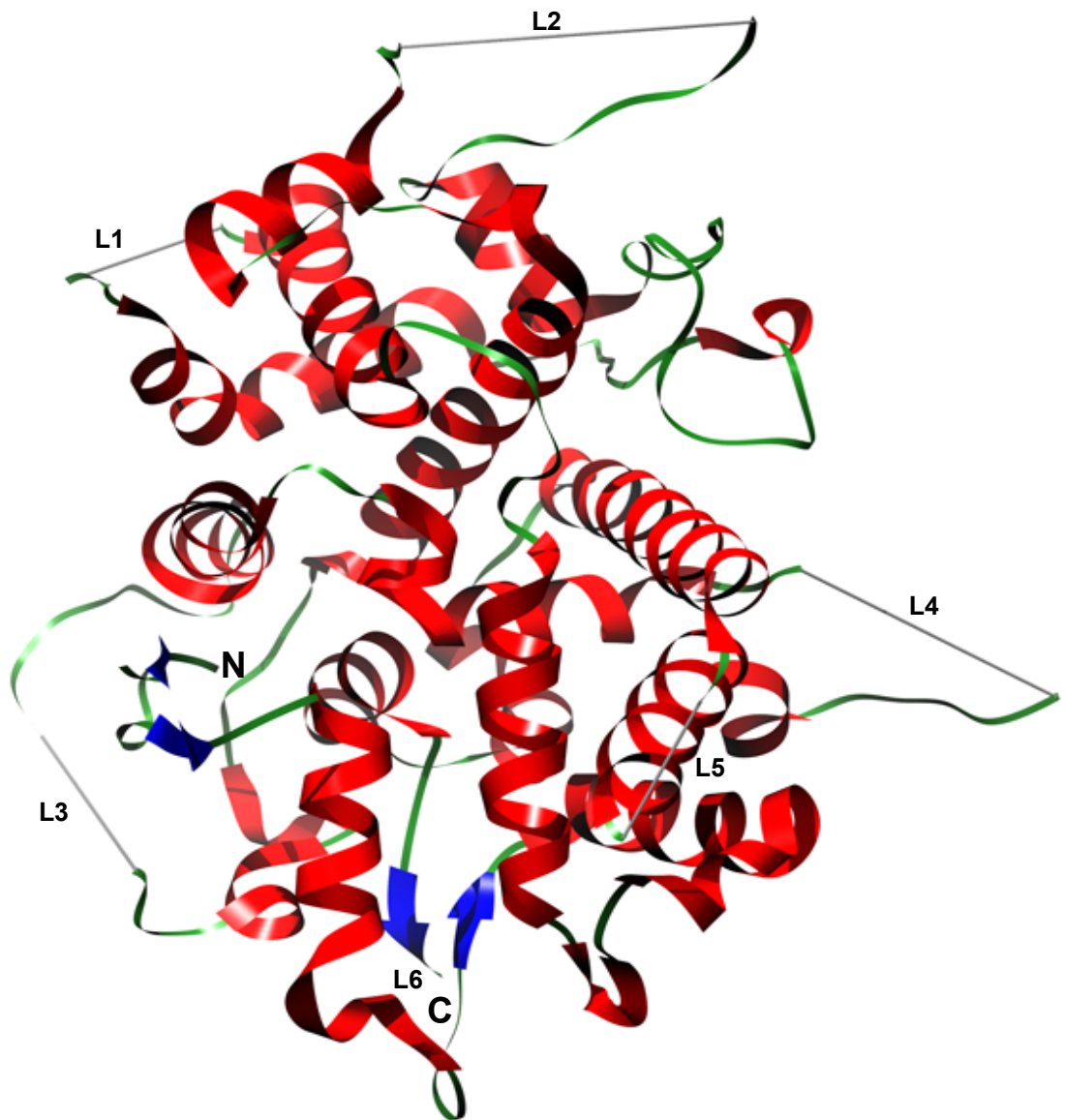


**Figure 1.21 Ribbon diagram of UL25nt**

The secondary structure elements are coloured red ( $\alpha$ -helices), blue ( $\beta$ -strands), green (extended loops) and grey (disordered loop regions). N and C labels identify the amino- and carboxyl-terminal ends, respectively. The unstructured looped out regions, L1-L5, are indicated, and the L6 unstructured residues located at the C-terminus are shown.

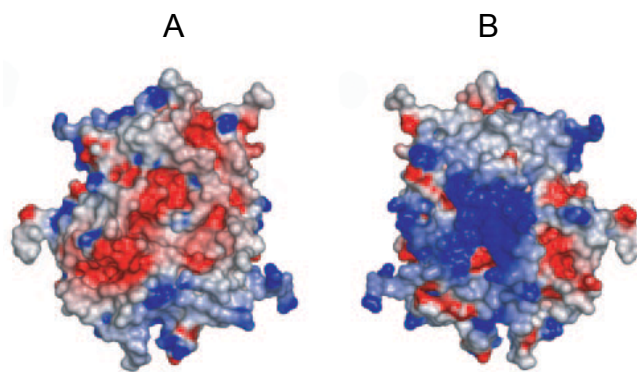


**Figure 1.22 Electrostatic surface charge of UL25nt**

(A) A space filling model showing the electrostatic surface representation of the electronegative face of UL25nt. (B) A 180° rotation of the view in panel A, showing the electropositive face of UL25nt (adapted from Bowman et al., 2006).

significance of the charged faces in UL25nt is unclear, but they may play a role in interactions of pUL25 with other proteins. Since pUL25 has been reported to bind DNA, the basic face may mediate this association, perhaps at some point during DNA packaging or during entry and release of the viral genome from the capsid at the NPC (Ogasawara et al., 2001, Bowman et al., 2006).

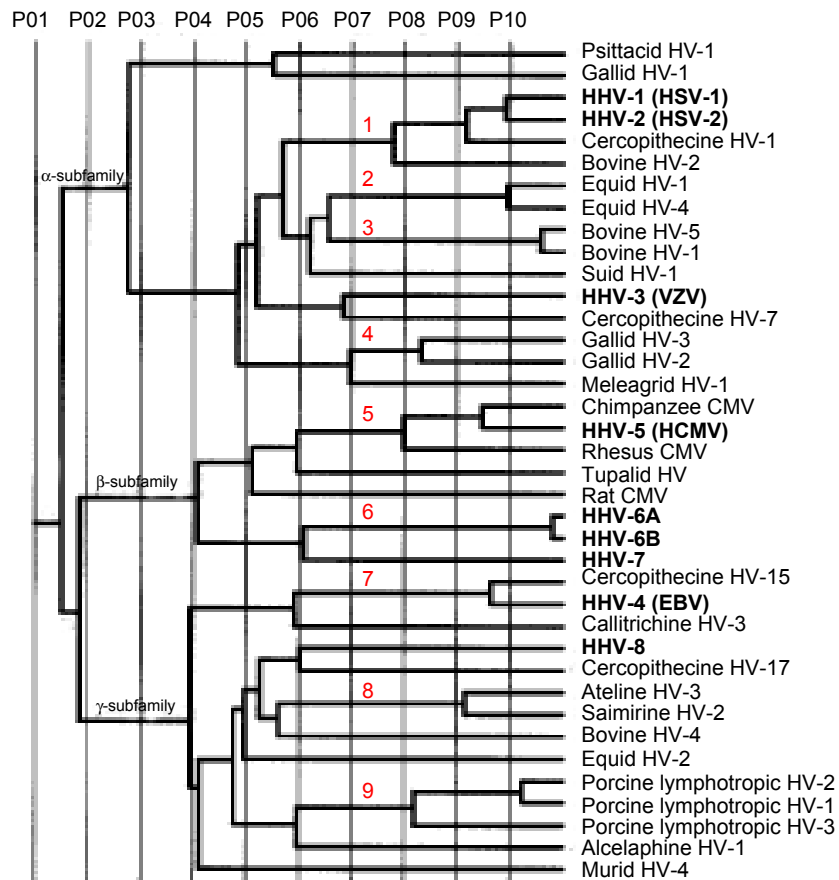
Loop Region	Residues	Unstructured residues
L1	H247 - T259	A249 - D254
L2	V325 - A347	R335 - G345
L3	A415- D437	P417 - A425
L4	Q475 - S490	P479 - T483
L5	R509 - P516	R511 - N513
L6	L577 - V580	S578 - V580

Table 1.4 Residues in the extended loops (L1-L5) and the unstructured L6 region of UL25nt.

### 1.4.1 The predicted functional interfaces

UL25 is one of approximately 40 core genes conserved among all members of the family of *Herpesviridae* (Davison, 2002). The sequence alignment of the UL25 protein homologues from the eight human herpesviruses revealed that the N-terminal 133 residues, in particular residues 1-45 that were predicted to be unstructured, were the least conserved part of pUL25. Within the UL25nt portion of the protein, 24 residues were identified that were completely conserved in the eight human herpesviruses. However, subsequent mapping of these residues onto the known structure of UL25nt showed that they were mostly hydrophobic core residues situated in the interior of the protein. Therefore, these amino acids are more likely to be critical for maintaining the structural integrity of the protein.

To identify important functional interfaces on the surface of UL25nt, an evolutionary trace (ET) analysis was performed on a multiple-sequence alignment of UL25 and homologous protein sequences. ET was developed by Lichtarge et al. (1996) and exploits the fact that residues important for the structure of a protein tend to be strongly conserved across species. The ET algorithm uses phylogenetic information to identify conserved amino acids within a protein family and then maps this information in the context of an atomic structure (Lichtartge & Sowa, 2002). The method has been successful in identifying functional sites in a wide range of proteins (Chakravarty et al., 2005, Mikalek et al., 2003, Sowa et al., 2001). The phylogenetic tree for UL25nt is shown in Figure 1.23. Partitioning of the tree divides the set of proteins into a number of classes; each containing related sequences derived from a node within that partition. Residues that are important for the protein's structural integrity usually are highly conserved and show the least variation in a family of related proteins, while residues that are functionally important are less well conserved but are invariant among a group of closely related proteins or subgroup. Clustering of these specific residues onto the structure of the protein implies a functional interface, since evolutionary divergence and functional specificity is associated with changes in the amino acid composition. By examining the pattern of conservation within a family of related proteins, ET analysis can reveal relationships that conventional sequence comparisons do not. At P07, there are nine protein classes defined that are distributed across the three herpesvirus subfamilies and contain more than a single member (Figure 1.23). Mapping of the class-specific residues at this level on the surface of UL25nt identified four clusters (C1-C4) of particular interest. The class-specific surface residues and the cluster to which they were assigned to are listed in Table 1.5, and illustrations of the four clusters and their constituent amino acids on the surface of UL25nt are shown in Figure 1.24. All four potential binding interfaces contain both charged and uncharged residues. Three of the four clusters are located on or near areas where there are disordered flexible loops and it is conceivable that these unstructured loops become ordered upon binding to another protein partner. C1 resides are on the same face as C2, which traverses the entire molecule and lies adjacent to L5. C3 is situated at the opposite end of the molecule from C1, near L3, whereas C4 also lies next to L3 but is located on the face 180° from C1 and C2. The wide distribution of the



**Figure 1.23 Evolutionary trace of herpesvirus UL25 homologues**

P01 to P10 represent the different partitions of the ET phylogenetic tree. The branches defining the three herpesvirus subfamilies are labelled  $\alpha$ ,  $\beta$  and  $\gamma$ . The numbers 1-9, which are highlighted in red, denote the nine protein classes at P07 that contain more than a single member. The virus species are listed next to the tree and the names in boldface are human viruses (adapted from Bowman et al., 2006).

Cluster	Cluster Residues								
<b>C1</b>	G225	R288	R305	P327	G331	H348	R362	G363	N365
<b>C2</b>	R148	D150	N152	D156	L214	N508			
<b>C3</b>	G169	S170	G172	R180	G202	R203	K206	P413	
<b>C4</b>	R390	N396	Y398	D400	L402	R552			

**Table 1.5 The residues within the four clusters (C1-C4) of pUL25 identified in the structural analysis**

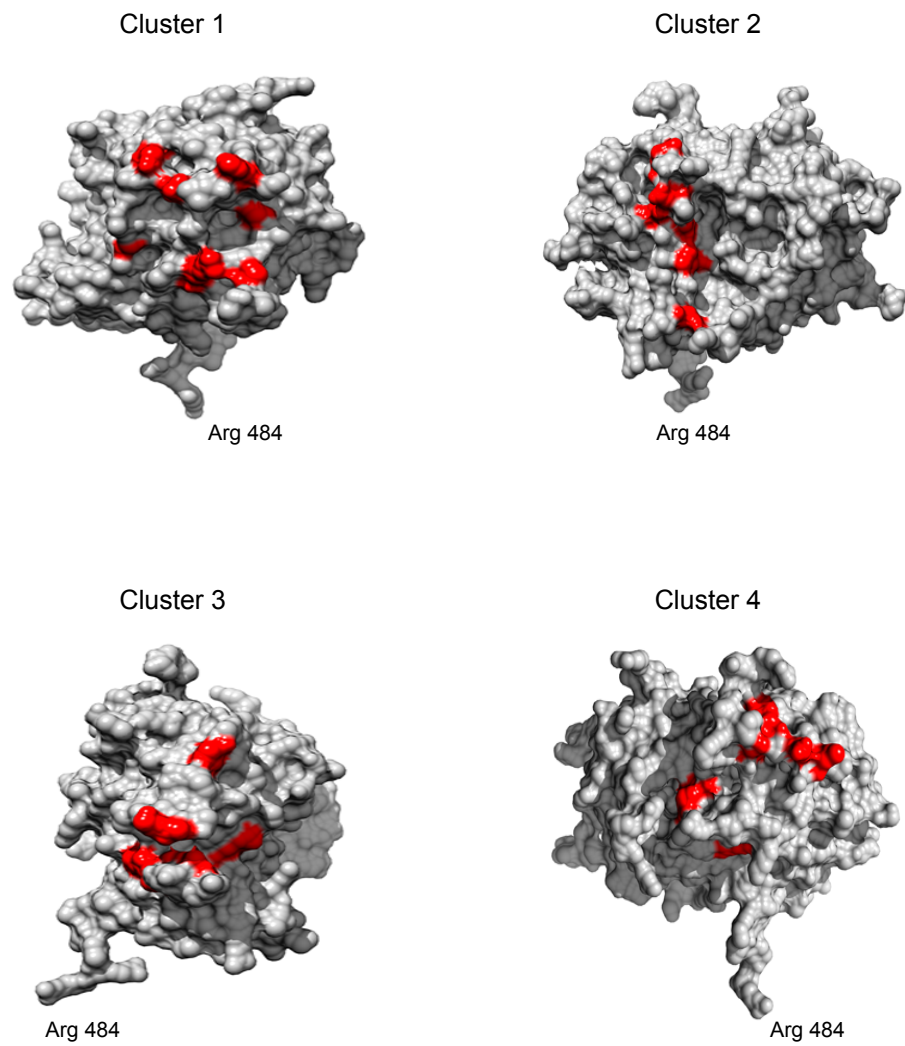


**Figure 1.24 UL25nt predicted functional amino acid clusters**

Space-filling models of UL25nt, with the exterior residues identified by the evolutionary trace for each cluster highlighted in red. The position of the residue arginine 484 (Arg 484) in UL25nt is indicated as a reference point.

predicted binding sites on UL25nt, its flexible architecture and distinctive electrostatic pattern, are consistent with an intrinsically plastic and dynamic protein that is capable of accommodating the multiple roles that pUL25 is implicated in.

## 1.5 The binding partners of pUL25

The HSV-1 UL25 gene product is a multifunctional capsid protein that is essential during viral DNA packaging (Section 1.3.5.2.5), is important for viral entry and has been implicated during viral egress. In addition, it interacts with an assortment of virus and cellular encoded proteins that are required during these processes (Table 1.6). The UL25 protein is located on the capsid surface and binds to the structure in increasing amounts as the capsid matures during DNA packaging, with the highest concentrations of pUL25 identified on C-capsids (Newcomb et al., 2006, Ogasawara et al., 2001, Sheaffer et al., 2001, Thurlow et al., 2006, Trus et al., 2007). This observation led to the proposal that pUL25 stabilises the C-capsid by attaching to binding sites that are exposed on the surface of the capsid as it matures during DNA packaging. In support of this model was the finding that removal of viral DNA from C-capsids led to a reduction in the amount of pUL25 attached to the A-capsids that were generated (Trus et al., 2007). The binding of pUL25 to capsids is also dependent on the presence of another essential DNA packaging protein, pUL17, since B-capsids lacking pUL17 contain low levels of pUL25 (Thurlow et al., 2006). Similarly, reduced levels of pUL17 are found on capsids isolated from non-permissive cells infected with a UL25 null mutant. These two observations led to the suggestion that pUL25 and pUL17 interact with each other (Thurlow et al., 2006).

A subsequent study involving cryoelectron microscopy and image reconstruction provided further evidence that pUL25 binds to pUL17. Extra mass was identified on the surface of the wt C-capsid, adjacent to the pentons at the capsid vertices, which was not seen on wt and UL25-null mutant A-capsids. This extra mass, referred to as the C-capsid specific component (CCSC), was proposed to be a complex of pUL25 and pUL17 (Trus et al., 2007). Additional contact points were also identified for pUL25 on the capsid that were calculated to be located

at the triplexes and peripentonal hexons surrounding the penton. These findings are corroborated by observations that pUL25 interacts directly with the triplex protein VP19C and the major capsid protein, VP5 (Ogasawara et al., 2001). Trus et al. (2007) proposed that the predicted triplex and hexon interaction sites for pUL25 are the binding sites, which are exposed as a consequence of the conformational changes induced in the capsid during DNA packaging. In addition they suggested that, as a consequence of the pUL25 binding to pUL17, VP19C and VP5, during capsid maturation, the shell is stabilised during encapsidation of full-length viral genomes.

UL25 protein partners	Reference
pUL6	Pasdeloup et al., 2009
pUL17	Thurlow et al., 2006; Trus et al., 2007
pUL36	Coller et al., 2007; Pasdeloup et al., 2009
VP5	Ogasawara et al., 2001
VP19C	Ogasawara et al., 2001
Nucleoporin CAN/Nup214	Pasdeloup et al., 2009
Nucleoporin hCG1	Pasdeloup et al., 2009

**Table 1.6 UL25 protein binding partners**

Immunofluorescence studies have demonstrated that the capsid-binding domain (CBD) of the HSV-1 large tegument protein pUL36 requires the presence of pUL25 for its recruitment onto capsids, indicating a role for pUL25 during tegumentation (Coller et al., 2007, Lee et al., 2006). Co-immunoprecipitation experiments have confirmed that the CBD, which consists of the 62 amino acid carboxyl-terminal region of pUL36, interacts directly with pUL25 (Coller et al., 2007). Previous studies have shown that the CBD of PrV pUL36 localises to nuclear capsid assembly sites when transiently expressed as a GFP-fusion protein in virus-infected cells (Lee et al., 2006). Although not addressing the site of tegumentation, Coller et al. (2007) proposed that the interaction between pUL25 and pUL36 is the initial step necessary for tegument acquisition during virus assembly.

## 1.6 The aims of the study

Although the 3D crystal structure of the N-terminally truncated form of pUL25 (UL25nt, residues 134-580) has been determined, the lack of structural similarity to a known protein has made it difficult to deduce the function of the protein with reference to the structural information alone (Bowman et al., 2006). ET analysis had identified clusters of external residues, which are likely to be important during protein interactions, and flexible loops that may be essential in accommodating the conformational alterations necessary for these interactions. The UL25 encoded gene product is a multifunctional protein that is important at a number of stages during the virus life cycle and has several protein partners that are also involved at these points of the HSV-1 growth cycle. The aim of the project was to exploit the 3D crystallographic information for HSV-1 pUL25 by engineering site-directed mutations into selected regions of the gene and characterising the resulting mutant proteins in order to relate the protein's structure to its function. It was anticipated that by determining the effect the mutations had on the function of pUL25 the project would lead to a better understanding of the protein's role(s) during HSV-1 lytic infection.

## 2 Materials and methods

### 2.1 Materials

#### 2.1.1 Chemicals and reagents

The chemicals and reagents used for EM analysis were purchased from Agar Aids or TAAB laboratories. All other chemicals and reagents were obtained from Sigma-Aldrich Co. Ltd, unless otherwise stated below or in subsequent sections.

Chemical	Supplier
Acetic acid	Rhone-Poulenc Ltd
Acrylamide solution (40% w/v)	Bio-Rad Laboratories
Acrylamide: N, N'methylene-bis acrylamide Solution, 19:1 (40% w/v)	Bio-Rad Laboratories
Ammonium persulphate	Bio-Rad Laboratories
BDMA	Bio-Rad laboratories
Blotting paper	Whatman International Ltd
Butanol	Prolabo
Chloroform	Prolabo
Copper grids	Agar Aids
Dimethyl sulphoxide (DMSO)	BDH laboratory Supplies
DNA (lambda) 1 Kb ladder	New England Biolabs
ECL reagent	GE Healthcare
EDTA (ethylenediaminetetraacetic acid disodium salt)	BDH

Chemical	Supplier
Ethanol	Prolabo
Epon 812 Resin	TAAB
Glacial acetic acid	Prolabo
Glass fibre discs	Whatman International Ltd
Glutaraldehyde	Agar Scientific
Hydrochloric acid	Rhone-Poulenc Ltd
IPTG (Isopropyl $\beta$ -D-1-thiogalactopyranoside)	Gibco BRL
Lipofectamine reagent	Invitrogen
Methanol	Prolabo
Optimem	BDH
Osmium tetroxide	TAAB
PCR tubes	Applied Biosystems
Plus reagent	Invitrogen
Mini protease inhibitor tablets	Boehringer Mannheim
Rainbow markers	GE Healthcare
Surfact-Amps <sup>TM</sup> NP40	Pierce
Uranyl acetate	BDH
X-omat film	Kodak Ltd

### 2.1.2 Enzymes

New England Biolabs, Sigma-Aldrich Co. Ltd, or Roche Diagnostics Ltd supplied the restriction enzymes and DNA modifying enzymes.

### 2.1.3 Antibiotics

The antibiotics used in this study together with their suppliers are listed below:

Antibiotic	Supplier
Ampicillin	Smithkline Beecham Research
Chloramphenicol	Sigma-Aldrich Co. Ltd
Gentamicin	Life Technologies
Kanamycin	Sigma-Aldrich Co. Ltd
Penicillin	Life Technologies
Streptomycin	Life Technologies
Tetracycline	Sigma-Aldrich Co. Ltd

### 2.1.4 Tissue culture cell lines

Vero cells (Rhim and Schell, 1967): These African green monkey kidney cells were obtained from the American Type Culture Collection and supplied by Dr. V. Preston.

8-1 cells (McNab *et al.*, 1998): This Vero cell line, which expressed the HSV-1 packaging gene UL25 under the control of the HSV-1 ICP6 promoter, was obtained from Dr P. Desai and supplied by Dr V. Preston.

Sf21 cells (Vaughn *et al.*, 1977): This insect cell line was derived from pupal ovarian tissue of the fall armyworm (species *Spodoptera frugiperda*) and obtained from the MRC Virology Unit's Cytology Department.

U2OS cells (Ponten and Saksela, 1967): This epithelial cell line was cultured from the cancerous bone tissue of a human female suffering from osteosarcoma.

It was obtained from the American Type Culture Collection and supplied by Dr V. Preston.

### **2.1.5 Tissue culture medium and growth conditions**

Tissue culture media were obtained from Gibco BRL and media supplements were purchased from Life Technologies, except for human serum (HS), which was supplied by MP Biomedicals LLC. The growth medium and supplement requirements for each of the cell lines used were as follows:

Vero and 8-1 cells were grown at 37°C in atmosphere containing 5% CO<sub>2</sub> in Dulbecco's modified Eagle's medium (DMEM) supplemented with 1X penicillin (pen)/streptomycin (stp) (100 units/ml pen and 100 µg/ml stp) plus 10% (v/v) foetal calf serum (FCS).

U2OS cells were grown under the same conditions as Vero and 8-1 cells except that a concentration of 5% (v/v) FCS was used.

Sf21 cells were cultured at 28°C in TC100 medium supplemented with 1X pen/stp and 5% (v/v) FCS.

### **2.1.6 HSV-1 stocks**

Wild-type (wt) HSV-1 strain 17 *syn*<sup>+</sup> (Brown *et al.*, 1973): This virus was obtained from the MRC Virology Unit's virus stocks.

ΔUL25MO: This deletion mutant lacks the complete UL25 ORF (nucleotide sequences 48,813 to 50,555 in the HSV-1 strain 17 *syn*<sup>+</sup> genome) and contains in its place the rpsL-neo antibiotic selection cassette (Chapter 3).

KUL25NS (McNab *et al.*, 1998): This UL25 null mutant was a gift from Dr P. Desai and was supplied by Dr V. Preston. The virus has a 14bp *SpeI* linker containing stop codons in all 3 open reading frames inserted at codon 104 of the UL25 ORF.

MRUL25MO: Marker rescuant of ΔUL25MO (Section 3.3.2).

### 2.1.7 Baculoviruses

The 11 recombinant baculoviruses listed below were used in this study. AcUL25- $\Delta$ 1-45, - $\Delta$ 1-59, - $\Delta$ 1-133 and AcUL17 were supplied by Dr V. Preston and the remaining viruses were constructed during this project using the procedure outlined in Section 2.2.12. The inserted genes in each virus were under the control of the HCMV IE promoter.

Baculovirus	Expressed HSV-1 Protein
AcpCI	None
AcWTUL25	pUL25
AcUL25-C3B	pUL25-C3B
AcUL25-C4A	pUL25-C4A
AcUL25-L3	pUL25-L3
AcUL25-L5	pUL25-L5
AcUL25-L6	pUL25-L6
AcUL25 $\Delta$ 1-45	pUL25 $\Delta$ 1-45
AcUL25 $\Delta$ 1-59	pUL25 $\Delta$ 1-59
AcUL25 $\Delta$ 1-133	pUL25 $\Delta$ 1-133
AcUL17	pUL17

### 2.1.8 *E. coli* strains and culture medium

DH5 $\alpha$  (Life Technologies): This strain of *E. coli* contains the *endA* and *recA* mutations. The *endA* mutation prevents the degradation of the plasmid DNA by eliminating endonuclease I activity in the bacterial cell, thereby improving the quality of the DNA preparations. The *recA* mutation enhances the stability of the plasmid by reducing homologous recombination between plasmid DNAs within the bacterial cell.

DH10Bac: This strain of *E. coli* contains the baculovirus shuttle vector (bacmid), bMON14272, and a helper plasmid, the mini-F replicon pMON7124. Electrocompetent DH10Bac cells (Section 2.2.5) were used to create the recombinant baculoviruses. Bacteria were grown in the presence of 50  $\mu$ g/ml

kanamycin (km) to maintain the bacmid and 10 µg/ml tetracycline (tet) to maintain the helper plasmid.

DH10B: This is a transformation competent strain of *E. coli* used as the host bacteria for the mutation of a bacterial artificial chromosome (BAC) possessing a copy of a mutated HSV-1 strain 17 syn<sup>+</sup> genome (fHSVΔpac) (Saeki et al., 1998) lacking the packaging signals. The bacteria containing the BAC were maintained in the presence of 15 µg/ml of chloramphenicol (cm) and 50 µg/ml of stp.

BL21: This strain was used for expression of the GST tagged fusion proteins and was purchased from Stratagene.

### *E. coli* culture medium

*E. coli* strains were cultured in L-broth containing the appropriate antibiotic, if required, for selection of the desired plasmid, BAC or recombinant bacmid.

## 2.1.9 Plasmids

pGEM-T Easy: This plasmid was used as a vector for cloning PCR products. The plasmid was obtained from Promega as a linearised DNA molecule with a 3'-terminal thymidine residue added to both ends. Since the Taq polymerase used in the PCR reactions described in this thesis adds a single deoxyadenosyl residue to the 3' ends of the PCR products produced, the PCR fragments were directly cloned into pGEM-T Easy (Figure 4.4) without further enzymatic manipulation.

pFBpCI: This plasmid was produced by Professor R. Everett from the MRC Virology Unit, Glasgow (Sourvinos & Everett, 2002) and was made by inserting a *Bgl*III/*Eco*RI fragment, containing the promoter and enhancer sequences from pCI-neo (Promega), into *Bam*HI/*Eco*RI digested pFastBac Hta (Life Technologies) (Figure 5.2). The plasmid was used as a cloning plasmid for the UL25 ORF, as a mammalian expression vector and as a baculovirus transfer vector for the production of the recombinant baculovirus.

pGX37: This plasmid contains the HSV-1 strain 17 syn<sup>+</sup> *Bam*HI G fragment, (HSV-1 strain 17 syn<sup>+</sup> nucleotides 52589-60363), inserted into the *Bam*HI site of the

plasmid vector pAT153 (Abbotts et al., 2000)). The *Bam*HI G probe used in Southern blot hybridisation was purified from the *Bam*HI-digested pGX37 vector.

pGX2: This plasmid contains the HSV-1 strain 17 syn<sup>+</sup> *Bam*HI K fragment (HSV-1 strain 17 nucleotides 123461-129403) inserted into the *Bam*HI site of pAT153. The *Bam*HI K fragment in this plasmid has a single *a* sequence.

pGX292: This plasmid contains the HSV-1 strain 17 syn<sup>+</sup> *Bam*HI U fragment inserted into the *Bam*HI site of pAT153. *Bam*HI U spans the HSV-1 strain 17 syn<sup>+</sup> nucleotides 48635 - 50929, which contains the entire UL25 ORF.

pBE1: This plasmid was derived from pGX2 and was constructed to detect the joint spanning region and the L terminus of the HSV-1 genome (Stow, 2001). It contains sequences corresponding to HSV-1 strain 17 syn<sup>+</sup> nucleotides 596 to 2905 of TR<sub>L</sub> (Figure 5.1).

pST17: This plasmid, like pBE1, was derived from pGX2 but was constructed to detect the joint spanning region and the S terminus of the HSV-1 genome (Stow, 2001). It contains sequences corresponding to HSV-1 strain 17 syn<sup>+</sup> nucleotides 148825 to 151857 of TR<sub>S</sub> (Figure 5.1).

pGEX-2TNMCR: This plasmid was produced by Professor R. Everett from the MRC Virology Unit, Glasgow, and was derived from a commercially available plasmid, pGEX2T (Pharmacia). The vector was designed for inducible, high-level bacterial expression of proteins or protein fragments as fusions with *Schistosoma japonicum* glutathione S-transferase (GST). Expression of GST fusion proteins was under the control of the IPTG-inducible tac promoter.

### 2.1.10 Antibodies

Anti-pUL25 MAb166: The mouse monoclonal antibody (MAb) was raised against purified HSV-1 UL25-His tagged protein (Thurlow et al., 2005) and diluted 1:1000.

**Anti-pUL25 RAb335:** The rabbit polyclonal antibody was raised against purified HSV-1 UL25 (residues 342 - 580) GST fusion protein (Thurlow et al., 2006) and diluted 1:1000.

**Anti-pUL17 MAb203:** The MAb was raised against purified HSV-1 UL17-NusA tagged protein (residues 154-703) (Thurlow et al., 2005) and diluted 1:1000.

**Anti-GST antibody:** The goat polyclonal antibody was raised against purified GST (GE Healthcare) and diluted 1:2000.

**Anti-goat IgG hrp-conjugate:** The donkey polyclonal antibody was raised against purified goat IgG conjugated to horseradish peroxidase (Santa Cruz Biotechnology) and diluted 1:80000.

**Protein A hrp-conjugate:** protein A-horseradish peroxidase (Sigma-Aldrich) was diluted 1:1000.

**Anti-mouse IgG hrp-conjugate:** The goat polyclonal antibody was raised against mouse IgG and conjugated to horseradish peroxidase (Sigma-Aldrich) and diluted 1: 1000.

**Anti-mouse IgG FITC-conjugate:** The goat polyclonal antibody was raised against purified mouse IgG and conjugated to the fluorophore FITC (Sigma-Aldrich) and diluted 1:100.

### 2.1.11 Buffers and solutions

Common solutions	Constituents
Acid wash	0.14 M NaCl, 0.1M glycine pH 3.0
Alkaline transfer solution	0.4 M NaOH, 0.6 M NaCl
Antibody buffer A	5% (w/v) marvel, 0.05% (v/v) Tween-20 in PBS
Antibody buffer B	2% (w/v) marvel, 0.05% (v/v) Tween-20 in PBS
Boiling mix (3X)	6% (w/v) SDS, 30% (v/v) glycerol, 0.3% (w/v) bromophenol blue, 210 mM $\beta$ -mercaptoethanol
Buffer A	50 mM Tris HCl pH 7.5, 100 mM NaCl, 5% Glycerol, 0.1% Triton X100
Chloroform:Isoamyl alcohol	24 parts chloroform:1 part isoamyl alcohol (v/v)

Common solutions	Constituents
CLB (Cell lysis buffer) (2X)	20 mM TrisHCl pH 7.5, 2 mM EDTA, 1.2% SDS
DABCO solution	25% DABCO in dH <sub>2</sub> O, stored at -20°C
Denhardt's solution	0.02% Ficoll 400, 0.02% polyvinylpyrrolidone, 0.02% bovine serum albumin
DNA loading buffer (4X)	0.1 M EDTA, 0.25% (w/v) bromophenol blue, 50% (w/v) sucrose
Elution buffer	500 mM NH <sub>4</sub> Acetate, 1 mM EDTA, 0.1% SDS
Epon 812 resin mix	150 µl DBMA, 10 ml Epon 812 resin
EZ lysis buffer	100 mM TrisHCl pH 8.0, 100 mM KCl, 10% glycerol, 1% NP40. 1 mini protease tablet per 10 ml buffer
Hybridisation buffer	50% formamide, 10% dextran sulphate and 4X SSC (1X SSC is 0.15 M NaCl, 0.015 M sodium citrate)
Loening's buffer (1X)	40 mM NaH <sub>2</sub> PO <sub>4</sub> , 36 mM Tris, 1mM EDTA
Lead citrate solution	1.33g Pb(NO <sub>3</sub> ) <sub>2</sub> , 1.76g Na <sub>3</sub> (C <sub>6</sub> H <sub>5</sub> O <sub>7</sub> ).2H <sub>2</sub> O, 30 ml boiled and cooled dH <sub>2</sub> O
Membrane wash buffer	0.2X SSC, 0.1% SDS
Mowiol mounting solution	2.4g Mowiol 4-88, 6g glycerol, 6 ml dH <sub>2</sub> O, 12 ml 0.2 M Tris HCl pH 8.5, 10% DABCO solution
Neutralising solution	0.5 M TrisHCl pH 7.0
PBS (Phosphate-buffered saline)	170 mM NaCl, 3.4 mM KCl, 10 mM Na <sub>2</sub> HPO <sub>4</sub> , 1.8 mM KH <sub>2</sub> PO <sub>4</sub> , pH 7.2
PBS-1% FCS	PBS containing 1% Foetal calf serum
10X Phosphate buffer	58 mM Na <sub>2</sub> HPO <sub>4</sub> , 17 mM NaH <sub>2</sub> PO <sub>4</sub> , 68 mM NaCl pH 7.5
Protease	20 mg/ml grade XIV protease
RGB (4X Resolving gel buffer)	1.5 M TrisHCl pH 8.8, 0.4% (w/v) SDS
RNase mix (200X)	1 mg/ml RNaseA, 10000 u/ml RNase T1 in TE
Sonication buffer	20 mM TrisHCl pH 7.5, 0.1% NP40., 10% glycerol, 1 miniprotease tablet per 7 ml of buffer
RSB (Reticulocyte standard buffer)	10 mM TrisHCl pH 7.5, 10 mM KCl, 1.5 mM MgCl <sub>2</sub>
SGB (4X Stacking gel buffer)	488 mM TrisHCl pH 6.8, 0.4% (w/v) SDS
Southern prehybridisation buffer	0.5 M sodium phosphate buffer pH 7.4, 7% SDS
SSC (20X)	3 M NaCl, 0.3 M sodium citrate
Tank buffer (1X)	52 mM Tris, 53 mM glycine, 0.1% SDS
TBE (Tris-borate-EDTA)	90 mM Tris base, 89 mM boric acid, 1 mM EDTA
TBS (Tris-buffered saline)	137 mM NaCl, 5 mM KCl, 0.7 mM NaH <sub>2</sub> PO <sub>4</sub> , 5.5 mM glucose, 25 mM TrisHCl pH 7.4
Towbin buffer	25 mM Tris, 192 mM glycine, 20% (v/v) methanol
Triton 1X buffer	0.1% Triton X100 diluted in PBS and 1 miniprotease tablet per 7 ml of solution
Trypsin	0.25% (w/v) trypsin (Sigma-Aldrich) dissolved in TBS
Versene	0.6 mM EDTA, 0.002% phenol red in PBS
X-gal solution	20 mg/ml X-gal in dimethyl formamide

### 2.1.12 Oligonucleotides

Oligonucleotides for PCR amplification and sequencing were synthesised and purified by either Sigma-Genosys or MWG Biotech.

### 2.1.13 Radiochemicals

5' ( $\alpha^{32}\text{P}$ ) dCTP and 5' ( $\alpha^{32}\text{P}$ ) dGTP, at 10  $\mu\text{Ci}/\mu\text{l}$  (3000 Ci/mMole), were purchased from GE Healthcare, UK.

### 2.1.14 Commercial kits

The commercial kits used in this study are listed in below or in the relevant sections.

Commercial Kits	Supplier
Advantage <sup>TM</sup> -GC 2 PCR Kit	Clontech
Counter-Selection BAC Modification Kit Version 2.4 (June 2005)	Gene Bridges
pGEM-T Easy Vector System	Promega
Qiagen Plasmid Purification – QIAGEN-tip 100 (3 <sup>rd</sup> Edition June 2005)	Qiagen
QIAprep Spin Miniprep Kit	Qiagen
QIAQuick Gel Extraction Kit	Qiagen

### 2.1.15 Computer software

Computer software used for analysis in this study and the manufacturer or web link is listed below:

Computer Software	Link/Manufacturer
ET analysis	<a href="http://www-cryst.bioc.cam.ac.uk/~jjye/evoltrace/evoltrace.html">http://www-cryst.bioc.cam.ac.uk/~jjye/evoltrace/evoltrace.html</a>
Protein Bank Database	<a href="http://www.rcsb.org">http://www.rcsb.org</a>
SIFT Analysis	<a href="http://sift.jcvi.org">http://sift.jcvi.org</a>
Webcutter	<a href="http://rna.lundberg.gu.se/cutter2/">http://rna.lundberg.gu.se/cutter2/</a>
Chimera	<a href="http://www.cgl.ucsf.edu/chimera">http://www.cgl.ucsf.edu/chimera</a>

## 2.2 Methods

### 2.2.1 DNA cloning and manipulation

#### 2.2.1.1 Restriction endonuclease digests

Typically, 1  $\mu\text{g}$  of plasmid DNA was digested with 10 units of the desired restriction endonuclease (REN) in a 20  $\mu\text{l}$  reaction volume containing the appropriate restriction buffer and 2  $\mu\text{g}$  BSA (if recommended) for 1-4 hours (h) at the recommended temperature. For double digests both RENs were added to the same reaction provided the enzyme conditions were compatible, if not, two sequential reactions were carried out. In this instance the DNA was digested with the first REN in a reaction volume of 20  $\mu\text{l}$  at the recommended temperature for 1-2 h. This was followed by the addition of the second REN and modification of the REN buffer in a final volume of 30  $\mu\text{l}$ . The incubation was continued for a further 1-2 h at the second enzyme's recommended temperature. All REN digests were confirmed by gel electrophoresis (Section 2.2.3.1).

#### 2.2.1.2 Polymerase chain reaction (PCR)

Each PCR was set up in thin-walled 0.2 ml PCR tube using the enzyme, buffer and dNTP mix from the Clontech Advantage<sup>TM</sup>-GC 2 PCR kit. A typical PCR reaction mix contained 50 ng of template DNA with the forward and reverse primers at a concentration of 100 pmoles/ $\mu\text{l}$  in a total volume of 50  $\mu\text{l}$ . The PCRs were performed using Applied Biosystems GeneAmp PCR System 9700 thermocycler running the following programmes:

PCR –cycle1	
Step 1: 1 cycle	95°C for 5 min
Step 2: 35 cycles	95°C for 30 sec
	58°C for 1 min
	68°C for 2 min
Step 3: 1 cycle	68°C for 7 min
Step 4	Hold at 4°C

PCR-cycle2	
Step 1: 1 cycle	95°C for 5 min
Step 2: 30 cycles	95°C for 30 sec
	68°C for 3 min
Step 3: 1 cycle	68°C for 7 min
Step 4	Hold at 4°C

### 2.2.1.3 Annealing overlapping oligonucleotides

Each oligonucleotide was supplied as a lyophilised powder and resuspended in the appropriate amount of dH<sub>2</sub>O to give a final concentration of 100 pmoles/ $\mu$ l. The two oligonucleotides were mixed together and diluted to a final concentration of 10 pmoles/ $\mu$ l in 1X T4 ligase buffer (BRL) in a total volume of 50  $\mu$ l. The reaction mix was heated to 100°C for 5 minutes (min) and allowed to cool slowly to room temperature (RT). The sample was stored at -20°C until required.

## 2.2.2 Ligation of DNA fragments

### 2.2.2.1 Standard ligation

Purified insert and vector DNA fragments were mixed at a 3:1 molar ratio in a 10  $\mu$ l reaction volume containing 1 unit of T4 DNA ligase and 1X T4 ligase buffer (BRL). The reaction was incubated overnight at 16°C followed by storage at -20°C until required.

### 2.2.2.2 Ligation of PCR products

Typically, a molar ratio of 3:1 of gel-purified PCR product to pGEM-T Easy vector was used for the ligation reactions. The identity of the cloned PCR product was confirmed by analytical REN digestion and DNA sequencing.

### **2.2.2.3 Ligation of overlapping oligonucleotides**

Annealed overlapping oligonucleotides, which were prepared as outlined in Section 2.2.1.3, were routinely diluted 1:3 or 1:10 in dH<sub>2</sub>O and 1 µl was used in the ligation reaction.

## **2.2.3 DNA analysis and purification**

### **2.2.3.1 Separation and purification of restriction endonuclease (REN) fragments on agarose gels**

Routine analysis of DNA REN digests was carried out on 1% agarose gels in 1X TAE. The gels were prepared by heating the agarose mixture in a microwave oven until the agarose was dissolved. After the solution had cooled to 55-60°C, 5 µl ethidium bromide (10 mg/ml) was added and the solution, which was then poured into a horizontal gel kit containing a 14-well comb. When the gel had set it was submerged in 1X TAE buffer, the comb was removed and the samples, containing 4X DNA loading buffer (1:4 loading buffer:sample), and the appropriate size markers were added to the wells. The gel was electrophoresed in a BRL horizontal electrophoresis apparatus at 100 V for 30-40 min. The DNA fragments were visualised under long-wave UV light and excised from the gel using a sterile scalpel. DNA fragments were purified from agarose gel slices using the Qiagen Qiaquick Gel Extraction kit in accordance with the standard protocol supplied.

### **2.2.3.2 Separation and purification of REN fragments on polyacrylamide gels**

#### **Separation**

DNA fragments of less than 500 bp were resolved on 5% polyacrylamide gels. The gels were prepared by mixing 8.3 ml 40% acrylamide bis-acrylamide (19:1) (Bio-Rad), 4.2 ml 40% acrylamide, 5 ml 10X TBE, 100 µl TEMED, 700 µl 10% ammonium persulphate in a final volume of 100 ml. The mixture was immediately poured between glass plates and a 12-well comb inserted. Once the gel had set the samples to be analysed were mixed with 4X DNA loading buffer and loaded onto the gel. The samples were run alongside a 100 bp ladder

and electrophoresed in 1X TBE at 100 V for 30-40 min, before the bromophenol blue dye front reached the bottom of the gel. The DNA fragments were stained by submersing the gel for 30 min in a 100ml solution of 1X TBE containing 5  $\mu$ l of ethidium bromide (10 mg/ml). The DNA was visualised under long-wave UV light and the DNA fragment was excised from the gel using a sterile scalpel.

### Purification

The excised fragment was transferred to a 0.5 ml reaction tube, containing a small aperture in the bottom, and the tube placed inside a 1.5 ml reaction tube. After the sample had been centrifuged at 13000 rpm for 5 min in a microcentrifuge, 400  $\mu$ l of elution buffer (Section 2.1.11) was added to the pulverised gel in the 1.5 ml reaction tube, and the mixture incubated overnight at 42°C. The polyacrylamide gel was removed from the mixture by filtering the sample through a glass fibre disc, pre-soaked briefly in elution buffer and placed in a 2 ml syringe. Two volumes of ethanol (200  $\mu$ l) were added to the filtered sample and the tube was placed on dry ice. After 1 h incubation the sample was centrifuged at 13000 rpm in a bench-top microcentrifuge for 10 min and the supernatant discarded. The DNA pellet was dissolved in 300  $\mu$ l of sodium acetate pH 5.5 and 600  $\mu$ l of ethanol was added to the solution to precipitate the DNA. The mixture was chilled on dry ice for 30 min prior to centrifugation at 13000 rpm for 10 min. The supernatant was removed and the DNA pellet was washed in 70% ethanol. The centrifugation step repeated and the supernatant was removed and discarded. The DNA pellet was left to air dry for 5 to 10 min at RT and then dissolved in 30  $\mu$ l 10mM TrisHCl pH 8.0. Typically, 3  $\mu$ l of the sample was analysed on an agarose gel (Section 2.2.3.1) to determine the yield and purity of the eluted DNA fragment, while the remainder of the sample was stored at -20°C until required.

#### 2.2.3.3 Plasmid DNA preparation

Plasmid DNA was routinely isolated from bacterial clones using 1.5 ml of a 5 ml overnight bacterial culture (Section 2.2.4). The culture was transferred into a 1.5 ml reaction tube and the bacteria centrifuged for 1 min at 13000 rpm in a bench-top microcentrifuge. The supernatant was discarded and the pelleted

bacteria were processed using the QIAprep Spin Miniprep Kit (Section 2.1.14) according to the manufacturer's instructions. The final concentration of the plasmid DNA was determined by measuring the absorbance at 260 nm ( $A_{260}$ ), based upon an  $A_{260}$  value of 1.0 corresponding to a dsDNA concentration of 50  $\mu\text{g}/\text{ml}$ . The identity of the plasmid DNA was confirmed by an analytical REN digest (Section 2.2.1.1) and DNA sequencing (Section 2.2.3.4). The plasmid stocks were stored at  $-20^{\circ}\text{C}$  until required.

#### **2.2.3.4 DNA sequencing**

All DNA sequencing was carried out commercially by Geneservices Ltd.

### **2.2.4 Growth and maintenance of *E. coli* bacteria**

#### **2.2.4.1 Culture of *E. coli***

For the production of small-scale *E. coli* cultures a tube containing 5 ml of L-broth supplemented with the appropriate antibiotic was inoculated with a single isolated bacterial colony and the culture grown overnight at  $37^{\circ}\text{C}$  in the orbital shaker at 225 rpm. These cultures were used in the preparation of small amounts of plasmid DNA (Section 2.2.3.3). The small-scale bacterial culture was also used as a starter culture for large-scale plasmid DNA production. A volume of 2.5 ml of the overnight culture was added to 250 ml of L-broth, containing the appropriate antibiotics, and the sample incubated as before at  $37^{\circ}\text{C}$  overnight.

#### **2.2.4.2 Storage of *E. coli***

A small-scale culture of *E. coli* was grown as outlined above (Section 2.2.4.1). After overnight incubation 900  $\mu\text{l}$  of the cell suspension was transferred to a 1.5 ml cryotube and mixed with 100  $\mu\text{l}$  DMSO, frozen on dry ice and stored at  $-70^{\circ}\text{C}$ .

### **2.2.5 Preparation and transformation of electrocompetent *E. coli***

Prior to preparation each of the *E. coli* stocks was thawed from long-term storage at  $-70^{\circ}\text{C}$ . The bacterial suspension was streaked onto L-broth agar plates containing the appropriate antibiotics. Following overnight incubation at  $37^{\circ}\text{C}$  a

single colony was selected from each strain and used to produce the following electrocompetent bacteria.

### **2.2.5.1 *E. coli* DH5 $\alpha$**

A single colony of *E. coli* DH5 $\alpha$  was inoculated into a 50 ml starter culture of L-broth and incubated at 37°C in the orbital shaker at 225 rpm. The following day 20 ml of the starter culture were added to 1 litre of pre-warmed L-broth and the culture incubated as before until an OD<sub>600</sub> of 0.5 to 0.6 was reached. The contents were then transferred to six pre-chilled 250 ml Falcon tubes and incubated on ice for 30 min, followed by centrifugation at 3000 rpm for 25 min in a Sorvall SLA-1500 rotor. The bacterial pellets were vigorously resuspended in 200 ml of ice-cold sterile dH<sub>2</sub>O. The bacterial suspensions were centrifuged again at 3000 rpm and the supernatants were subsequently discarded. The dH<sub>2</sub>O wash was repeated twice more. After the final wash the combined cell pellet was vigorously resuspended in 20 ml of sterile dH<sub>2</sub>O containing 10% glycerol (v/v). The cell suspension was transferred to a pre-chilled 50 ml SS34 tube and centrifuged at 5800 rpm in a Sorvall SS34 rotor for 15 min at 0°C. After centrifugation the supernatant was discarded and the cell pellet was resuspended in 2 ml ice-cold sterile 10% glycerol. Aliquots (80  $\mu$ l) of the competent bacteria were stored at -70°C until required.

Aliquots of electrocompetent *E. coli* DH5 $\alpha$  were removed from -70°C storage and thawed slowly on ice immediately prior to electroporation using a Hybaid Cell Shock Electroporator. A 1  $\mu$ l volume of the appropriate ligation reaction was added to each aliquot of DH5 $\alpha$ . The mixture was transferred into a pre-chilled Gene Pulser cuvette (Bio-Rad), placed into the Hybaid Cell Shock CS 100 system set at 1.8 kV and the machine activated. The bacteria were subsequently resuspended in 1 ml of unsupplemented L-broth, transferred to a 25 ml universal and incubated in the orbital shaker at 37°C for 1 h. The bacterial suspension was diluted 1:10 in unsupplemented L-broth and a 100  $\mu$ l aliquot was plated onto an L-broth agar plate containing the appropriate antibiotic, followed by incubation overnight at 37°C. Plasmid DNA was prepared from the recombinant bacteria obtained as outlined in Section 2.2.3.3.

### 2.2.5.2 *E. coli* DH10Bac

Electrocompetent DH10Bac cells were prepared and transformed essentially as described for DH5 $\alpha$  (Section 2.2.5.1), except DH10Bac were grown in the presence of 50  $\mu\text{g}/\text{ml}$  km and 10  $\mu\text{g}/\text{ml}$  tet and following electroporation they were incubated for 4 h at 37°C. Serial dilutions of  $10^{-1}$  to  $10^{-3}$  of the bacterial suspension were prepared. A 100  $\mu\text{l}$  sample of each dilution was plated onto L-broth agar plates containing 50  $\mu\text{g}/\text{ml}$  km, 7  $\mu\text{g}/\text{ml}$  gentamicin (gm), 10  $\mu\text{g}/\text{ml}$  tet, 100  $\mu\text{g}/\text{ml}$  X-gal and 40  $\mu\text{g}/\text{ml}$  IPTG and the plates incubated at 37°C for 48 h. White bacterial colonies, unable to express functional  $\beta$ -galactosidase, were streaked onto fresh supplemented agar plates and incubated at 37°C overnight. Bacmid DNA was prepared from the recombinant bacteria obtained as outlined in Section 2.2.12.1.

### 2.2.5.3 *E. coli* DH10B

A single colony of *E. coli* DH10B carrying fHSV $\Delta$ pac was inoculated into 50 ml of L-broth, supplemented with 15  $\mu\text{g}$  cm and 50  $\mu\text{g}$  of stp, and grown overnight at 37°C. A 30  $\mu\text{l}$  aliquot of the bacterial suspension was inoculated into a universal containing 1.4 ml of L-broth and the antibiotics described above. After incubation at 37°C for 2 h on a platform shaker at 1000 rpm the bacterial suspension was transferred to a pre-chilled reaction tube and centrifuged at 11000 rpm for 30 sec at 4°C. The bacterial pellet was resuspended in 1 ml of ice-cold dH<sub>2</sub>O and centrifuged as before. The electrocompetent bacteria were resuspended in a residual volume of the supernatant (30  $\mu\text{l}$ ) and stored on ice prior to transformation as outlined in section 2.2.8.

### 2.2.5.4 *E. coli* BL21

A single colony of *E. coli* BL21 was inoculated into 5 ml L-broth and incubated at 37°C in the orbital shaker at 225 rpm overnight. A 30  $\mu\text{l}$  aliquot of the overnight culture was inoculated into 1.4 ml of L-broth in a universal and the culture incubated as before. After 2-3 h incubation the culture was transferred to a pre-chilled reaction tube and the bacteria pelleted by centrifugation at 13000 rpm for 30 sec in a microcentrifuge located in the 4°C cold room. The

supernatant was discarded and the pellet was resuspended in ice-cold dH<sub>2</sub>O, followed by centrifugation at 13000 rpm for 30 sec. The wash was repeated twice more. After the final wash the bacterial pellet was resuspended in a volume of 30 µl of the residual supernatant and the remaining supernatant was discarded. The bacterial suspension was stored on ice prior to transformation as outlined in Section 2.2.5.1.

## **2.2.6 Maintenance and passage of tissue culture cells**

### **2.2.6.1 Mammalian cell lines**

Cells were grown overnight in a 175 cm<sup>2</sup> tissue culture dish and the confluent cell monolayer was rinsed with 20 ml of versene, followed by a brief wash in 20 ml of 1X trypsin (diluted in versene) at RT. The trypsinised cells were detached from the culture vessel by gentle agitation and resuspended in 10 ml of fresh medium. Typically, 1/5<sup>th</sup> of the total volume of resuspended Vero or 8-1 cells and 1/3<sup>rd</sup> of the total volume of resuspended U2OS cells was seeded into a new flask. The cells were passaged every 3-4 days.

### **2.2.6.2 Insect cell line**

Cells were grown overnight in a 175 cm<sup>2</sup> tissue culture dish. Confluent Sf21 monolayers were detached from the flask by agitation alone and resuspended in 10 ml of fresh medium. Generally, 2 ml of the cell suspension was seeded into a fresh flask and the cells passaged every 3-4 days.

### **2.2.6.3 Counting cells**

Tissue culture cells were diluted 1:10 in cell culture medium and counted in a haemocytometer (Neubauer) under an inverted light microscope (Olympus).

## **2.2.7 Complementation analysis**

### **2.2.7.1 Transfection of mammalian cells**

Duplicate transfections were prepared for each DNA sample that was analysed. Vero cells were seeded at a density  $1 \times 10^5$  cells/well in 24-well tissue culture dishes and incubated at 37°C. The following day 0.5 µg of the appropriate recombinant plasmid DNA was diluted in Optimem to a final volume of 21 µl in a 0.5 ml reaction tube and mixed with 4 µl of Plus reagent. After 15 min at RT 25 µl of diluted Lipofectamine (1 µl Lipofectamine + 24 µl Optimem) was added to each sample and the mixture was incubated for a further 15 min at RT. During the incubation the Vero cell monolayers were washed twice with unsupplemented growth medium and then overlaid with 200 µl of the same medium. The transfection mix (50 µl) was added to each cell monolayer and the cells incubated at 37°C for 3 h. The transfection mix was removed from the transfected cells and 1 ml of supplemented growth medium was added to each monolayer. One set of transfected cells was incubated overnight at 37°C and crude mammalian protein extracts were prepared (Section 2.2.7.2). The other set of transfected cells was incubated at 37°C for a further 2 h prior to virus infection and subsequent analysis using the complementation yield assay described in Section 2.2.7.3.

### **2.2.7.2 Production of crude mammalian protein extract**

The transfected cell monolayer (Section 2.2.7.1) in each well of the 24-well tissue culture dish was washed in 1 ml of PBS followed by the addition of 500 µl of fresh PBS. Each cell monolayer was scraped into PBS and the suspension was transferred to a reaction tube. After the sample had been centrifuged at 6000 rpm for 30 sec in a bench top microcentrifuge, the cell pellet was resuspended in 20 µl dH<sub>2</sub>O and the cells lysed by the addition of 10 µl of 3X boiling mix. The cell lysate was then stored at -20°C, if necessary. To determine the level of the recombinant proteins produced, a 15 µl sample of the cell lysate was analysed by Western blotting (Section 2.2.18.2).

### **2.2.7.3 Complementation yield assay**

The transfection mix was removed from each sample prepared in Section 2.2.7.1 and the transfected cells were washed once with 1ml of growth medium. Each monolayer was infected with 100  $\mu$ l HSV-1 UL25 null virus ( $\Delta$ UL25MO) at a concentration of 2 PFU/cell and incubated at 37°C for 1 h. To ensure that the virus was equally absorbed over the cell monolayer and that the cells did not dry out, the tissue culture dishes were gently rocked every 15 min throughout the incubation. After viral absorption, the cells were treated with acid as described in Section 2.2.7.4, followed by incubation in 1 ml of growth medium at 37°C. The next day each cell monolayer was scraped into the medium and transferred to a 15 ml Falcon tube prior to sonication at 4°C. The yield of the progeny virus produced was determined by titrating the virus on 8-1 cells (Section 2.2.10).

### **2.2.7.4 Acid wash of cell monolayers**

The acid wash was carried out in order to eliminate residual viral particles from the cell surface after viral absorption. The viral inoculum was removed from each monolayer, the cells were washed twice with 1 ml 0.14 M NaCl and then overlaid with 1 ml acid wash (Section 2.1.11) for 1 min at RT. The acid wash was promptly removed after incubation. The cells were washed with 1 ml of growth medium, then overlaid with 1 ml of fresh medium and incubated at 37°C.

## **2.2.8 Generation of HSV-1 UL25 null mutant ( $\Delta$ UL25MO)**

To generate the new HSV-1 UL25 null virus the commercially supplied Counter-Selection BAC Modification Kit (Gene Bridges version 2.4, 2005) was utilised. The manufacturer's recommended controls were included throughout the procedure to ensure that the techniques were correctly applied. A synopsis of the methodology and theory behind the strategy is outlined in Section 3.2. A revised and amended version of the manual used in the procedure can be seen at the link below:

<http://www.genebridges.com/gb/pdf/K001%20Q%20E%20BAC%20Modification%20Kit-version2.6-2007->

### **2.2.8.1 Transformation of DH10B carrying fHSV $\Delta$ pac with the Red/ET plasmid (pRed/ET) and expression of recombination enzymes**

A 1  $\mu$ l (20 ng) aliquot of the Red/ET plasmid (pRed/ET) (Gene Bridges) was electroporated into 30  $\mu$ l of freshly prepared electrocompetent DH10B cells (Section 2.2.5.3) containing the HSV-1 strain 17 syn<sup>+</sup> BAC (fHSV $\Delta$ pac). After electroporation the bacteria were resuspended in 1 ml of L-broth and incubated at 30°C for 70 min in a platform shaker at 1000 rpm. The transformed DH10B culture was plated onto L-broth agar plates, supplemented with 15  $\mu$ g/ml of cm and 3  $\mu$ g/ml of tet, and incubated at 30°C for 18-24 h. Since tet is light sensitive the agar plates containing this antibiotic were wrapped in tin foil during incubations. Following incubation a well-isolated single colony was selected and inoculated into 50 ml of L-broth containing cm/tet and the culture was incubated at 30°C for 18-24 h on the platform shaker at 1000 rpm. The next day duplicate samples (one set for the induced cultures and one set for the uninduced cultures), were prepared by adding 30  $\mu$ l of the overnight culture to 1.4 ml of L-broth supplemented with cm/tet. The duplicate bacterial suspensions were incubated at 30°C for 2 h on a platform shaker at 1000 rpm until the OD<sub>600</sub> reached 0.3. The expression of the genes mediating Red/ET homologous recombination was induced by adding 50  $\mu$ l of 10% L-arabinose to one set of samples (induced) and shifting the temperature from 30°C to 37°C. Both the induced and uninduced cultures were incubated at 37°C for 45-60 min on a platform shaker at 1000 rpm. After incubation the induced and uninduced bacterial suspensions were prepared for electroporation as described in section 2.2.5.3. The competent bacteria were subsequently transformed with the PCR product, rps-L neo-PCR1, as described below.

### **2.2.8.2 Step 1 of the Counter-Selection BAC Modification procedure:- insertion of rpsL-neo-PCR1 selection cassette into the HSV-1 BAC (fHSV $\Delta$ pac )**

A 2  $\mu$ l (200 ng) aliquot of the rpsL-neo-PCR1 product (Section 3.2.2) was electroporated into the induced and uninduced bacteria as described in Section 2.2.5.3. After electroporation 1 ml of L-broth was added to each cuvette and

the bacterial suspension was divided between two universals, representing the recombinant and non-recombinant samples. The non-recombinant samples for the induced and uninduced suspensions were retained on ice. The recombinant samples from the induced and uninduced cultures were incubated at 37°C for 70 min on the platform shaker at 1000 rpm to allow recombination between the PCR product and fHSV $\Delta$ pac to take place. After incubation each of the four cultures was streaked onto an L-broth agar plate supplemented with 15  $\mu$ g/ml cm, 3  $\mu$ g/ml tet and 15  $\mu$ g/ml km and incubated at 30°C for 36-48 h. Bacterial colonies from the recombinant induced samples were each inoculated into 100  $\mu$ l of L-broth, supplemented with cm/tet/km, and incubated for 1-2 h at 30°C on a platform shaker at 1000 rpm. After incubation four aliquots of each overnight culture were used as follows: an aliquot was prepared for storage (Section 2.2.4.2) and the other aliquots were used for the functional analysis of the rpsL-neo-PCR1 cassette (Section 2.2.8.3), preparation of recombinant BAC DNA (Section 2.2.8.4) and step 2 of the Counter-Selection BAC Modification procedure (Section 2.2.8.5).

### **2.2.8.3 Functional analysis of the rpsL-neo-PCR1 selection cassette**

To verify the km resistance (km<sup>R</sup>) of selected colonies from the induced recombinant plates (Section 2.2.8.2) each colony was replica plated onto L-broth agar plates containing either cm/tet and 50  $\mu$ g/ml stp or cm/tet/km and incubated at 37°C for 2 days. Bacteria containing an inserted and functional rpsL-neo-PCR1 cassette within the BAC should display km<sup>R</sup> and sensitivity to stp (stp<sup>S</sup>).

### **2.2.8.4 Preparation of BAC DNA and confirmation of correct insertion of the rpsL-neo-PCR1 selection cassette**

BAC DNA was prepared from bacterial cultures that were km<sup>R</sup> and stp<sup>S</sup>. A 30  $\mu$ l aliquot of bacterial culture from the 30°C incubation described in Section 2.2.8.2 was transferred into 2 ml of L-broth supplemented with cm/km and the sample incubated at 37°C on the platform shaker at 1000 rpm. After an overnight incubation the culture was inoculated into 100 ml of L-broth containing cm/km and incubated again at 37°C in the orbital shaker at 225 rpm overnight. A

modified version of the QIAGEN-tip 100 protocol (Section 2.1.14), designed for the production of very low-copy number plasmids, was utilised for the preparation of the BAC DNA. Following the manufacturer's instructions, 100 ml of the bacterial culture was used, along with proportional amounts of the reagents supplied with the QIAGEN-tip 100 kit for the preparation of DNA. Each purified BAC DNA sample was resuspended in a final volume of 50  $\mu$ l 10 mM TrisHCl pH 8.0 and stored at 4°C until required.

**2.2.8.5 Step 2 of the Counter-Selection BAC Modification procedure:-  
replacment of the rpsL-neo-PCR1 selection cassette with the non-  
selectable PCR product (non-sm)**

An aliquot of each of the 100  $\mu$ l km<sup>R</sup>/stp<sup>S</sup> cultures from the 1-2 h 30°C incubation described in Section 2.2.8.2 was used for Step 2 of the BAC counter-selection procedure (Section 3.2.6). A 300  $\mu$ l aliquot of L-broth, supplemented with cm/tet/km, was added to each sample and the cultures were incubated at 30°C overnight on a platform shaker at 1000 rpm. A 30  $\mu$ l aliquot of each of the cell cultures was transferred to a tube containing 1.4 ml of L-broth, supplemented with the same antibiotics as before, and the incubation continued at 30°C until the OD<sub>600</sub> was 0.3. The bacterial culture was divided into the uninduced control and the induced samples. A volume of 50  $\mu$ l of 10% L-arabinose was added to each of the induced samples, to initiate the expression of the genes mediating Red/ET recombination, and Step 2 of the procedure was started by shifting the temperature from 30°C to 37°C. Both the induced and uninduced cultures were incubated at 37°C for 45-60 min on a platform shaker at 1000 rpm and subsequently prepared for electroporation (Section 2.2.5.3). A 2  $\mu$ l aliquot of a 1:2 dilution of the overlapping nucleotide non-sm (Section 3.2.5) was added to each sample and the DNA electroporated. Following electroporation 1 ml of L-broth was added to each cuvette and each culture was divided into two, one representing the recombinant sample and the other representing the non-recombinant sample. The induced and uninduced non-recombinant samples were retained on ice as controls. The induced and uninduced recombinant cultures were incubated at 37°C for 70 min on the platform shaker at 1000 rpm to allow recombination between non-sm and the inserted rpsL-neo-PCR1 product

contained in fHSV $\Delta$ pac. After incubation each culture was replica plated onto L-broth agar plates containing cm/tet/stp or cm/tet/km.

#### **2.2.8.6 Transfection of 8-1 cells with HSV-1 BAC DNA containing the rpsL-neo-PCR1 cassette**

UL25 expressing (8-1) cells were seeded at a density of  $5 \times 10^5$  cells/dish on 35 mm dishes and incubated at 37°C. The following day 5  $\mu$ l of HSV-1 BAC DNA and 0.5  $\mu$ g of the *Bam*HI K fragment, purified from plasmid pGX2, were diluted in 100  $\mu$ l Optimem prior to the addition of 3  $\mu$ l of Plus reagent. The solution was mixed and incubated at RT for 15 min. A 3  $\mu$ l aliquot of Lipofectamine mix, diluted in 100  $\mu$ l of Optimem, was added to each sample and the transfection mix was incubated for a further 15 min at RT. During the incubation the medium was removed from the monolayers and the cells were washed with 1 ml of Optimem. The transfection mix was added to each dish containing 800  $\mu$ l Optimem and the cells were incubated at 37°C. After 4.5 h the medium was removed and the cells were washed with 1 ml of fresh medium prior to being overlaid with 2 ml of growth medium and incubated at 37°C. After 2-3 days incubation the monolayer was scraped into the growth medium, and the viral particles were released by sonication. The virus was plaque-purified (Section 2.2.9) and a large-scale virus stock prepared.

#### **2.2.9 Virus plaque purification**

Eighty percent sub-confluent cell monolayers, seeded in 35 mm tissue culture dishes, were overlaid with 100  $\mu$ l of the sonicated viral preparation (Section 2.2.8.6). The dishes were incubated at 37°C for 1 h and the dishes were gently rocked every 15 min to stop the cells drying out. After viral absorption the cells were overlaid with 2 ml of methyl cellulose medium, to reduce the spread of the resulting plaques, and incubated as before for another 2-3 days. Well-isolated plaques were picked from the virus-infected monolayers and transferred into 1 ml of growth medium, then frozen on dry ice before being stored at -70°C. The titres of the plaque-purified stocks were determined as described in Section 2.2.10 prior to large-scale viral production (Section 2.2.11).

### 2.2.10 Titration of HSV-1 stocks (plaque assay)

Serial tenfold dilutions of the virus sample were prepared and 100  $\mu$ l aliquots from each dilution were added to 80% sub-confluent cell monolayers. After incubation at 37°C for 1 h with intermittent rocking, the cells were overlaid with 2 ml of DMEM supplemented with 2% FCS, 3% human serum and 1X pen/stp. Human serum was added to the growth medium during the viral titrations to neutralise any unabsorbed virus and to prevent secondary plaque formation. Following incubation at 37°C for 2-3 days the medium was removed from the cells and replaced with 1 ml of Giemsa stain per dish. After 20 min at RT the stain was washed off the cells under gently running water and the plaques counted using a dissecting microscope. The virus titre was determined by the following calculation:

Titre = number of plaques on  $10^{-n}$  dilution  $\times 10^{n+1} \times 10^{n+1}$  PFU/ml.

### 2.2.11 Large scale production of HSV-1 stocks

Four 850 cm<sup>2</sup> roller bottles, containing 80% sub-confluent monolayers, were each infected with virus at a concentration of 0.01 PFU/cell in a 40 ml volume of medium and incubated at 37°C. After 3-4 days the virus-infected cells were harvested into the medium by agitation and pelleted by centrifugation at 1,500 rpm in a Sorval RT7 centrifuge for 10 min at 4°C. The supernatant was centrifuged at 12000 rpm in a Sorval RC 5B Plus centrifuge for 2 h at 4°C to concentrate the cell-released virus. The resulting pellets of cell-released virus were combined in a total volume of 5 ml of medium, dispersed in a bath sonicator and divided into aliquots, which were subsequently frozen on dry ice and stored at -70°C. The virus-infected cell pellet was resuspended in 5 ml of medium, disrupted by bath sonication and the cell debris removed by centrifugation at 3000 rpm in a Sorval RT7 centrifuge for 10 min at 4°C. The supernatant, containing the cell-associated virus, was divided into aliquots and frozen on dry ice prior to storage at -70°C.

## 2.2.12 Generation of recombinant baculoviruses

The recombinant baculoviruses were generated using the Bac-to-Bac system from Life Technologies and a synopsis of the procedure used is described in Section 5.2.

### 2.2.12.1 Preparation of recombinant bacmid DNA

Recombinant bacmid DNA was isolated from transformed DH10Bac using a modified version of the Qiagen Plasmid Purification QIAGEN-tip 100 procedure (Section 2.1.14). A single white colony was inoculated into 5 ml of L-broth containing 50 µg/ml km, 7 µg/ml gm and 10 µg/ml tet and incubated at 37°C. The following day 1.5 ml of the bacterial suspension was transferred to a reaction tube and the cells were pelleted by centrifugation at 13000 rpm for 1 min. The cell pellet was resuspended in 300 µl of ice-cold solution P1 (Qiagen), gently mixed in 300 µl of solution P2 (Qiagen) and the lysate was incubated at RT for 5 min. Subsequently, 300 µl of P3 (Qiagen) solution was slowly added to the sample, producing a white precipitate that contained both protein and *E. coli* genomic DNA. The sample was incubated at 4°C for 5-10 min prior to centrifugation at 13000 rpm for 10 min. The supernatant was transferred to a fresh reaction tube and 800 µl of isopropanol was added. The samples was mixed and placed on ice for 5-10 min prior to centrifugation for 15 min at 13000 rpm. The residual salt was washed off the pelleted DNA by the addition of 500 µl of 70% ethanol. The sample was centrifuged for 5 min at 13000 rpm and the supernatant discarded. The bacmid DNA pellet was air dried for 5 min, then resuspended in 40 µl 10 mM TrisHCl and stored at 4°C until required.

### 2.2.12.2 Transfection of Sf21 cells with the modified BAC DNA

Sf21 cells were seeded onto 35 mm dishes at a concentration of  $1 \times 10^6$  cells per dish and incubated at 28°C overnight. A 10 µl aliquot of the prepared recombinant bacmid DNA (Section 2.2.12.1) was added to 6 µl of Lipofectamine diluted in 100 µl of Optimem and incubated at RT for 15 min. This was followed by the addition of 4 µl of Plus diluted in 100 µl of Optimem. The transfection mix was then incubated for a further 15 min at RT. During the incubation the

Sf21 monolayers were washed twice with Optimem and overlaid with 300  $\mu$ l Optimem. The transfection mix was added to the cell monolayers and the dishes placed inside a sealed sandwich box containing a small amount of dry ice. After incubation at 28°C for 5 h the transfection mix was replaced with growth medium and the incubation continued for a further 3 days. The medium was then transferred to a 15 ml Falcon tube and the residual Sf21 cells were removed by centrifugation at 1,500 rpm for 5 min at 4°C in a bench top centrifuge. The supernatant containing the cell-released virus was retained and stored at -70°C.

### **2.2.12.3 Production of high-titre baculovirus stocks**

Four 850 cm<sup>2</sup> roller bottles of Sf21 cells were each seeded at a density of  $2 \times 10^5$  cells/ml in a total volume of 300 ml of growth medium and incubated at 28°C. After two days, when the cells had reached a density of  $5 \times 10^5$  cells/ml, they were infected with the recombinant baculovirus at a multiplicity of infection (MOI) of 0.1 PFU/cell ( $1.5 \times 10^7$  PFU) and the incubation was continued for a further 6 days. The virus-infected cells were removed from the medium by centrifugation at 3000 rpm in a Sorval RT7 centrifuge for 10 min at 4°C. The clarified supernatant was centrifuged at 12000 rpm in a Sorval RC 5B Plus centrifuge for 2 h at 4°C. The resulting viral pellet was resuspended in 2-3 ml of growth medium, sonicated, divided into aliquots and fast-frozen on dry ice prior to storage at -70°C.

### **2.2.12.4 Titration of baculovirus stocks**

Sf21 cells were seeded onto 35 mm dishes at a density of  $1 \times 10^6$  per plate in 2 ml of growth medium and incubated overnight at 28°C. The next day the medium was removed and 100  $\mu$ l of serial tenfold dilutions of the viral sample was added to the cells. The dishes were incubated at RT for 1 h with periodic rocking. The cells were then overlaid with 1.5 ml of TC100 growth medium containing 1.5% (w/v) LGT agarose, prewarmed to 45 °C. When the agarose had set 1.5 ml of TC100 growth medium was added to each dish and the incubation continued at 28°C. At 4-5 days post-infection the liquid overlay was removed and the cell monolayers were overlaid with 1 ml TC100 medium containing 2% neutral red and incubated for 3-4 h at 28°C. After the stain was removed, the

dishes were inverted overnight at 28°C. The following day the plaques were counted using the dissecting microscope.

#### **2.2.12.5 Preparation of baculovirus protein extract from insect cells**

Sf21 cells were seeded into a 175cm<sup>2</sup> flask at a density of  $3 \times 10^7$  cells in 40 ml of growth medium and incubated at 28°C. The following day the cells were infected with the appropriate recombinant baculovirus at a MOI of 5 PFU/cell. After incubation at 28°C for 2 days the cells were detached from the flask into the medium by gentle agitation and pelleted by centrifugation at 3000 rpm in a Sorval RT7 centrifuge for 10 min at 4°C. The supernatant was discarded and the cells were washed twice in PBS, before being resuspended in 1 ml of sterile 1X phosphate buffer (Section 2.1.11) containing protease inhibitors (Boehringer Mannheim). The cell suspension was sonicated and then centrifuged at 35000 rpm for 30 min in a TLA 100.2 rotor using a BECKMAN TL-100 centrifuge. The supernatant, containing the protein extract, was retained and divided into aliquots prior to fast-freezing on dry ice and storage at -70°C.

#### **2.2.12.6 Baculovirus infection of mammalian cells**

U2OS cells were seeded onto 35 mm dishes at a density of  $8 \times 10^5$  cells per dish and incubated at 37°C. After incubation overnight the cell density was assumed to be  $1.6 \times 10^6$ . The medium was removed from the monolayers and the cells were singly infected with baculovirus at an MOI of 50 PFU/cell in a final volume of 100 µl or infected with two viruses, each at an MOI of 25 PFU/cell/ in a final volume of 50 µl. After absorption of the virus at RT for 1 h the inocula were removed and the cells were washed twice with fresh growth medium. The cells were then infected with  $\Delta$ UL25MO at an MOI of 2 PFU/cell in a final volume of 100 µl. After virus absorption at 37°C for 1 h the inocula were removed and the cells were washed twice with fresh medium. The cells were overlaid with 2 ml of growth medium and incubated at 37°C for 18-24 h. If the cells were to be analysed using immunofluorescence (Section 2.2.12.8 and 2.2.17.2) they were seeded at a density of  $1 \times 10^5$  cells onto 13 mm glass coverslips placed at the bottom of a 24-well dish and overlaid with 1 ml of growth medium. After overnight incubation at 37°C, viral infection of the cells was carried out as described above.

### **2.2.12.7 Preparation of baculovirus protein extract from mammalian cells**

U2OS cells were grown on 35 mm tissue culture dishes and infected with the appropriate baculovirus stock as described in Section 2.2.12.6. At 24 hpi the cell monolayers were scraped into the growth medium, and each transferred to a 1.5 ml reaction tube. The cells were pelleted, by centrifugation at 2000 rpm for 1 min, resuspended in TBS containing protease inhibitor tablets and the centrifugation step was repeated. The cell pellet was mixed with 500  $\mu$ l ice-cold EZ lysis buffer and placed on ice for 20 min, with periodic vortexing. A 20  $\mu$ l aliquot, referred to as the total protein sample (TP), was transferred to a reaction tube containing 10  $\mu$ l 3X boiling mix and stored at  $-20^{\circ}\text{C}$  until required. The remaining lysed cells were clarified by pelleting the cell debris at 35000 rpm for 20 min at  $4^{\circ}\text{C}$  in a TLA 100.2 rotor, using a BECKMAN TL-100 ultra centrifuge. After centrifugation another 20  $\mu$ l sample, referred to as the soluble protein extract (SP), was transferred to a reaction tube containing 10  $\mu$ l of 3X boiling mix and stored at  $-20^{\circ}\text{C}$  until required.

### **2.2.12.8 Assessment of the efficiency of baculovirus infection using an immunofluorescence assay**

Baculovirus-infected U2OS cell monolayers were prepared as described in Section 2.2.12.6. The monolayers, grown on the coverslips placed in 24-well plates, were washed twice with PBS and then carefully overlaid with 1 ml PBS containing 5% (v/v) formaldehyde, 2% (w/v) sucrose in a fume hood at RT. After 10 min the monolayers were washed three times with PBS prior to permeabilisation of the cells with 1 ml PBS containing 0.5% NP40 10% sucrose. Following incubation for 5 min at RT the cells were washed three times with PBS-1% FCS (Section 2.1.11). With the cell monolayer facing down, the coverslips were each transferred on to a 20  $\mu$ l droplet of the UL25 monoclonal antibody MAb166, diluted 1:500 in PBS-1% FCS, placed in the well of the lid from a 24-well dish. The coverslips on the lid were put inside a sealed box to reduce evaporation and incubated for 1 h at RT. Unbound antibody was subsequently removed by immersing each coverslip three times in PBS-1% FCS for 5 min at RT. Each coverslip was then transferred to a 20  $\mu$ l droplet of the secondary antibody

anti-mouse IgG conjugated to FITC, diluted 1:100 in PBS-1% FCS, and incubated for 1 h as before. Unbound antibody was removed by washing each coverslip three times in PBS-1% FCS. The cell nuclei were stained with 20  $\mu$ l propidium iodide solution (20  $\mu$ l propidium iodide in 20 ml PBS) for 2 min at RT and the coverslips were again washed three times in PBS-1% FCS, followed by two rinses in dH<sub>2</sub>O to remove any residual salt remaining from the PBS washes. With the cell monolayer facing up, the coverslips were transferred onto Whatman's number 1 blotting paper and allowed to dry. Each coverslip was subsequently transferred, with the cell monolayer facing down, onto a 5  $\mu$ l droplet of Mowiol (Harco) mounting fluid on a glass slide. The cells were examined using the Zeiss Axioplan 2 confocal microscope and the images were obtained using the associated LSM 510 software.

### **2.2.13 Sterility of viral stocks**

The sterility of the viral stocks was checked by streaking a small sample onto a blood agar plate. The plate was sealed with Parafilm<sup>TM</sup> and incubated at 37°C for up to 5 days. Contaminated viral stocks were discarded.

### **2.2.14 Detection of full length packaged viral DNA**

#### **2.2.14.1 Preparation of total and DNase I resistant viral DNA**

##### **DNA preparation for Southern blots**

U2OS cells, seeded onto 35 mm dishes, were grown and infected with the appropriate baculovirus, as described in Section 2.2.12.6. Following incubation at 37°C for 24 h the medium was removed and 2.3 ml of ice-cold TBS was added to each monolayer. The cells were scraped into the TBS, placed in a 15 ml Falcon tube and dispersed by vortexing. Each cell suspension was divided into two 1 ml aliquots and transferred to reaction tubes labelled (A) and (B), with sample (A) representing the total viral DNA content of the cells and sample (B) representing the DNase I resistant (packaged) DNA fraction of the cells. Both aliquots were centrifuged at 13000 rpm in a bench top microfuge for 12 sec and the supernatant discarded. A 184  $\mu$ l aliquot of RSB containing 0.5% NP40 was added to sample (A) and the mixture vortexed. This was immediately followed

by the addition of 184  $\mu$ l of 2X CLB containing 1 mg/ml of protease. The sample was mixed by gentle inversion of the reaction tube and incubated at 37°C for 1 h. A 184  $\mu$ l aliquot of RSB containing 0.5% NP40 and 200  $\mu$ g/ml DNase I was added to sample (B), followed by incubation at 37°C for 20 min, with occasional vortexing. Subsequently, 184  $\mu$ l of 2X CLB containing 1 mg/ml of protease was added to (B) and the incubation continued for 1 h.

Following incubation, 32  $\mu$ l of 4 M NaCl, 50 mM EDTA solution was added to (A) and (B) samples and the DNA was sequentially extracted with phenol and chloroform:isoamyl alcohol. After the addition of phenol the sample was mixed by rotation for 15 min. The organic and aqueous phases were subsequently separated by centrifugation at 13000 rpm for 1 min and the DNA-containing top phase was transferred to a fresh reaction tube. A 400  $\mu$ l aliquot of chloroform:isoamyl alcohol (24:1) was added to the DNA solution and the sample mixed by rotation for 15 min. The DNA-containing top phase was removed and the DNA was precipitated from the solution by adding 1 ml of ethanol to each sample, mixing and then placing them overnight at -20°C. The following day the samples were centrifuged at 13000 rpm for 10 min, after which the DNA pellet was allowed to air dry for 5-10 min. A 160  $\mu$ l and 80  $\mu$ l aliquot of 10 mM TrisHCl pH8.0 containing 1X RNase was added to each of the (A) and (B) samples, respectively. After the DNA was dissolved thoroughly by incubating the samples for 6 h at 37°C, the samples were stored at 4°C until required.

### **DNA preparation for pulse field gels**

U2OS cells were grown on 35 mm dishes as outlined in Section 2.2.12.6, except that after virus-absorption the residual virus was removed from the cells by an acid wash (Section 2.2.7.4). DNA was prepared from infected U2OS cells in essentially the same manner as for Southern blots except for the following modifications. The amount of RSB containing 0.5% NP40 and the amount of 2X CLB containing 1 mg/ml of protease added to samples (A) were reduced to 100  $\mu$ l. Similarly, the amount of RSB containing 0.5% NP40, plus 200  $\mu$ g/ml DNase I, and the amount of 2X CLB containing 1 mg/ml of protease added to sample (B) were reduced to 100  $\mu$ l. The samples were carefully mixed throughout, and both phenol extraction and ethanol precipitation of the DNA were omitted to minimise shearing of the high molecular weight DNA. The DNA molecules

obtained were separated using pulse field gel electrophoresis as described in Section 2.2.16.

#### **2.2.14.2 Preparation of a $^{32}\text{P}$ -labelled DNA probe**

DNA was labelled with  $^{32}\text{P}$  using Roche's Random Primed DNA Labelling kit. Briefly, 500 ng of plasmid DNA in a total volume of 9  $\mu\text{l}$  was boiled for 10 min and chilled on ice before the addition of 20  $\mu\text{Ci}$  of  $\alpha$ - $^{32}\text{P}$  dCTP, 20  $\mu\text{Ci}$  of  $\alpha$ - $^{32}\text{P}$  dGTP, 3  $\mu\text{l}$  dNTP mix, 2  $\mu\text{l}$  10X reaction mix containing random primers and 1 unit of Klenow in a final volume of 20  $\mu\text{l}$ . After incubation at 37°C for 1 h the reaction was stopped by the addition of 5  $\mu\text{l}$  0.2 M EDTA pH 8.0 and diluted to a final volume of 50  $\mu\text{l}$  with 25  $\mu\text{l}$  10 mM TrisHCl pH 8.0. Unincorporated  $^{32}\text{P}$ -labelled nucleotides were removed from the sample using a Microspin Sephadex G-50 spin column, following the manufacturer's instructions. The probe was diluted by the addition of 40  $\mu\text{l}$  10 mM Tris pH 8.0 and subsequently denatured by the addition of 20  $\mu\text{l}$  1 M NaOH. After incubation at RT for 5 min the reaction was neutralised by the addition of 20  $\mu\text{l}$  1 M HCl.

### **2.2.15 Southern blots**

#### **2.2.15.1 DNA digestion and electrophoresis**

Following digestion of a 36  $\mu\text{l}$  aliquot of DNA with *Bam*HI the reaction was stopped by the addition of 10  $\mu\text{l}$  of DNA loading buffer. Subsequently, the sample was loaded onto a 0.8% agarose gel in 1X Loening's buffer (Section 2.1.11) and the DNA separated by electrophoresis at 15-20 V overnight in a BRL horizontal electrophoresis apparatus. To confirm that the DNA was both completely digested and that equal amounts had been loaded into each well, the gel was examined under short wave UV light the following day and the ethidium bromide-stained DNA photographed using a gel documentation system (Bio-Rad) prior to Southern blot transfer (Section 2.2.15.2).

### **2.2.15.2 Southern blot transfer**

DNA was denatured by immersing the gel in 400 ml of alkaline transfer solution for 15-30 min and then transferred to a Hybond-XL membrane (Amersham) by capillary transfer in alkaline transfer solution overnight at RT. The following day the membrane was removed from the gel and soaked in 100 ml of neutralising solution for 15 min with occasional agitation. The membrane-bound DNA was cross-linked by exposure to 120 mJ/cm<sup>2</sup> UV light in a Stratalinker (Stratagene). The membrane was then placed in a Hybaid bottle containing 50 ml of Southern blot prehybridisation buffer. After incubation in the Hybaid oven at 68°C for 1-2 h the solution was replaced with 20 ml Southern blot prehybridisation buffer containing 0.01 mg/ml of denatured sheared calf thymus DNA and the incubation continued for a further 3-5 h. The purified denatured <sup>32</sup>P-labelled probe (Section 2.2.14.2) was added to the solution and the hybridisation carried out at 68°C for a further 16-24 h. The radioactive solution was removed and the membrane was washed with 50 ml Southern blot prehybridisation buffer at 68°C for 45 min. This was followed by two 30 min washes with membrane wash buffer (Section 2.1.11) at 68°C and final rinse of the membrane with dH<sub>2</sub>O. The Hybond-XL membrane was exposed to a phosphorimager screen and the screen was analysed on a Bio-Rad Personal Molecular Imager FX using Quantity One software.

### **2.2.16 Pulse field gels**

DNA was prepared and treated with DNase as described in Section 2.2.14.1. A 25 µl aliquot of each DNA sample was analysed on the Bio-Rad DR-II apparatus as recommended by the manufacturer. Using a wide-bored tip, DNA samples were loaded onto a 1% agarose (Bio-Rad: pulse field gel electrophoresis [PFGE] certified) gel in 0.5X TBE buffer. The DNA was resolved with a voltage gradient of 6 volts/cm for 18 h at 14°C, with a linear time switch gradient from 1 to 15 sec. After electrophoresis the gel was stained with ethidium bromide and photographed. The DNA fragments were transferred onto a Hybond-XL membrane by Southern blotting (Section 2.2.15.2).

## 2.2.17 Analysis of viral assembly in infected cells

### 2.2.17.1 Electron microscopy

Cells were grown on 35 mm dishes and infected at 37°C with the appropriate baculovirus as outlined in Section 2.2.12.6. At 24 hpi the medium was removed, the cells were washed twice with 1 ml of PBS and then fixed by the addition of 500 µl of 2.5% glutaraldehyde in PBS overnight at 4°C. The following day the cells were rinsed twice with 1 ml of PBS and incubated at RT in 200 µl of osmium tetroxide, with occasional rocking of the dishes. After 1 h the monolayers were washed twice with PBS, scraped into 0.5 ml of PBS and each transferred to a 1.5 ml reaction tube. The cells were pelleted by centrifugation at 3000 rpm for 5 min and then each sample was resuspended in 0.5 ml of 1% SeaPlaque agar (Lonza) pre-warmed to 50°C. The samples were spun at 5000 rpm for 5 min in a swing-out rotor in a Beckman Microfuge 12 to ensure the pellet formed at the bottom of the reaction tube. Following centrifugation the samples were left at 4°C for 1-2 h to allow the agar to set. The bottom of the tube was then cut off to release the agar embedded cell pellet and the cell/agar plugs were trimmed to approximately 2 mm<sup>3</sup>. Each agar plug was transferred to a beam capsule and the pellets were dehydrated by sequential 1 h incubations at RT in increasing concentrations (30, 50, 70, 90, 100%) of ethanol, with a final incubation at RT overnight in 100% ethanol. The following day the ethanol was carefully removed from each sample and replaced with freshly prepared Epon 812 resin mix (Section 2.1.11). The samples were incubated overnight at RT, with the lids of the beam capsules left open to allow residual ethanol to evaporate from the mix. The next day the cell pellets were drained and fresh Epon 812 resin mix added. The samples were incubated overnight at RT before being labelled and placed in an embedding oven at 65°C for 2 days to allow the resin to harden.

The embedded samples were sectioned using an ultra-microtome (Leica Ultracut E) and the thin sections mounted onto 400 mesh uncoated copper grids by Dr F. Rixon or Mr J. Aitken at the MRC Virology Unit. The sections were each subsequently stained in 100 µl of a saturated solution of uranyl acetate in 90% ethanol for 1 h, and washed twice by immersion in 300 µl of sterile dH<sub>2</sub>O for 5 min. The excess water was drained off each grid, by carefully blotting the grid

onto Whatman's no. 1 filter paper. Each grid was subsequently transferred into 100  $\mu$ l lead citrate solution (Section 2.1.11) and stained for 1 min, followed by three 10 min washes in sterile dH<sub>2</sub>O and then dried. The grids were examined at 80 KV using a JEOL 100S electron microscope.

### **2.2.17.2 Fluorescent in-situ hybridisation (FISH)**

To determine the location of viral DNA within the cell, the U2OS cells on coverslips were infected with the appropriate baculovirus and prepared as outlined in Section 2.2.12.6. Following overnight incubation at 37°C the cells were washed twice with 1 ml of PBS-1% FCS and then fixed in 1 ml of pre-chilled 95% ethanol containing 5% acetic acid at -20°C for 5 min. After fixation the cells were carefully rinsed three times with 1 ml of PBS-1% FCS and stored at 4°C until required. Preparation of the Cy3-labelled cos56 probe, containing HSV-1 strain 17 syn<sup>+</sup> nucleotide sequences 79,442-115,152, and FISH were carried out by Mrs J. Murray from the MRC Virology Unit (Cunningham & Davison, 1993, Everett et al., 2007). The probe was labelled by nick translation using Cy3-dCTP (Amersham), following the manufacturer's protocol. After DNase I treatment the cells were incubated for 30 min at 37°C in 20  $\mu$ l hybridisation buffer (Section 2.1.11) per coverslip in a humidified microarray hybridisation chamber (Camlab). The coverslips were removed from the chamber, drained and incubated in 20  $\mu$ l hybridisation buffer containing the probe at a concentration of 1 ng/ $\mu$ l for 2 min at 95°C to denature the probe. The coverslips containing the probe were then placed in the humidified chamber and the hybridisation was continued overnight at 37°C. The cells were washed at 60°C for 5 min with 2x SSC and once with 2x SSC at RT. After two washes with PBS-1% FCS, the coverslips were incubated in PBS-1% FCS containing 1  $\mu$ g/ml DAPI for 2.5 min. The cells were then washed three times with PBS-1% FCS, air dried, and mounted in Citifluor AF1 (Citifluor Ltd) on glass slides. The prepared slides were examined using a Zeiss LSM 510 confocal microscope with 405 and 543-nm laser lines, scanning each channel separately under image capture conditions that eliminated channel overlap. The images were exported for analysis as tagged-image format files and then processed using Adobe Photoshop.

## **2.2.18 Protein analysis**

### **2.2.18.1 SDS-polyacrylamide gel electrophoresis (SDS-PAGE)**

Proteins were resolved by electrophoresis on 10% SDS-polyacrylamide gels in 1X RGB (Section 2.1.11) prepared from a stock solution of 30% w/w acrylamide:0.8% bisacrylamide (37.5:1) (Protogel, National Diagnostics). The resolving gel layer was polymerised by the addition of 200  $\mu$ l of 10% ammonium persulphate and 20  $\mu$ l TEMED and cast into the Mini Protean II gel sandwich (Bio-Rad) to approximately 5 mm below the gel comb slot. The gel solution was overlaid with 1X RGB. After the gel had polymerised, the 1X RGB solution was removed and the resolving gel was overlaid with 5% polyacrylamide in 1X SGB (Section 2.1.11) containing the polymerisation reagents. The comb was inserted into the solution and gel was allowed to polymerise at RT. Boiling mix (3X) (Section 2.1.11) was added to the protein samples at a final concentration of 1X, and the samples were heated to 100°C in a boiling water bath for 3 min shortly before they were loaded onto the gel. The molecular weight markers used were either Rainbow Markers (Amersham Pharmacia) or MagicMark (Life Technologies). The proteins were separated by electrophoresis in 1X Tank buffer (Section 2.1.11) at 200 V until the tracking dye had reached the bottom of the resolving gel. The gels were then prepared for Western blotting (Section 2.2.18.2).

### **2.2.18.2 Western blotting**

#### **Protein transfer and detection**

Proteins separated by SDS-PAGE (Section 2.2.18.1) were transferred onto a Hybond-ECL membrane using a Mini Protean II blotting apparatus (Bio-Rad), according to the manufacturer's instructions. Transfer of the protein to the Hybond-ECL membrane was carried out in 1X Towbin buffer (Section 2.1.11) at 100 V for 1-2 h. To block non-specific protein-binding sites, the Western blot was transferred into blocking buffer (5% (w/v) dried skimmed milk powder, 0.05% (v/v) Tween-20 in PBS) and incubated overnight at 4°C with gentle shaking. The following day the blot was placed in fresh blocking buffer, containing the appropriately diluted primary antibody (Section 2.1.10), and incubated for 1-4 h at RT with gentle shaking. Unbound primary antibody was

removed by rinsing the blot twice in wash buffer (0.05% (v/v) Tween-20 in PBS), followed by incubation in fresh wash buffer for 15 min at RT with gentle shaking. The blot was washed twice more in wash buffer for 5 min at RT and subsequently placed in the appropriate secondary antibody solution (Section 2.1.10) diluted in 2% (w/v) dried skimmed milk powder, 0.05% (v/v) Tween-20 in PBS and incubated for 1 h at RT with gentle shaking. Unbound secondary antibody was washed off the blot as outlined for the unbound primary antibody. Bound antibody was detected using an ECL chemiluminescence kit (Amersham) with Kodak X-OMAT autoradiograph film.

### **Stripping antibodies from Hybond-ECL membranes**

After Western blotting the Hybond-ECL membrane was stored in PBS supplemented with 0.05% (v/v) Tween-20 at 4°C. To remove the antibodies the Western blot was immersed in a solution containing 100 mM  $\beta$ -mercaptoethanol, 2% SDS and 2.5 mM Tris HCl pH 6.0 and incubated at 55°C for 1 h with gentle shaking. The membrane was then washed extensively in wash buffer at RT.

## **2.2.19 GST-fusion protein expression and GST pull-down assay**

### **2.2.19.1 Induction of GST-UL36CBD and GST proteins expressed in *E. coli* BL21**

*E. coli* BL21 cells were transformed (Section 2.2.5.4) with either the GST expression plasmid, pGEX-2TNMCR (Section 2.1.9), or the recombinant pGEX-2TNMCR plasmid containing the pUL36 capsid binding domain (UL36cbd), pGEX-UL36cbd (Section 7.1.1). Single colonies were selected from the recombinants obtained and inoculated into 10 ml of L-broth, supplemented with 100  $\mu$ g/ml amp. After the samples had been incubated overnight at 37°C, a 2.5 ml aliquot from each culture was inoculated into 250 ml of amp containing L-broth and the bacterial suspensions were incubated at 37°C in the orbital shaker at 225 rpm until the OD<sub>600</sub> reached 0.4-0.6. At this point 1ml of each culture, representing the uninduced sample, was removed and stored at 4°C for further analysis by SDS-PAGE. Expression of the GST-fusion proteins was induced in the remainder of each culture by the addition of IPTG to a final concentration of 0.2 mM. After the induced cultures had been incubated for 3 h at 37°C, a 1 ml aliquot was

removed from each sample and stored at 4°C for further analysis. The remainder of each culture was used for protein purification (Section 2.2.19.2). The 1 ml uninduced and induced samples were removed from 4°C storage and centrifuged at 13000 rpm for 5 min at RT. The bacterial pellets were resuspended in 100µl of 10mM TrisHCl pH8.0 and 5µl of each sample was resolved by SDS-PAGE (Section 2.2.18.1).

### **2.2.19.2 Purification of GST-UL36CBD and GST proteins from *E. coli* BL21**

The induced bacterial culture retained for protein purification (Section 2.2.19.1) was centrifuged at 5000 rpm in a SORVAL RC 5B Plus for 10 min at 4°C. After centrifugation the bacterial pellet was resuspended in 2.5 ml of sonication buffer (Section 2.1.11) and placed on ice. Subsequently, the bacterial cells were lysed by sonication using a Branson sonifier 450 soni-probe, with the machine giving five 15 sec bursts set at 90% intensity. Following sonication the sample was centrifuged in a SORVAL RC 5B Plus at 6000 rpm for 30 min at 4°C, and the supernatant was retained for analysis. The pellet was resuspended in sonication buffer and the sample was resonicated for two 15 sec bursts at the same intensity as before. The cell debris was subsequently removed by repeating the previous centrifugation step. The supernatants obtained were pooled and were clarified further by centrifugation at 30000 rpm for 30 min at 4°C in TLA 100.2 rotor using a BECKMAN TL-100 ultra centrifuge. The supernatants containing the soluble GST-UL36CBD or GST protein extracts were divided into 500µl aliquots, frozen on dry ice and stored at -70°C until required.

### **2.2.19.3 GST pull-down assay**

Aliquots of 200 µl of either the GST or GST-UL36cbd protein extracts (bait proteins) or the target protein extracts expressing the wt pUL25 or mutant UL25 proteins, which were prepared as described in Section 2.2.12.5, were mixed with 400 µl of Triton 1X buffer (Section 2.1.11). Gluthathione-Sepharose 4B beads were rehydrated in PBS-A to make a 1:1 (v/v) slurry according to the manufacturer's instructions (GE Healthcare) and 50 µl of the suspension was added to each sample and mixed by rotation for 1.5 h at 4°C. The samples were then centrifuged at 13000 rpm for 30 sec at 4°C. The beads that had been

incubated with the bait protein extracts were retained and washed three times with 100  $\mu\text{l}$  of Triton 1X buffer. After each wash the beads were concentrated by centrifugation as described above. The washed beads were resuspended in 100  $\mu\text{l}$  of Triton 1X buffer and each sample transferred to a fresh 1.5 ml reaction tube. The beads were again concentrated by centrifugation and the supernatant discarded. Beads that had been incubated with the target protein extracts were discarded but the supernatants were retained. This procedure was used to pre-clear the target protein lysates of any aggregated or insoluble proteins that could bind non-specifically to the bait-bound beads. A 300  $\mu\text{l}$  volume of the pre-cleared target protein extract was added to the tubes containing the bait-bound beads, and the samples were mixed by rotation at 4°C for 1.5 h. The beads were pelleted by centrifugation at 13000 rpm for 30 sec at 4°C, washed three times in 750  $\mu\text{l}$  of Buffer A (Section 2.1.11). The beads were concentrated by centrifugation and the supernatant discarded. A volume of 40  $\mu\text{l}$  of Triton 1X buffer was added to each sample together with 10  $\mu\text{l}$  of 3X boiling mix prior to storage of the samples at -20°C. Before the samples were loaded onto an SDS-polyacrylamide gel they were heated to 100°C for 3 min to elute the bound proteins, and the beads were removed by centrifugation at 13000 rpm for 1 min at RT. A 25  $\mu\text{l}$  aliquot of each supernatant was loaded onto an SDS-polyacrylamide gel and the presence of a particular protein was detected by Western blot analysis (Section 2.2.18.2).

## 3 Generation of the HSV-1 UL25 deletion mutant $\Delta$ UL25MO

### 3.1 Introduction

An existing HSV-1 UL25 null virus, KUL25NS (McNab *et al.*, 1998), which was constructed by the insertion of an in-frame stop codon in the UL25 open reading frame, was available at the beginning of this study (Figure 3.1). However, the problem with KUL25NS is that during complementation assays recombination can occur between the UL25 sequences in KUL25NS and the UL25 sequences present in the expression plasmid, resulting in the production of wt progeny. The presence of wt virus among the progeny makes it difficult to distinguish between non-functional mutant constructs and those that have a low level of activity. To increase the sensitivity of the functional assay, an HSV-1 UL25 deletion mutant was generated using the Counter-Selection BAC Modification kit, supplied by Gene Bridges (Section 3.2). This kit utilises homologous recombination *in vivo* in *E. coli* to introduce mutations into BACs, which are large stable genetic elements that are replicated in *E. coli* vectors and can harbour foreign DNA sequences of up to 300 kb. The BAC used in this study (fHSV $\Delta$ pac) has the cm resistance gene, ensuring the BAC is maintained in the *E. coli* host strain DH10B in the presence of chloramphenicol, and contains a mutant HSV-1 strain 17 syn<sup>+</sup> genome lacking the packaging signals. The mutated HSV-1 containing BAC was transfected into UL25-expressing 8-1 cells together with the *a* sequence to generate the HSV-1 UL25 deletion virus  $\Delta$ UL25MO.

### 3.2 The Counter-Selection BAC Modification technique

#### 3.2.1 Red/ET recombination

Conventional methods of DNA cloning and manipulation rely on the use of restriction enzymes and DNA ligases to construct novel combinations of DNA molecules *in vitro*. Restriction enzymes generally cut on average about every 250-4000 bp, limiting manipulations to only short segments of DNA. Rare cutting enzymes are available which can produce fragments of up to approximately 50

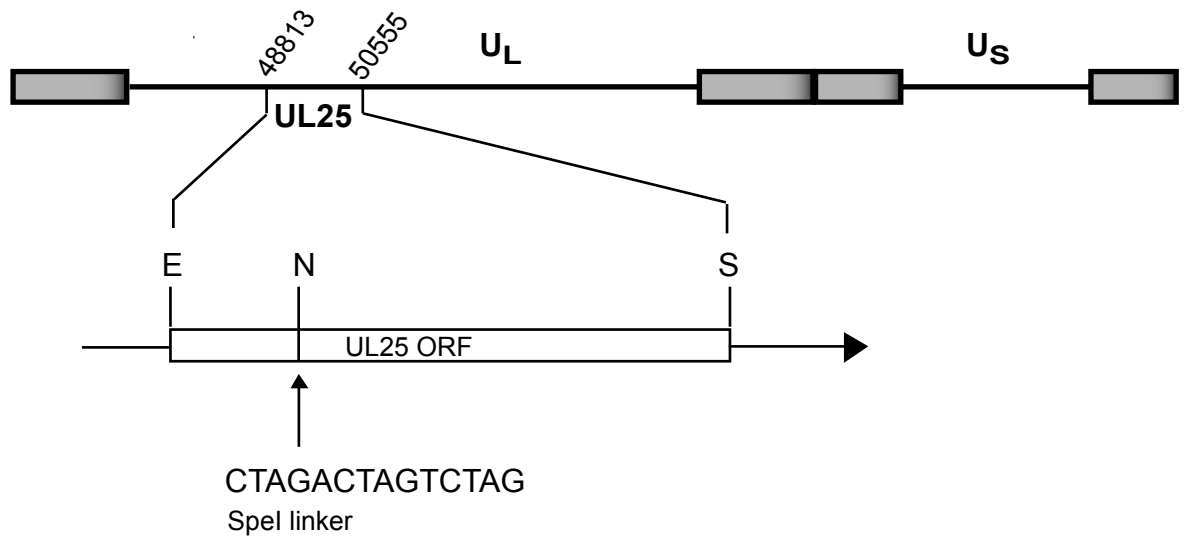


**Figure 3.1 Strategy used by McNab et al. (1998) to create a UL25 null mutant**

The HSV-1 genome is shown at the top with long and short unique region sequences labelled as  $U_L$  and  $U_S$ , respectively. Below, the 6,282 bp *EcoRI* (E) - *SnaBI* (S) fragment is expanded, which contains the UL25 ORF specified by sequences 48,813 to 50,555. This fragment was cloned into a vector and the single *NotI* (N) site present was converted to a *SpeI* site by insertion of a 14 bp linker. The linker contained stop codons in all three reading frames. The *NotI* site is located at codon 104 of the UL25 ORF, therefore insertion of the *SpeI* linker would terminate translation of UL25 at this point (adapted from McNab et al., 1998).

kb, but ligating these *in vitro* is difficult. The advent of PCR reduced the reliance on restriction enzymes but amplifying pieces of DNA larger than 10 kb is difficult, and the technique also suffers from poor fidelity that becomes more significant the larger the sequence being amplified. The Counter-Selection BAC Modification procedure was designed to address some of the limitations by using the Red/ET recombination system, which is also referred to as lambda-mediated recombination. Red/ET recombination relies on homologous recombination *in vivo* in *E. coli* strains that express the phage-derived protein pair, Red $\alpha$  and Red $\beta$ , an exonuclease and DNA annealing protein, respectively. A functional interaction between Red $\alpha$  and Red $\beta$  is necessary for the proteins to catalyse the homologous recombination event, which is illustrated in Figure 3.2. This process is assisted further by the lambda encoded Gam protein that inhibits the RecBCD exonuclease activity of *E. coli*. The advantage of this approach is that a range of modifications, such as insertions, deletions or substitutions, can be precisely introduced at any target site as the regions of homology can be chosen freely in DNA molecules of any size. Since the recombination event is carried out *in vivo*, it is considered inherently more accurate than PCR, because the endogenous proofreading and repair machinery of *E. coli* are constantly monitoring the process.

### 3.2.2 RpsL-neo counter-selection system

The technique relies on the *rpsL* gene, which encodes the S12 ribosomal protein, and *stp* selection. Bacterial resistance to high concentrations of *stp* is the result of recessive mutations in the *rpsL* gene. However, if both the wt and mutant alleles of *rpsL* are expressed in the same strain of *E. coli*, the strain is sensitive to *stp* (*stp*<sup>S</sup>). The *rpsL*-neo counter-selection cassette (Figure 3.3) used in the BAC modification procedure exploits this feature by introducing the wt *rpsL* gene and hence conferring *stp*<sup>S</sup> to the host bacteria that were previously *stp*<sup>R</sup>. An additional antibiotic marker, *km*, is also carried on the *rpsL*-neo cassette and consequently both positive and negative drug selection markers are introduced into the host.

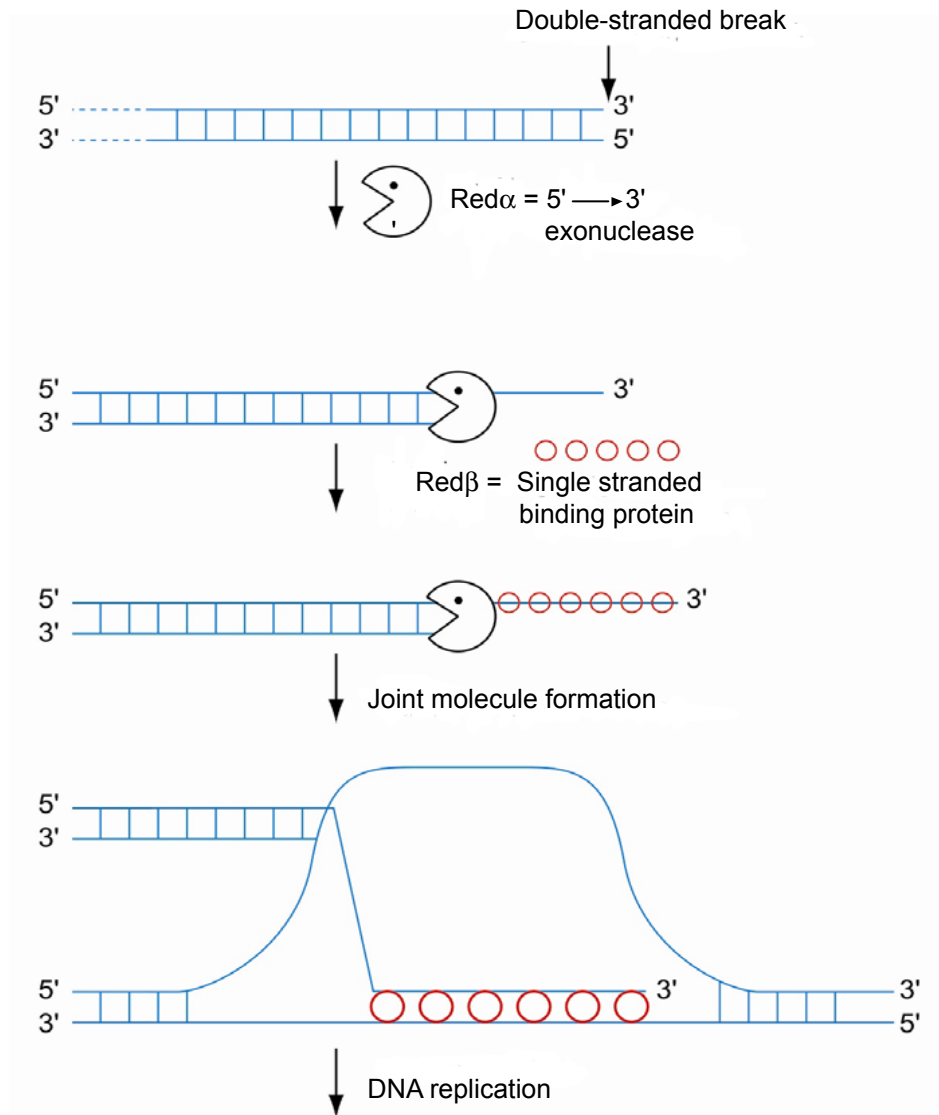


**Figure 3.2 Red/ET recombination**

A functional interaction between Red $\alpha$  and Red $\beta$  is required to catalyse the homologous recombination event. The double-stranded break (DSB) is initiated by the protein pair. First, Red $\alpha$  digests one strand of the DNA from the DSB, leaving the other strand as a 3' ended single-stranded DNA overhang. Red $\beta$  then binds to and coats the single-stranded DNA and then aligns with homologous DNA. Once the protein-nucleic acid filament is aligned it acts as a primer for DNA replication. The recombination enzymes can be expressed from the plasmid pRed/ET and are therefore transferrable to any *E.coli* strain (adapted from the Counter-Selection BAC Modification manual, version 2.4, June 2005).



**Figure 3.3 A schematic representation of the rpsL-neo counter-selection cassette**

Counter-Selection BAC Modification is essentially a two-step approach. In the first step the rpsL-neo cassette (rpsL-neo) flanked by homology arms is inserted by a Red/ET mediated recombination event into the target DNA, conferring  $km^R/stp^S$  onto the host bacteria. In the second step the counter-selection cassette is replaced with markerless (non-selectable) DNA using Red/ET recombination, and the host bacteria containing the markerless DNA are identified by their  $km^S/stp^R$ . The recombination events are initiated in the host bacteria after transformation with the Red/ET expression plasmid, pRed/ET, which is shown in Figure 3.4. This plasmid carries the genes specifying the recombination proteins Red $\alpha$  and Red $\beta$  that are under the control of the arabinose-inducible pBAD promoter and also contains the tet resistance marker, conferring tet resistance ( $tet^R$ ) to the host cell. The experimental approach used is summarised in Figure 3.5 and the methods employed are described in detail in Section 2.2.8.

For the counter-selection technique to work it is important that the *E. coli* strain used in the procedure carries a mutated *rpsL* gene and consequently is  $stp^R$ . Prior to using the Counter-Selection BAC Modification kit, DH10B bacteria carrying the HSV-1 BAC were plated onto L-broth agar supplemented with *stp*, *cm*, *km* or *tet* to verify they were indeed  $stp^R$ ,  $cm^R$ ,  $km^S$  and  $tet^S$ . Subsequently, the DH10B bacteria were transformed with pRed/ET and grown at 30°C in order to maintain the temperature sensitive plasmid within the host cells. To induce expression of the Red $\alpha$  and Red $\beta$  genes from the pRed/ET plasmid in DH10B cells L-arabinose was added to the bacterial culture and the incubation temperature was shifted from 30°C to 37°C.

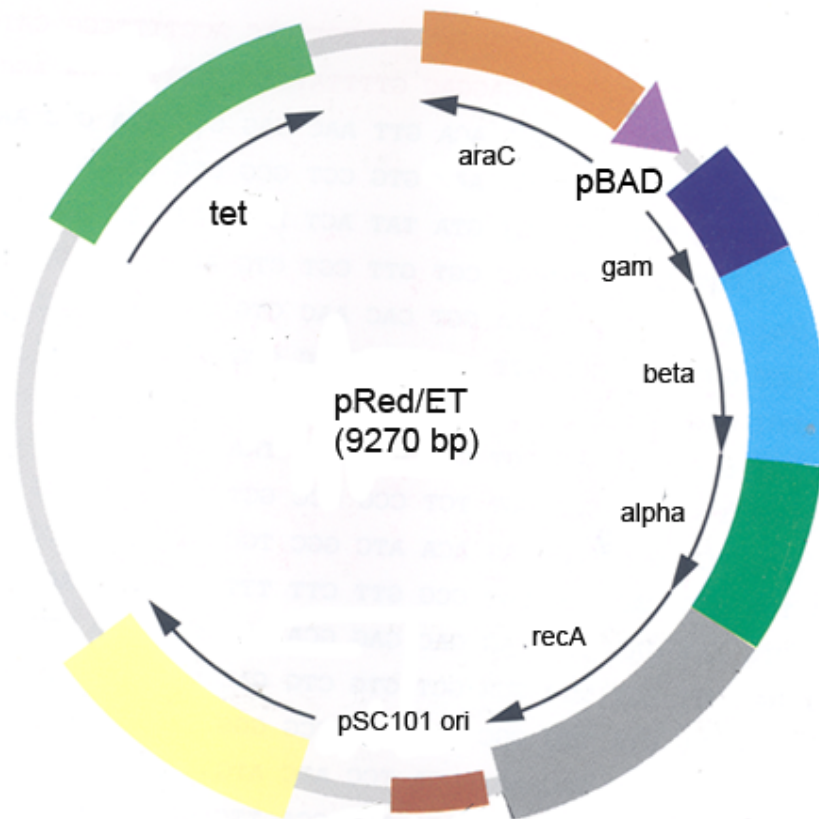


**Figure 3.4 Map of Red/ET expression plasmid pRed/ET**

The plasmid carries the lambda red alpha and beta genes that express the Red/ET recombination proteins, which together with the gam and recA genes are located in a polycistronic operon under the control of the inducible promoter pBAD. Expression of the Red/ET recombination proteins is induced by L-arabinose activation of pBAD at 37°C. The pBAD promoter is both positively and negatively regulated by the product of the araC gene. AraC is a transcriptional regulator that forms a complex with L-arabinose and allows transcription to begin. In the presence of glucose, or the absence of arabinose, transcription is blocked by the AraC dimer.

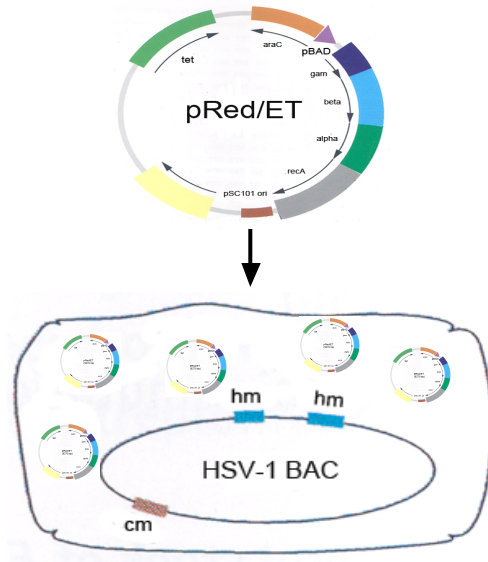
**Figure 3.5 Flow diagram of the experimental outline for the generation of the UL25 null HSV-1 BAC**

**(A)** The *E. coli* strain DH10B carrying the HSV-1 BAC (fHSV $\Delta$ pac) was transformed with the expression plasmid pRed/ET. The chloramphenicol marker (cm) highlighted in brown is shown on the HSV-1 BAC together with the homology regions (hm) highlighted in blue. The expression of genes mediating Red/ET recombination was induced by the addition of L-arabinose and a temperature shift from 30°C to 37°C.

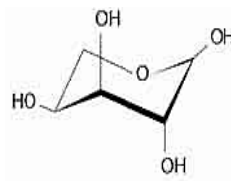
**(B)** Following induction of the Red/ET recombination enzymes, step 1 of the Counter-selection BAC Modification technique was carried out. The bacteria were prepared for electroporation and the linear rpsL-neo counter-selection/selection cassette (rpsL-neo-PCR1 PCR product) flanked by HSV-1 homology arms (shown in blue) was electroporated into the bacteria. Red/ET recombination inserts the functional cassette into the target locus in the fHSV $\Delta$ pac BAC. Only colonies carrying the modified BAC will survive km selection and will also become stp<sup>S</sup>.

**(C)** Following selection of km<sup>R</sup>/stp<sup>S</sup> colonies and verification that they contained a modified BAC, step 2 of the Counter-selection BAC Modification technique was performed. The expression of genes mediating Red/ET was induced by the addition of L-arabinose and a temperature shift from 30°C to 37°C, after which the bacterial cells were prepared for electroporation. The non-selectable DNA fragment (Non-sm) consisting of sequences from the right and left homology arms of the selection cassette was electroporated. Red/ET recombination should replace the rpsL-neo-PCR1 selection/counter-selection cassette with the markerless Non-sm fragment. Only colonies that have lost the cassette will grow on stp containing plates and will also be km<sup>S</sup>.

**A**



+



L-arabinose  
30°C to 37°C

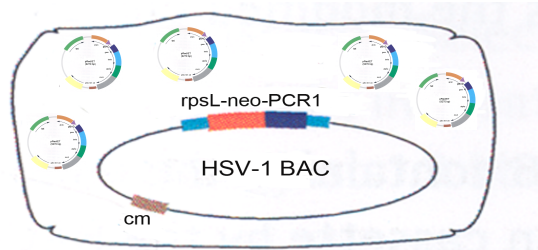
rpsL-neo-PCR1

PCR product  
rpsL-neo-PCR1

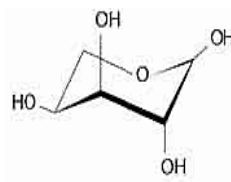
**B**



↓



+



L-arabinose  
30°C to 37°C

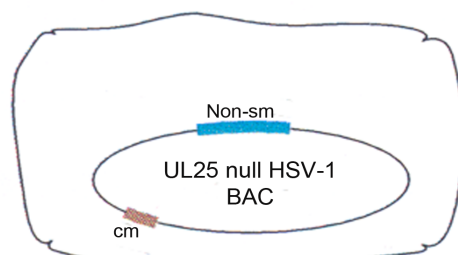
Non-sm

non-selectable overlapping  
oligonucleotide (Non-sm)

**C**



↓



### **3.2.3 Generation of the rpsL-neo counter selection cassette flanked by homology arms (rpsL-neo-PCR1)**

To target the UL25 gene of fHSV $\Delta$ pac, a PCR product (rpsL-neo-PCR1) that contained the rpsL-neo counter-selection cassette flanked by sequences homologous to 50 bp immediately upstream and downstream of the UL25 ORF was generated. The 1.4 kb rpsL-neo-PCR-1 fragment was produced using the forward primer PRC1-For and the reverse primer PRC1-Rev (Table 3.1) and amplified from the rpsL-neo DNA template supplied by the manufacturer using the PCR-cycle1 conditions described in Section 2.2.1.2. The purified 1.4 kb rpsL-neo-PCR-1 PCR product obtained is shown in Figure 3.6.

### **3.2.4 Step 1 - insertion of rpsL-neo-PCR1 into fHSV $\Delta$ pac**

Following incubation at 30°C overnight, DH10B bacteria containing fHSV $\Delta$ pac that had been transformed with the pRed/ET expression plasmid (Section 2.2.8.1), and control cells consisting of *E.coli* strain HS996 that contained a control BAC (pBeloBAC11) and pRed/ET, were divided into two aliquots. One bacterial suspension from each *E. coli* strain was induced by the addition of arabinose to express the genes mediating Red/ET recombination, while the other bacterial suspension acted as a control and remained uninduced. To allow expression of the genes mediating the Red/ET recombination enzymes, the induced and uninduced samples were incubated at 37°C for 45-60 min (Section 2.2.8.1). Step 1 of the BAC modification procedure was initiated by electroporating the purified 1.4 kb rpsL-neo-PCR-1 PCR product into the induced and uninduced DH10B cells. In addition, the induced and uninduced aliquots of HS996 cells were transformed with an rpsL-neo PCR product that had complementary sequences to pBeloBAC11 and was supplied by Gene Bridges. Following transformation of DH10B and HS996 with their respective rpsL-neo PCR products the induced and uninduced bacterial suspensions were subsequently divided into two further aliquots, representing the recombinant and non-recombinant samples. To allow recombination of the rpsL-neo PCR product into the BAC DNA contained in the host cell, the recombinant samples from each bacterial strain were incubated at 37°C for 70 min, while the non-recombinant control samples were stored on ice. A summary of the experimental outline and

Primer ID	Primer Sequence
PCR1-For	5'-GACAACGACCGCAGTTCTCGTGTGTTATTTTCGCTCTCCGCCTCTCGCAGGGCCTGGTGGTGGCGGGATCG-3'
PCR1-Rev	5'-TCTTGTTTTTTTCTCCCTAATGCCCCCTCCCCCTCGCCCACCACCCACTATCAGAAGAACTCGTCAAGAAGGCG-3'
Non-smF	5'-GCAGTTCTCGTGTGTTATTTTCGCTCTCCGCCTCTCGCAGΔTAGTGGGTGGTGGGCGAGGGGGGAGGGGGCATTAGGGAGA-3'
Non-smR	5'-TCTCCCTAATGCCCCCTCCCCCTCGCCCACCACCCACTAΔCTGCGAGAGGCGGAGAGCGAAAATAACACACGAGAACTGC-3'

**Table 3.1 Oligonucleotides used to generate the DNA fragments required for the Counter-Selection BAC Modification procedure**

The PCR primers, PCR1-For and PCR1-Rev, were used to generate rpsL-neo-PCR1 and contained 50 bp of HSV-1 homology directly upstream and downstream of the UL25 ORF and 24 bp of homology to the rpsL-neo cassette template (highlighted in red). The complementary oligonucleotides Non-smF and Non-smR were annealed to produce the non-selectable overlapping oligonucleotide, Non-sm. The symbol Δ represents the deleted UL25 ORF sequences.

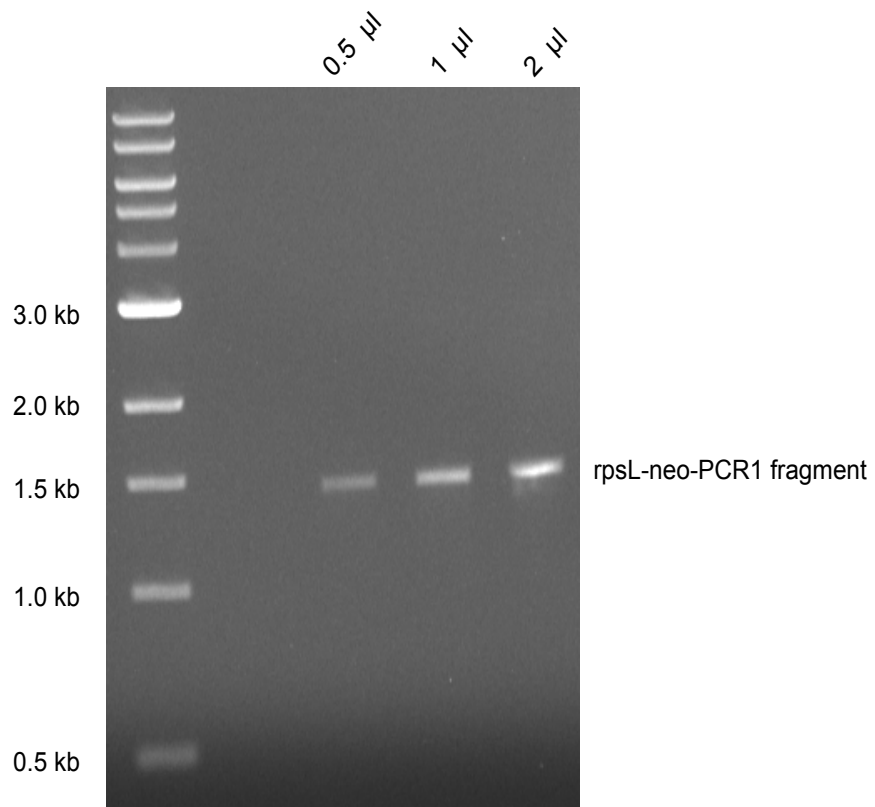


**Figure 3.6 Gel photograph showing the purified rps-neo-PCR1 PCR product**

0.5, 1 and 2 µl aliquots of the purified 1.4 kb rpsL-neo-PCR1 product were run on a 1% TAE gel to determine the purity and concentration of the fragment obtained. Band sizes were estimated using a 1 kb DNA ladder (New England Biolabs), the sizes of the bands upto 3.0 kb are shown on the left of the diagram.

the bacterial samples generated are illustrated in Figure 3.7. Following incubation, the DH10B and HS996 induced and uninduced recombinant and non-recombinant samples were plated onto L-broth agar containing tet/cm/km. As expected, the uninduced recombinant and non-recombinant bacterial samples remained  $km^S$ , reflecting the presence of an unmodified BAC in DH10B and HS966 cells. The efficiency of Red/ET recombination in the procedure is determined by the ratio of recombinant to non-recombinant  $km^R$  colonies produced by the induced bacterial suspensions during the experiment. The observed frequency was close to the expected frequency of 100 recombinant: 1 non-recombinant colony per plate, signifying that the majority of induced recombinant *E.coli* isolates had successfully undergone Red/ET recombination. To verify the fidelity of the amplified rpsL-neo-PCR1 product present in the induced recombinant bacteria and to confirm that the bacteria were  $km^R/stp^S$ , fifteen  $km^R$  DH10B colonies were selected for replica plating onto L-broth agar plates containing either tet/cm/km or tet/cm/stp. Included in the screen were five colonies of the  $km^R$  HS996 bacteria that were predicted to contain a modified BAC, and two  $km^S$  DH10B bacteria containing unmodified BACs. The results, shown in Table 3.2, revealed that only one of the  $km^S$  DH10B colonies was also  $stp^R$  and therefore contained an unmodified BAC. However, the results confirmed that nine of the recombinant DH10B and three of the recombinant HS996 colonies selected were  $km^R/stp^S$  and therefore contained fully functional rpsL-neo cassettes.

### 3.2.5 Verification of the modified HSV-1 BAC by Southern blot analysis

To confirm that the rpsL-neo-PCR1 product was inserted at the correct location within the modified fHSV $\Delta$ pac BACs, DNA was prepared from each of the nine  $km^R/stp^S$  DH10B clones and digested with *Bam*HI. The *Bam*HI fragments were separated on an agarose gel and analysed by Southern blotting. The DNA bound to nylon membrane was probed with the  $^{32}P$ -radiolabelled rpsL-neo-PCR1 fragment to detect any rpsL-neo-PCR1 sequences present in the modified BAC DNAs. The expected *Bam*HI restriction digest patterns of the modified and unmodified HSV-1 BACs were obtained using Vector NTi software (Invitrogen). The digested wt HSV-1 or HSV-1 BAC DNA contains the 2,294 bp *Bam*HI U

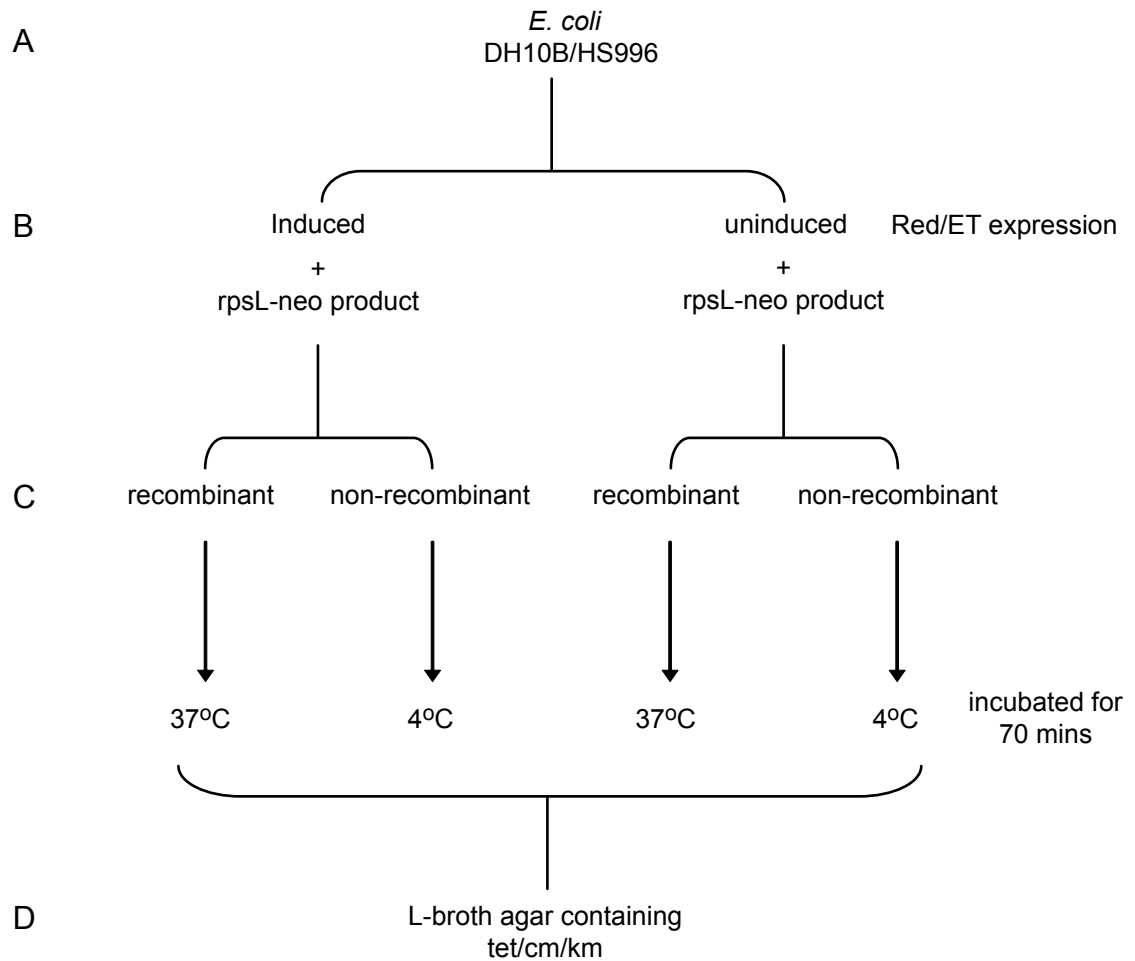


**Figure 3.7 DH10B and HS966 samples generated during Step 1 of the Counter-Selection BAC Modification procedure**

(A) Bacterial cultures of *E. coli* strains DH10B and HS966, each containing their respective BACs and pRed/ET, were grown at 30°C overnight and then divided into two aliquots. (B) Expression of the genes mediating Red/ET expression were 'induced' in one of the bacterial suspensions by the addition of arabinose, while the control cells remained 'uninduced'. Both bacterial suspensions were then incubated at 37°C for 45-60 min to allow expression of the Red/ET recombination enzymes and then electroporated with their respective rpsL-neo PCR products as indicated. (C) The induced and uninduced bacterial cells were subsequently divided into two further aliquots, representing the recombinant and non-recombinant samples for each strain. The recombinant samples for induced and uninduced DH10B and HS966 were incubated at 37°C for 70 min, while the non-recombinant bacterial suspensions for the induced and uninduced samples were stored on ice for 70 min. (D) After incubation each bacterial culture was plated onto L-broth agar containing tet/cm/km.

Step 1 Results			Modified BAC
Colony	stp <sup>R</sup>	km <sup>R</sup>	km <sup>R</sup> / stp <sup>S</sup>
<b>Recombinant DH10B Colonies</b>			
1	+	+	
2	-	+	Positive
3	-	-	
4	+	+	
5	-	+	Positive
6	-	+	Positive
7	-	-	
8	-	+	Positive
9	-	-	
10	-	+	Positive
11	-	+	Positive
12	-	+	Positive
13	+	+	
14	-	+	Positive
15	-	+	Positive
<b>Recombinant HS996 Colonies</b>			
1	-	+	Positive
2	-	+	Positive
3	-	-	
4	-	-	
5	-	+	Positive
<b>Non-recombinant DH10B Colonies</b>			
1	+	-	
2	-	-	

**Table 3.2 Counter-Selection BAC Modification Step 1 results for DH10B and HS996 cells with modified BACs**

The table shows DH10B and HS996 clones obtained after replica plating them onto L-broth agar containing either kanamycin or streptomycin after Step 1 of the BAC Modification Counter-Selection procedure. The bacterial colonies that screened positive for kanamycin resistance (km<sup>R</sup>) and streptomycin sensitivity (stp<sup>S</sup>) are ones that contained a modified BAC with the functional rpsL-neo-PCR1 product.

fragment (nucleotide sequences 48,635-50,929) spanning the UL25 gene of the HSV-1 strain 17 syn<sup>+</sup> genome (McGeoch et al., 1988). When the rpsL-neo-PCR1 product is recombined in this region of the HSV-1 genome, two *Bam*HI fragments, 1,873 bp and 863 bp, are obtained instead of the wt *Bam*HI 2,294 bp fragment. A representative phosphorimage of a Southern blot is shown in Figure 3.8. Lanes 1-3 of the image, containing the *Bam*HI-digested unmodified BAC DNA control (km<sup>S</sup>/stp<sup>R</sup> DH10B) samples, show the expected 2,294 bp *Bam*HI U fragment, whereas the remaining lanes (4-13) display the profiles of *Bam*HI-digested modified BAC DNAs. Lane 4 of the Southern blot contains the positive control consisting of digested km<sup>R</sup>/stp<sup>S</sup> HS996 modified BAC DNA, which shows the expected *Bam*HI fragment of 8,907 bp generated by the insertion of the rpsL-neo PCR product. Lanes 5-13 of the Southern blot contain digested BAC DNA preparations from the nine recombinant km<sup>R</sup>/stp<sup>S</sup> DH10B clones. Although the *Bam*HI 1,873 bp fragment was present in all nine km<sup>R</sup>/stp<sup>S</sup> DH10B samples, it was most clearly visible in lanes 6 (clone 14), and 9-13 (clones 10, 8, 6, 5 and 2, respectively). Lane 9, 10 and 13 also contained a *Bam*HI U fragment, which is most clearly visible in lane 13, indicating that these samples had a mixture of both modified and unmodified BAC DNAs. However, the presence of the *Bam*HI 1,873 bp fragment and the absence of the *Bam*HI U fragment in the remaining samples suggest that these BACs contain the inserted rpsL-neo-PCR1 cassette with the concomitant deletion of the UL25 ORF.

### 3.2.6 Generation of the non-selectable DNA product (Non-sm)

In the second stage of the Counter-Selection procedure the rpsL-neo cassette in the BAC is replaced with the non-selectable DNA. Two complementary oligonucleotides, Non-smF and Non-smR (Table 3.1), were annealed (Section 2.2.1.3) to produce the non-selectable, or markerless, product Non-sm. The 80 bp Non-sm fragment contains HSV-1 sequences present in the right and left HSV-1 homology arms of the rpsL-neo-PCR1 product to allow insertion by homologous recombination of the annealed overlapping oligonucleotide into fHSV $\Delta$ pac, with the concomitant excision of the rpsL-neo-PCR1 cassette, to produce an HSV-1 BAC lacking the UL25 ORF.

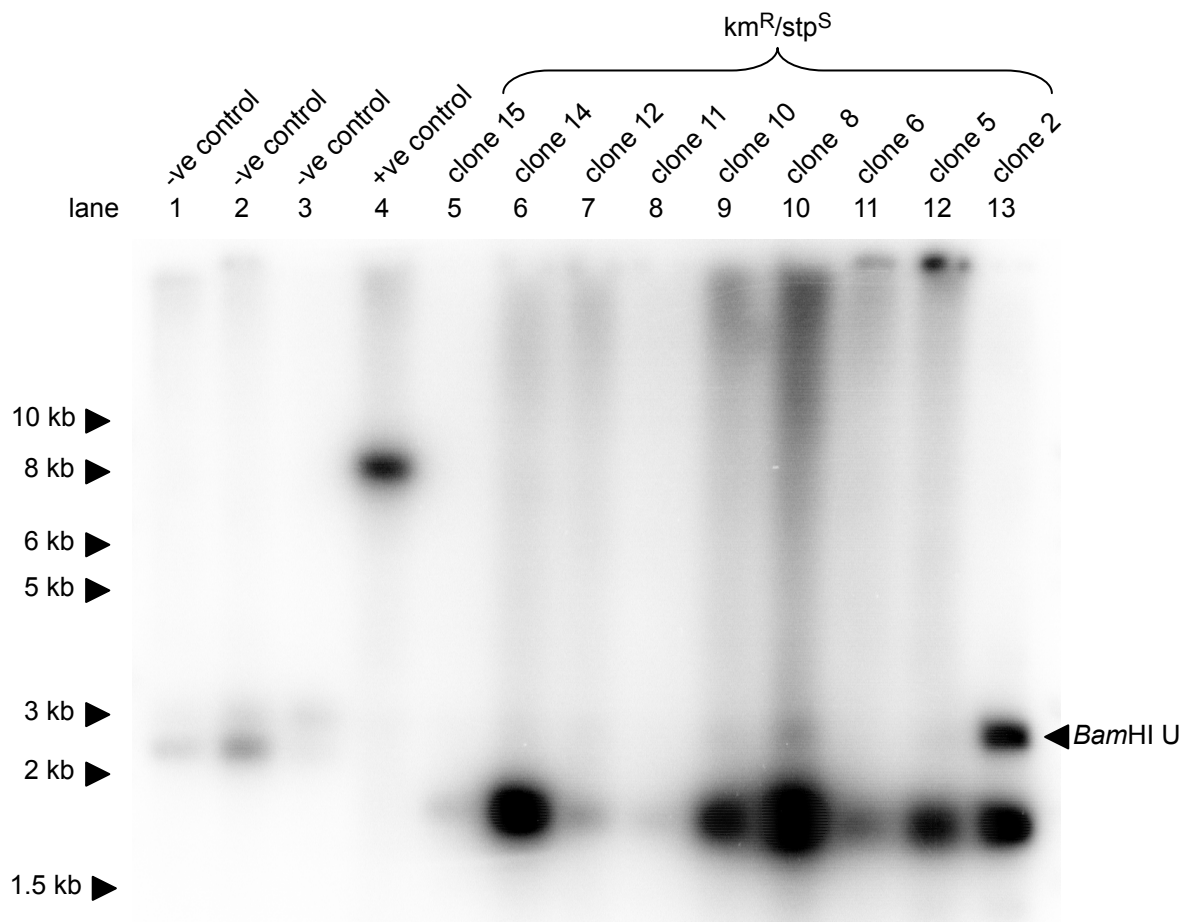


**Figure 3.8 Southern blot of BamHI digested BAC DNAs from Step 1**

The phosphorimage shows the *Bam*HI digested BAC DNA samples from Step 1 of the Counter-Selection BAC Modification procedure. Lane 1 is a negative control of an unmodified HSV-1 BAC from a DH10B clone. Lanes 2 and 3 are negative controls of an unmodified HSV-1 BAC from km<sup>S</sup>/stp<sup>R</sup> DH10B clones. Lane 4 is a positive control of a modified BAC containing a *rpsL*-neo cassette from the km<sup>R</sup>/stp<sup>S</sup> HS996 colony 1 (Table 3.2). Lanes 5-13 are the recombinant km<sup>R</sup>/stp<sup>S</sup> DH10B clones listed in Table 3.2, with the colony numbers for each clone indicated above the lanes. The position of the 2,294 bp *Bam*HI U fragment is indicated.

### 3.2.7 Step 2 - replacing the rpsL-neo-PCR1 cassette with the non-selectable (Non-sm) DNA in fHSV $\Delta$ pac

The second stage of the procedure was initiated by the addition of L-arabinose and induction of the Red/ET proteins in km<sup>R</sup>/stp<sup>S</sup> modified BAC containing DH10B samples 11 and 12 and the control km<sup>R</sup>/stp<sup>S</sup> HS996 samples 1 and 5 (Table 3.2). Subsequently, electrocompetent DH10B were transformed with the annealed overlapping oligonucleotide Non-sm (Section 2.2.1.3), and the electrocompetent HS996 were transformed with a BAC-repair oligonucleotide (Gene Bridges) designed to replace the rpsL-neo product inserted in the modified pBeloBAC11. Each transformed *E. coli* strain was divided into two aliquots with one representing the recombinant sample, which was incubated at 37°C to allow Red/ET recombination to proceed, and the other representing the non-recombinant sample, which was retained on ice. Following incubation for 70 minutes the recombinant and non-recombinant samples from each bacterial strain were plated onto L-broth agar containing tet/cm/stp and the results are shown in Table 3.3.

Step 2	Bacterial colonies per plate		Ratio (Rec:Non)
	Recombinant (Stp <sup>R</sup> )	Non-recombinant (Stp <sup>R</sup> )	
<b>DH10B</b>			
11	1.5 x 10 <sup>5</sup>	9.0 x 10 <sup>3</sup>	16:1
12	1.6 x 10 <sup>4</sup>	1.5 x 10 <sup>3</sup>	10:1
<b>HS996</b>			
1	9.2 x 10 <sup>3</sup>	8.0 x 10 <sup>2</sup>	11:1
5	1.0 x 10 <sup>4</sup>	9.0 x 10 <sup>2</sup>	11:1

**Table 3.3** The ratio of DH10B and HS996 recombinant:non-recombinants colonies obtained in step 2 of the Counter-Selection BAC Modification procedure

As in step 1 of the technique, a high ratio of about 100 recombinant: 1 non-recombinant colonies is indicative of efficient Red/ET recombination. The frequency of recombination observed was lower than expected for both the experimental and control samples tested. At this stage of the procedure

successful Red/ET recombination should result in the removal of the inserted rpsL-neo PCR product present in the host's modified BAC and its replacement with the non-selectable DNA fragment. Positive bacterial recombinants are selected on the basis of being km<sup>S</sup>/stp<sup>R</sup>. The antibiotic integrity of two of the stp<sup>R</sup> DH10B and two of the HS966 recombinants obtained in step 2 (Table 3.3) was tested by replica plating them onto to L-broth agar containing either tet/cm/km or tet/cm/stp. Unexpectedly, the stp<sup>R</sup> DH10B and HS996 colonies tested had acquired dual drug resistance and were both km<sup>R</sup> and stp<sup>R</sup>. Additional attempts to obtain the desired recombinants at this stage produced the same results.

### **3.3 Construction of $\Delta$ UL25MO and its marker rescuant MRUL25MO**

#### **3.3.1 $\Delta$ UL25MO**

Results from the Southern blot analysis of the modified fHSV $\Delta$ pac DNA (Section 3.2.5) revealed that the rpsL-neo-PCR1 cassette was present, replacing the UL25 ORF, and confirming that an HSV-1 UL25-deleted BAC had been created. Column-purified BAC DNA was prepared from *E. coli* carrying one of the modified BACs analysed by Southern blotting (lanes 6 in Figure 3.8, colony 14 from Table 3.2) and transfected together with the HSV-1 BamHI K fragment, which was added to repair the deleted *a* sequences encoding the Pac signals in the modified fHSV $\Delta$ pac, into UL25 expressing 8-1 cells. Three of the viral plaques that formed were plaque-purified and each of their viral titres was determined as outlined in Section 2.2.4. The stock with the highest titre was selected and subsequently referred to as  $\Delta$ UL25MO. The yield of  $\Delta$ UL25MO was compared to KUL25NS, the original HSV-1 UL25 null mutant, by infecting 8-1 cells with virus at MOI of 5 PFU/cell. After incubation for 24 hrs at 37°C the cells were harvested and the progeny virus was titrated on complementing (8-1) and non-complementing (Vero) cells. As expected,  $\Delta$ UL25MO and KUL25NS both failed to form plaques on Vero cells. In the complementing cells, although the size of the plaques obtained for both HSV-1 UL25 mutants were similar,  $\Delta$ UL25MO produced

a yield that was approximately ten-fold lower than KUL25NS (Table 3.4). The experiment was repeated twice more and the results produced were similar.

Virus	Yield of virus from 8-1 cells (PFU/ml)	
	Non-complementing cells (Vero)	Complementing cells (8-1)
$\Delta$ UL25MO	$<10^2$	$5.0 \times 10^7$
KUL25NS	$<10^2$	$5.1 \times 10^8$

**Table 3.4 Growth of HSV-1 UL25 null viruses on non-complementing and complementing cells**

A complementation assay (Section 2.2.7) was carried out to determine how well transiently expressed wt UL25 protein (pUL25) complemented the growth of  $\Delta$ UL25MO and KUL25NS. Vero cells were transfected with either the wt UL25 expressing recombinant plasmid (pFB-UL25) or the empty vector control (pFBpCI) and subsequently infected with  $\Delta$ UL25MO or KUL25NS at an MOI of 5 PFU/cell. At 24 hpi the cells were harvested and the progeny viruses were titrated on Vero and 8-1 cells. The results obtained are shown in Table 3.5 and are the average of three independent experiments. The progeny virus from  $\Delta$ UL25MO-infected Vero cells expressing wt pUL25 did not form plaques on Vero cells, whereas some of the progeny from KUL25NS-infected Vero cells expressing wt pUL25 produced plaques on the non-complementing cells. Furthermore, the total yield of virus from  $\Delta$ UL25MO-infected Vero cells expressing wt pUL25 on 8-1 cells was approximately ten-fold higher than that obtained from KUL25NS-infected Vero cells expressing pUL25.

Virus	Plasmid	Yield of virus (PFU/ml)	
		Vero cells	8-1 cells
KUL25NS	pFBpCI	$< 10^1$ (+/- 0.6)	$< 10^1$ (+/- 1.0)
	pFB-UL25	$2.6 \times 10^1$ (+/- 0.3)	$4.6 \times 10^5$ (+/- 1.1)
$\Delta$ UL25MO	pFBpCI	$< 10^1$ (+/- 0)	$< 10^1$ (+/- 0)
	pFB-UL25	$< 10^1$ (+/- 0)	$3.3 \times 10^6$ (+/- 1.3)

**Table 3.5 Complementation efficiencies of HSV-1 UL25 null viruses**

### 3.3.2 MRUL25MO

To confirm that there were no secondary mutations in the  $\Delta$ UL25MO genome that affected its viability, a marker rescuant of the virus was generated. The plasmid pGX292 was digested with *Bam*HI to release the HSV-1 strain 17 syn<sup>+</sup> *Bam*HI U fragment (nucleotide sequences 48,635-50,929), which contains the entire UL25 ORF (McGeoch et al., 1988). Marker rescue of the deleted UL25 sequences in  $\Delta$ UL25MO is obtained by homologous recombination between the complementary sequences of the HSV-1 *Bam*HI U fragment and the  $\Delta$ UL25MO genome. Vero cells were seeded into a well of a 24-well dish (Section 2.2.7.1) and transfected with *Bam*HI-digested pGX292 and subsequently infected with 5 PFU/cell of  $\Delta$ UL25MO (Section 2.2.7.3). After 24 h at 37°C the cells were harvested and the ability of the progeny virus to grow on Vero cells was determined. A single well-isolated plaque was picked and the virus was plaque purified (Section 2.2.9) twice on Vero cells prior to the production of a high titre stock of the marker rescuant virus, which was referred to as MRUL25MO. To compare the growth characteristics and phenotypes of  $\Delta$ UL25MO, MRUL25MO and wt HSV-1, the yield of the viruses were compared in duplicate on complementing and non-complementing cells grown on 35 mm tissue culture dishes. Each of the cell monolayers were infected with 10 PFU/cell of wt HSV-1,  $\Delta$ UL25MO or MRUL25MO virus and incubated at 37°C. After 1 h, the cells were treated with acid to remove residual input virus (Section 2.2.7.4) and then overlaid with supplemented DMEM and incubated at 37°C. At 24 hpi the cells were harvested and the progeny viruses were titrated onto 8-1 cells (Table 3.6). HSV-1 and MRUL25MO grew to comparable levels on permissive and non-permissive cells, confirming that the marker rescuant contained no deleterious secondary mutations. As expected,  $\Delta$ UL25MO grew on 8-1 cells but failed to grow on Vero cells, confirming that the mutation is lethal for growth.

Virus	Yield of virus on 8-1 cells (PFU/ml)	
	Growth in Vero cells	Growth in 8-1 cells
wt HSV-1	$5.7 \times 10^8$	$4.9 \times 10^8$
MRUL25MO	$3.3 \times 10^8$	$2.25 \times 10^8$
$\Delta$ UL25MO	$<10^1$	$4.0 \times 10^8$

**Table 3.6 Yield of HSV-1 viruses from non-complementing and complementing cells**

### 3.3.3 Single-step virus growth of HSV-1 viral stocks

Replicate 35 mm tissue culture dishes of complementing cells were infected with 10 PFU/cell of wt HSV-1,  $\Delta$ UL25MO or MRUL25MO virus. After 1 h at 37°C the cells were treated with acid wash and then overlaid with supplemented DMEM and incubated at 37°C. At 3, 6, 12 and 24 hpi the cells were harvested and the progeny virus was titrated onto 8-1 cells. The single-step growth analysis was performed only once, but demonstrated that  $\Delta$ UL25MO and MRUL25MO exhibited similar growth patterns and grew to titres comparable to wt HSV-1 (Figure 3.9), indicating that no secondary mutations were contributing to the growth defect of  $\Delta$ UL25MO.

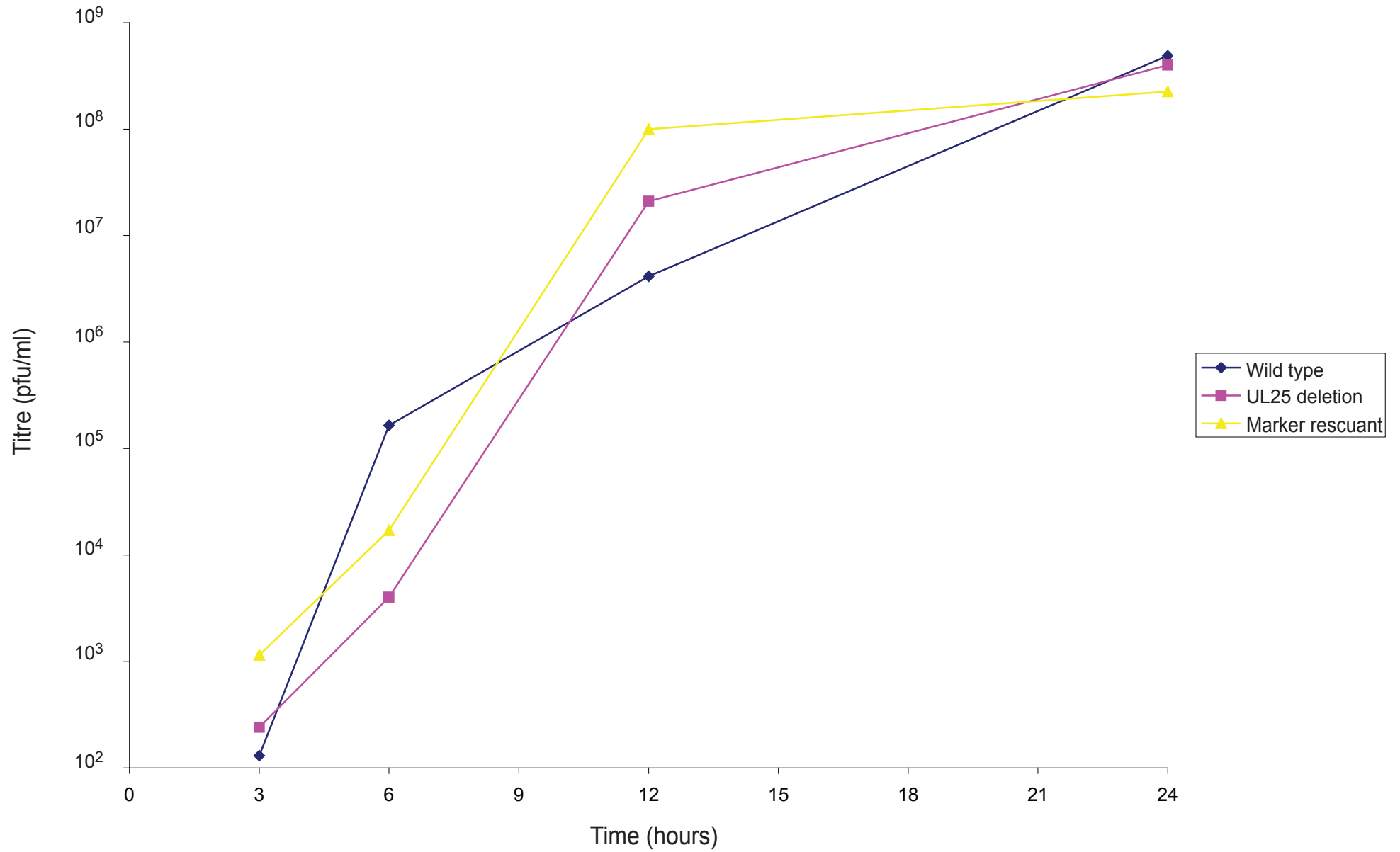
## 3.4 Discussion

During the first step of the Counter-Selection BAC Modification technique no problems were encountered and the rpsL-neo selection/counter-selection cassette was readily inserted at the correct position in the HSV-1 fHSV $\Delta$ pac genome. Despite several attempts, I was unsuccessful in completing the second step of the procedure in which the inserted cassette is replaced with non-selectable DNA that should result in the seamless deletion of the UL25 ORF in HSV-1 fHSV $\Delta$ pac. The inserted rpsL-neo cassette in the modified BACs of the host cells allows both positive and negative antibiotic selection of the recombinants obtained. The cassettes are then replaced with the desired markerless DNA by a second recombination event and subsequent antibiotic

**Figure 3.9 Comparison of the growth of wt HSV-1,  $\Delta$ UL25MO and MRUL25MO in 8-1 cells**

Single-step virus growth. Replicate 35 mm dishes of complementing cells were infected with 10 pfu/cell of HSV-1 strain 17 syn<sup>+</sup>,  $\Delta$ UL25MO or MRUL25MO. After 1 h at 37°C the cells were treated with acid to remove residual input virus and overlaid with supplemented DMEM and the incubation was continued at 37°C. At 3, 6, 12 and 24 hpi the cells were harvested and the progeny virus were titrated onto 8-1 cells.

Comparison of the growth of wt HSV-1,  $\Delta$ UL25MO and MRUL25MO in 8-1 cells



counter-selection to obtain  $stp^R/km^S$  bacteria. An inherent problem with the system used here appears to be the potential for spurious recombination events. Viral genomes contain a high number of repeated sequences and intramolecular recombination between them could result in the loss of the markers used in the system's selection process (Tischer et al., 2006). To ensure that the techniques for the system were being applied correctly, the manufacturer's additional controls were included throughout the procedure. However, the  $stp^R$  recombinant colonies obtained in step 2 for both the DH10B and the control HS996 bacterial cells were shown to be  $stp^R$  and  $km^R$ . Subsequently, several colleagues using the same method encountered similar problems and also detected only  $stp^R/km^R$  colonies at the second stage. They also confirmed that non-specific recombination events were occurring in fHSV $\Delta$ pac DNA. Recent improvements to the technology by Tischer et al. (2006), in which the recombination event is targeted to specific sequences, has resulted in the successful production of mutated HSV-1 virus. The difficulties encountered using the Counter-Selection BAC Modification system led to baculovirus vectors being used for subsequent functional analysis of the HSV-1 UL25 mutants generated.

The ability of the UL25 expressing 8-1 cell line to complement the growth of  $\Delta$ UL25MO suggested that no secondary mutations were contributing to growth defects of the mutant virus. This was confirmed by single-step growth analysis on complementing cells, which showed that  $\Delta$ UL25MO, MRUL25MO and wt HSV-1 grew to comparable levels (Figure 3.8). However, a ten-fold reduction in the yield of  $\Delta$ UL25MO in comparison to the original HSV-1 UL25 null mutant KUL25NS was observed in 8-1 cells when the viral stocks were titrated on to complementing cells (Section 3.3). The replication efficiency of  $\Delta$ UL25MO might be compromised, since the virus was obtained from the HSV-1 BAC fHSV $\Delta$ pac (Saeki et al., 1998) that lacks *oriL*. In addition, the presence of the rpsL-neo cassette that replaces the UL25 ORF in the viral genome may also affect the viability of  $\Delta$ UL25MO. UL25 lies in a nested transcription region with UL26, a capsid maturation protease, and the transcription levels of UL26 may be affected as both UL25 and UL26 share 3' co-terminal transcripts. However, none of these possibilities seems likely, since the yield of  $\Delta$ UL25MO from complementing cells was comparable to the yields observed for its marker rescuant, MRUL25MO, which were in turn similar to the yields obtained for wt

HSV-1 strain 17 syn<sup>+</sup> (Table 3.6). Alternatively, the disparity in yields observed between the two HSV-1 UL25 null mutants might be due to strain variations between the HSV-1 KOS derived KUL25NS and the HSV-1 strain 17 syn<sup>+</sup> derived  $\Delta$ UL25MO virus. Although  $\Delta$ UL25MO gave lower yields of virus in 8-1 cells in comparison to KUL25NS, it performed better in transient complementation assays than KUL25NS. Since KUL25NS can produce a low level of wt virus as a consequence of recombination during complementation experiments, using  $\Delta$ UL25MO increased the sensitivity of the assay making it easier to distinguish between non-functional and poorly complementing UL25 mutants.

## 4 Generation and complementation analysis of the mutant pUL25s

### 4.1 Introduction

As discussed previously (Section 1.4.1), Bowman et al. (2006) used both the 3D structural information and ET analysis of the N-terminally truncated version of pUL25 (residues 134-580) to identify four clusters of amino acids (C1-C4) on the surface of pUL25 that were predicted to be involved in protein-protein interactions. Their study also revealed five looped out regions (L1-L5) containing unstructured residues, and three residues at the carboxyl terminus of pUL25 that were also disordered (L6). The aim of the work described in this chapter was to relate the structure of pUL25 to its function by constructing a series of mutant UL25 genes and to characterise the expressed proteins. Specifically, amino acids within C1, C2, C3 and C4, were targeted as well as the unstructured residues in L1-L6. Initially, residues mutated in C1, C2, C3 and C4 were substituted with alanine. Since alanine is the smallest chiral amino acid, substitution with this residue will remove side-chain atoms that are present on the wt residue. The observed effect of this removal during analysis is typically interpreted to indicate the contribution of the deleted side chain to the stability of any protein-protein interactions. Alanine substitution is also considered to be a relatively conservative change due to the ambivalent nature of the amino acid. Since it is only slightly hydrophobic it can reside both inside and outside a protein molecule. The codons of several residues within a cluster were mutated simultaneously to increase the probability of creating a functionally impaired pUL25.

Although the amino acid sequence normally codes for the 3D structure of a protein, it may code for an entirely unfolded protein, or protein region, as indicated by the unstructured residues identified in the L1-L6 regions of pUL25. These disordered portions of a protein molecule are often highly flexible areas that are involved in molecular recognition. To examine the functional roles of the unstructured portions of the molecule, a panel of deletion mutant proteins, pUL25-L1 - pUL25-L6, were generated that lacked the unstructured amino acids

of their particular regions. Deletion mutants were created in preference to those with substitutions or insertions of additional amino acids at the disordered regions in order to increase the possibility of observing a phenotypic affect. The absence of unstructured residues in a looped out region of the protein may compromise its flexibility and, as a consequence, affect the ability of pUL25 to interact with other proteins. As well as an L6 mutant protein lacking the unstructured residues, an additional L6 mutant was constructed by substituting two of the three unstructured amino acids (S578 and V580) with alanine, since the wt residue at position 579 was alanine.

To assess the functional impact of each of the mutant UL25 proteins generated, their ability to complement the growth of the HSV-1 UL25 null virus,  $\Delta$ UL25MO, in non-permissive cells was examined. Three deletion mutant proteins, pUL25 $\Delta$ 1-45, pUL25 $\Delta$ 1-59 and pUL25 $\Delta$ 1-133 were also included in the study to establish the significance of the uncrystallised portion of UL25 (residues 1-133). The plasmid constructs expressing these proteins were supplied by Dr V. Preston.

## 4.2 Methods used for site-directed mutagenesis

To create the mutated UL25 fragments, which were used to construct the mutant UL25 genes, either annealed complementary oligonucleotides were prepared or PCR was performed. Convenient REN cloning sites, located upstream and downstream from the target residues, were included in the mutated fragments generated and used to transfer the sequences into the UL25 gene. If possible, additional REN sites were introduced by silent mutagenesis into the nucleotide sequence of the PCR primers or the complementary oligonucleotides. These sites were useful for detecting plasmid constructs containing the mutated UL25 fragment. The additional REN sites, which did not alter the protein sequence of the gene, were identified in the UL25 ORF using the Webcutter bioinformatics program (<http://rna.lundberg.gu.se/cutter2/>). When the distance between the cloning sites was less than 90 bp, overlapping oligonucleotides were prepared. When the distance between the cloning sites was greater than 90 bp and the mutated residues were not sufficiently close to one of the cloning sites to amplify the required UL25 fragment in a single PCR, a two-step approach, referred to as overlap extension PCR (Ho, 1989), was used.

Summaries of the single-step and overlap extension PCR procedures are illustrated in Figure 4.1 and Figure 4.2, respectively.

Dr. V. Preston had previously cloned the wt HSV-1 strain 17 syn<sup>+</sup> UL25 ORF into pFBpCI to produce the recombinant plasmid, pFB-UL25 (Figure 4.3). The pFB-UL25 construct was used as the template DNA to generate and amplify the mutated UL25 fragments during PCR. Each purified PCR product was subcloned into the pGEM-T Easy vector (Figure 4.4) and plasmid DNA was prepared from each of the isolates obtained. The DNA samples containing UL25 inserts were identified with the appropriate REN digestion, and DNA sequencing with the M13 DNA sequencing primers (Table 4.1) verified that the recombinant pGEM-T Easy DNAs contained the desired UL25 mutations. To generate the recombinant plasmids, the purified PCR REN fragment from recombinant pGEM-T Easy plasmid or the annealed overlapping oligonucleotide was ligated to REN fragments from pFB-UL25. The recombinant constructs produced, together with the mutated residues present in the UL25 gene, are listed in Table 4.2. Prior to further analysis the entire UL25 mutant gene in each of the recombinant pFBpCI constructs was sequenced, using the DNA sequencing primers pFB-Forward and Reverse (Table 4.1), to confirm that each construct contained the expected UL25 nucleotide sequence with the desired alterations. A summary of the cloning procedures used is illustrated in Figure 4.5. In addition to containing the HCMV IE promoter that allows the expression of foreign proteins in mammalian cells, pFBpCI is also a baculovirus transfer vector. This plasmid was selected on the basis that recombinant baculoviruses were required for subsequent experiments to investigate the DNA packaging and capsid assembly functions of the encoded mutant UL25 proteins (Section 5.2).

## 4.3 Cluster mutants

### 4.3.1 C1 mutant construct (pFB-UL25-C1)

The nucleotide sequence that specifies three (R362, G363 and N365) of the nine residues in C1 is located between the REN sites *DdeI* (1100 bp) and *NruI* (1199 bp) of pFB-UL25 (Figure 4.6). A fragment was generated using the PCR primers C1-F that encoded the mutations R363A, G363A and N365A and the cloning site

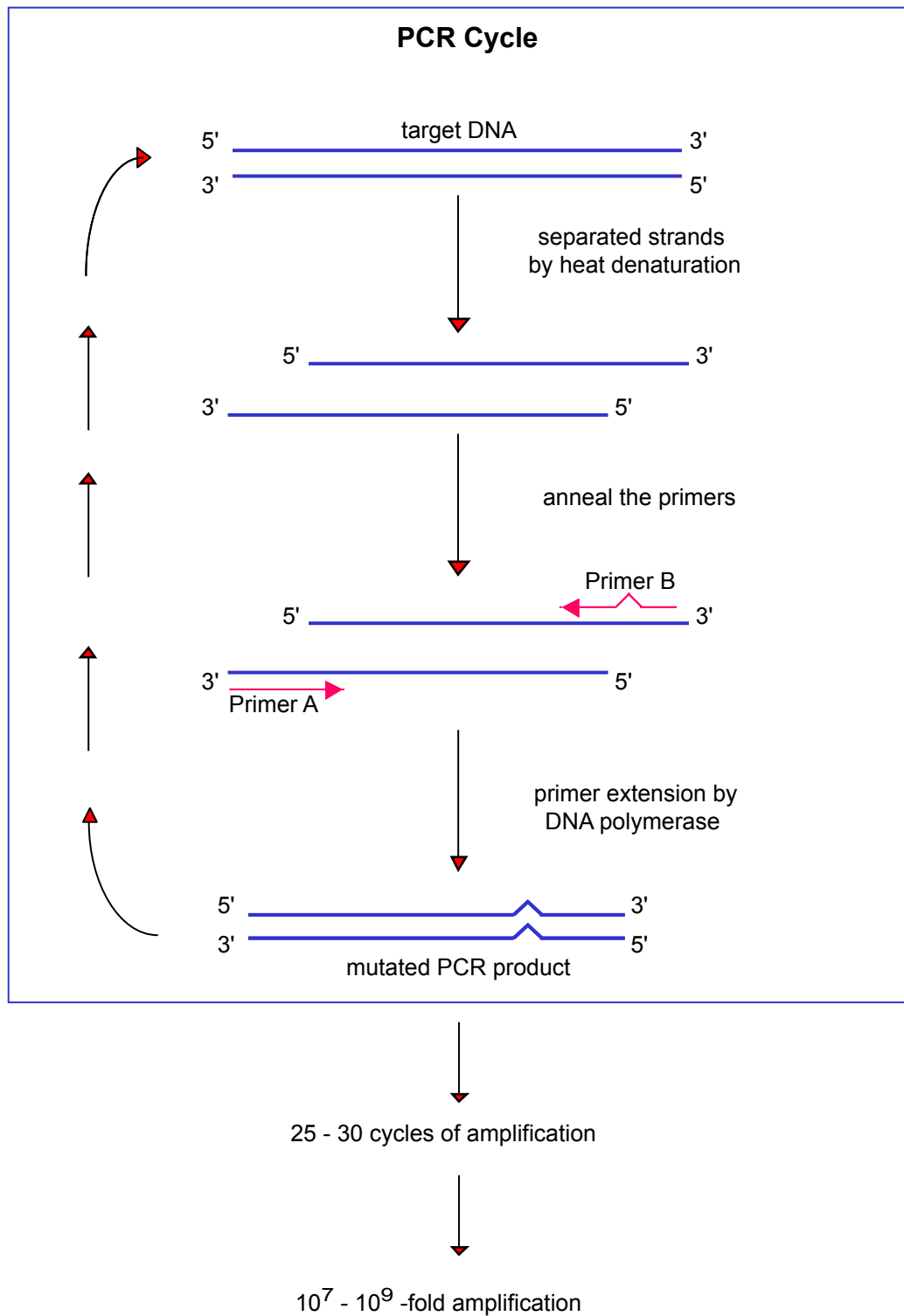


**Figure 4.1 Site-directed mutagenesis by PCR**

PCR is a cyclic process of double-stranded separation of the target DNA by heat denaturation, specific hybridisation or annealing of short oligonucleotide primers to the single-stranded DNA, and synthesis of double-stranded DNA by DNA polymerase (Saiki *et al.*, 1985). This process is illustrated in the boxed area of the diagram. The full-length mutated DNA is amplified during subsequent amplification cycles to produce multiple copies of the fragment. In site-directed mutagenesis using PCR, the target gene is amplified using a flanking primer (Primer A) and a primer (Primer B), which overlaps the target area and contains the required mutation. The primer pair are designed such that the amplified product can be REN digested and the full-length UL25 gene reconstructed in a ligation reaction with vector and wt UL25 REN fragments.

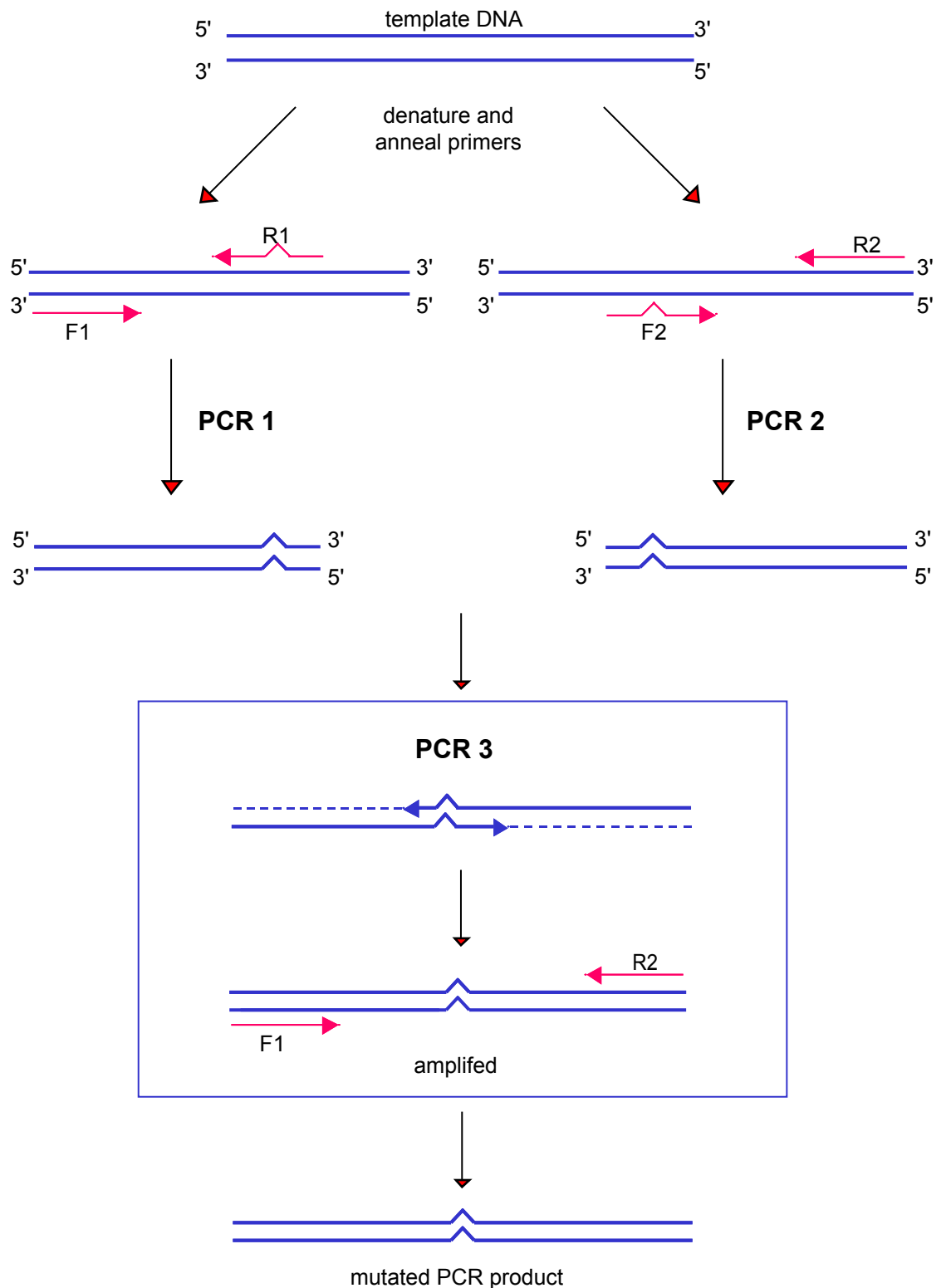


**Figure 4.2 Site-directed mutagenesis by overlap extension PCR**

Two fragments of the target gene are amplified in two separate PCRs (PCR 1 and 2). Both PCRs use a set of flanking (F1 and R2) and mutagenic primers (F2 and R1), with PCR 1 using the primer pair, F1 and R1, and PCR 2 using the F2 and R2 primers. The fragments produced from each reaction contain a region of overlap where, in both products, the desired mutations are located. During PCR 3 the fragments from PCR 1 and 2 are mixed, denatured and annealed at the regions of overlap to form heteroduplexes that are extended, as indicated by the dashed lines, to form full-length double-stranded mutant DNA. The full-length DNA is subsequently amplified during PCR 3 using the flanking primers, F1 and R2.

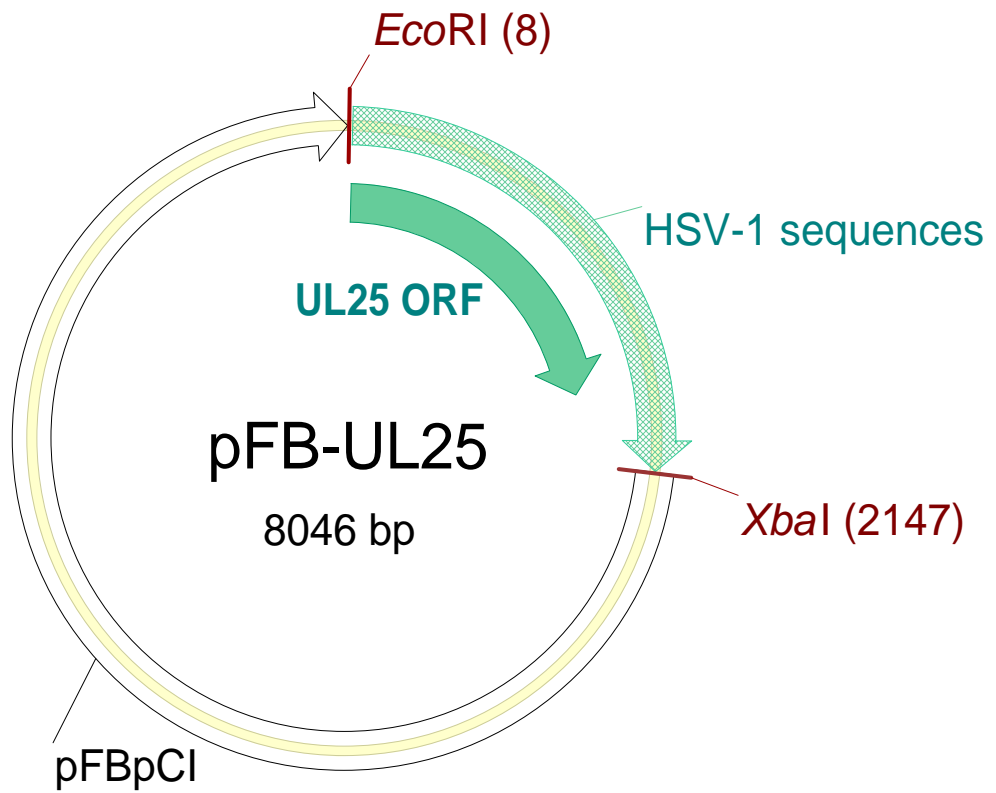


**Figure 4.3 Plasmid map of pFB-UL25**

The green-hatched arrow represents the HSV-1 sequences inserted in the pFBpCI backbone, with the UL25 ORF denoted by the block green arrow. The position of the unique REN sites, *EcoRI* and *XbaI*, are highlighted in red.

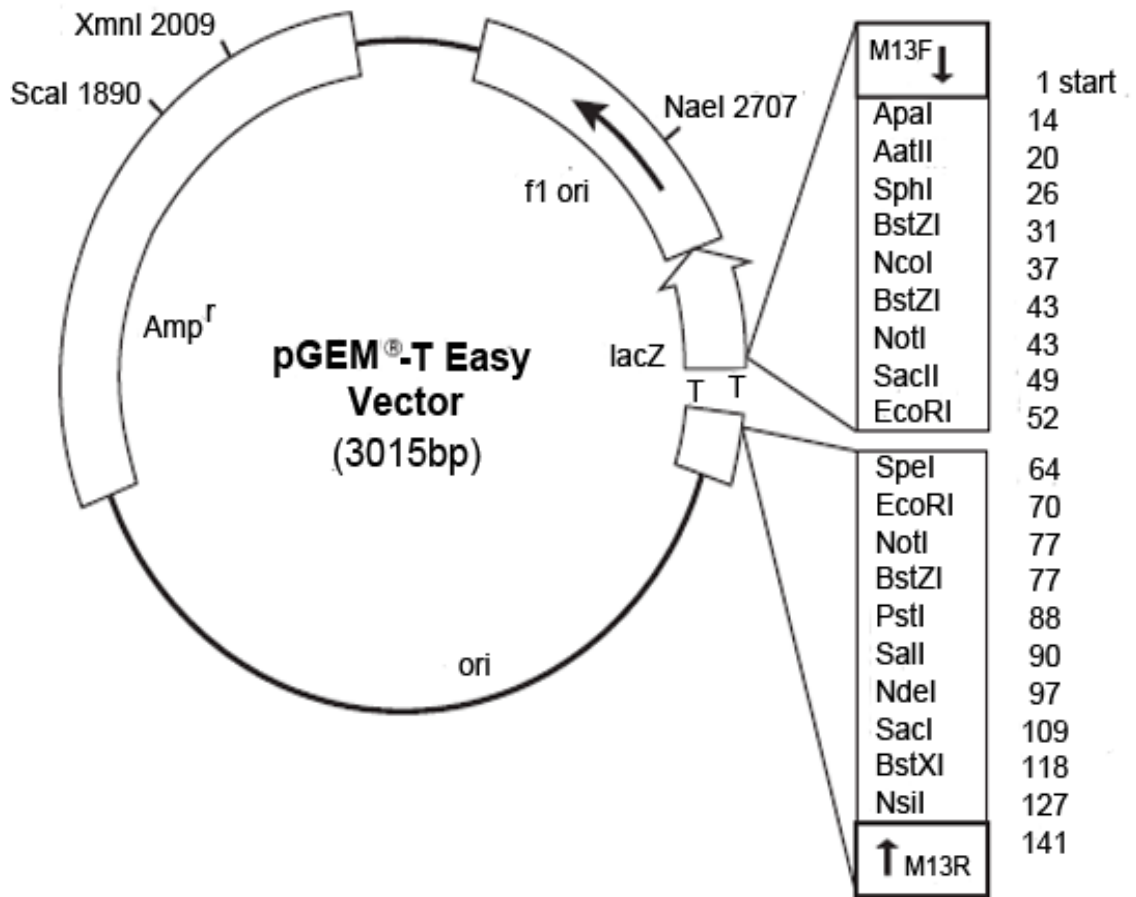


**Figure 4.4 pGEM-T Easy vector map**

The position of the REN sites and the location of the ampicillin (Amp) gene, f1 origin of replication (f1 ori) and origin of replication (ori) are shown. The broken arrow represents the site where the vector has been linearised with *EcoRI* and a T has been added to both 3' ends (position 60 bp on the map) (adapted from Promega Technical Manual).

<b>DNA Sequencing Primers</b>	
<b>pGEM-T Easy primers</b>	
M13 Forward	5'-TCACACAGGAAACAGCTATGAC-3'
M13 Reverse	5'-CGCCAGGGTTTTCCCAGTCACGAC-3'
<b>pFB-UL25 primers</b>	
pFB-Forward	5'-TCTCCACAGGTGTCCACTCC-3'
pFB-Reverse	5'-TTCTCGACAAGCTTGGTACC-3'

**Table 4.1 DNA sequencing primers**

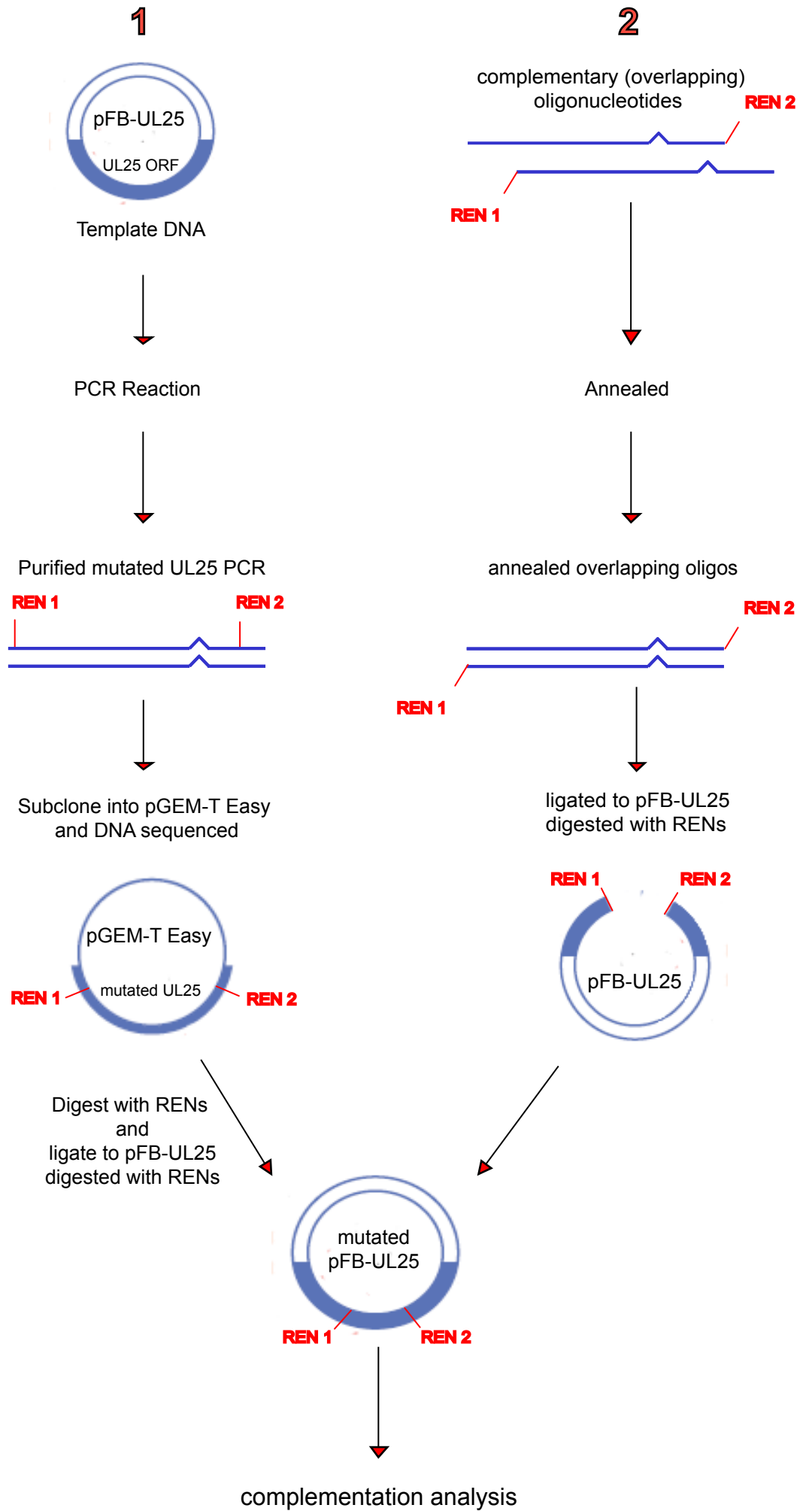
<b>Plasmids</b>	<b>Expressed protein</b>	<b>Substituted residues in UL25</b>					
pFB-UL25	pUL25						
pFB-UL25-C1	pUL25-C1	R362A	G363A	N365A			
pFB-UL25-C2	pUL25-C2	R148A	D150A	N152A	D156A		
pFB-UL25-C3A	pUL25-C3A	G169A	S170A	G172A			
pFB-UL25-C3B	pUL25-C3B	G169A	S170A	G172A	G202V	R203A	K206A
pFB-UL25-C4A	pUL25-C4A	N396A	Y398A	D400A	L402A		
pFB-UL25-C4B	pUL25-C4B	R390A	N396A	Y398A	D400A	L402A	
pFB-UL25-L6sub	pUL25-L6sub	S578A	V580A				
<b>Plasmids</b>	<b>Expressed protein</b>	<b>Deleted residues in UL25</b>					
		<b>From</b>	<b>To</b>	<b>Number of deleted residues</b>			
pFB-UL25-L1	pUL25-L1	A249	D254	6			
pFB-UL25-L2	pUL25-L2	R335	G345	11			
pFB-UL25-L3	pUL25-L3	P417	A425	9			
pFB-UL25-L4	pUL25-L4	P479	T483	5			
pFB-UL25-L5	pUL25-L5	R511	N513	3			
pFB-UL25-L6	pUL25-L6	S578	V580	3			
pFB-UL25 $\Delta$ 1-45 *	pUL25 $\Delta$ 1-45	M1	R45	45			
pFB-UL25 $\Delta$ 1-59 *	pUL25 $\Delta$ 1-59	M1	R59	59			
pFB-UL25 $\Delta$ 1-133 *	pUL25 $\Delta$ 1-133	M1	V133	133			
<b>Plasmids</b>	<b>Expressed protein</b>	<b>Combination mutant</b>					
pFB-UL25-C1L2	pUL25-C1L2	C1 mutations R362A, G363A and N365A and L2 deleted residues A249-D254					

**Table 4.2 List of the pFB-UL25 constructs generated and their mutated residues**

(constructs marked \* were supplied by Dr V. Preston)

**Figure 4.5 Summary of the cloning strategies and methods used to generate the mutant UL25 constructs**

The mutated UL25 sequences were generated either by using primers containing the required nucleotide changes in a PCR reaction (Section 2.2.1.2) with pFB-UL25 as a template (1) or by annealing complementary (overlapping) oligonucleotides (Section 2.2.1.3) containing the desired mutations (2). The PCR products were resolved on 5% polyacrylamide gels and the purified fragments (Section 2.2.3.2) were sub-cloned into the pGEM-T Easy vector (Section 2.1.9). The ligated DNA (Section 2.2.2) was electroporated into DH5 $\alpha$  (Section 2.2.5) and DNA samples were prepared from the ampicillin resistant colonies using the QIAprep spin miniprep protocol (Section 2.1.14). Each plasmid isolate was screened for the presence of the desired UL25 insert using REN analysis (Section 2.2.1.1) and by DNA sequencing (Section 2.2.3.4) with the primers M13 forward and reverse (Table 4.1). PCR products with the correct UL25 insert were released from pGEM-T Easy recombinants using the appropriate REN digests and purified. Mutant pFB-UL25 plasmids were generated by ligating the appropriate gel purified pFB-UL25 fragments to the mutated UL25 fragments and electroporating the DNA into DH5 $\alpha$ . DNA was prepared from the recombinant pFB-UL25 clones using the QIAprep spin miniprep protocol and recombinants containing the correct UL25 sequences were identified using REN analysis and by DNA sequencing with the pFB-UL25 sequencing primers, pFB-Forward and pFB-Reverse, shown in Table 4.1.



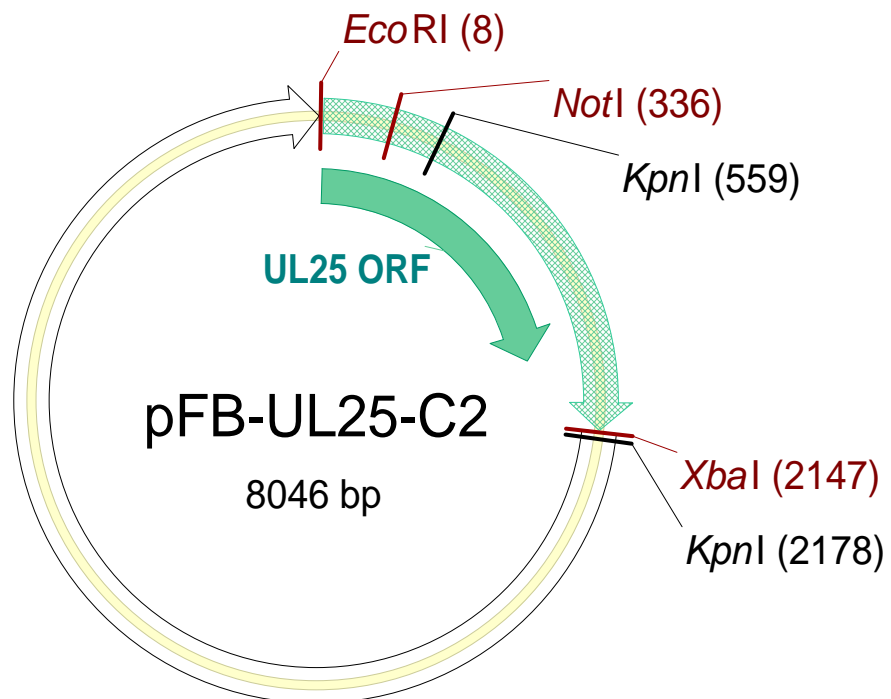
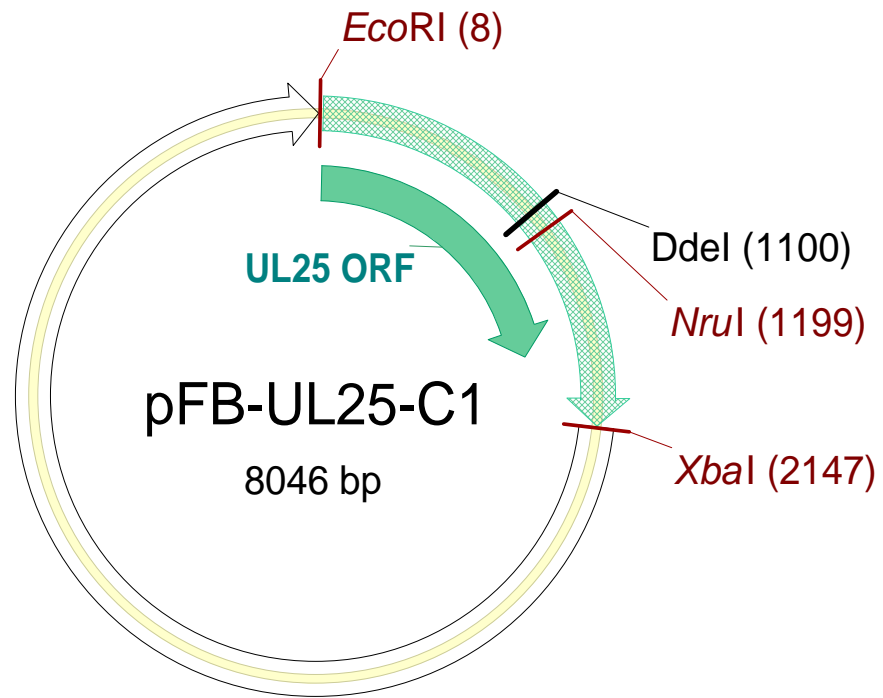


**Figure 4.6 Plasmid maps of pFB-UL25-C1 and pFB-UL25-C2**

The REN sites used in the construction and analysis of each plasmid are shown. The green-hatched arrow represents the HSV-1 sequences inserted in the pFBpCI backbone, with the UL25 ORF denoted by the block green arrow. Multiple cutting REN sites are coloured black and unique REN sites are highlighted in red.

*DdeI*, and C1-R that contained the *NruI* site (Table 4.3A). The purified PCR product was cloned into pGEM-T Easy and plasmid DNA was prepared from the isolates obtained. The recombinant pGEM-T Easy DNA was identified by the presence of a single *NruI* site located in the UL25 gene. DNA samples from these plasmids were sequenced using the M13 sequencing primers, which revealed that one contained the desired mutations. The 99 bp UL25 insert was released from the pGEM-T Easy recombinant by digestion with *DdeI* plus *NruI*. The purified fragment was ligated to the pFB-UL25 *EcoRI*-*DdeI* 1092 bp and *NruI*-*EcoRI* 6855 bp fragments and then electroporated into DH5 $\alpha$ . Plasmid DNA samples, prepared from five recombinant bacterial clones, were digested with *EcoRI* plus *NruI*, and *EcoRI* alone. Three of the plasmids produced the expected 1191 bp *EcoRI*-*NruI* and 8046 bp *EcoRI* fragments. One of the plasmids was selected and renamed pFB-UL25-C1.

### 4.3.2 C2 mutant construct (pFB-UL25-C2)

The nearest convenient cloning sites flanking the codons specifying four (R148, D150, N152 and D156) of the six residues in the C2 region were *NotI* (336 bp) and *KpnI* (559 bp), which are shown in Figure 4.6. Since the distance between the two REN sites and the desired mutations was too great to use either annealed overlapping oligonucleotides or to amplify the mutated sequences in a single PCR, overlap extension PCR (Ho, 1989) was utilised (Figure 4.2). Unlike the single-step PCR procedure used previously, where two primers and one PCR reaction are required, overlap extension PCR uses four primers and three separate PCR reactions to introduce the desired site-specific mutations. In the first PCR, one pair of primers amplifies the DNA that includes the mutations together with the upstream sequences. The forward, or flanking, primer in this PCR contains the wt sequences and an appropriate REN cloning site, while the reverse primer contains the desired mutations. In the second PCR, the primer pair amplifies the DNA that includes the mutations and the downstream sequences, with the forward primer in this pair containing the required mutations and the reverse, or flanking, primer containing the wt sequences and an appropriate REN cloning site. The products generated during these initial two PCRs contain a region of overlap located at the site of the mutations. These two fragments are mixed during a third PCR cycle and denatured and annealed at the

UL25 Mutant	Primer ID	C1 – C2 Primers
pFB-UL25-C1	C1-F	5'-TTCCTCAGC <u>GCTGCACATGCC</u> CCTATTCCTGTGGGAGGACCAGACTCTGC-3' <i>Ddel</i>
	C1-R	5'-ACGTTACCGTT <u>TCGCGAG</u> AAGACGCTGGATAACGCCAGGGCCGTTATGG-3' <i>NruI</i>
pFB-UL25-C2	C2-F1	5'-CGAAACGTACATGAATTGCAGGTGCTCTAGAAGCACTAGAAACAGCA <u>GCGGCCGCCG</u> CCGAAGAGGCGGATGC-3' <i>NotI</i>
	C2-R1	5'-CGTACACCATGTGTAGCAGAGCTACAGGAAGTGCAGTAGCATATGCTAGCGGCGGGTTCGTTGCGCACGATCTGG-3'
	C2-F2	5'-CAGATCGTGCGCAACGACCCGCCGCTAGCATATGCTACTGCACTTCCTGTAGCTCTGCTACACATGGTGTACGC-3'
	C2-R2	5'-GGTCAGGGGAAAATCTGTAAATAGTACGATCCTGGATAGTG <u>CGGTACC</u> AGGTCCCGAACACCACCCCGACGAGC-3' <i>KpnI</i>

**Table 4.3A – The primers used to generate the UL25 mutant constructs listed**

Bases highlighted in red are the base pair changes resulting in substitutions of amino acids within the UL25 protein. The bases highlighted in green are nucleotide changes used to adjust the percentage of G + C bases in a primer so that a pair of primers had an equal percentage. The REN sites included in the primers are underlined and their respective names are shown underneath.

region of overlap to generate heteroduplexes, which are subsequently extended to form full-length double-stranded mutant DNA. The full-length DNA is amplified during the third PCR cycle, using the two flanking primers from PCR reaction one and two that contain the REN cloning sites.

To mutate the four C2 codons using overlap extension PCR, the flanking primers C2-F1 and C2-R2 (Table 4.3A), containing the cloning sites *NotI* (336 bp) and *KpnI* (559 bp) respectively, and the mutagenic primers C2-F2 and C2-R1 (Table 4.3A), containing the desired mutations and including overlapping sequences at their 3'-ends, were constructed. Two initial PCR reactions, PCR1 and PCR2, were performed using the primers C2-F1 and C2-R1, and C2-F2 and C2-R2, respectively. The purified 165 bp PCR1 fragment and 223 bp PCR2 fragment were denatured and annealed during the third PCR cycle (PCR3) and extended, using the flanking primers C2-F1 and C2-R2 from PCR1 and PCR2, respectively, to form the full-length double-stranded mutant DNA. The purified PCR3 315 bp product was subsequently ligated to pGEM-T Easy and electroporated into DH5 $\alpha$ . Recombinant plasmids, prepared from pGEM-T Easy isolates, were identified by the presence of a single *SmaI* site that was located in the UL25 sequences. Three recombinant plasmids, which contained a single *SmaI* site, were digested with *KpnI* plus *NotI*. One of the plasmids produced the expected 223 bp fragment, indicating that it contained the UL25 insert. DNA sequencing of this plasmid verified that the UL25 insert encoded the mutated residues R148A, D150A, N152A and D156A. The purified 223 bp fragment was subsequently ligated to the pFB-UL25 *KpnI*-*XbaI* 1588 bp and *XbaI*-*NotI* 6235 bp fragments to produce pFB-UL25-C2.

### 4.3.3 C3 mutant constructs (pFB-UL25-C3A and pFB-UL25-C3B)

Two C3 mutant constructs were generated. The first construct, pFB-UL25-C3A, encoded three mutated residues and the second, pFB-UL25-C3B, encoded six mutated residues of the eight amino acids assigned to the cluster.

#### 4.3.3.1 pFB-UL25-C3A

The *KpnI* (559 bp) and *NotI* (336 bp) sites in the UL25 gene flanked the nucleotide sequences specifying three of the six residues in C3 (Figure 4.7). These two REN sites were incorporated in the PCR primers used to create the fragment encoding the three missense mutations G169, S170 and G172. The primer C3A-F (Table 4.3B) contained the wt sequences upstream from the mutated codons and included the unique *NotI* (336 bp) site. The reverse primer C3A-R (Table 4.3B) encoded the mutated residues G169A, S170A and G172A and wt sequences downstream of these mutations that encompassed a *KpnI* (559 bp) site. Initial attempts using these primers and the PCR-cycle1 cycle (Section 2.2.1.2) to obtain the required PCR product produced various sized fragments, none of which corresponded to the size of the predicted 284 bp PCR product. To increase the specificity of the reaction a new PCR programme, PCR-cycle2 (Section 2.2.1.2), was used that had a higher annealing temperature than PCR-cycle1. A PCR product of the correct size was identified and the purified fragment was cloned into pGEM-T Easy. DNA was prepared from the recombinant bacterial clones and those containing UL25 inserts were identified by the presence of a single *SmaI* in the UL25 gene. The recombinant plasmids containing a single *SmaI* site were digested with *KpnI* plus *NotI* and several produced a 223 bp fragment, confirming the presence of the PCR fragment. DNA sequencing verified that one of the recombinant plasmids encoded a UL25 insert with the desired mutations. The purified *KpnI-NotI* 223 bp insert from this bacterial clone was ligated to the pFB-UL25 *KpnI-XbaI* 1588 bp and *XbaI-NotI* 6235 bp fragments and the ligated DNA was electroporated into DH5 $\alpha$ . Plasmid DNA samples, prepared from the recombinant bacterial clones and the control plasmid (pFB-UL25), were digested with *KpnI* plus *NotI* and *EcoRI* plus *XbaI*. A recombinant plasmid contained the expected *KpnI-NotI* fragments of 223 bp, 1619 bp and 6204 bp and the *EcoRI-XbaI* fragments of 2139 bp and 5907 bp and was named pFB-UL25-C3A.

#### 4.3.3.2 pFB-UL25-C3B

Preliminary complementation experiments indicated that pUL25-C3A supported viral growth in non-permissive cells infected with  $\Delta$ UL25MO. A new construct

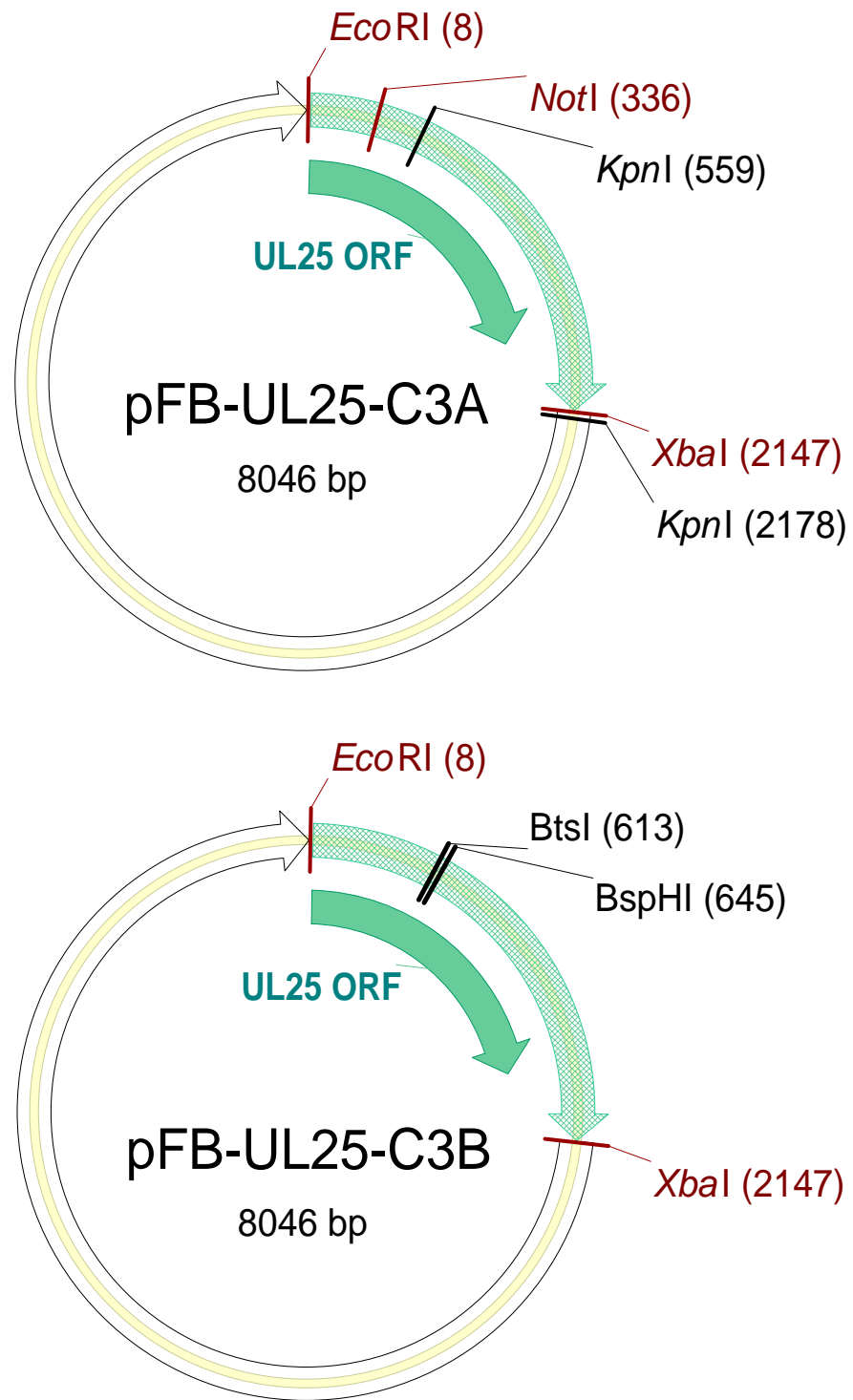


**Figure 4.7 Plasmid maps of pFB-UL25-C3A and pFB-UL25-C3B**

The REN sites used in the construction and analysis of each plasmid are shown. The green-hatched arrow represents the HSV-1 sequences inserted in the pFBpCI backbone, with the UL25 ORF denoted by the block green arrow. Multiple cutting REN sites are coloured black and unique REN sites are highlighted in red.

UL25 Mutant	Primer ID	C3 – C4 Overlapping Oligonucleotides and Primers
pFB-UL25-C3A	C3A-F	5'-GAAACGTACATGAAATTGCAGGTGCTCTAGAAGCACTAGAAACAGCA <u>GCGGCCGCCGCCGAAGAGGCGGATGC</u> -3' <i>NotI</i>
	C3A-R	5'-AGTCTTGAAATAGTACGGTACCAAGTTCCAAATACTACTGCTGAAGCTGC <u>GGTCGCCCCCGGCCGCGTACACC</u> -3' <i>KpnI</i>
pFB-UL25-C3B	C3B-F	5'-GACTTTCGGGAC <u>GTCGCT</u> ATGTCC <u>GCG</u> ACCTT-3' <i>BtsI</i> <i>BspHI</i>
	C3B-R	5'-CATGAAGGT <u>GCG</u> GGACATAG <u>GCG</u> ACGTCCCGAAAGT <u>CGG</u> -3' <i>BspHI</i> <i>BtsI</i>
pFB-UL25-C4A	C4A-F	5'-CGAACGGC <u>GCA</u> GTG <u>GCGGCCGC</u> ACGC <u>GCT</u> AACAACCGCCTGCA-3' <i>NruI</i> <i>NotI</i> <i>PstI</i>
	C4A-R	5'-GGCGGTTGTTAGCGCGT <u>GCGGCCGC</u> CACTGC <u>GCCGTTCG</u> -3' <i>PstI</i> <i>NotI</i> <i>NruI</i>
pFB-UL25-C4B	C4B-F	5'-TCTGTTCTCAGCCGGGGCCACAACCTATTCCTGTGGGAGGACC-3' <i>DdeI</i>
	C4B-R	5'-ACAGTTTCGCGAGGAGTGCCTGGATAACGCCAGGGCCGTTATGG-3' <i>NruI</i>

**Table 4.3B – The overlapping oligonucleotides and primers used to generate the UL25 mutant constructs listed**

Bases highlighted in red are base pair changes resulting in substitutions of amino acids in the UL25 protein. The bases highlighted in green are nucleotide changes used to adjust the percentage of G + C bases in a primer so that a pair of primers had an equal percentage. The REN sites included in the primers are underlined and their respective names are shown underneath.

pFB-UL25-C3B was therefore created, containing the mutations in pFB-UL25-C3A (G169A, S170A and G172A) together with additional mutations, specifying substitutions at residues G202, R203 and K206 (Figure 4.7). Substituting alanine at the mutated sites in pUL25-C3A resulted in a minimal reduction in the observed function of the protein. As discussed earlier (Section 3.1), due its size and neutral nature, alanine is generally regarded as the preferred choice of amino acid when performing mutational analysis by substitution of any particular residue in a protein. The problem with this general mutational approach is that it does not incorporate information specific to the protein of interest. To help address this problem a bioinformatics program, SIFT (<http://sift.jcvi.org>), which had been brought to my attention at this time, was used. Given a particular protein sequence, SIFT analysis will predict a list of residues that are considered tolerant or intolerant at each position along a protein sequence, hence the name SIFT, sorting intolerant from tolerant. SIFT is a multi-step procedure that searches for and chooses similar sequences, makes an alignment of these sequences and then calculates scores based on the amino acids appearing at each position in the alignment. The analysis of any particular residue is based on the conservation of each amino acid along the protein sequence and the physical properties of the residue at that position. Tolerated amino acids, which included the wt residue, are predicted not to alter the protein's function. Conversely, intolerant residues are predicted to affect the protein's function if the amino acid is positioned at a functional interface.

Prior to creating pFB-UL25-C3B, SIFT analysis was used to determine the predicted tolerant and intolerant residues at positions G202, R203 and K206. Although SIFT predicted that two of the residues, R203 and K206, would be intolerant to alanine substitution, the program calculated that the substitution of G202 with alanine would be tolerated and, therefore, would be expected not to alter the protein's function. From the list of intolerant residues that were suggested at position G202, valine was chosen as the amino acid substitute since its physical properties were the most closely related to alanine. Consequently, two overlapping oligonucleotides, C3B-F and C3B-R (Table 4.3B), containing the necessary nucleotide changes for the substitutions G202V, R203A and K206A and the complementary ends of the REN cloning sites *BtsI* (613 pb) and *BspHI* (645 bp) were constructed. The annealed *BtsI*-*BspHI* 32 bp fragment was ligated to

the pFB-UL25-C3A *EcoRI-BtsI* 605 bp fragment, which encoded the G169A, S170A and G172A mutated residues, the pFB-UL25 *BspHI-XbaI* 1502 bp fragment and the *XbaI-EcoRI* 5907 bp fragment. The ligated DNA was electroporated into DH5 $\alpha$  and plasmid DNA samples were prepared from the recombinant bacterial clones. Double digestion of two recombinant plasmids with *EcoRI* and *XbaI* produced two fragments, one of 2139 bp in size and the other of 5907 bp. These fragments co-migrated on an agarose gel with the two fragments from pFB-UL25 digested with the same enzymes, indicating that the complete UL25 gene was present in each of the mutant constructs. One of these plasmids was selected for further analysis and referred to a pFB-UL25-C3B.

#### 4.3.4 C4 mutant constructs (pFB-UL25-C4A and pFB-UL25-C4B)

Two mutant constructs were generated for C4. The plasmid pFB-UL25-C4A encoded four mutated residues and pFB-UL25-C4B specified five mutated residues of the six amino acids assigned to the region (Table 4.2). These two constructs were created at the same time and it was only evident during subsequent complementation analysis that the four mutated residues encoded in pFB-UL25-C4A were sufficient to alter the function of pUL25.

##### 4.3.4.1 pFB-UL25-C4A

This plasmid encoded four mutated amino acids N396A, Y398A, D400A and L402A from the C4 region of the protein. The annealed complementary oligonucleotides, C4A-F and C4A-R (Table 4.3B), included the nucleotide changes for the desired amino acid substitutions, an additional *NotI* (1213 bp) site and the complementary ends of the cloning sites *NruI* (1199 bp) and *PstI* (1242 bp) (Figure 4.8). The annealed 43 bp oligonucleotide was ligated to the purified pFB-UL25 *XbaI-NruI* 7098 bp and *XbaI-PstI* 905 bp fragments. To obtain the *XbaI-PstI* 905 bp fragment, pFB-UL25 was digested with *EcoRI* in addition to *XbaI* and *PstI*, in order to remove a 929 bp *PstI-PstI* fragment that was difficult to separate from the 905 bp *XbaI-PstI* fragment on a 1% TAE gel. *EcoRI* cut the unwanted *PstI-PstI* 929 bp fragment into two products (265 bp and 664 bp) that were easily resolved from the required *XbaI-PstI* 905 bp fragment after electrophoresis on an agarose gel. The ligation mixture was electroporated into DH5 $\alpha$  and plasmid DNA was prepared from the recombinant bacteria. The DNA

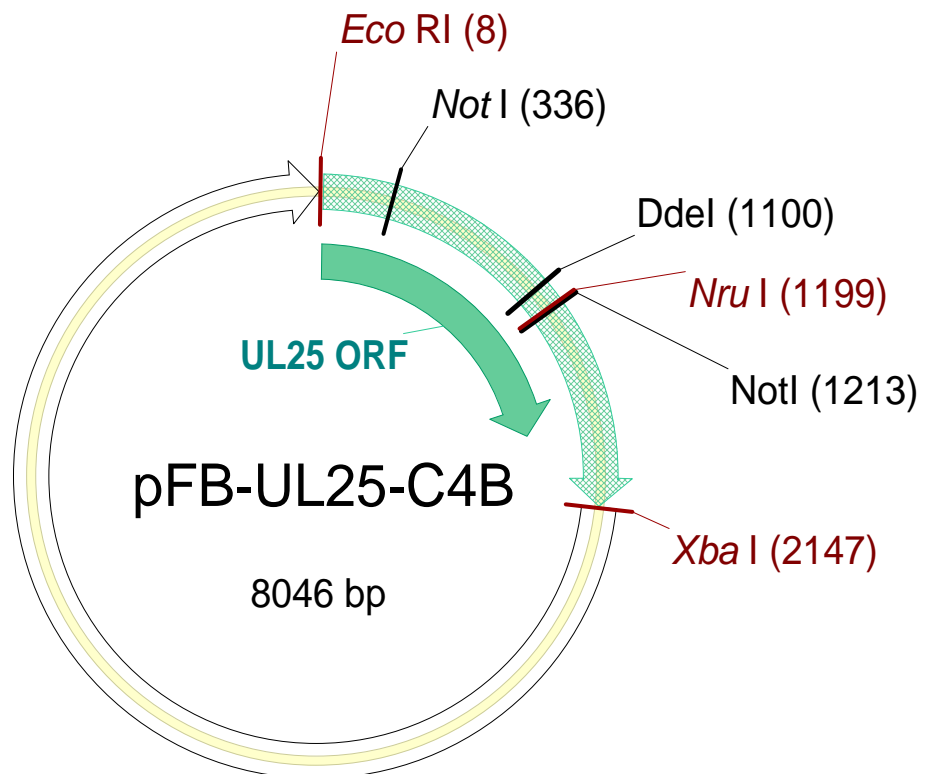
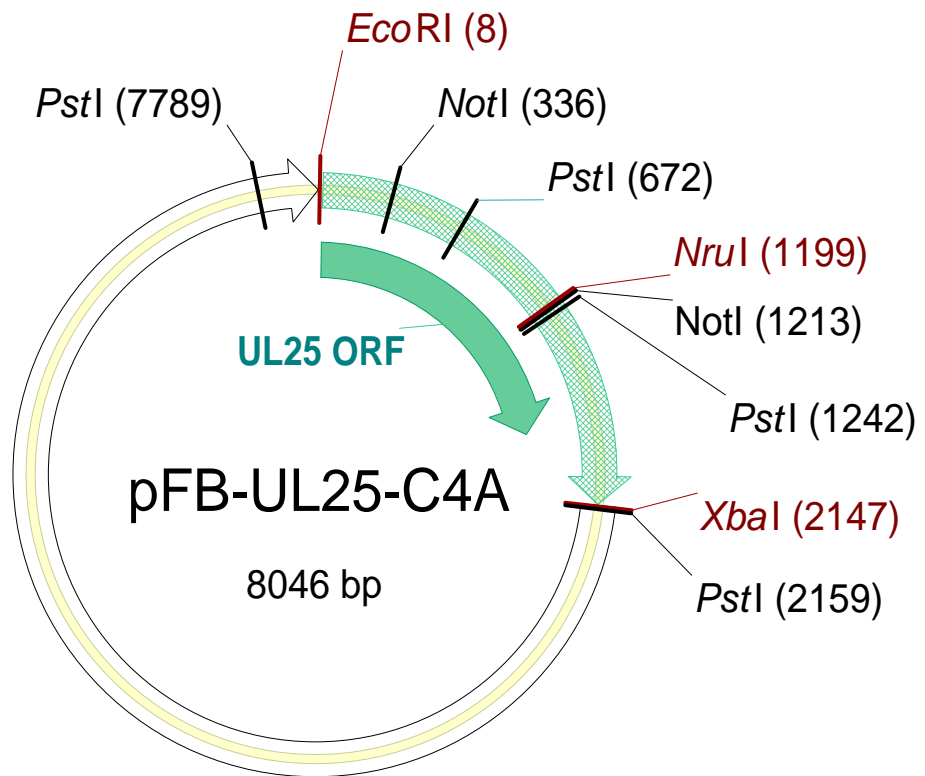


**Figure 4.8 Plasmid maps of pFB-UL25-C4A and pFB-UL25-C4B.**

The REN sites used in the construction and analysis of each plasmid are shown. The green-hatched arrow represents the HSV-1 sequences inserted in the pFBpCI backbone, with the UL25 ORF denoted by the block green arrow. Multiple cutting REN sites are coloured black and unique REN sites are highlighted in red.

samples and the control plasmid (pFB-UL25) DNA were digested with *NotI* to confirm that the DNA fragment with the mutations and the *NotI* site was present. One of the recombinant DNAs produced the two expected fragments, 877 bp and 7169 bp, which verified that it contained the additional *NotI* site together with the mutated UL25 sequences and this plasmid was renamed pFB-UL25-C4A (Figure 4.8).

#### 4.3.4.2 pFB-UL25-C4B

The pFB-UL25-C4B construct contained the mutations in pFB-UL25-C4A, encoding N396A, Y398A, D400A, L402A substitutions and specified an additional alanine substitution at R390 in the UL25 protein. The REN sites, *DdeI* (1100 bp) and *NruI* (1199 bp), were conveniently located 5' and 3' of R390 codon, respectively (Figure 4.8). The *NruI* site, together with the nucleotide changes required for the R390A mutation, were included in the PCR primer C4B-R (Table 4.3B) and the *DdeI* cloning site was incorporated into the primer C4B-F (Table 4.3B). The 99 bp PCR product was purified and cloned into pGEM-T Easy. Two recombinant plasmids were obtained and digested with *NruI* and *DdeI*. The REN digested plasmid DNAs were separated on a 5% polyacrylamide gel, and the presence of the expected 99 bp fragment confirmed that the correct HSV-1 *NruI-DdeI* insert had been cloned. DNA sequencing of one of the pGEM-T Easy recombinants verified it contained the UL25 sequences specifying the R390A mutation. The purified *NruI-DdeI* 99 bp fragment was subsequently ligated to the purified pFB-UL25-C4A *NruI-EcoRI* 6855 bp fragment, containing the mutated residues N396A, Y398A, D400A and L402A, and to the pFB-UL25 *EcoRI-DdeI* 1092 bp fragment. The ligated DNA was electroporated into DH5 $\alpha$  and the recombinant plasmids obtained were digested with *NruI* and *EcoRI*. One of the recombinant plasmids, which produced the expected fragments of 1191 bp and 6855 bp, was selected for further analysis and renamed pFB-UL25-C4B.

## 4.4 Loop mutants

The disordered residues deleted in each of the six regions (L1-L6) are shown in Table 4.2.

#### 4.4.1 L1 mutant construct (pFB-UL25-L1)

A PCR product that contained a deletion of the nucleotides encoding the L1 unstructured residues A249-D254, and included the cloning sites *Pst*I (672 bp) and *Bsa*WI (772 bp) flanking the deletion, was produced using the primers L1-F and L1-R (Table 4.3C). Initial attempts to generate the required PCR product with L1-F and L1-R using the PCR-cycle1 cycle were unsuccessful. The UL25 fragment was successfully amplified after repeating the experiment using the PCR-cycle2 cycle, which increased the specificity by raising the annealing temperature from 58°C used during PCR-cycle1 to 68°C. The purified 116 bp PCR product was sub-cloned into pGEM-T Easy and plasmid DNA was prepared from the recombinant bacteria obtained. Recombinant plasmids containing the correctly mutated UL25 insert were identified by REN analysis and confirmed by sequencing the DNA samples. The purified HSV-1 100 bp *Pst*I-*Bsa*WI insert was subsequently ligated to the pFB-UL25 *Eco*RI-*Nru*I 6855 bp, *Eco*RI-*Pst*I 664 bp and *Bsa*WI-*Nru*I 409 bp fragments and the DNA was electroporated into DH5 $\alpha$ . Plasmid DNAs prepared from ten recombinant bacterial clones and the control pFB-UL25 DNA were digested with *Eco*RI and *Xba*I. Three plasmids produced the expected *Eco*RI-*Xba*I fragments, 2121 bp and 5907 bp, giving the same pattern of digestion as the control pFB-UL25 plasmid. One of these plasmids was used for subsequent analysis and was renamed pFB-UL25-L1 (Figure 4.9).

#### 4.4.2 L2 mutant construct (pFB-UL25-L2)

To remove the DNA sequences specifying the unstructured residues in L2 two overlapping oligonucleotides, L2-F and L2-R, were designed (Table 4.3C). The annealed fragment contained the cohesive ends of the cloning sites *Aat*II (1020 bp) and *Dde*I (1067 bp), an additional *Not*I (1051 bp) site and a 33 bp deletion that removed the sequences encoding the unstructured residues R335-G345 of L2 (Figure 4.9). The annealed 47 bp oligonucleotide was ligated to the purified pFB-UL25 *Not*I-*Xba*I 6253 bp, *Not*I-*Aat*II 684 bp and *Dde*I-*Xba*I 1029 bp fragments and the ligation mixture was electroporated into DH5 $\alpha$ . Plasmid DNAs were prepared from six recombinant bacterial colonies and together with the control plasmid (pFB-UL25) were digested with *Not*I. Each of the recombinant plasmid DNA samples produced two fragments of the expected size (7298 bp and 715 bp),

UL25 Mutant	Primer ID	L1 – L3 Overlapping Oligonucleotides and Primers
pFB-UL25-L1	L1-F	5'-TAATATTATCCCTGCAGGCCTGCGGCCGGCTGTATGTGGGCCAGCGCCACTATTCC-3' <i>PstI</i>
	L1-R	5'-ATATGACCGGAGCGCG <del>Δ</del> CCCGTGCCTGTTTCGGTACAGCAGGTAGAGACACAACACG-3' <i>BsaWI</i>
pFB-UL25-L2	L2-F	5'-CCCC <del>Δ</del> GTGGCGCACCACGACGACATAAACCGCGCGGCCCGCGCTTCC-3' <i>AatII</i> <i>NotI</i> <i>DdeI</i>
	L2-R	5'-TGAGGAACGCGGCCGCCCGCGCGGTTTATGTCGTCGTGGTGCGCCAC <del>Δ</del> GGGGACGT-3' <i>DdeI</i> <i>NotI</i> <i>AatII</i>
pFB-UL25-L3	L3-F	5'-TAGGCATGCTGATTCCTGGAGCCGTC <del>Δ</del> TCCGGATCCGACTCGGGGGCCATCAAGAGCGGAGACAACAATCTGG -3' <i>NspI</i> <i>BamHI</i>
	L3-R	5'-ATATAGCAGTAAGACGTACTAGTGCTGCTTGGCGGGCCCCCGATGACATATCCACCACCCGCCGCTCGACC-3' <i>ApaI</i>

**Table 4.3C The overlapping oligonucleotides and primers used to generate the UL25 mutant constructs listed**

The symbol **Δ** represents deleted UL25 sequences. The REN sites included in the primers are underlined and their respective names shown underneath. Bases highlighted in bold are the silent base pair changes used to introduce REN sites without altering the protein sequence. The bases highlighted in green are nucleotide changes used to adjust the percentage of G + C bases in a primer so that a pair of primers had an equal percentage.

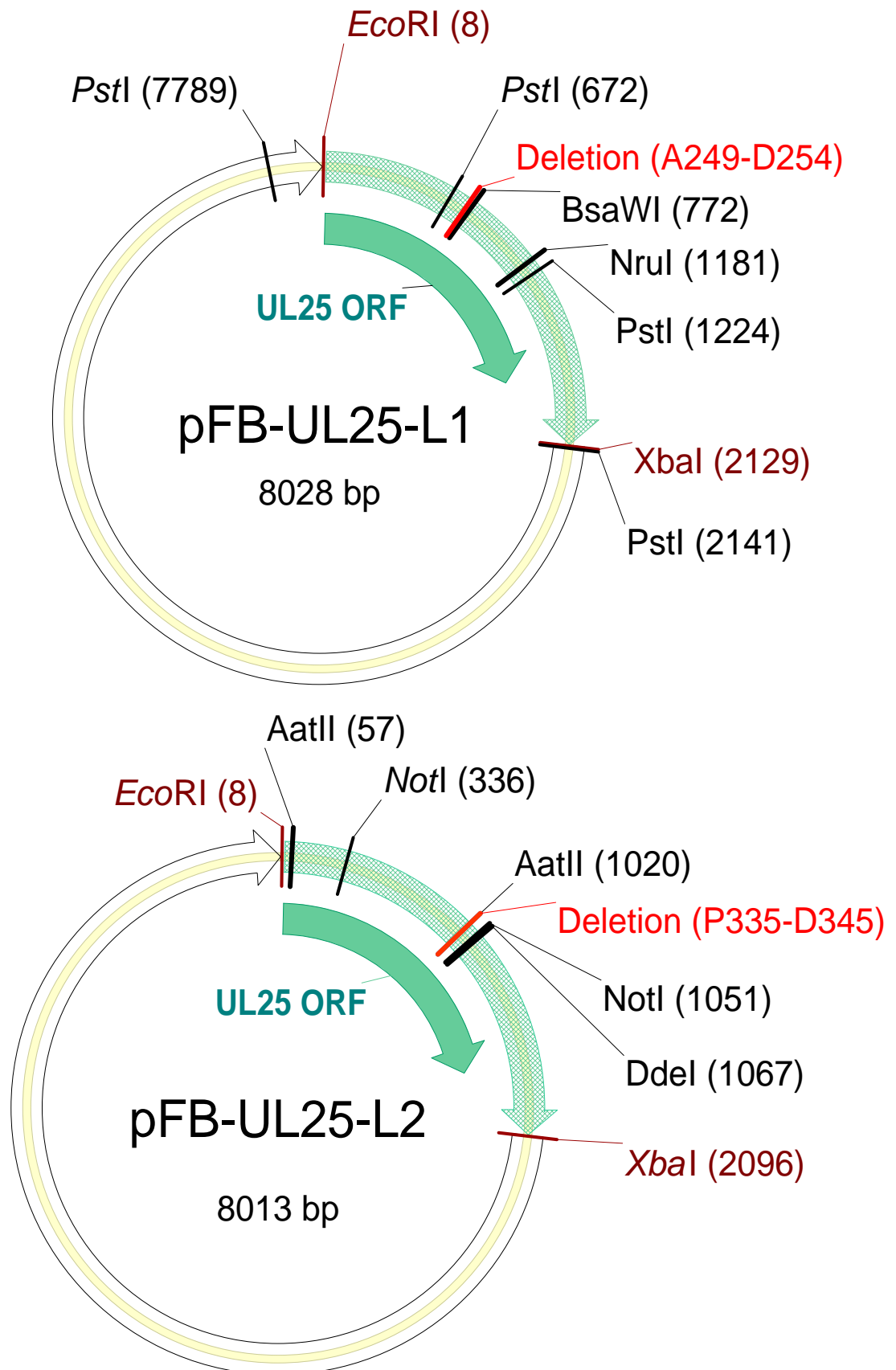


**Figure 4.9 Plasmid maps of pFB-UL25-L1 and pFB-UL25-L2**

The REN sites used in the construction and analysis of each plasmid are shown, together with the location of the deleted (unstructured) residues from the looped out regions. The green-hatched arrow represents the HSV-1 sequences inserted in the pFBpCI backbone and the block green arrow represents the UL25 ORF. Multiple cutting REN sites are coloured black and unique REN sites are highlighted in red.

confirming they contained an additional *NotI* site, which was present in the mutated UL25 insert. One of the plasmids was selected for further study and renamed pFB-UL25-L2.

#### 4.4.3 L3 mutant construct (pFB-UL25-L3)

A PCR product containing a 27 bp deletion of sequences specifying the nine unstructured residues (P417-A425) of L3, the cloning sites *NspI* (1252 bp) and *ApaI* (1474 bp) flanking the deletion, and an additional *BamHI* (1273 bp) site was produced using the primers L3-F and L3-R (Table 4.3C). The purified PCR product was ligated to pGEM-T Easy and the DNA was electroporated into DH5 $\alpha$ . Plasmid DNA was prepared from a series of recombinant bacterial clones and digested with *BamHI*, which does not cut pGEM-T Easy, and those containing the desired UL25 insert were linearised. DNA sequencing of the positively identified recombinants confirmed that one encoded the required deletion. The purified 222 bp *NspI*-*ApaI* mutated fragment was ligated to the pFB-UL25 *EcoRI*-*NspI* 1244 bp and *ApaI*-*EcoRI* 6553 bp fragments. To detect the recombinant plasmids containing the mutated fragment, DNA was prepared from six bacterial clones and digested with *BamHI*. Five of the recombinant pFB-UL25 plasmids produced the three expected *BamHI* fragments of 838 bp, 1259 bp and 5922 bp, verifying that they contained the UL25 insert with the additional *BamHI* site. One plasmid was selected for further analysis and referred to as pFB-UL25-L3 (Figure 4.10).

#### 4.4.4 L4 mutant construct (pFB-UL25-L4)

Overlapping oligonucleotides, L4-F and L4-R (Table 4.3D), were constructed that when annealed contained *DrdI* (1391 bp) and *ApaI* (1486 bp) cohesive ends, an additional *XbaI* (1434 bp) site and a deletion of 15 bp removing the codons of the five unstructured residues (P479-T483) of L4 (Figure 4.10). The annealed 95 bp fragment was ligated to the purified pFB-UL25 *EcoRI*-*DrdI* 521 bp, *DrdI*-*DrdI* 862 bp and *ApaI*-*EcoRI* 6553 bp fragments and the DNA was electroporated into DH5 $\alpha$ . Plasmid DNA samples from two recombinant bacterial clones were digested with *KpnI* and *XbaI*. Only one produced the expected fragments *KpnI*-*KpnI* 6427 bp, *KpnI*-*XbaI* 875 bp, *XbaI*-*XbaI* 698 bp and *XbaI*-*KpnI* 31 bp that

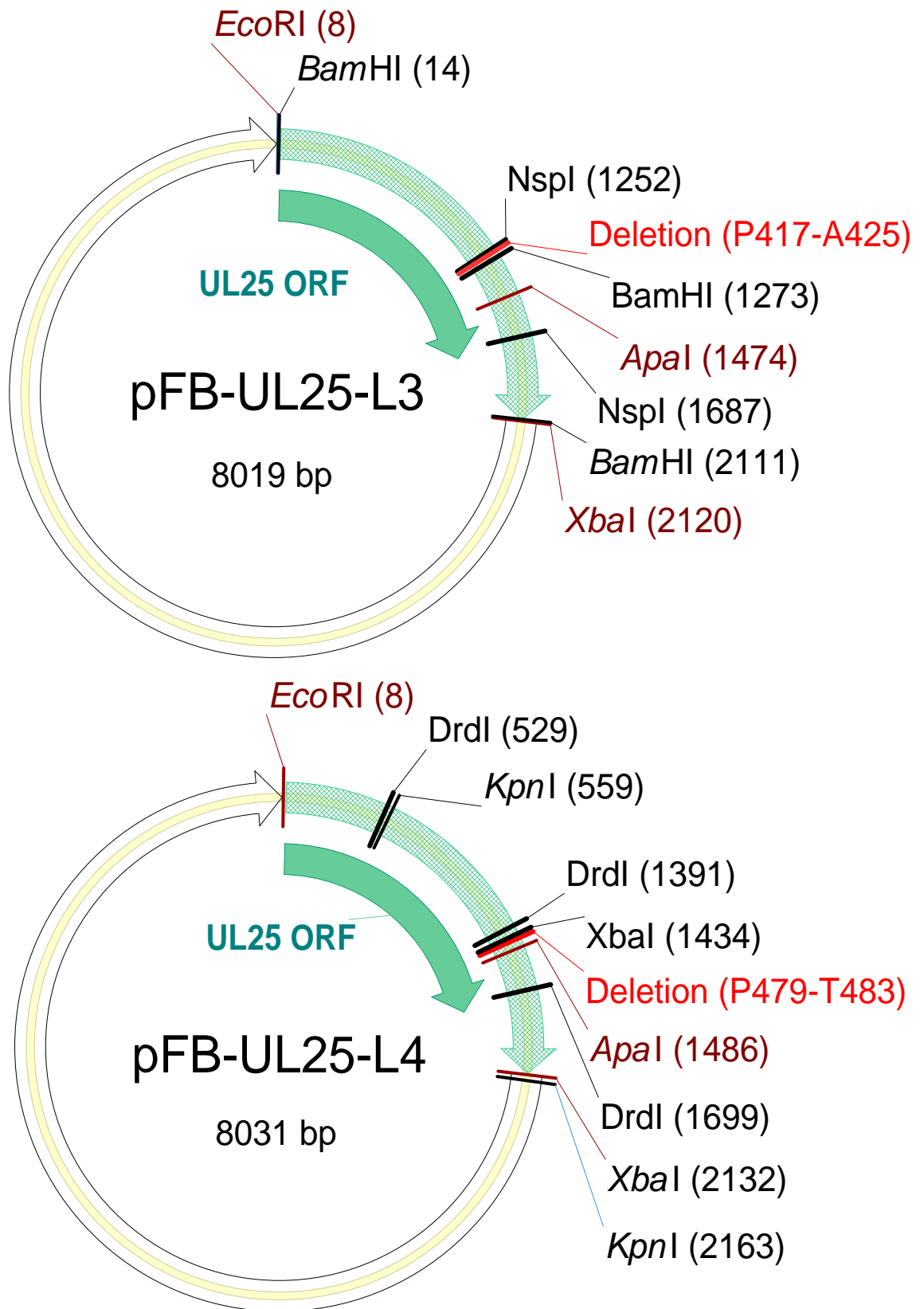


**Figure 4.10 Plasmid maps of pFB-UL25-L3 and pFB-UL25-L4**

The REN sites used in the construction and analysis of each plasmid are shown, together with the location of the deleted (unstructured) residues from the looped out regions. The green-hatched arrow represents the HSV-1 sequences inserted in the pFBpCI backbone and the block green arrow represents the UL25 ORF. Multiple cutting REN sites are coloured black and unique REN sites are highlighted in red.

**Table 4.3D – The overlapping oligonucleotides used to generate the UL25 mutant constructs listed**

The symbol **Δ** represents deleted UL25 sequences. The REN sites included in the primers are underlined and their respective names shown underneath. Bases highlighted in bold are the silent base pair substitutions used to introduce or eliminate REN sites without altering the protein sequence. The REN sites eliminated from UL25 are shown in grey.

UL25 Mutant	Primer ID	L4 – L6 Overlapping Oligonucleotides
pFB-UL25-L4	L4-F	5'- <u>CGGTCGAGCTGACCCAGCT</u> <u>ATTTCCCGCCTGGCCGCCCTGTGTCTAGACGCCAGGCGGGGCGG</u> <u>ΔCGG</u> <i>DrdI</i> no <i>PvuII</i> site <i>XbaI</i> CGGGTGGTGGATATGTCATCGGGGGCC-3' <i>ApaI</i>
	L4-R	5'- <u>CCCGATGACATATCCACCACCCGCCG</u> <u>ΔCCGCCCGCCTGGGCGTCTAGACACAGGGCGGCCAGGCCGGG</u> <i>ApaI</i> <i>XbaI</i> AAATAGCTGGGTCAGCTCGACCGCC-3' no <i>PvuII</i> site <i>DrdI</i>
pFB-UL25-L5	L5-F	5'- <u>CGCCAGGCGGCGCTGGTGCGCCTCACCGCCCTCGAG</u> <u>GCTCATCAACCGCACC</u> <u>ΔCCCACCCCT</u> -3' <i>ApaI</i> <i>XhoI</i> <i>BstXI</i>
	L5-R	5'- <u>GTGGG</u> <u>ΔGGTGCGGTTGATGAGCTCGAGGGCGGTGAGGCGCACCAGCGCCGCCTGGCGGGCC</u> -3' <i>BstXI</i> <i>XhoI</i> <i>ApaI</i>
pFB-UL25-L6	L6-F	5'- <u>TTGTACTTTTTATGTCTGGGGTTCATTCCACAGTACCTG</u> <u>ΔTAGT</u> -3' <i>NspI</i> <i>XbaI</i>
	L6-R	5'- <u>CTAGACTA</u> <u>ΔCAGGTA</u> <u>CTGTGGAATGAACCCAGACATAAAAAGTACAACATG</u> -3' <i>XbaI</i> <i>NspI</i>
pFB-UL25-L6sub	L6sub-F	5'- <u>TTGTACTTTTTATGTCTGGGGTTCATTCCACAGTACCTG</u> <u>GCGGCCGCT</u> <u>TAGT</u> -3' <i>NspI</i> <i>NotI</i> <i>XbaI</i>
	L6sub-R	5'- <u>CTAGACTA</u> <u>AGCGGCCGCGC</u> <u>CAGGTA</u> <u>CTGTGGAATGAACCCAGACATAAAAAGTACAACATG</u> -3' <i>XbaI</i> <i>NotI</i> <i>NspI</i>

indicated the pFB-UL25 *Drdl-Drdl* 862 bp fragment was inserted in the correct orientation. This plasmid was subsequently named pFB-UL25-L4.

#### 4.4.5 L5 mutant construct (pFB-UL25-L5)

Overlapping oligonucleotides, L5-F and L5-R (Table 4.3D), were produced that when annealed contained the *ApaI* (1501 bp) and *BstXI* (1561 bp) cohesive ends, an additional *XhoI* (1531 bp) site, and a deletion of 9 bp encoding the unstructured residues (R511-N513) of L5 (Figure 4.11). The 60 bp annealed product was ligated to the pFB-UL25 *XbaI-ApaI* 7400 bp, *BstXI-NspI* 144 bp and *NspI-XbaI* 433 bp fragments and the DNA was electroporated into DH5 $\alpha$ . Plasmid DNAs prepared from six recombinant bacterial isolates were digested with *XhoI*, with two producing fragments of 5880 bp, 1378 bp, 622 bp and 157 bp, which confirmed that they contained the additional *XhoI* site. One was selected and subsequently renamed pFB-UL25-L5.

#### 4.4.6 L6 mutant constructs (pFB-UL25-L6 and pFB-UL25-L6sub)

L6 consists of three unstructured residues (S578-V580) located directly at the carboxyl terminus of the UL25 ORF. Initially, the mutant construct pFB-UL25-L6 was created that contained a deletion of sequences encoding S578-V580. Preliminary complementation studies indicated that the pUL25-L6 failed to complement the growth of  $\Delta$ UL25MO. To determine if alanine residues located at all three codons elicited the same functional impact as the deletion mutant, pFB-UL25-L6sub encoding the amino acid substitutions S578A and V580A in the UL25 ORF was generated.

##### 4.4.6.1 pFB-UL25-L6

The primers L6-F and L6-R (Table 4.3D) were annealed to give an oligonucleotide that included a deletion of the 9 bp encoding the unstructured residues of L6, and the cloning sites *NspI*(1714) and *XbaI*(1756) flanking the deletion (Figure 4.12). The annealed 42 bp fragment was ligated to the pFB-UL25 *EcoRI-BstXI* 1562 bp, *BstXI-NspI* 144 bp and *EcoRI-XbaI* 5901 bp fragments and the ligated DNA was electroporated into DH5 $\alpha$ . Recombinant plasmid DNA was prepared from the bacterial isolates and digested with *NotI*, those containing the

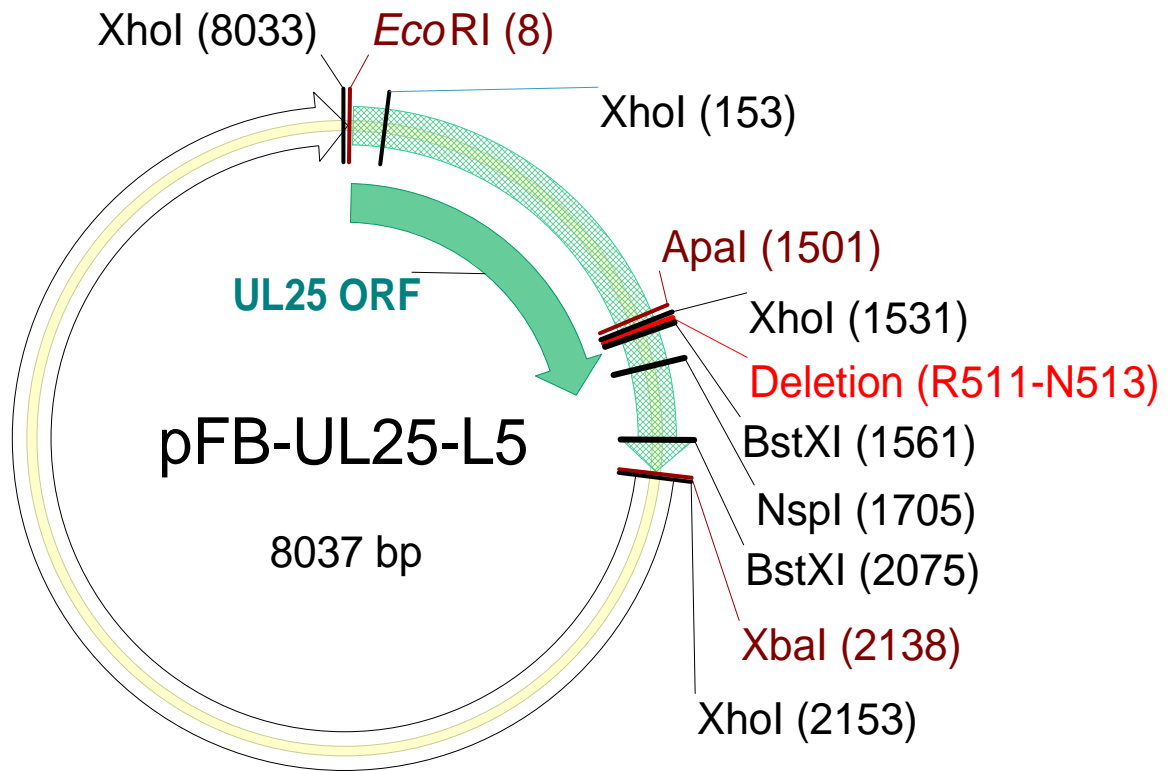


**Figure 4.11 Plasmid map of pFB-UL25-L5**

The REN sites used in the construction and analysis of each plasmid are shown, together with the location of the deleted (unstructured) residues from the looped out regions. The green-hatched arrow represents the HSV-1 sequences inserted in the pFBpCI backbone and the block green arrow represents the UL25 ORF. Multiple cutting REN sites are coloured black and unique REN sites are highlighted in red.

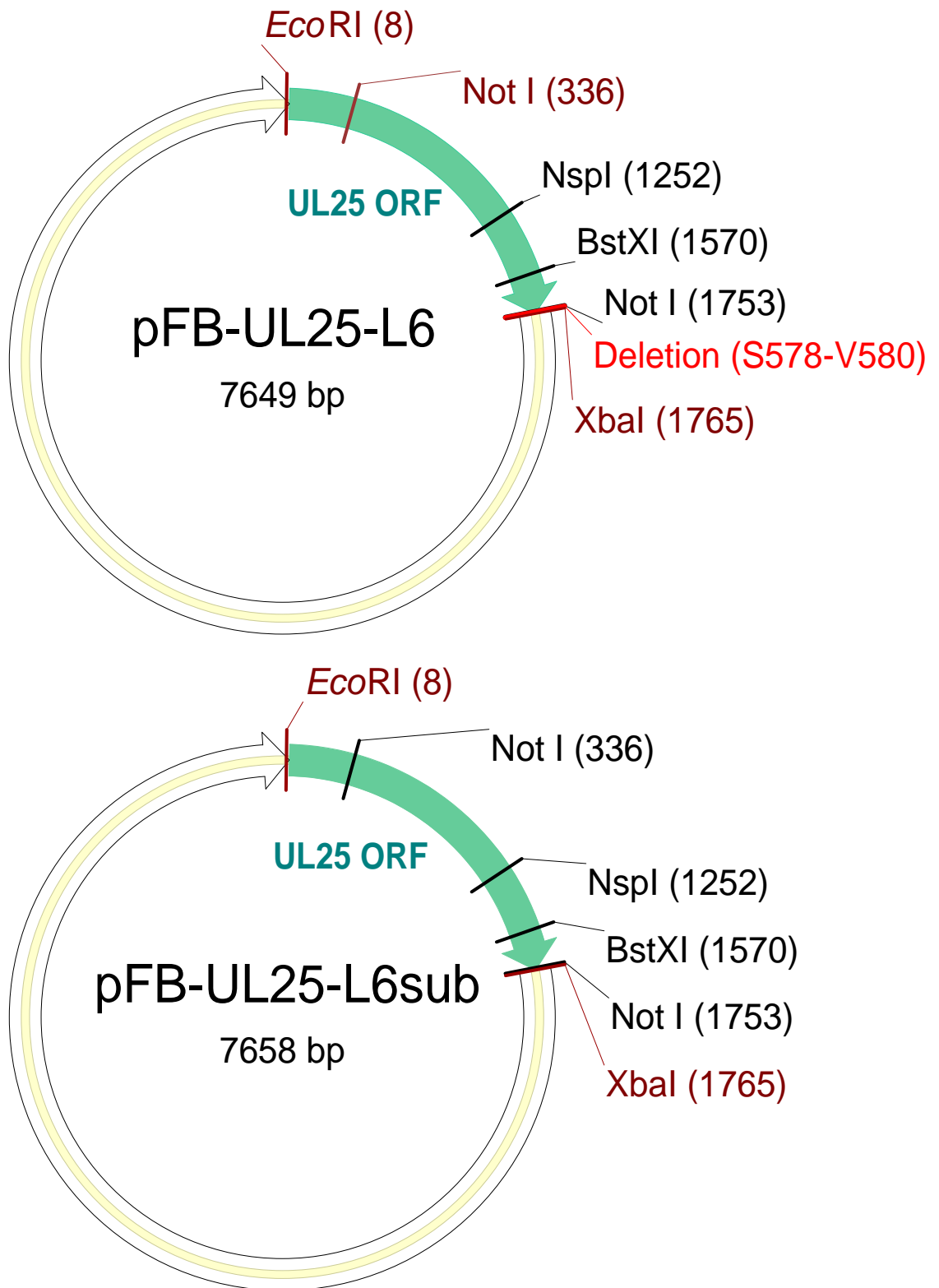


**Figure 4.12 Plasmid maps of pFB-UL25-L6 and pFB-UL25-L6sub**

The REN sites used in the construction and analysis of each plasmid are shown, together with the location of the deleted (unstructured) residues in pFB-UL25-L6. The block green arrow represents the UL25 ORF. Multiple cutting REN sites are coloured black and unique REN sites are highlighted in red.

expected UL25 insert were linearised and produced a fragment of 7649 bp. One of these recombinants was selected for further analysis and named pFB-UL25-L6.

#### 4.4.6.2 pFB-UL25-L6sub

This mutant was constructed in the same manner as pFB-UL25-L6, using the overlapping oligonucleotides, L6sub-F and L6sub-R (Table 4.3D) that specified the amino acid substitutions S578A and V580A and contained an internal *NotI* site (Figure 4.12). Recombinants containing the mutated UL25 insert and the additional *NotI* site were identified by the production of two *NotI* fragments of 1417 bp and 6241 bp. One of these recombinants was selected for further analysis and named pFB-UL25-L6sub.

### 4.5 Combination mutant (pFB-UL25-C1L2)

As referred to in Section 1.4, pUL25 and pUL17 interact to form the C-capsid-specific component (CCSC) (Trus et al., 2007). Specific residues in pUL25 have been speculated to be the sites of the protein that interact with the capsid during the formation of the CCSC (A. Steven, personal communication). The predicted amino acids included H348, R362 and G363 from C1 and H323 and G324, which lie in the extended L2 region of pUL25 (Table 1.4). Substitutions affecting two of the residues, R362A and G363A, were encoded in the UL25 gene within pFB-UL25-C1, whereas pFB-UL25-L2 has a deletion in UL25 that removes the codons specifying the unstructured residues R335-G345 that are adjacent to H323 and G324 in L2. To determine the functional impact of these mutations in combination, a construct containing both the C1 and L2 mutated residues was generated. The purified fragments pFB-UL25-C1 *Ddel-XbaI* 1047 bp, pFB-UL25-L2 *EcoRI-Ddel* 1059 bp and pFB-UL25 *EcoRI-XbaI* 5907 bp were ligated and the ligated DNA was electroporated into DH5 $\alpha$ . Recombinant plasmid DNA was prepared from the bacterial isolates and analysed by REN digestion and DNA sequencing. One of the plasmids, pFB-UL25-C1L2 (Figure 4.13), had the correct REN pattern and the expected UL25 sequence containing the desired mutations.

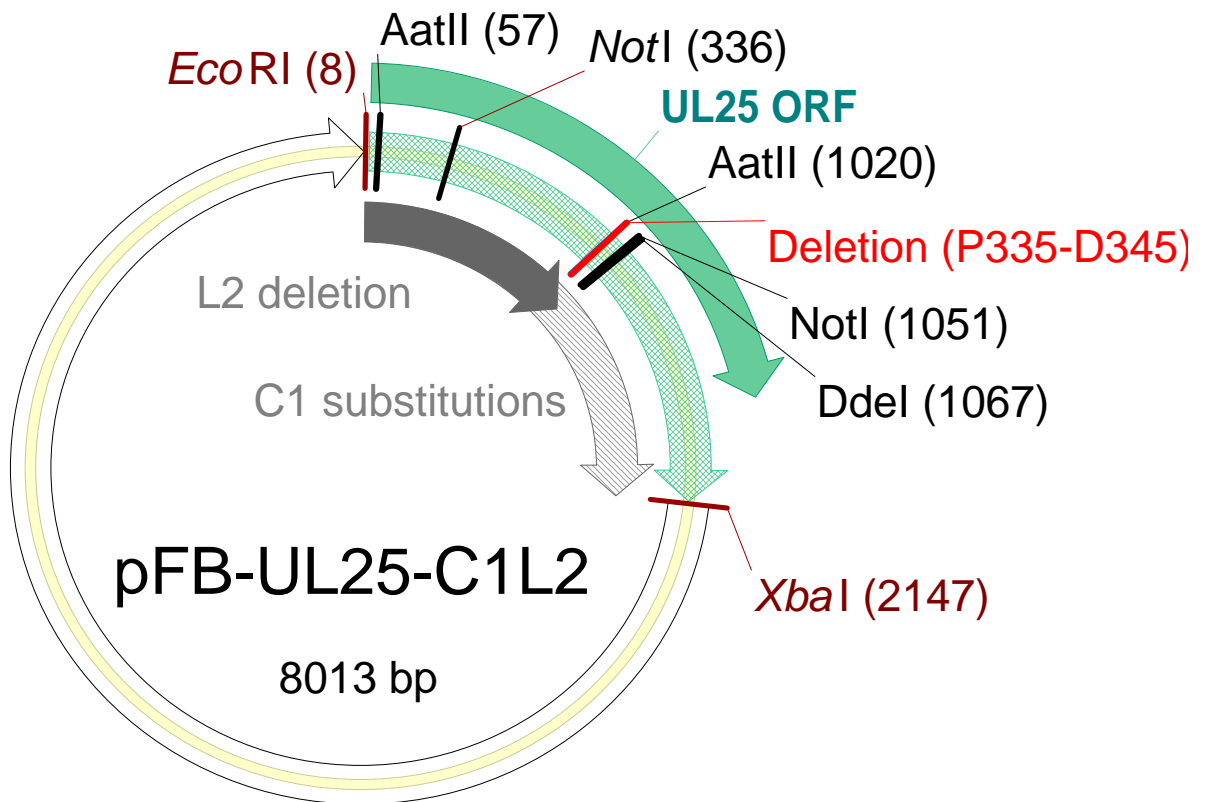


**Figure 4.13 Plasmid map of pFB-UL25-C1L2**

The REN sites used in the construction and analysis of the plasmid are shown and the positions of two of the fragments used to generate the complete plasmid are indicated. The block grey arrow represents the pFB-UL25-L2 *AatII-Ddel* fragment (L2 deletion) that contained the deleted (unstructured) residues from pFB-UL25-L2. The second fragment contained the mutated residues from pFB-UL25-C1 in the *Ddel-XbaI* fragment from this plasmid (C1 substitutions) and is denoted by the hatched grey arrow. The green-hatched arrow represents the HSV-1 sequences inserted in the pFBpCI backbone, with the UL25 ORF highlighted by the block green arrow. Multiple cutting REN sites are coloured black and unique REN sites are highlighted in red.

## 4.6 Complementation assay

This assay determines the ability of proteins supplied *in trans* to complement the growth of a mutant virus lacking a functional version of the protein, under conditions non-permissive for input virus replication. The yield of the progeny virus is subsequently determined by titrating the virus under permissive conditions. Vero cells were transfected with either pFB-UL25, the empty vector pFBpCI or individual mutated pFB-UL25 plasmids and subsequently infected with  $\Delta$ UL25MO (Section 2.2.7.3). After incubation at 37°C for 24 h the cells were harvested and the viral yields were determined on 8-1 cells and expressed as a percentage of the yield obtained from positive control cells containing pFB-UL25 (Figure 4.14). Eight of the 17 mutants analysed had a minimal effect on the ability of the protein to support virus growth, giving yields of over 40% of the wt pUL25 positive control level in the complementation assay. The remaining nine mutant proteins displayed significantly lower levels of complementation that were 5% or below that of the positive control sample. For each of the complementation assays performed, a duplicate set of cell monolayers from the experiment was harvested and the proteins contained in the cell lysates were separated by SDS-PAGE on 10% polyacrylamide gels. The proteins were blotted onto nitrocellulose membrane and incubated with primary anti-pUL25 antibody. The blot containing the N-terminally truncated pUL25 proteins was screened with anti-pUL25 RAb335, which was raised against pUL25 residues 342-580. Whereas, the other blots were screened with anti-pUL25 MAb166, which recognises an epitope located between pUL25 residues 59-133. Although no loading control was used to determine the quantities of the proteins expressed in each sample, Western blot analysis confirmed the expression of pUL25 in each of the cell lysates analysed, confirming that the cells had been successfully transfected with the recombinant plasmid. A representative image for each of the samples analysed during complementation analysis is shown Figure 4.15.

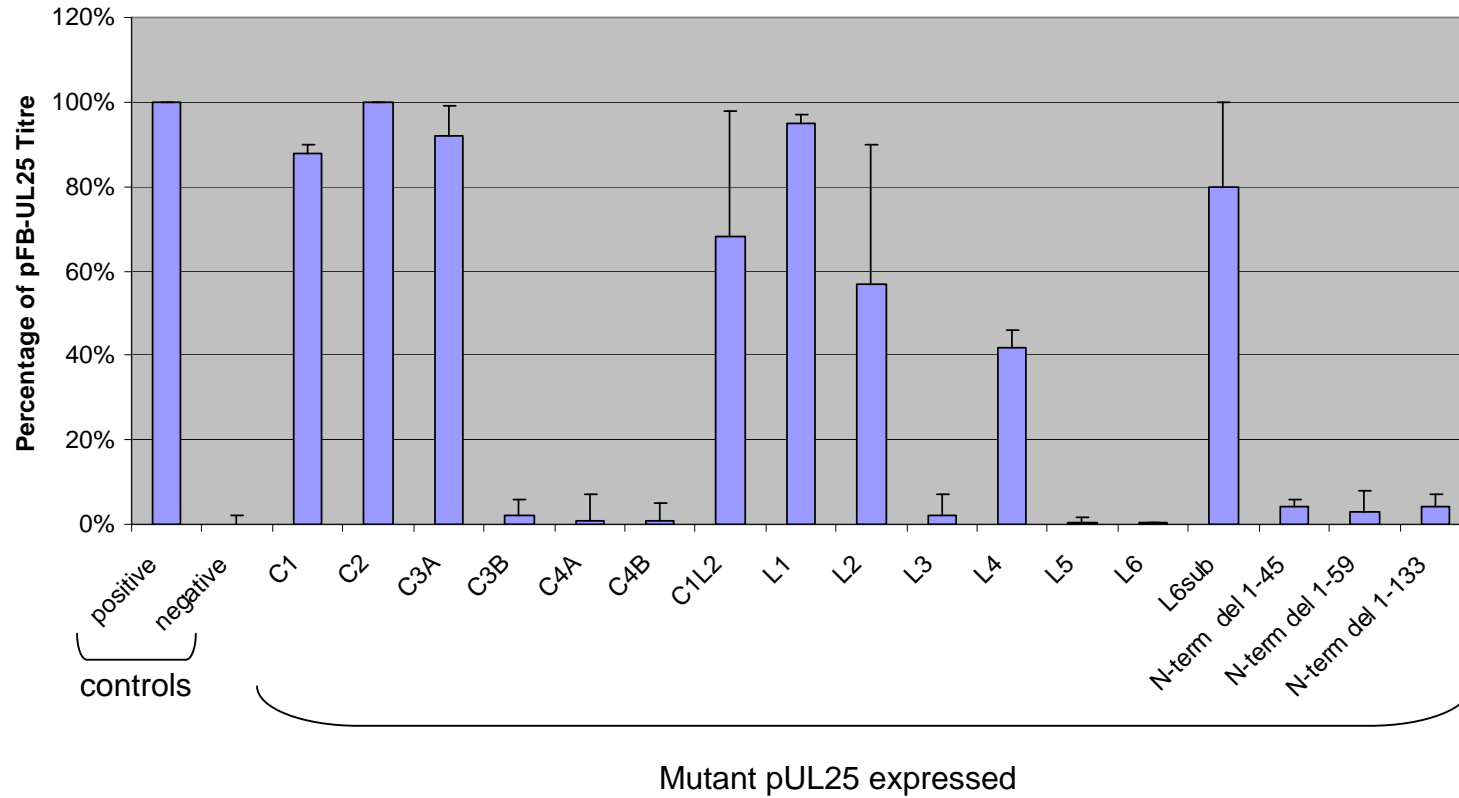
## 4.7 Discussion

UL25 must interact with its essential protein partners to ensure production of functional capsids and hence infectious virions. Eight of the UL25 mutant proteins examined retained the ability to complement the growth of  $\Delta$ UL25MO,

#### **Figure 4.14 Complementation of $\Delta$ UL25MO by mutant UL25 proteins**

Vero cell monolayers in 24 well tissue culture dishes were transfected with a plasmid expressing a mutant UL25 protein. As a positive control, cells in one well were transfected with pFB-UL25 expressing the wt protein and as a negative control, cells in another well were transfected with the empty vector pFBpCI that did not express pUL25 instead of a plasmid expressing a mutant UL25 protein. Subsequently, each of the wells was infected with  $\Delta$ UL25MO, and after virus absorption the cells were acid washed to remove residual viral particles from the cell surface. Following incubation at 37°C for 18 h, cells were harvested and the yield of  $\Delta$ UL25MO determined on 8-1 cells. For each plasmid, the average yield of the viral progeny obtained from three independent experiments was calculated and expressed as a percentage of the average yield obtained from  $\Delta$ UL25MO-infected cells expressing pFB-UL25. Error bars represent the standard deviation of the mean.

# Complementation Analysis



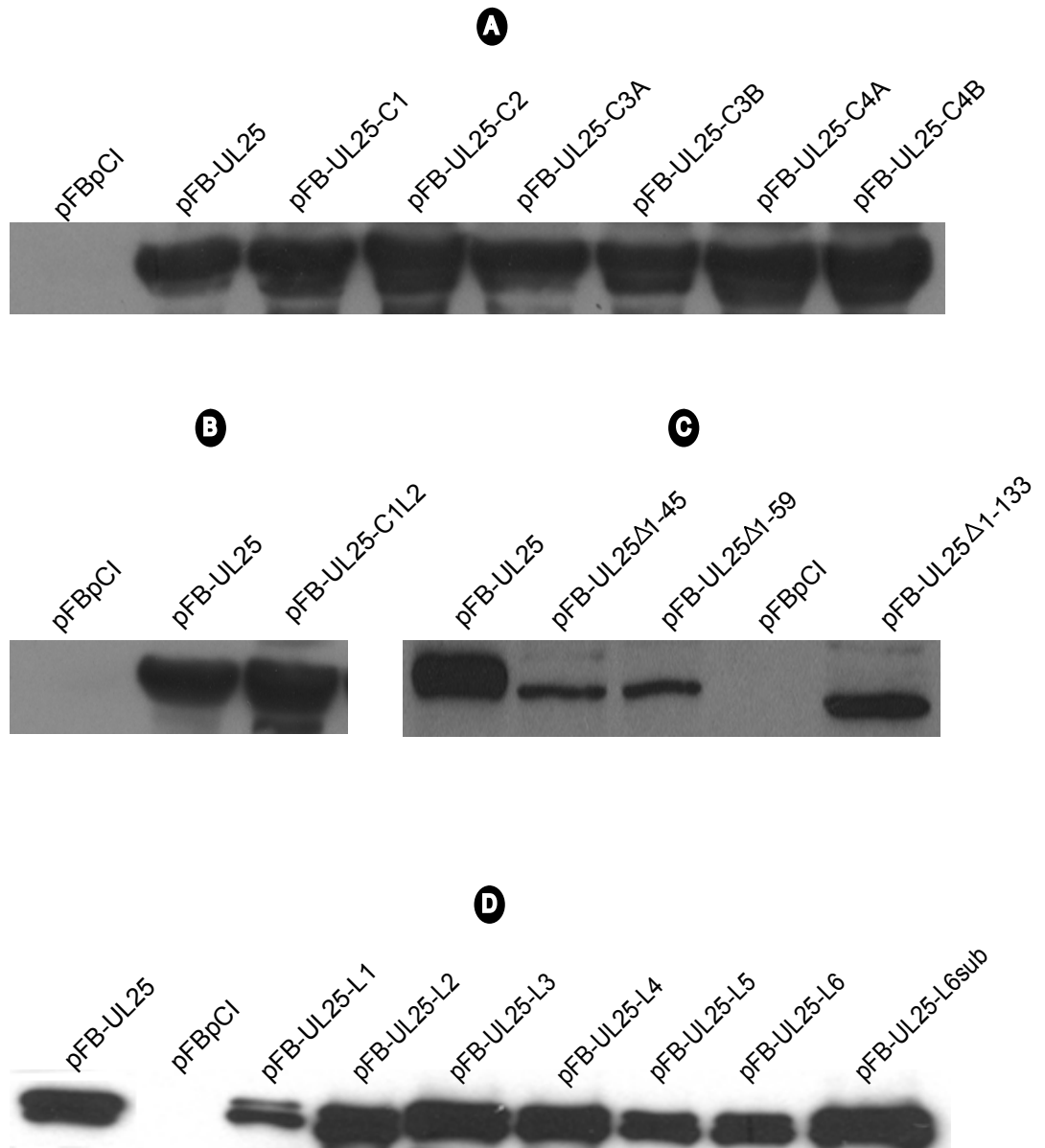


**Figure 4.15 Western blot analysis of pUL25 in the complementation assays**

Vero cell monolayers seeded in a 24-well dish were transfected with a plasmid expressing a mutant UL25 protein. As a positive control cells in one well were transfected with pFB-UL25 expressing the wt protein and as a negative control, cells in another well were transfected with the empty vector pFBpCI that did not express pUL25. Following incubation a 37°C for 18 h, cell lysates were prepared from the harvested cells and the proteins were separated by SDS-PAGE on 10% polyacrylamide gels and blotted onto nitrocellulose. UL25 proteins in A, B and D were detected using primary MAb166 antibody and secondary hrp-conjugated anti-mouse antibody. UL25 proteins in C were detected using primary RAb335 antibody and secondary hrp-conjugated protein A.

and reasonable virus yields of over 40% of the yield from the wt positive control sample were produced (Figure 4.14). Several possibilities are suggested by these observations. The corresponding wt residues of the mutated amino acids in pUL25-C1, -C2, -C3A, -L1, -L2, -L4, -L6sub and -C1L2 may not be essential for the interactions required during viral assembly. Alternatively, the number of predicted functional residues mutated in each of the clusters, or the size of the deletion in the looped out regions, may be insufficient to produce a functional impact. For instance, pUL25-C1 contained only three mutated residues of the nine predicted functional amino acids for C1, and pUL25-C2 contained four mutated residues out of the possible six for C2. In addition, the mutated residues in the cluster regions may be tolerated as defined by SIFT analysis. Certainly, retrospective SIFT analysis on the amino acids mutated in pUL25-C1, pUL25-C2 and pUL25-C3A predicted that several of the alanine substitutions included in each of these constructs would be tolerated, and thus would be expected not to alter the protein's function. Ideally, if time had allowed, new C1 and C2 constructs would have been created that contained the additional mutated residues from the list of predicted functional amino acids for these regions. In addition, SIFT analysis would have been used to potentially optimise the type of amino acid substitution performed at each of the target sites in the new constructs.

Nine of the 17 mutant proteins analysed displayed significant reductions in the efficiency of complementation of the growth of  $\Delta$ UL25MO, and virus yields of 5% or less of the level observed for the positive control sample were obtained (Figure 4.14). These mutant proteins were pUL25-C3B, -C4A, -C4B, -L3, -L5, -L6 and the three N-terminal deletion mutants, pUL25 $\Delta$ 1-45, pUL25 $\Delta$ 1-59 and pUL25 $\Delta$ 1-133. Since the residues mutated in UL25 are located on the surface of the protein they are unlikely to affect the overall structure of the protein. Consequently, the reduction in complementation observed in  $\Delta$ UL25MO-infected Vero cells expressing the individual mutant proteins listed above suggests that the wt residues mutated in each of the proteins, are crucial to the function of pUL25. Two of the loop mutants, pUL25-L5 and pUL25-L6, with the smallest number of deleted residues (3 each), produced a profound effect on the ability of the protein to complement, and virus yields of less than 1% of the wt yield were obtained. In contrast,  $\Delta$ UL25MO-infected Vero cells expressing pUL25-L2

produced a mean complementation level of 68%, despite the protein having an 11 amino acid deletion in L2. The unstructured portions of the protein are assumed to relate to the molecule's flexibility, which in turn influences the conformational parameters the protein requires to function effectively. Since the large deletion of the unstructured residues in pUL25-L2 was tolerated, alterations in the flexibility of the protein appear to be localised with little long-range impact on the function of the highly flexible pUL25 (Bowman et al., 2006).

The level of complementation of  $\Delta$ UL25MO by pUL25-C3A was comparable to the value obtained for the positive control. However, by expanding the number of mutated residues within the C3 region of UL25 from the three in pUL25-C3A (G169A, S170A and G172A) to the six in pUL25-C3B, which contained the additional mutated residues G202V, R203A and K206A, the mean complementation efficiency was reduced from 92% to 2%, respectively. A study is presently under way to determine if the two groups of mutated residues G169A, S170A, G172A plus G202V, R203A, K206A, contained in pUL25-C3B work in concert with each other or if the mutated amino acids G202V, R203A and K206A operate independently to produce the low levels of complementation observed with pUL25-C3B.

The mutant pUL25-C1L2 (Section 4.5) had been created to examine the combined effects of the mutations contained in pUL25-C1 plus pUL25-L2 on the properties of pUL25. A combination of the mutations was chosen since they either contained, or were close to, residues that were predicted to be the interaction sites on pUL25, which were involved in the formation of the CCSC (Trus et al., 2007). In the complementation analysis the mutations in pUL25-C1L2 had little effect on the protein's ability to support viral growth, and virus yields of over 68% of the wt positive control level were produced. However, the results do not conclusively rule out the possibility that these regions may be important during viral assembly. The mutant pFB-UL25-C1 encodes mutations for only two of the possible three residues in C1 identified as significant for CCSC formation, while pUL25-L2 was chosen because the deleted amino acids in this protein were in close proximity to the two residues in L2 that were predicted to be the interaction sites for the formation of the CCSC on mature capsids. Further experiments are required that specifically target the proposed interaction residues for CCSC formation on mature capsids. Analysis of a single

mutant construct containing the appropriate SIFT selected substitutions at H348, R362, G363, H323 and G324 would help to clarify the functional significance of the amino acids identified.

Complementation assays with pUL25-C4B and -C4A generated virus yields of less than 1% of the wt positive control level. Since pUL25-C4A contained only four of the five mutated residues in pUL25-C4B, this demonstrated that one or more of the wt residues N396, Y398, D400 and L402 mutated in pUL25-C4A was functionally important. The amino acids mutated in pUL25-C4A are located along a loop on the surface of UL25, which lies adjacent to the extended looped out region, L3 (Figure 4.16). Since the pUL25-L3 protein also failed to complement the growth of  $\Delta$ UL25MO, the combined results for pUL25-C4A and pUL25-L3 suggests that this whole area of the protein is essential for viral assembly.

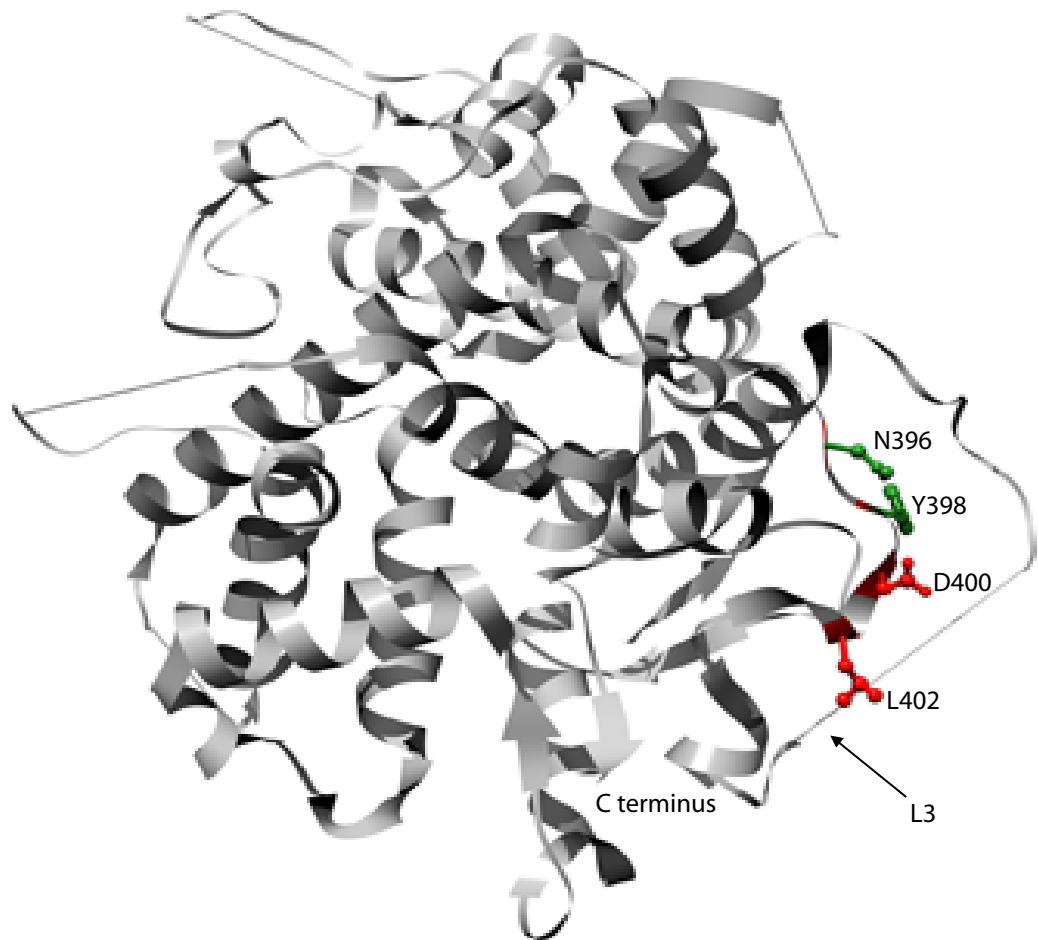


**Figure 4.16 Ribbon diagram of UL25nt**

The location of the wt residues, N396, Y398, D400 and L402, which are mutated in pUL25-C4A and their proximity to L3 are illustrated.

## 5 Ability of the mutant pUL25s to support DNA packaging

### 5.1 Introduction

As discussed in Section 1.3.5.2.5, UL25 has been shown to play an important role during the later stages of viral DNA packaging prior to the release of capsids into the cytoplasm. The available evidence supports a model for DNA packaging in which the viral genome is inserted into the capsid in the direction of the L to S terminus (McVoy et al., 2000, Stow, 2001). Stow (2001) used the original UL25 null mutant, KUL25NS, to analyse HSV-1 DNA packaging in Vero and BHK cells in the absence of UL25 and showed that the proportion of encapsidated DNA present as full-length genomes was much lower than the values obtained in wt virus-infected cells. Consequently, in KUL25NS-infected cells there was a significant overrepresentation of the L terminus and underrepresentation of the S terminus of the packaged HSV-1 genome (Figure 5.1). The aim of the experiments carried out in this section was to determine the effect of each of the eight non-complementing mutant proteins pUL25-L3, -L5, -L6, -C3B, -C4A,  $\Delta$ 1-45,  $\Delta$ 1-59 and  $\Delta$ 1-133 on the ability of  $\Delta$ UL25MO to encapsidate unit-length viral DNA in non-permissive U2OS cells.

The UL25 mutant genes were initially cloned into the plasmid pFBpCI (Figure 5.2), which had been selected on the basis that it could also be used as a baculovirus transfer vector. Transfection of Vero cells with plasmid DNA was a convenient method of introducing the UL25 gene into cells for screening the expressed mutant UL25 proteins for their ability to complement the growth of  $\Delta$ UL25MO. However, the efficiency of transfection and the level of expression of the UL25 proteins in individual cells were variable. To determine whether the mutant proteins altered the packaging phenotype of  $\Delta$ UL25MO in non-permissive cells, a system was required in which the majority of the cells expressed the recombinant pUL25. Various mammalian cell lines, in particular human osteosarcoma cell lines such as U2OS, have been reported to be efficiently transduced by a recombinant baculovirus containing a reporter gene under the control of the HCMV IE promoter (Condreay et al., 1999, Song et al., 2003).

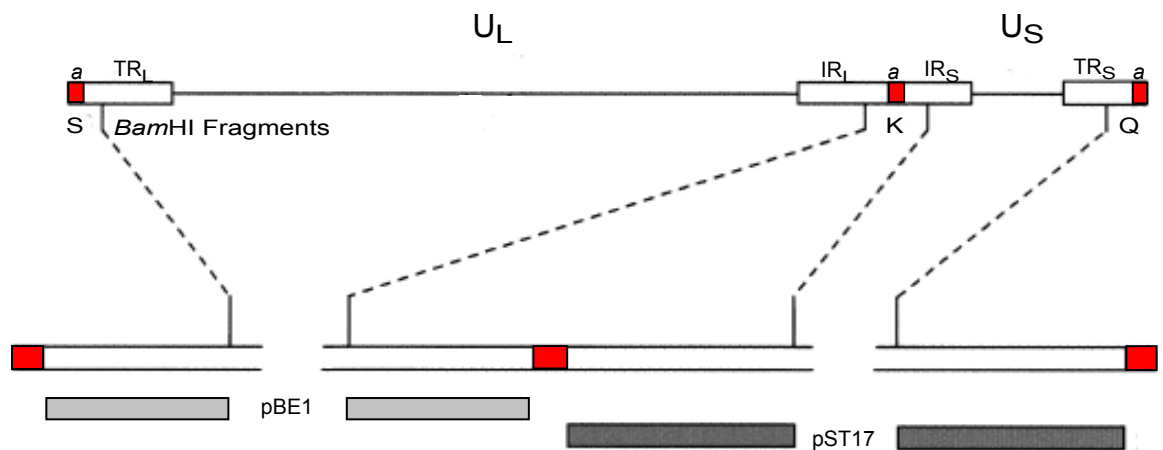


**Figure 5.1 The structure of the HSV-1 genome**

The HSV-1 genome is represented at the top and shows the positions of the unique ( $U_L$  and  $U_S$ ) and repeated regions ( $TR_L$ ,  $IR_L$ ,  $IR_S$  and  $TR_S$ ). The locations of the BamHI fragments S, K and Q are indicated and the positions of the a sequence are shown in red. The expanded representation of the BamHI K (joint-spanning) fragment and the terminal fragments S and Q are shown along the bottom. The shaded boxes represent the regions within these fragments that correspond to the inserts in the plasmids pBE1 and pST17.  $^{32}\text{P}$ -labelled pBE1 and pST17 were used as probes to determine the genomic location of the BamHI fragments generated and analysed by Southern blot hybridisation during the DNA packaging assays carried out in Section 5.3 (adapted from Stow, 2001).

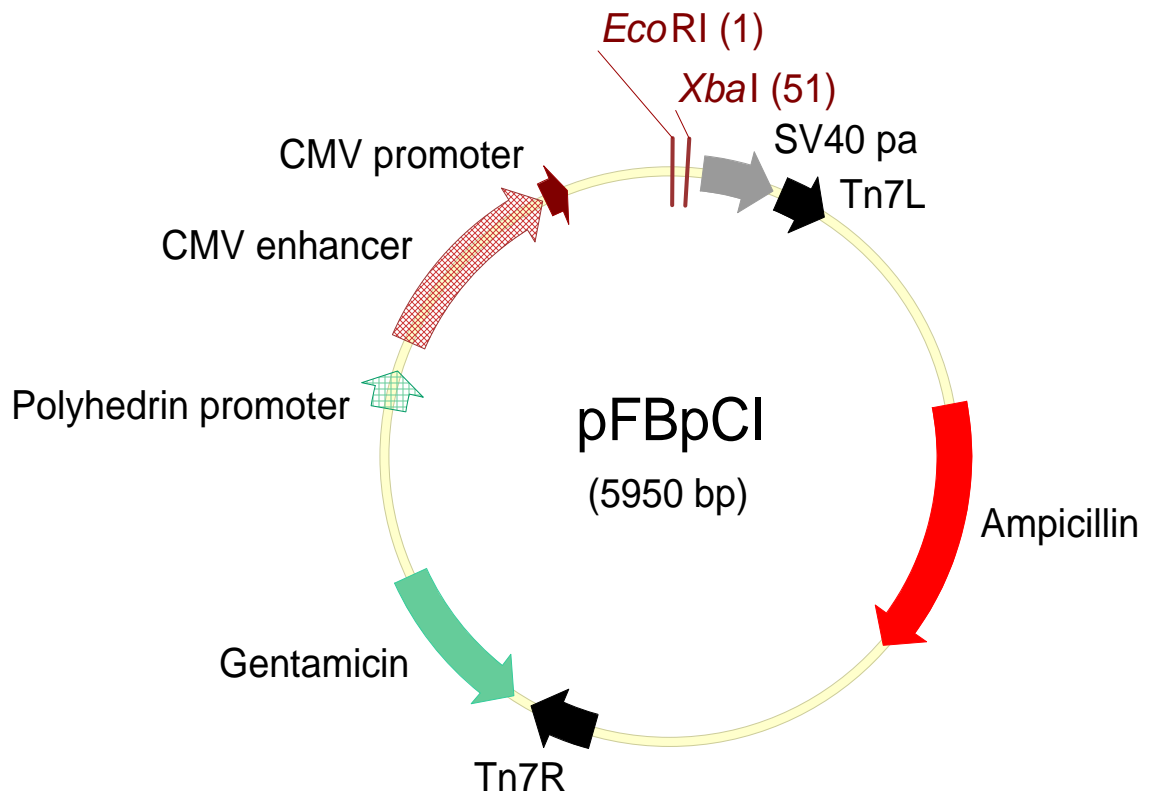


**Figure 5.2 Plasmid map of pFBpCI**

The HCMV IE promoter and enhancer, polyhedrin promoter, ampicillin and gentamicin genes are represented by different coloured arrows. The position of the right and left arms of the Tn7 transposon (Tn7R and Tn7L, respectively) are shown by the black arrows, while the grey arrow represents the position of the SV40 polyadenylation signal (SV40 pa). The positions of the unique *EcoRI* and *XbaI* sites are highlighted in red.

Furthermore, provided cells were infected with recombinant baculovirus at a high MOI, a reproducible number of transduced cells could be achieved. An additional safety feature of this system is that recombinant baculovirus infections are contained, since mammalian cells are non-permissive for baculovirus replication (Kost et al., 2005). To perform the packaging assay a series of recombinant baculoviruses were generated, each expressing one of the eight non-complementing mutant UL25 proteins under the control of HCMV IE promoter. Two control recombinant baculoviruses were also constructed, one expressing the wt UL25 protein, AcWTUL25, and one expressing no foreign proteins, AcpCI.

## 5.2 Generation of the baculovirus expressing the recombinant pUL25s

The recombinant baculoviruses were produced using the Bac-to-Bac system (Life Technologies) and an overview of this procedure is shown in Figure 5.3. Based on a method developed by Luckow et al. (1993), the system takes advantage of the site-specific transposition properties of the Tn7 transposon to generate recombinant bacmid DNA. The bacmid was propagated in *E.coli* DH10Bac containing the helper plasmid pMON7124, which confers tet<sup>R</sup> to the bacterial cells and encodes a transposase enzyme providing the Tn7 transposition function *in trans* (Barry, 1988). The mutated and wt UL25 genes were cloned into the baculovirus transfer vector pFBpCI downstream of the HCMV IE promoter, which controls the expression of the recombinant UL25 genes in mammalian cells (Figure 5.2). The mini-Tn7 in pFBpCI contains the expression cassette, which is flanked by the right and left arms of Tn7 and includes the gm<sup>R</sup> gene. Following transformation of *E. coli* DH10Bac with the recombinant pFBpCI, site-specific transposition occurs between the mini-Tn7 region from the recombinant plasmid gene and the receptor attTn7 sites in the baculovirus genome within the bacmid. Transposition of the recombinant gene to the attTn7 attachment site disrupts the expression of  $\beta$ -galactosidase from the *LacZ $\alpha$*  gene in the bacmid, thereby allowing blue/white recombinant selection on medium containing the colourimetric substrate X-gal and the inducer IPTG. Transformants are also selected for km<sup>R</sup>, gm<sup>R</sup> and tet<sup>R</sup>, which confirms the presence of the bacmid, pFBpCI and the helper plasmid, respectively.

### Figure 5.3 Experimental outline used to generate the recombinant baculovirus

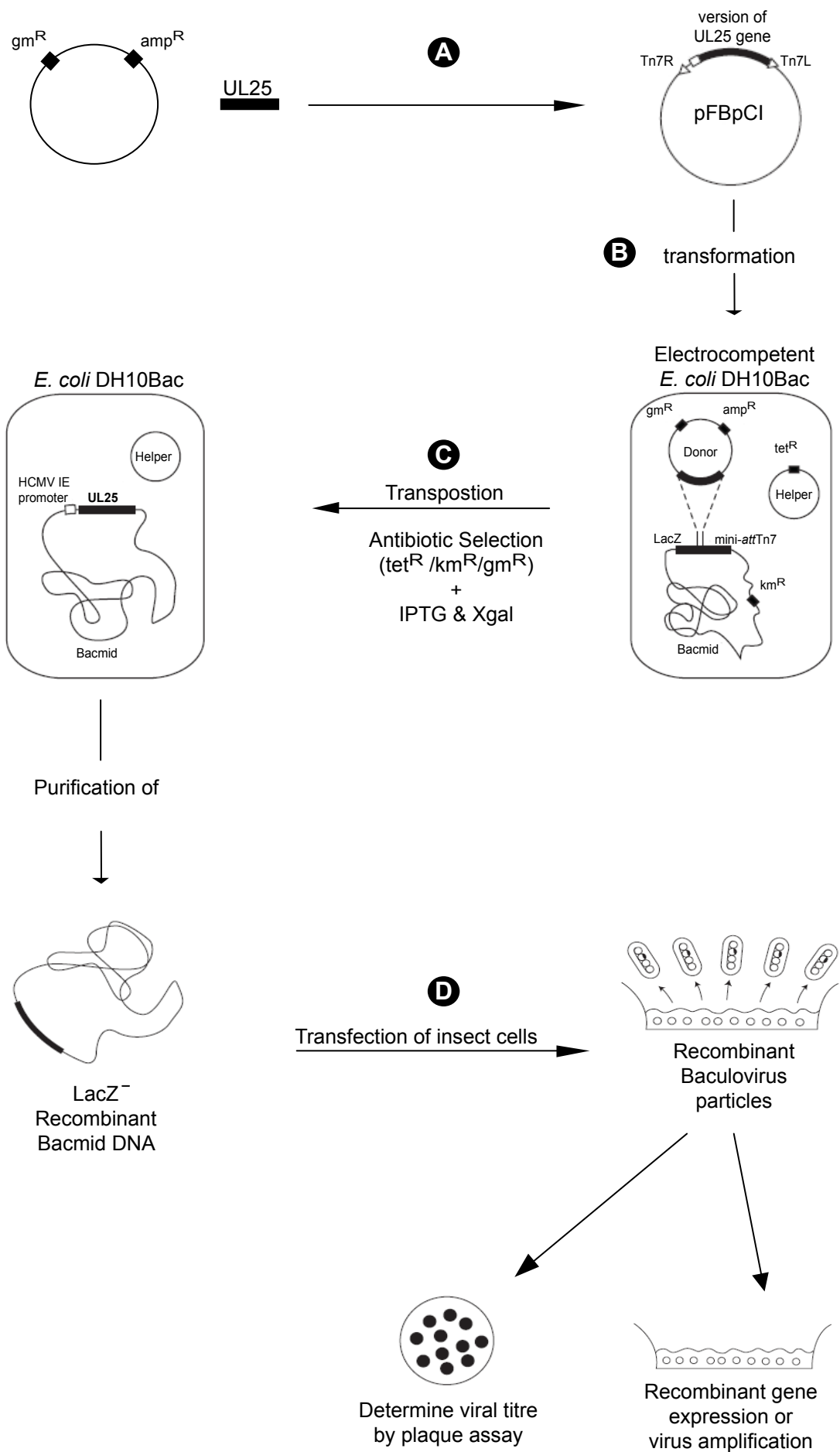
The recombinant baculovirus were generated using the Bac-to-Bac system (Life Technologies).

(A) A wt or mutant UL25 gene was cloned into the baculovirus transfer vector, pFBpCI, downstream of the HCMV IE promoter within the mini-Tn7.

(B) The recombinant vector was electroporated into electrocompetent *E. coli* DH10Bac cells that contained the baculovirus shuttle vector, bMON14272, which encodes the *LacZ $\alpha$*  gene possessing a mini-*att*Tn7 site.

(C) The helper plasmid pMON7124 provided the Tn7 transposition function *in trans*, allowing transposition of the UL25 gene into, and disruption of, the *LacZ $\alpha$*  gene in the bacmid. Bacteria, containing recombinant bacmids, were plated out onto L broth agar supplemente with tet, km and gm, which selects for bacteria carrying the bacmid, pFBpCI and the helper plasmid respectively. In addition, the plates contained X-gal so that recombinant bacmids with the *LacZ $\alpha$* <sup>-</sup> phenotype could be identified.

(D) The recombinant bacmid DNA was transfected into insect cells, resulting in the production of infectious recombinant baculovirus, which expressed the UL25 gene under the control of the HCMV IE promoter in mammalian cells.



Bacmid DNA encoding the modified UL25 gene was isolated from  $km^R$ ,  $gm^R$  and  $tet^R$  bacteria using an adapted alkaline lysis procedure (Section 2.2.12.1). To obtain infectious recombinant baculovirus, bacmid DNA was transfected into Sf21 cells (Section 2.2.12.2) and the cells were incubated at 28°C for three days. The progeny viruses were harvested and amplified to produce high-titre virus stocks, as described in Section 2.2.12.3. Each of the recombinant baculoviruses generated and the proteins they express are listed in Table 5.1 (The N-terminal deletion mutants AcUL25 $\Delta$ 1-45,  $\Delta$ 1-59 and  $\Delta$ 1-133 were supplied by Dr V. Preston). To confirm that each baculovirus expressed UL25 protein in mammalian cells, U2OS cells were infected with baculovirus expressing wt UL25 or a mutant protein. As a negative control a sample of cells was infected with baculovirus AcpCl. After 24 h at 37°C, the cells were harvested and each sample was analysed for UL25 protein expression using the Western blotting technique described in Section 2.2.18.2. The proteins expressed by AcUL25-C3B, -C4A, -L3, -L5 and -L6 were screened with anti-UL25 MAb166, which recognises an epitope located between pUL25 residues 59-133. Since this epitope was not present in the N-terminally truncated proteins, the proteins expressed by AcUL25- $\Delta$ 1-45, - $\Delta$ 1-59 and - $\Delta$ 1-133 were screened with anti-UL25 RAb335, which was raised against UL25 residues 342-580. The images obtained for the Western blots are shown in Figure 5.4, and demonstrate that each UL25 recombinant baculovirus expressed a UL25 protein of the correct size.

To confirm that the infection efficiency of each of the recombinant baculovirus in mammalian cells was similar, U2OS monolayers were infected with virus at MOI of 50 PFU per cell and prepared for immunofluorescence as outlined in Section 2.2.12.6. To detect virus-infected cells in each sample, the mounted monolayers were probed with the appropriate anti-UL25 primary antibody at a concentration of 1:500 and secondary FITC-conjugated anti-mouse antibody at a concentration of 1:100. To identify all of the cells in each sample the cell nuclei were stained with propidium iodide and then visualised using the confocal microscope. The total number of cells and the number of cells infected with baculovirus were counted in a selected area of each coverslip. For each recombinant baculovirus the proportion of virus-infected cells ranged from 41% to 47% of the total number of cells counted (data not shown), verifying that

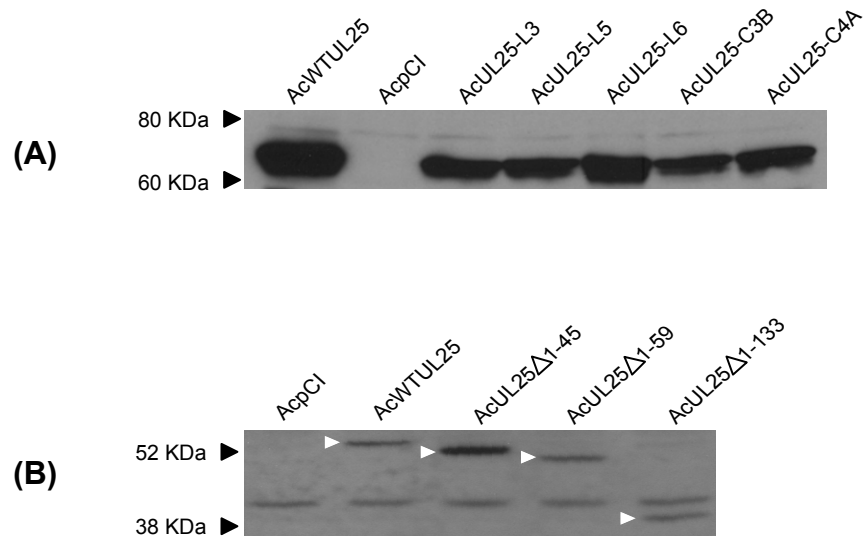


**Figure 5.4 Western analysis of baculovirus- infected U2OS cell extracts for UL25 expression**

U2OS cells were infected with the baculovirus at an MOI of 50 PFU/cell and incubated overnight at 37°C. Cell extracts were prepared and the proteins were separated by SDS-PAGE and then analysed by Western blotting. No loading control was used during this experiment. Blot (A) was screened with primary anti-pUL25 MAb166 antibody at a concentration of 1:1000 and secondary hrp-conjugated anti-mouse antibody at 1:1000 dilution. Blot (B) was screened with primary anti-pUL25 RAb335 antibody at a concentration of 1:1000 and with secondary hrp-conjugated protein A antibody at 1:1000 dilution. The white arrowheads indicate the position of the wt or truncated UL25 proteins.

each virus stock showed a similar and therefore comparable efficiency of infection.

Baculovirus	Expressed HSV-1 UL25 Protein
AcpCI	None
AcWTUL25	pUL25
AcUL25-C3B	pUL25-C3B
AcUL25-C4A	pUL25-C4A
AcUL25-L3	pUL25-L3
AcUL25-L5	pUL25-L5
AcUL25-L6	pUL25-L6
AcUL25 $\Delta$ 1-45	pUL25 $\Delta$ 1-45
AcUL25 $\Delta$ 1-59	pUL25 $\Delta$ 1-59
AcUL25 $\Delta$ 1-133	pUL25 $\Delta$ 1-133

**Table 5.1 List of recombinant baculoviruses**

### 5.3 Viral DNA packaging assay

The DNA packaging assay of Stow (2001) was used to determine whether any of the mutant UL25 proteins expressed by the recombinant baculoviruses listed in Table 5.1 could alter the DNA packaging phenotype of  $\Delta$ UL25MO in U2OS cells. A summary of the assay is shown in Figure 5.5. At 24 hpi the cells were harvested and total and DNase-resistant DNA samples were prepared as described in Section 2.2.14.1. Since DNase I treatment should degrade all of the DNAs present in virus-infected cells, except the encapsidated viral DNA, the DNase-resistant fraction represents the DNA that has been stably packaged. DNA samples from both the total and DNase-resistant fractions were digested with *Bam*HI. The fragments were separated on a 0.8% agarose gel and analysed by Southern blot hybridisation (Section 2.2.15) using either <sup>32</sup>P-labelled pBE1 or pST17 probes. Figure 5.1 shows the genomic location of each of the *Bam*HI fragments that hybridised to the HSV-1 sequences present in pBE1 and pST17. During the packaging process the replicated concatemeric viral DNA is cleaved

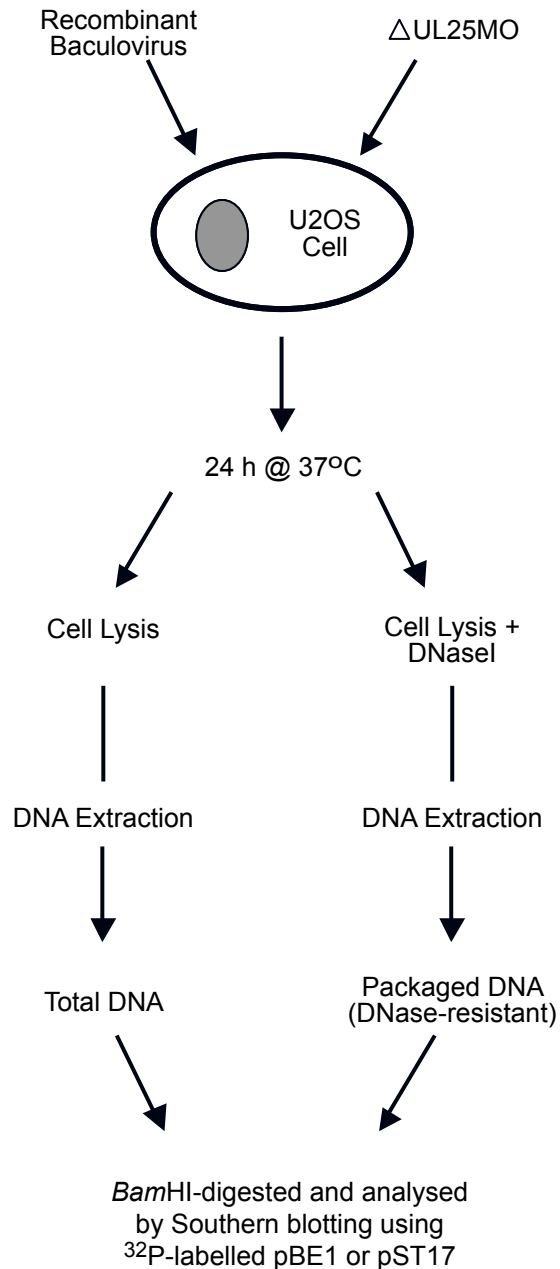


**Figure 5.5 Summary of the packaging assay**

U2OS cells infected with a recombinant baculovirus and  $\Delta$ UL25MO were incubated at 37°C for 24 h. The cells were harvested and divided into two aliquots. One aliquot of infected cells, which represented the total DNA fraction, was lysed and the DNA was extracted. The other infected cell sample was lysed and treated with DNaseI prior to DNA extraction. This fraction represented the packaged DNA. Duplicate DNA samples from both the total and packaged fractions were digested with *Bam*HI, the fragments were separated on a 0.8% agarose gel and then transferred by blotting onto nitrocellulose. The DNA was hybridised to  $^{32}$ P-labelled pBE1 or pST17.

into monomeric units, which, when digested with *Bam*HI, give rise to the terminal *Bam*HI S and Q fragments. The pBE1 probe hybridises to the *Bam*HI S fragment, which is located in the R<sub>L</sub> region of the L terminus, and the joint-spanning *Bam*HI K fragment of the HSV-1 genome. The pST17 probe recognises the *Bam*HI Q fragment, which is located in the HSV-1 R<sub>S</sub> region of the S terminus, and the *Bam*HI K fragment. In non-permissive cells infected with an HSV-1 UL25 null mutant, viral DNA is cleaved and encapsidation of the DNA is initiated but fails to go to completion. As a consequence, in packaged DNA digested with *Bam*HI the L terminus (*Bam*HI S) is overrepresented and S terminus (*Bam*HI Q) is underrepresented relative to the joint-spanning fragment, *Bam*HI K (Stow, 2001).

Representative phosphorimages of total and DNase-resistant DNA samples analysed by Southern blot hybridisation are shown in Figure 5.6. Inspection of the images revealed that in  $\Delta$ UL25MO-infected cells expressing any of the five UL25 mutant proteins, pUL25-L5, -C3B,  $\Delta$ 1-45,  $\Delta$ 1-59 and  $\Delta$ 1-133, the DNA packaging profile of  $\Delta$ UL25MO was indistinguishable from the one obtained from the negative control sample, in which cells were co-infected with AcpCI and  $\Delta$ UL25MO. In the DNase-resistant samples the L terminal fragment (*Bam*HI S) was present but the joint-spanning K fragment was detectable in considerably reduced amounts (Figures 5.6, B, lanes 2,4 and 6; F, lanes 2-5). The S terminal fragment (*Bam*HI Q) was also present at low levels in these DNA samples (Figure 5.6 D, lanes 2, 4 and 6; C and D lanes, 2-5). In contrast, in  $\Delta$ UL25MO-infected cells expressing pUL25-L3, -L6 or -C4A the DNA packaging profile of  $\Delta$ UL25MO was comparable to the pattern from positive control sample expressing the wt pUL25 protein, where both the *Bam*HI S and Q fragments were detected in similar amounts in the DNase-resistant DNA samples (Figure 5.6 B and D, lanes 1, 3, 5 and 7). To quantify the results the amounts of radioactivity in the bands corresponding to the joint fragment and the L and S terminal fragments (*Bam*HI K, S and Q, respectively) were measured in DNase-resistant samples. When calculating the amount of radioactivity in *Bam*HI S, the measurements included the major fragment, which had a single copy of the *a* sequence and the higher molecular weight fragments containing two or three copies. The ratio of joint to terminal fragment was calculated for each recombinant baculovirus-infected cell sample from three independent packaging assays and the results are summarised

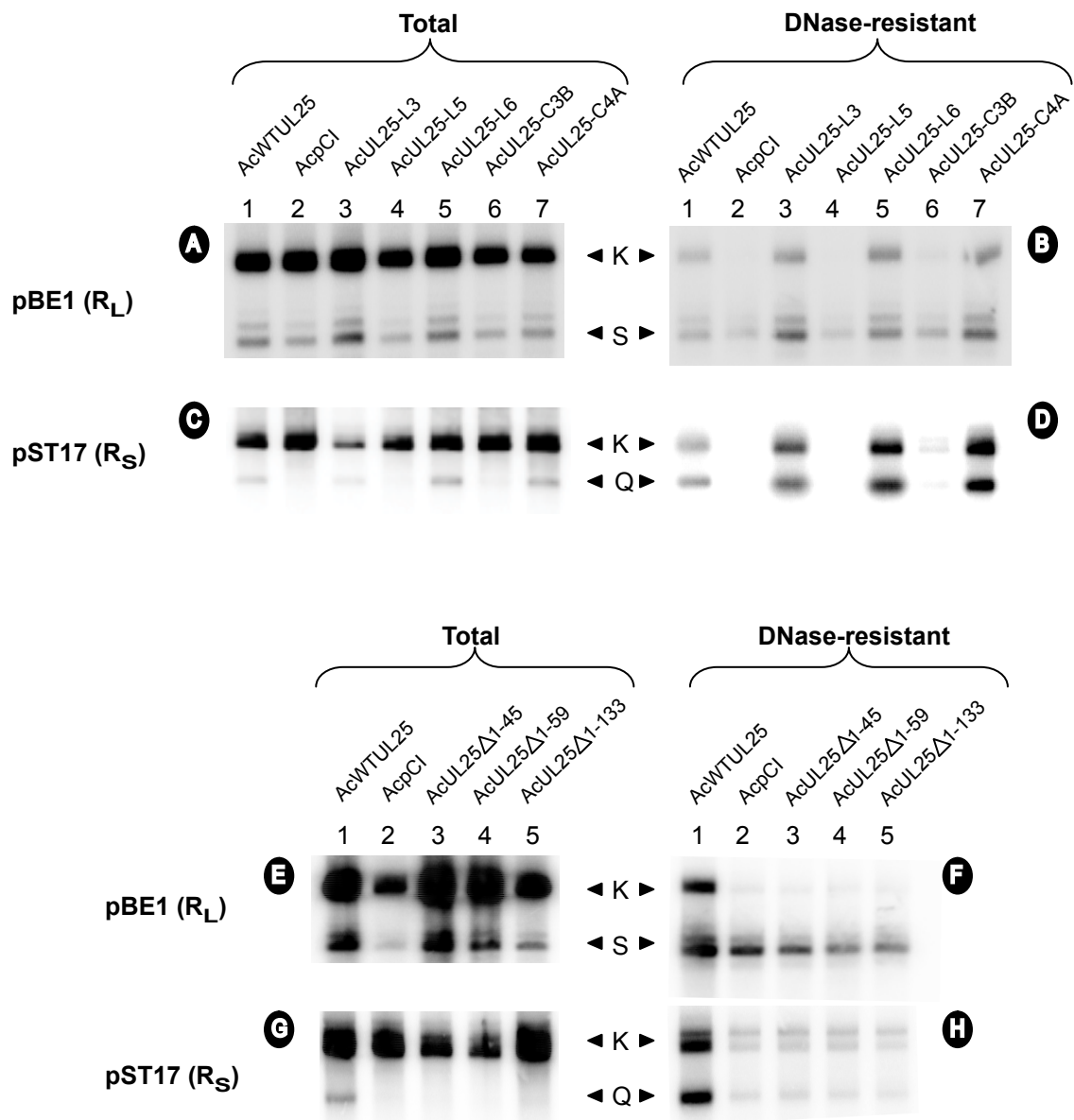


**Figure 5.6 Southern blots of the packaging assays**

U2OS monolayers were co-infected with the recombinant baculovirus indicated and  $\Delta$ UL25MO. At 24 hpi the cells were harvested and total and DNase-resistant DNAs were prepared. Duplicate samples were digested with *Bam*HI and the fragments were resolved by electrophoresis through 0.8% agarose gel and transferred onto Hybond-XL membranes. The membranes were hybridised to either  $^{32}$ P-labelled pBE1 ( $R_L$  probe) or pST17 ( $R_S$ ) probe as shown. The position of the joint-spanning (*Bam*HI K) and terminal fragments (*Bam*HI S and Q) detected are indicated.

in Table 5.2. In cells co-infected with the negative control baculovirus, AcpCI and  $\Delta$ UL25MO the DNA packaging profile was similar to the one previously reported by Stow (2001) for KUL25NS-infected cells alone, with a ratio of 3.5:1 overrepresentation of the L terminal fragment, *Bam*HI S, and a ratio of 0.6:1 underrepresentation of the S terminal fragment, *Bam*HI Q, relative to the joint-spanning *Bam*HI K fragment. In addition, in  $\Delta$ UL25MO-infected cells expressing pUL25-C3B, -L5,  $\Delta$ 1-45,  $\Delta$ 1-59 and  $\Delta$ 1-133 the *Bam*HI digested packaged viral DNA samples produced ratios of the L and S terminal fragments relative to *Bam*HI K that were similar to the ratios observed in the negative control sample (Table 5.2), indicating that the mutant proteins expressed by AcUL25-C3B, -L5,  $\Delta$ 1-45,  $\Delta$ 1-59 and  $\Delta$ 1-133 failed to support encapsidation of full-length viral DNA in  $\Delta$ UL25MO-infected cells. By contrast, the ratios obtained from *Bam*HI-digested packaged DNA from cells co-infected with  $\Delta$ UL25MO and baculovirus expressing pUL25-C4A, -L3 or -L6, were comparable to the positive control, indicating that the defect in each of these proteins did not affect their ability to support packaging of full-length DNA.

## 5.4 Pulse-field gel electrophoresis (PFGE) of encapsidated viral DNA

To confirm that the genomic termini present in the DNase-resistance samples from  $\Delta$ UL25MO-infected cells expressing pUL25-C4A, -L3 or -L6 resulted from encapsidation of mature unit-length genomes, each of the fractions were analysed by PFGE (Section 2.2.16) together with the DNase-resistant fraction from  $\Delta$ UL25MO-infected U2OS cells expressing wt UL25. PFGE is a technique used to separate large DNA molecules greater than 50 kb, which is the limit for the separation of DNA fragments by electrophoresis on standard agarose gels. U2OS monolayers were co-infected with  $\Delta$ UL25MO and either AcWTUL25, AcpCI, AcUL25-L3, AcUL25-L6 or AcUL24-C4A, or singly infected with wt HSV-1, AcWTUL25 or  $\Delta$ UL25MO. At 24 hpi the cells were harvested, and DNase-resistant DNA was carefully prepared as described in Section 2.2.14.1 to minimise DNA shearing. The DNAs were resolved by PFGE, transferred to Hybond-N membrane and hybridised to  $^{32}$ P-labelled HSV-1 pGX2, which contains the *Bam*HI K fragment. The phosphorimage obtained is shown in Figure 5.7 and reveals that a major band, corresponding to the full-length 152 kb HSV-1 genome, was

Recombinant baculovirus	Packaging competent	Terminus	Ratio relative to <i>Bam</i> HI K			Mean ratio	Mean ratio relative to AcWTUL25
			Exp 1	Exp 2	Exp 3		
AcWTUL25	+	L	1.3	1.8	1.6	1.6	1.0
		S	0.9	1.0	1.0	1.0	1.0
AcpCI	-	L	4.3	2.7	2.7	3.5	2.2
		S	0.6	0.6	0.6	0.6	0.6
AcUL25-C3B	-	L	3.5	4.7	1.2	3.1	1.9
		S	0.7	0.5	1.1	0.7	0.7
AcUL25-C4A	+	L	1.8	2.0	1.4	1.7	1.0
		S	1.0	0.7	0.8	0.8	0.8
AcUL25-L3	+	L	2.3	2.1	1.8	2.0	1.3
		S	1.1	0.7	0.9	0.9	0.9
AcUL25-L5	-	L	3.5	5.0	2.1	3.5	2.2
		S	0.5	0.5	0.5	0.5	0.5
AcUL25-L6	+	L	1.8	1.0	1.1	1.3	0.8
		S	1.0	0.7	0.9	0.9	0.9
AcUL25-Δ1-45	-	L	4.0	4.0	5.5	4.5	2.8
		S	0.5	0.7	0.5	0.6	0.6
AcUL25-Δ1-59	-	L	6.5	6.4	9.2	7.4	4.6
		S	0.7	0.6	0.4	0.6	0.6
AcUL25-Δ1-133	-	L	7.1	7.4	10.3	8.3	5.2
		S	0.8	0.5	0.5	0.6	0.6

**Table 5.2 Quantification of the L and S terminal fragments encapsidated during packaging assays**

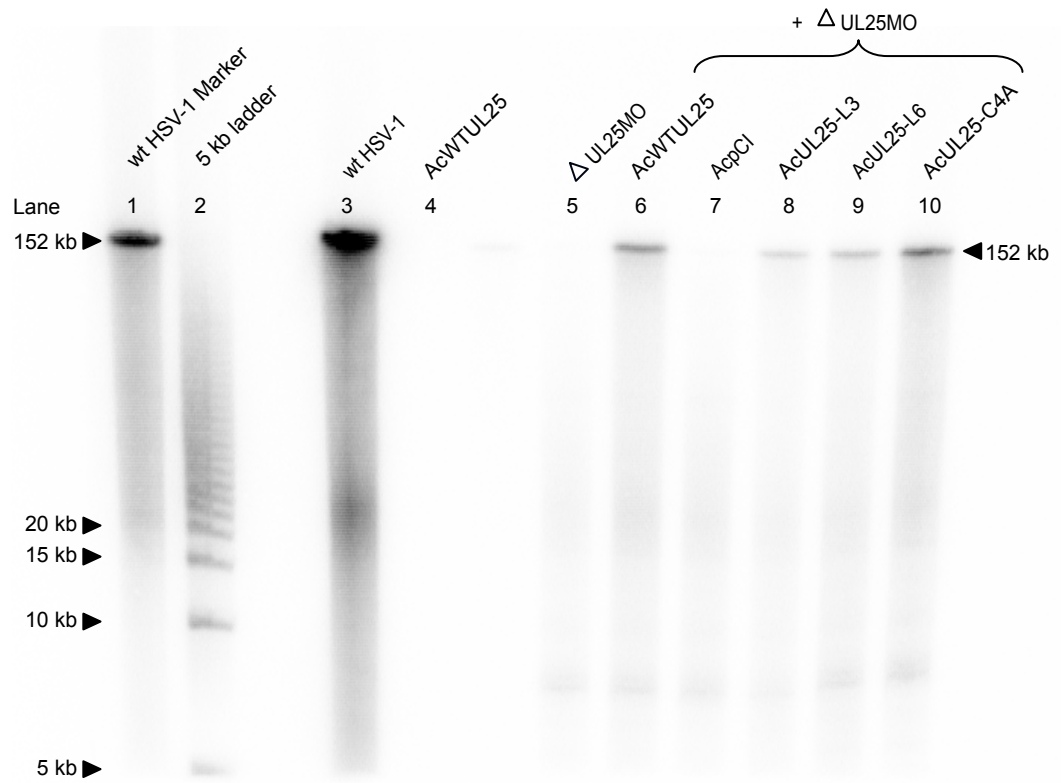


**Figure 5.7 PFGE analysis of packaged DNA**

U2OS monolayers were co-infected with the recombinant baculovirus indicated and  $\Delta$ UL25MO. At 24 hpi the cells were harvested and DNase-resistant DNA was prepared, using a gentle method without phenol extraction to reduce shearing. After the DNA molecules had been separated by PFGE, the DNA was blotted onto Hybond-N membrane and hybridised to  $^{32}$ P labelled pGX2, which contains the HSV-1 *Bam*HI K fragment. The position of the 152 kb viral genomes are indicated by the black arrowheads.

detected in packaged DNA from cells infected with either the wt HSV-1 virus (lane 3) or co-infected with AcWTUL25 and  $\Delta$ UL25MO (lane 6). In addition, a 152 kb band was also observed in the packaged DNA from cells co-infected with  $\Delta$ UL25MO and AcUL25-L3, -L6 or -C4A (lanes 8, 9 and 10). In contrast, no full-length encapsidated DNA was evident in the negative control sample from cells co-infected with AcpCI and  $\Delta$ UL25MO (lane 7), or in the other control samples from cells infected with either AcWTUL25 or  $\Delta$ UL25MO alone (lanes 4 and 5).

## 5.5 Discussion

The ratio of L and S terminal fragments to joint fragment detected in *Bam*HI digested packaged DNA samples from  $\Delta$ UL25MO-infected U2OS cells expressing pUL25-L3, -L6 or -C4A were similar to values obtained for mutant-infected cells expressing the wt protein. The results suggested that unit length genomes were encapsidated in  $\Delta$ UL25MO-infected cells expressing these mutant proteins. These observations were confirmed by PFGE analysis of the packaged DNA extracted from cells co-infected with  $\Delta$ UL25MO and AcUL25-L3, -L6 or -C4A, which showed that full-length HSV-1 DNA molecules were present in these samples. The evidence presented here indicates that the UL25 mutant proteins, pUL25-C4A, -L3 and -L6, do not disrupt viral assembly during DNA packaging but at some stage after encapsidation. In contrast, in  $\Delta$ UL25MO-infected cells expressing pUL25-C3B, pUL25-L5, pUL25 $\Delta$ 1-45, pUL25 $\Delta$ 1-59 or pUL25 $\Delta$ 1-133, the L terminal region from the HSV-1 genome was overrepresented and the S terminal region was underrepresented. These results signified that the mutated residues contained in pUL25-C3B, the unstructured region of L5 (residues 511-513) and the first 45 residues in the N-terminal portion of UL25, are critical for HSV-1 packaging of unit-length DNA.

Using the imaging program Chimera (<http://www.cgl.ucsf.edu/chimera/>), five of the six residues that were mutated in pUL25-C3B were located in or near a deep cleft situated in the C3 region of UL25 and their position on the molecule is indicated in Figure 5.8. The image shows that four of the residues mutated in pUL25-C3B are situated directly in the crevice, with G169, S170 and G172 present on one side of the cleft and R203 lying directly opposite, while the fifth residue (R202) lies along the ridge at the entrance to the cleft. It is easy to

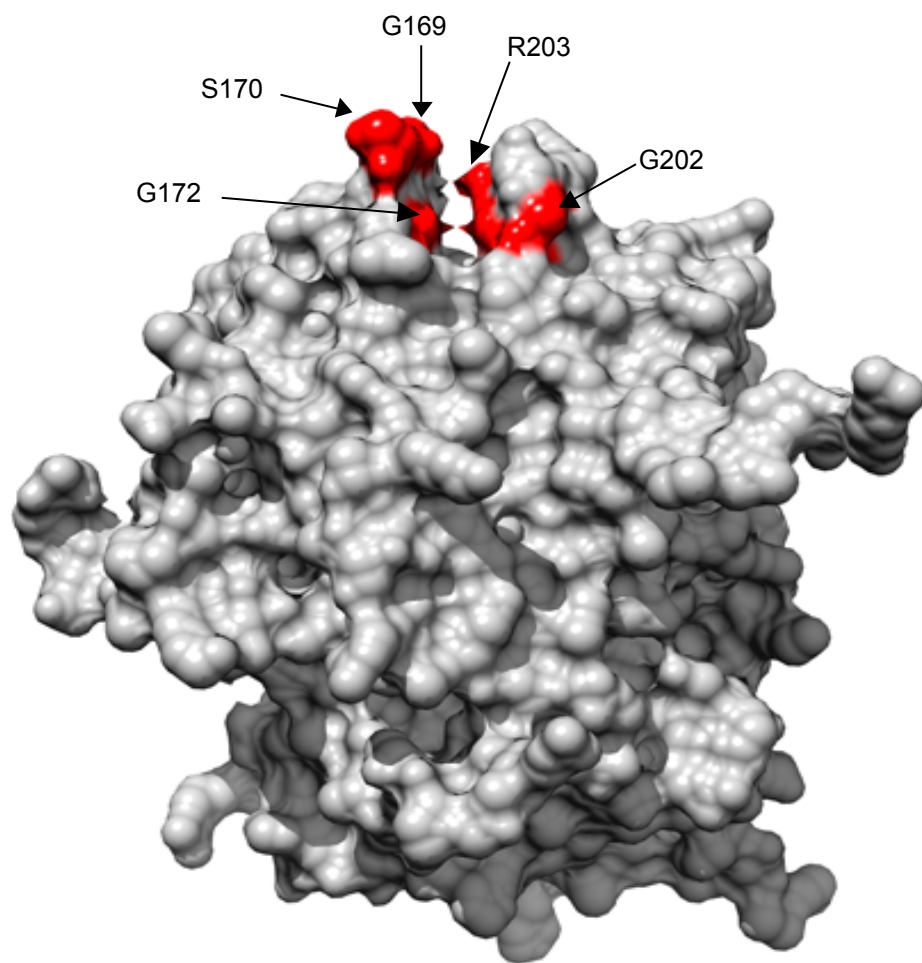


**Figure 5.8 The C3 cleft of UL25**

The image shows a solid surface representation of wt pUL25 and indicates the locations of the five residues in the C3 cleft that were mutated in pUL25-C3B. Four of the amino acids are situated directly in the crevice, with R203 lying on the opposing face from G172, S170 and G169. The fifth residue, G202, is positioned along the ridge at the entrance to the cleft.

envisage an essential protein partner of pUL25, which is required during DNA packaging, docking with pUL25 at this region and interacting directly with the important residue(s) that have been identified here. The position of C3 relative to L5, which contains the unstructured residues deleted in pUL25-L5, is indicated in Figure 5.9. On the view shown L5 is situated on the front face of the molecule, while C3 lies on the opposing side at the base of the protein, approximately  $180^{\circ}$  from L5. Since each of these regions appear to be some distance apart and on opposite sides of the structure, it is possible that the C3 and L5 regions interact with different binding partners that are required during DNA packaging.

Since the N-terminal region of pUL25 (residues 1-133) is not included in the crystallographic structure of the protein, the position of this region relative to L5 and C3 is unclear. However, the predicted secondary structure for this portion of UL25 includes a long alpha helix (residues 48-110) preceded by a 45-residue unstructured N-terminal loop, which may become structured following protein binding. Although sequence analysis of this region revealed that the N-terminal loop is the least conserved portion of the protein (Bowman et al., 2006), from the data presented here it does appear to be essential for packaging the full-length genome. This finding is supported by a recent report by Cockrell et al. (2009), who constructed an HSV-1 mutant expressing an N-terminally truncated pUL25 lacking the first 50 residues, and showed that failure of the virus to replicate in Vero cells was due to aberrant cleavage of the  $U_S$  end of the viral genome during packaging. They also provided evidence that residues 1-50 of the protein mediated capsid attachment of UL25 *in vitro*.

The work presented here indicates that UL25 contains at least three distinct regions, the N-terminal portion, L5 and C3, which are critical for the protein interactions necessary for efficient encapsidation of unit-length viral DNA. However, further analysis is necessary to clarify if the mutations contained in pUL25-C3B, pUL25-L5 and pUL25 $\Delta$ 1-45 disrupt a single functional interface on the protein, or if each interacts with a different binding partner during viral DNA packaging.

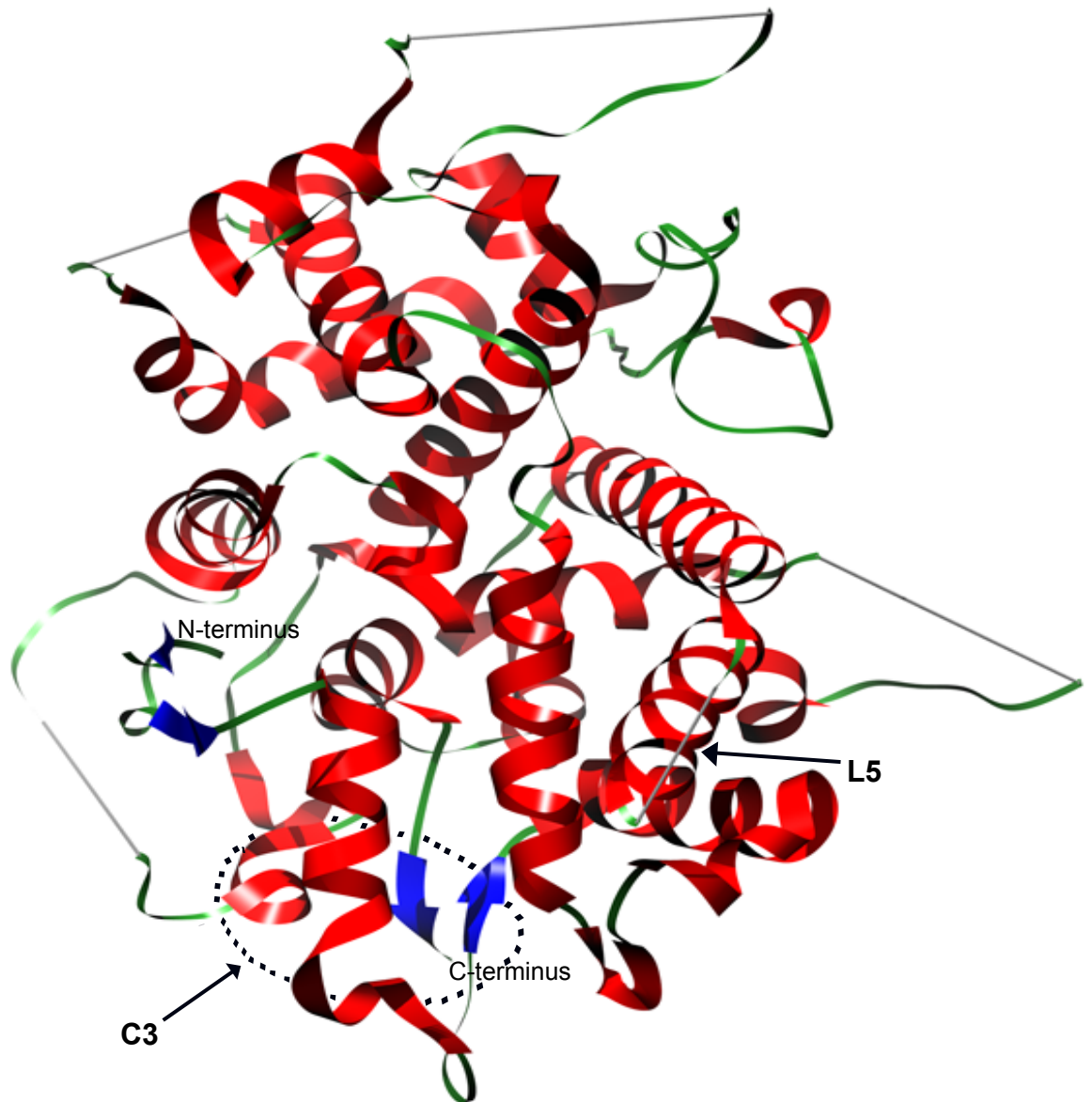


**Figure 5.9 Ribbon diagram of UL25nt with C3 and L5**

The position of L5 relative to the C3 region is indicated. The location of C3 is highlighted by the broken circle. On the view shown, C3 is located on the opposing face, approximately 180° from L5.

## **6 The effect of pUL25-L3, -L6 and -C4A on virus assembly in $\Delta$ UL25MO-infected U2OS cells**

### **6.1 Introduction**

The finding that the non-complementing mutant proteins, pUL25-L3, -L6 or -C4A, altered the DNA packaging phenotype of  $\Delta$ UL25MO, allowing the mutant to encapsidate unit-length viral DNA, indicated that virus assembly was disrupted after DNA packaging. The aim of the experiments described here was to determine at which point(s) during viral assembly these post-packaging blocks occurred. Two different approaches were used,  $\Delta$ UL25MO-infected U2OS cells expressing pUL25-L3, -L6 or -C4A were examined under the electron microscope to investigate the patterns of virus assembly, and fluorescent in-situ hybridisation (FISH) analysis was carried out on the cells to determine the distribution of virus DNA.

### **6.2 Electron microscopic (EM) analysis**

U2OS cells were co-infected with  $\Delta$ UL25MO and AcWTUL25, AcpCI, AcUL25-L3, -L6 or -C4A (Section 2.2.12.6). At 24 hpi the cells were harvested and embedded in resin. Thin sections of the virus-infected cells were prepared, stained with uranyl acetate and osmium tetroxide, and examined under the electron microscope (Section 2.2.17.1). Representative images from the samples analysed are shown in Figure 6.1A-6.1F. In the positive control sample, in cells co-infected with  $\Delta$ UL25MO and AcWTUL25, C-capsids were found in both the nuclear and cytoplasmic compartments as expected (Figure 6.1A). In the negative control sample, in cells co-infected with  $\Delta$ UL25MO and AcpCI, DNA-containing capsids were seen in the nuclei but not in the cytoplasm (Figure 6.1B). In  $\Delta$ UL25MO-infected cells expressing either pUL25-C4A or pUL25-L3, the pattern of virus assembly resembled that of the negative control where DNA-containing capsids were detected in the nuclei but not in the cytoplasm (Figure 6.1C and D). In contrast, in  $\Delta$ UL25MO-infected cells expressing pUL25-L6 the distribution of virus capsids was similar to that observed in the positive control, and DNA-containing C-capsids were detected in both the nuclear and

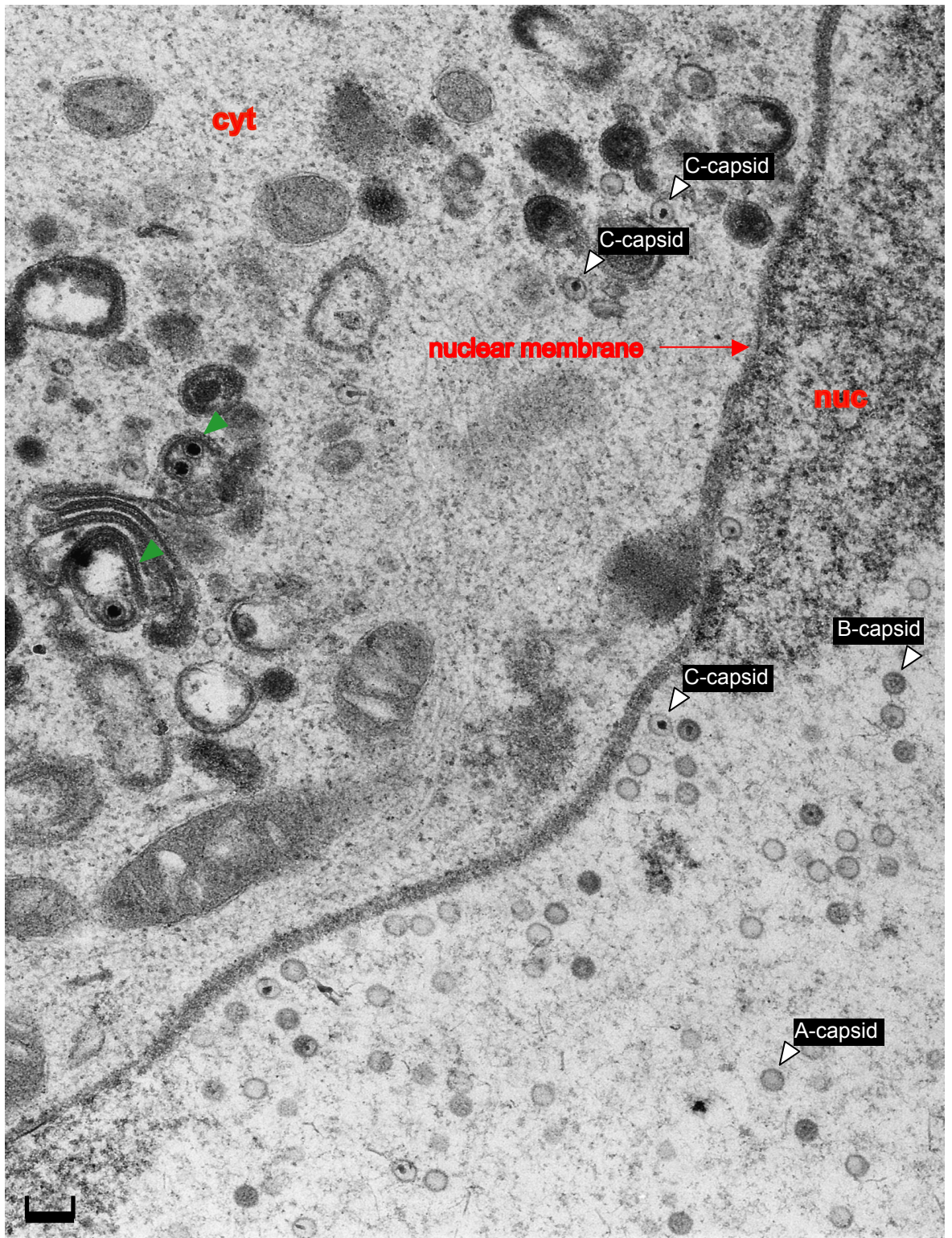


**Figure 6.1A Cells co-infected with  $\Delta$ UL25MO and AcWTUL25**

Monolayers of U2OS cells were co-infected with 2 PFU/cell  $\Delta$ UL25MO and 50 PFU/cell AcWTUL25. At 24 hpi cells were fixed and prepared for EM (Section 2.2.17.1). The nucleus (nuc), cytoplasm (cyt) and nuclear membrane are labelled. As expected, in infected cells expressing wt pUL25, free A- and B-capsids were located only in the nuclear compartment, while free C-capsids were present in the nuclear and cytoplasmic compartments. C-capsids located in vesicles are highlighted by the green arrowhead. The size bar represents 500 nm.

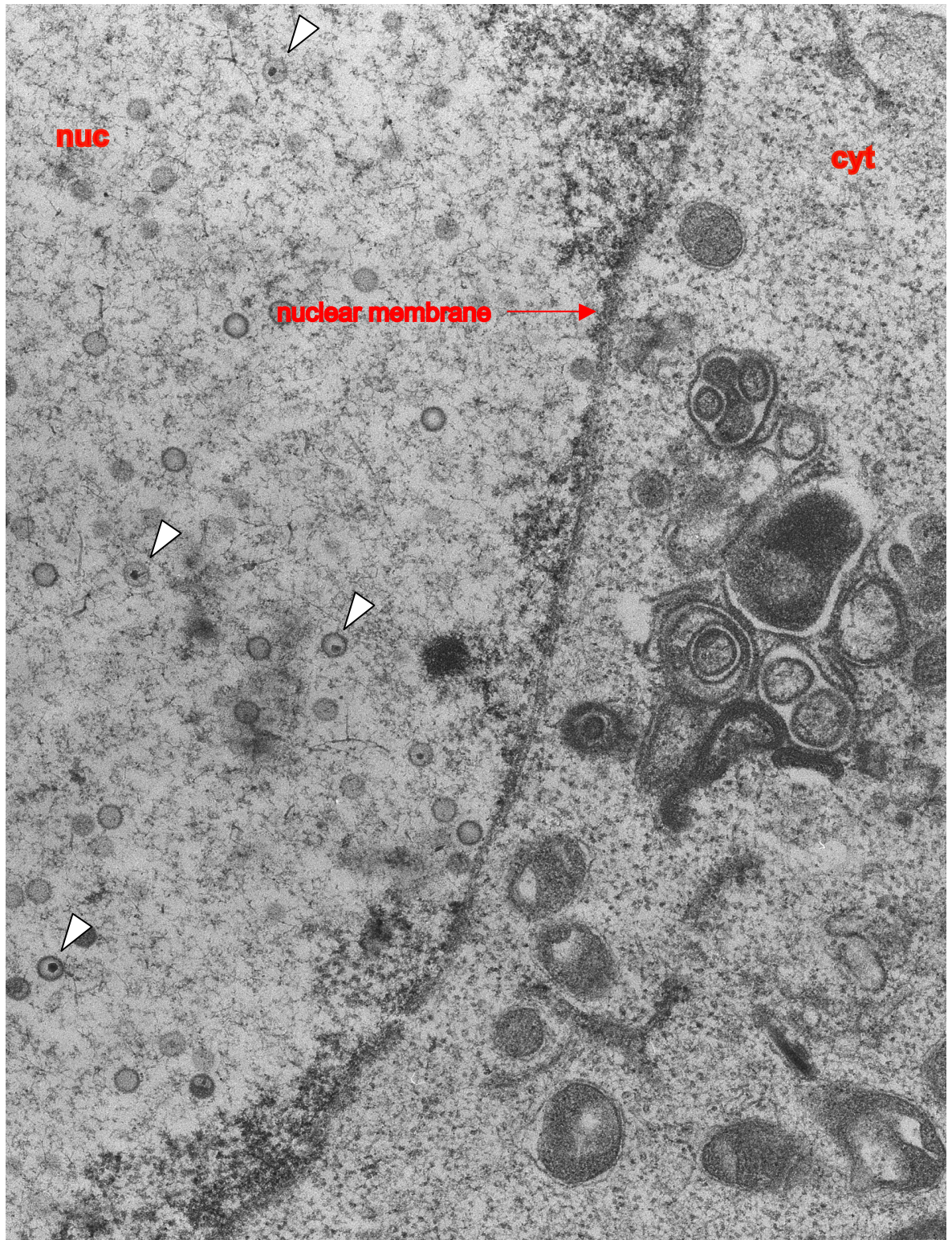


**Figure 6.1B Cells co-infected with  $\Delta$ UL25MO and AcpCI**

Monolayers of U2OS cells were co-infected with 2 PFU/cell  $\Delta$ UL25MO and 50 PFU/cell AcpCI. At 24 hpi cells were fixed and prepared for EM (Section 2.2.17.1). The nucleus (nuc), cytoplasm (cyt) and nuclear membrane are labelled. DNA-containing capsids (white arrowhead) were present in the nuclear compartment, but not the cytoplasm of infected cells.

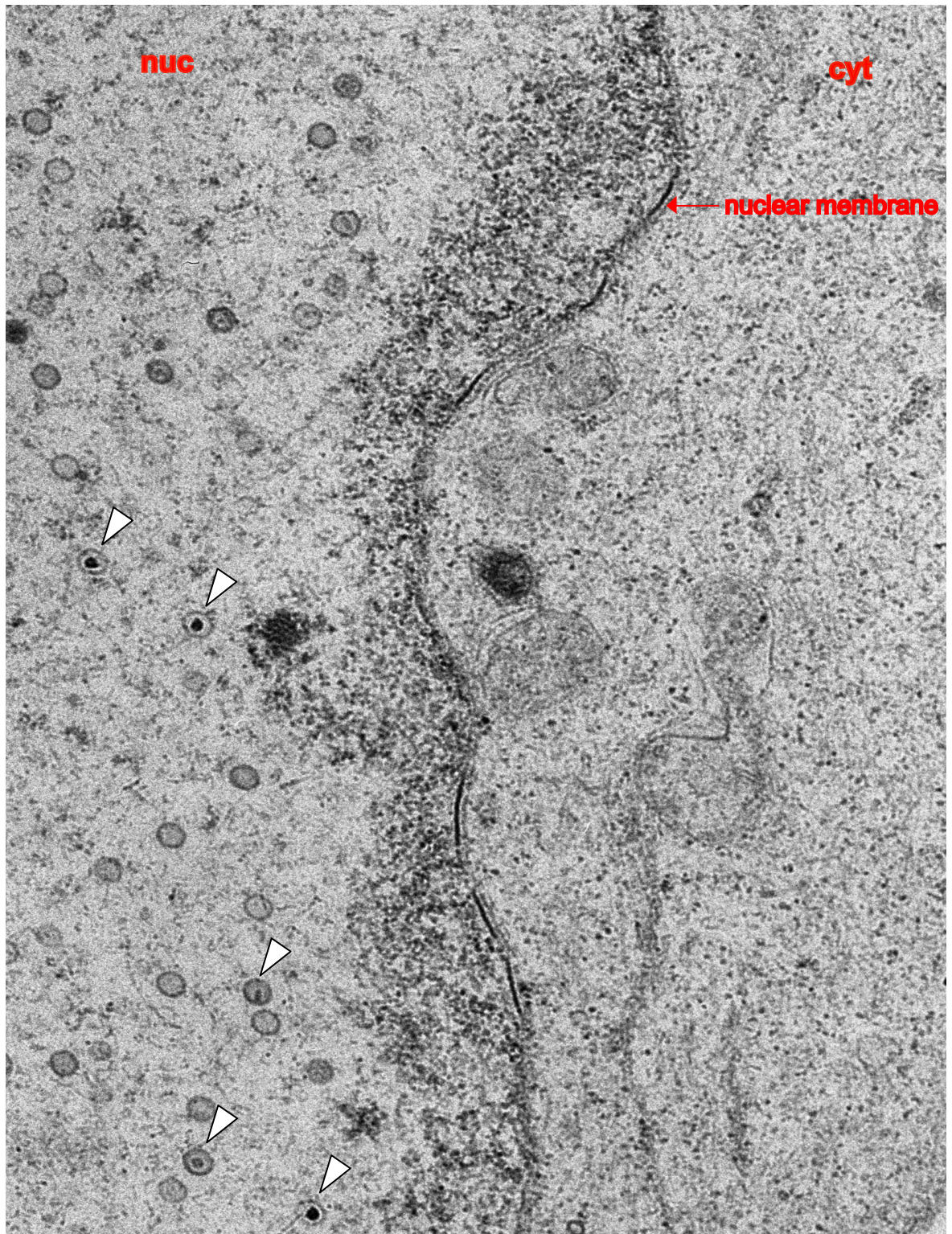


**Figure 6.1C Cells co-infected with  $\Delta$ UL25MO and AcUL25-C4A**

Monolayers of U2OS cells were co-infected with 2 PFU/cell  $\Delta$ UL25MO and 50 PFU/cell AcUL25-C4A. At 24 hpi cells were fixed and prepared for EM (Section 2.2.17.1). The nucleus (nuc), cytoplasm (cyt) and nuclear membrane are labelled. DNA-containing C-capsids (white arrowhead) were retained in the nucleus of infected cells.

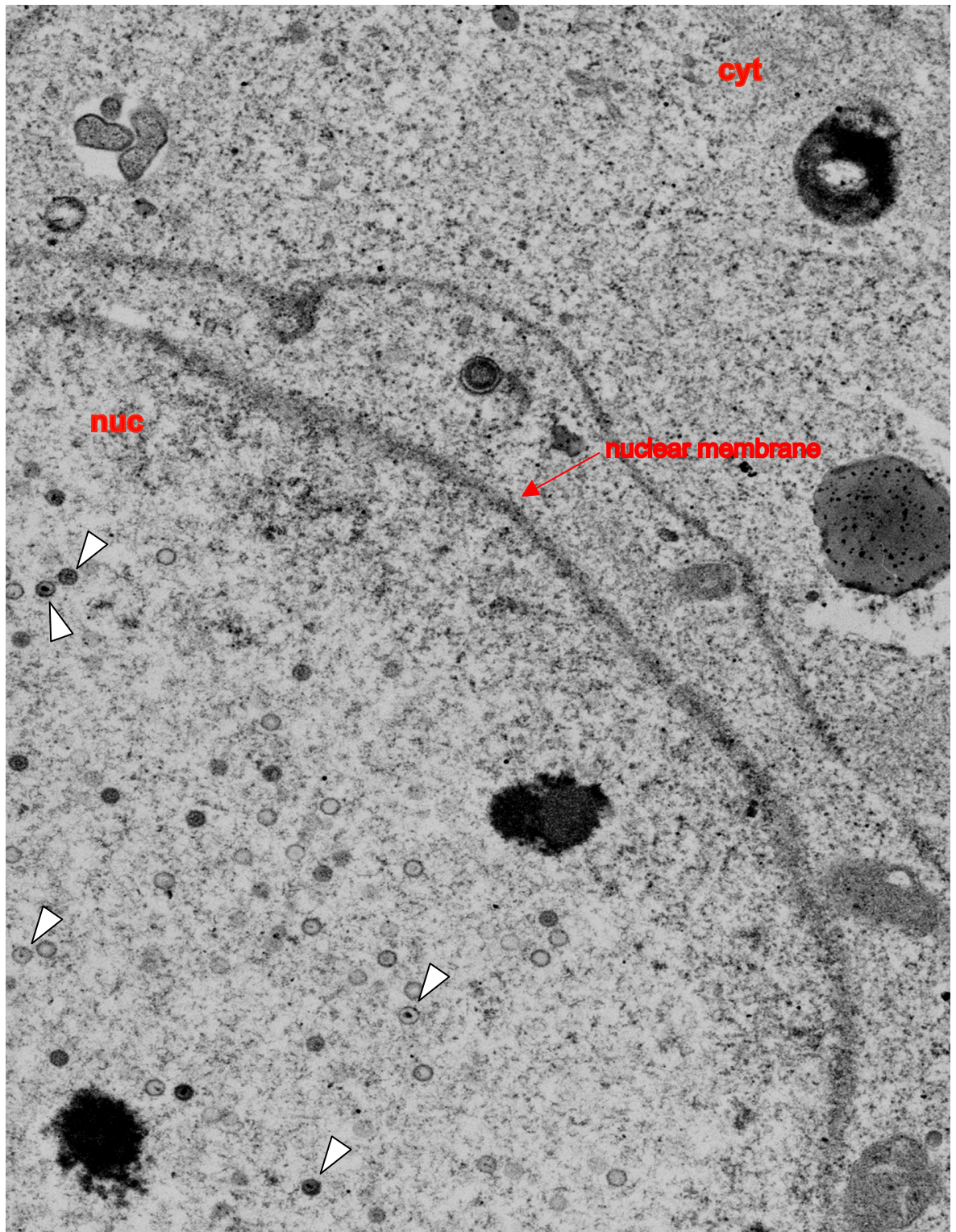


**Figure 6.1D Cells co-infected with  $\Delta$ UL25MO and AcUL25-L3**

Monolayers of U2OS cells were co-infected with 2 PFU/cell  $\Delta$ UL25MO and 50 PFU/cell AcUL25-L3. At 24 hpi cells were fixed and prepared for EM (Section 2.2.17.1). The nucleus (nuc), cytoplasm (cyt) and nuclear membrane are labelled. Free DNA-containing C-capsids (white arrowhead) were retained in the nucleus of infected cells.



**Figure 6.1E Cells co-infected with  $\Delta$ UL25MO and AcUL25-L6**

Monolayers of U2OS cells were co-infected with 2 PFU/cell  $\Delta$ UL25MO and 50 PFU/cell AcUL25-L6. At 24 hpi cells were fixed and prepared for EM (Section 2.2.17.1). The nucleus (nuc), cytoplasm (cyt) and nuclear membrane are labelled. DNA-containing C-capsids (white arrowhead) were present in the nuclear and cytoplasmic compartments of infected cells. Some cytoplasmic capsids surrounded by dense material (blue arrowhead), but not in vesicles, were also observed.

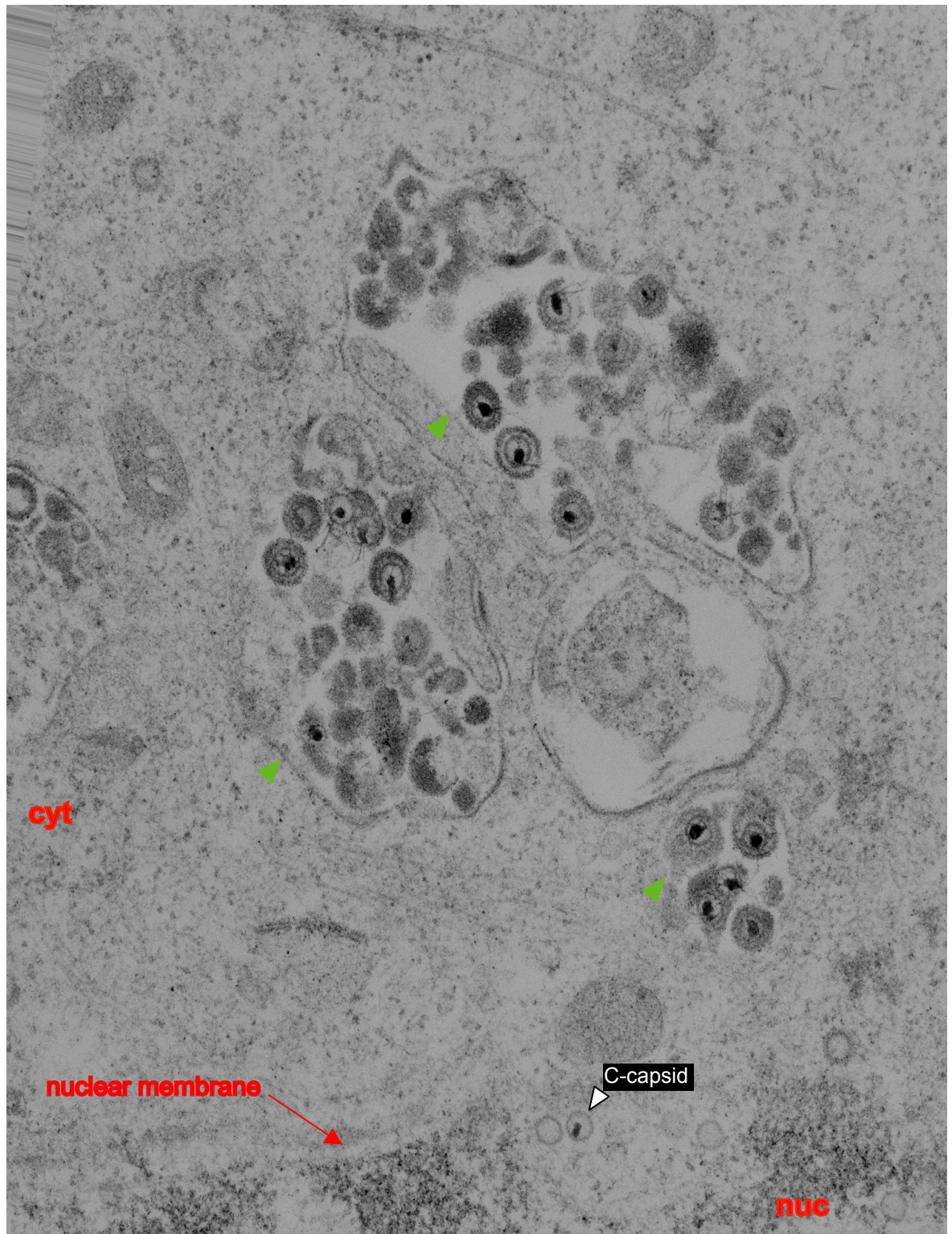


**Figure 6.1F Cells co-infected with  $\Delta$ UL25MO and AcUL25-L6**

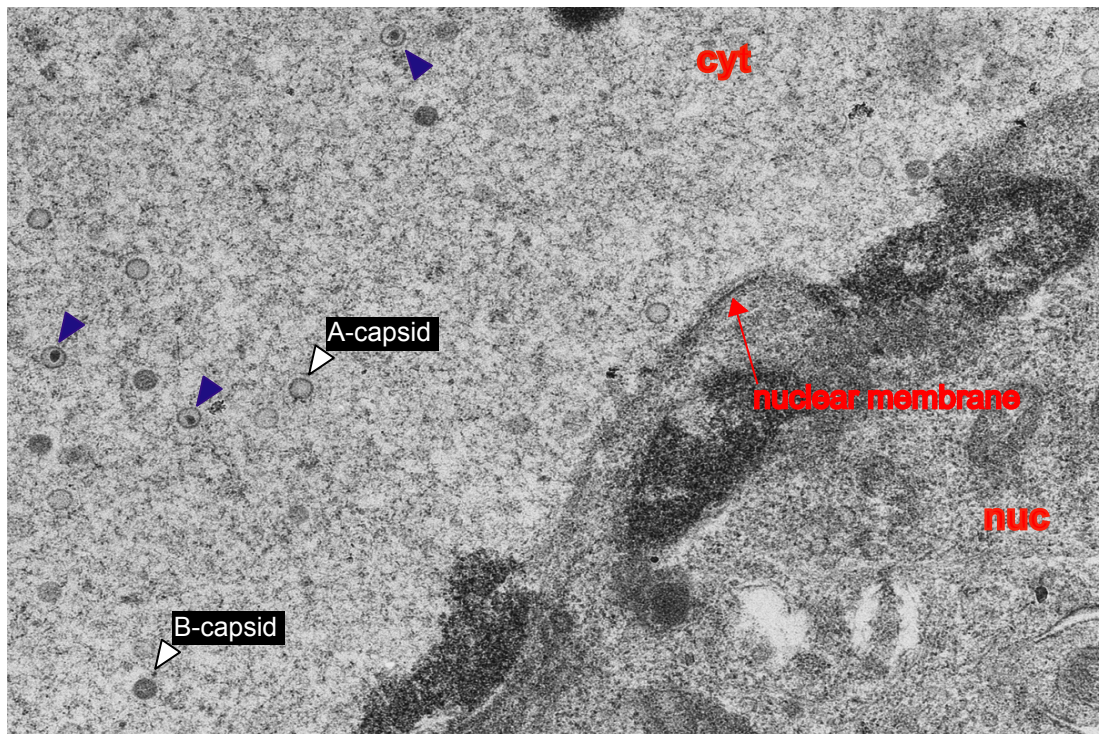
Monolayers of U2OS cells were co-infected with 2 PFU/cell  $\Delta$ UL25MO and 50 PFU/cell AcUL25-L6. At 24 hpi cells were fixed and prepared for EM (Section 2.2.17.1). The nucleus (nuc), cytoplasm (cyt) and nuclear membrane are labelled. The enveloped C-capsids located in vesicles in the cytoplasm are indicated by the green arrowheads and a C-capsid located in the nucleus is labelled.

cytoplasmic compartments of infected cells (Figure 6.1E). Interestingly, groups of cytoplasmic C-capsids in  $\Delta$ UL25MO-infected U2OS cells expressing pUL25-L6 or the wt protein were frequently found embedded in dense material (Figure 6.1E), a feature not observed in Vero or U2OS cells infected with wt HSV-1. In addition, enveloped virus particles were found in cytoplasmic vesicles in  $\Delta$ UL25MO-infected U2OS cells expressing wt pUL25 and to a lesser extent in the mutant-infected cells containing pUL25-L6. An image showing the enveloped C-capsids seen in  $\Delta$ UL25MO-infected cells expressing pUL25-L6 is shown in Figure 6.1F.

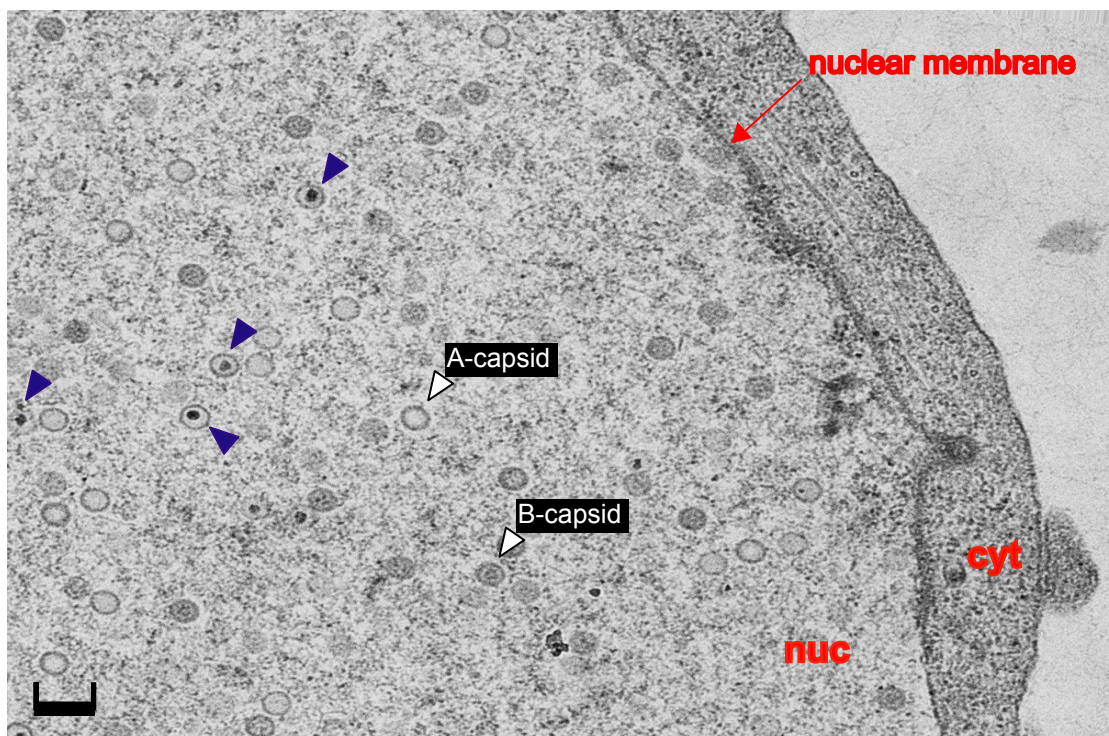
The finding that the nuclei of U2OS cells co-infected with  $\Delta$ UL25MO and AcpCI contained DNA-containing capsids, in addition to A- and B-capsids, was in contrast to earlier findings by McNab et al. (1998), who failed to detect DNA-containing capsids in the nuclei of UL25 null KUL25NS-infected Vero cells. The data from the packaging assays and the PFGE analysis described in this thesis confirmed that virus DNA was packaged in U2OS cells co-infected with  $\Delta$ UL25MO and AcpCI, although most of the encapsidated DNA was less than unit-length. In view of the different results obtained for the HSV-1 UL25 null mutants, the pattern of capsid assembly of  $\Delta$ UL25MO was compared with that of KUL25NS in Vero cells, together with wt HSV-1-infected Vero cells. As expected, C-capsids were detected in the nuclei and cytoplasm of wt virus-infected cells. However, in contrast to the previous results of McNab et al. (1998), DNA-containing capsids in addition to A- and B-capsids were detected in the cell nuclei of KUL25NS-infected Vero cells and in the nuclei of  $\Delta$ UL25MO-infected Vero cells (Figure 6.2). However, no cytoplasmic C-capsids were observed in cells infected with either mutant.

### **6.3 Fluorescent in-situ hybridisation (FISH) analysis**

To substantiate the conclusions from the EM data for the three post-packaging mutants, pUL25-L3, -L6 and -C4A, the distribution of the virus DNA in the infected U2OS cells was analysed using FISH (Section 2.2.17.2). U2OS cells were infected with  $\Delta$ UL25MO and the recombinant baculoviruses as described above and the cells were prepared for FISH analysis. FISH is a technique that detects and localises specific DNA sequences within the cell by using a fluorescent DNA



KUL25NS



$\Delta$ UL25MO

**Figure 6.2 Vero cells infected with KUL25NS or  $\Delta$ UL25MO**

Monolayers of Vero cells were infected with 2 PFU/cell KUL25NS (top) or  $\Delta$ UL25MO (bottom). At 24 hpi cells were fixed and prepared for EM (Section 2.2.17.1). The nucleus (nuc), cytoplasm (cyt) and nuclear membrane are labelled. The DNA containing capsids in the nucleus are indicated by the blue arrowheads and the A- and B-capsids are labelled. The size bar represents 250 nm.

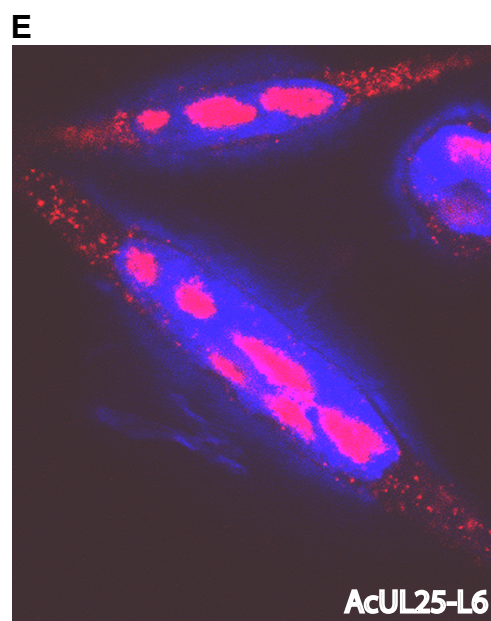
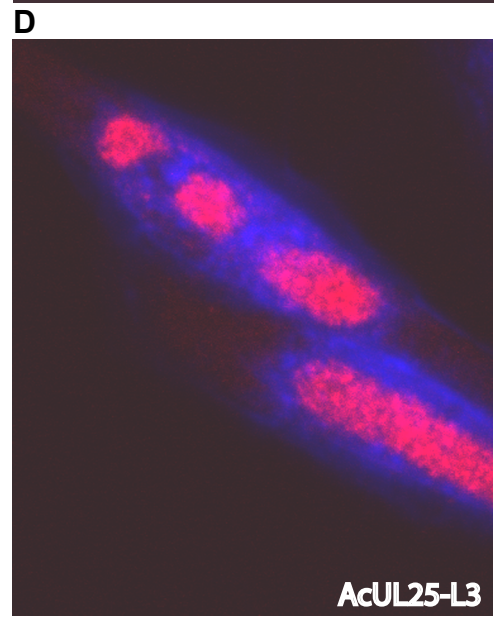
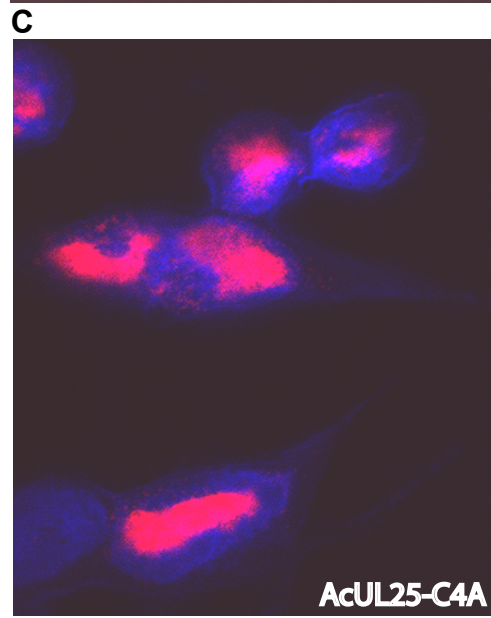
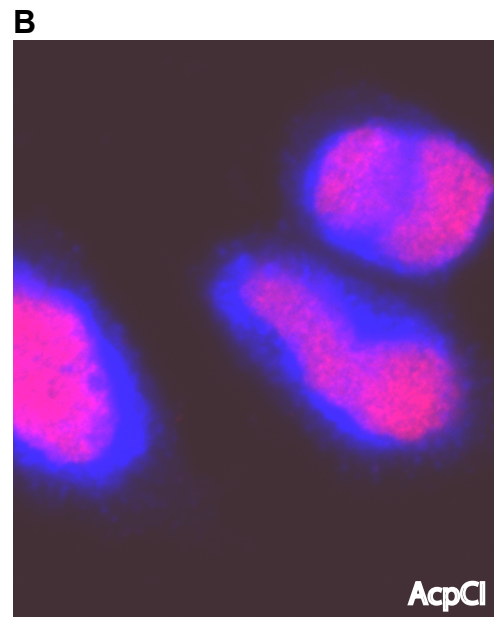
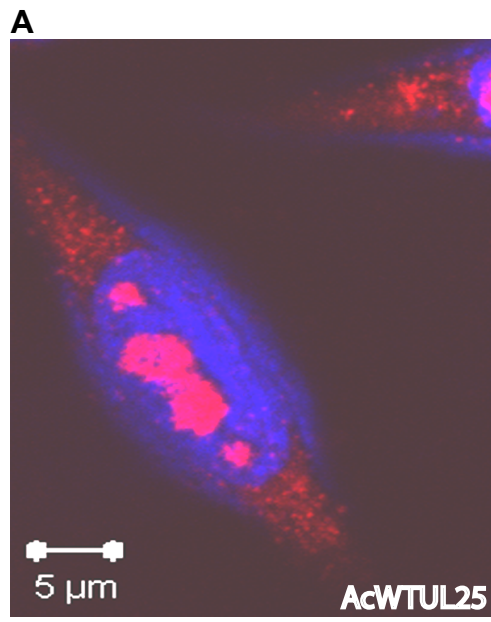
probe. The viral DNA probe used in this study consisted of HSV-1 sequences 79,442-115,152, which lie outwith the UL25 ORF, to eliminate the possibility of detecting baculovirus DNA containing the HSV-1 UL25 gene in the cells. To visualise the virus DNA, the HSV-1 DNA probe was labelled by nick translation with cy3-dCTP, and to highlight the cell nuclei the cells were counterstained with DAPI (4', 6'-diamidino-2-phenylindole) (Everett & Murray, 2005). A representative image obtained for each sample is shown in Figure 6.3. As expected, co-infection of cells with  $\Delta$ UL25MO and AcWTUL25 gave rise to fluorescently labelled virus DNA in both in the nuclear and cytoplasmic compartments of the cell (Figure 6.3A). In the negative control sample, where cells were co-infected with  $\Delta$ UL25MO and AcpCI, fluorescence from the labelled DNA was visible only in the nucleus as predicted (Figure 6.3B). In virus-infected cells expressing pUL25-L3 or pUL25-C4A the viral DNA was detected only in the nuclei, whereas in samples expressing pUL25-L6, viral DNA was observed in both the nuclear and cytoplasmic compartments of the infected cells (Figure 6.3C, D and E). These results support the data obtained from the electron microscopic study.

## 6.4 Discussion

DNA-containing capsids as well as A- and B-capsids were detected in the nuclei of both KUL25NS and  $\Delta$ UL25MO-infected Vero cells. The reason for the anomaly between the observations made by McNab et al. (1998) in KUL25NS-infected Vero cells and the results obtained during this study is unclear. However, the presence of DNA-containing capsids in the nuclei of HSV-1 UL25 null-infected cells is in agreement with a recent report on the pattern of virus assembly of another HSV-1 UL25 deletion mutant, HSV-1- $\Delta$ UL25. In the non-permissive rabbit kidney cell line RK13 infected with this mutant, numerous electron-dense DNA-containing capsids were seen in the nuclei but not the cytoplasm (Kuhn et al., 2008). In addition, DNA-containing capsids were also detected in the nuclei of cells infected with a BHV-1 UL25 null mutant and in the nuclei of cells infected with a PrV UL25 null mutant (Desloges & Simard, 2003, Klupp et al., 2006, Kuhn et al., 2008). The electron microscopic results on  $\Delta$ UL25MO and KUL25NS are also consistent with the data from the DNA packaging experiments presented in this thesis and earlier findings by Stow (2001), showing that in the absence of

### **Figure 6.3 Spread of viral DNA within the cell**

Monolayers of U2OS cells were co-infected with 2 PFU/cell UL25MO and 50 PFU/cell AcWTUL25 (A), AcpCI (B), AcUL25-C4A (C), AcUL25-L3 (D) or AcUL25-L6 (E). At 24 hpi cells were fixed and prepared for confocal microscopy (Section 2.2.17.2). The viral DNA was visualised by FISH using Cy3-labelled probe (orange) and the nuclei were stained with DAPI (blue).



pUL25 the cleaved HSV-1 DNA is encapsidated, although the packaged DNA is shorter than the full-length viral genomes.

In  $\Delta$ UL25MO-infected U2OS cells expressing the mutant proteins pUL25-L3, -L6 or -C4A, the UL25 null mutant acquired the capacity to encapsidate full-length viral DNA but failed to produce infectious virus particles. The EM and FISH data from  $\Delta$ UL25MO-infected cells expressing pUL25-C4A or pUL25-L3 demonstrate that the wt UL25 residues mutated in these proteins are essential for egress of mature C-capsids from the nuclear compartment during infection. In contrast, the three unstructured amino acids that were deleted in pUL25-L6 are critical for viral replication after nuclear egress and once the capsids have been released into the cytoplasm. These results indicate that pUL25 has at least two further distinct roles to play during virus assembly in addition to DNA-packaging.

Using Southern blot analysis Stow (2001) demonstrated that in non-permissive cells infected with KUL25NS less than unit-length DNA was stably packaged in the nuclear capsids and that these DNA-containing capsids were not translocated to the cytoplasm. These observations led to the suggestion that pUL25 is important during nuclear egress. However, a possible mechanism for the failure of the DNA-containing capsids to exit the nucleus in UL25 null-infected cells is that encapsidated full-length DNA may be necessary for the conformational changes required that allow more pUL17 and consequently pUL25 to bind, stabilising the structure and triggering primary envelopment. The results obtained in this study with  $\Delta$ UL25MO-infected U2OS cells expressing pUL25-C4A or pUL25-L3 revealed that after full-length DNA is packaged, pUL25 is required for egress of capsids from the nucleus.

In a non-permissive rabbit kidney cell line (RK13) infected with a PrV UL25 null mutant, although capsids failed to exit the nucleus, DNA-containing capsids were found in close association with the INM (Klupp et al., 2006). These results suggest that the lack of pUL25 does not affect the transport machinery required to relocate capsids to the site of primary envelopment at the INM, but does affect the ability of the capsids to bud into the INM. In contrast, in RK13 cells infected with the HSV-1 UL25 mutant, HSV-1- $\Delta$ UL25, DNA-containing capsids were dispersed throughout the nuclei and were not found frequently lining the INM (Kuhn et al., 2008). Similarly, in  $\Delta$ UL25MO-infected cells expressing either

pUL25, pUL25-C4A, -L3 or -L6, and in the negative control sample C-capsids were dispersed throughout the nuclear compartment and did not appear to be specifically associated with the INM during infection (Figure 6.1A-6.1E). In addition, since no capsids were observed in the perinuclear space this suggested that there was a defect during primary envelopment in virus-infected cells expressing pUL25-C4A or -L3. Therefore, it is not clear whether C-capsids trapped in the nuclei of virus-infected cells expressing either pUL25-C4A or pUL25-L3 were unable to be transported to the site of envelopment, or lacked the ability to interact with the proteins essential for primary envelopment, pUL31 and/or pUL34, or other viral or cellular proteins required during this process. As discussed in Chapter 4, the residues mutated in pUL25-C4A and pUL25-L3 lie in close proximity to one another, along a loop on the surface of UL25nt and illustrated in Figure 4.17. Since both regions lie in the same area of pUL25 and  $\Delta$ UL25MO has a similar phenotype in U2OS cells expressing either pUL25-C4A or pUL25-L3, it is conceivable that each mutated region disrupts the same functional interface of the protein. Potentially, one or more of the wt residues that were mutated in pUL25-C4A could be directly involved in the interactions that are required during primary envelopment. In contrast, the region that is deleted in pUL25-L3 may operate indirectly, by changing the conformation of the protein and blocking the ability of pUL25 to establish new interactions that are critical during egress. Since HSV-1-C4A and -L3 have recently been constructed in the lab, it would be interesting to determine whether these two mutant viruses complement, which would clarify if the C4 and L3 regions of pUL25 do indeed constitute a single interaction site.

In  $\Delta$ UL25MO-infected cells expressing pUL25-L6, some of the C-capsids located in the cytoplasm were surrounded with a dense material that may reflect the presence of tegument (Figure 6.1E). None of these capsids were enveloped and located inside vesicles, which would be expected following secondary envelopment. Since cytoplasmic C-capsids were often detected in clusters embedded in dense material, a feature that was not observed in wt HSV-1-infected Vero or U2OS cells or in U2OS cells co-infected with  $\Delta$ UL25MO and the negative control baculovirus, AcpCI, it is possible that some of the material associated with cytoplasmic C-capsids could be aggregates of pUL25. In U2OS cells the UL25 gene in the recombinant baculovirus is under the control of the

powerful HCMV IE promoter, therefore higher levels of pUL25 may be present in the U2OS cells than in wt virus-infected Vero cells. Although envelopment of C-capsids was observed in cells expressing pUL25-L6, there were fewer enveloped virus particles both inside the cell and on the cell surface than in  $\Delta$ UL25MO-infected U2OS cells expressing wt pUL25. Consistent with these observations, the mutant-infected cells expressing pUL25-L6 contained more angularised capsids in the cytoplasm than cells expressing the wt protein. Since the original complementation experiments had been performed in non-permissive  $\Delta$ UL25MO-infected Vero cells expressing pUL25-L6, the presence of enveloped particles in  $\Delta$ UL25MO-infected U2OS cells did raise some concern that pUL25-L6 may complement the growth of the mutant virus in these cells. However, subsequent complementation analysis confirmed that the defect in pUL25-L6 was also apparent in U2OS cells expressing the pUL25-L6 mutant protein (M. Murphy, personal communication). In addition, electron microscopic studies with a new mutant HSV-1-UL25-L6 virus that had been generated in our lab corroborated the findings with  $\Delta$ UL25MO-infected U2OS cells expressing the pUL25-L6 mutant protein (V. Preston, personal communication).

L6 is made up of three unstructured residues that are located directly at the C-terminus of pUL25, which may become structured during the correct protein-protein interaction. Interestingly, these last three residues of pUL25 (S578, A579 and V580) form a potential class I PDZ domain-binding motif. The sequence requirements for the different PDZ-binding motifs are outlined in Table 6.1. PDZ domains are modular protein interaction domains that are approximately 90 amino acids long, which bind the C-termini of target proteins in a sequence-specific manner. Their structural features allow them to mediate specific protein-protein interactions that underlie the assembly of large protein complexes involved in signalling and subcellular transport (Ham & Hendriks, 2003, Hung & Sheng, 2002). They are amongst the most common protein domains represented in sequenced genomes and have been recognised in numerous proteins from organisms as diverse as bacteria, plants, yeast, *Drosophila* and metazoans (Ponting, 1997). Interestingly, the three C-terminal residues from one of the head stabilising proteins of bacteriophage  $\lambda$ , gpW, which are thought to be unstructured, display sequence specificity for a Class II PDZ domain-binding motif and are critical for the protein's

PDZ Binding Motifs	
Class	C-terminal Sequence
Class I	X-S/T-X- $\phi$ -COOH
Class II	X- $\phi$ -X- $\phi$ -COOH
Class III	X-D/E-X- $\phi$ -COOH
Class I - UL25 loop 6	L-S-A-V-COOH

X = unspecified amino acid

$\phi$  = a hydrophobic amino acid

**Table 6.1 Classes of PDZ domain-binding motifs**

activity (Maxwell et al., 2000). The PROSITE bioinformatics program (<http://www.expasy.org/prosite/>) searches a given protein sequence for patterns that reflect protein domains, including PDZ domains. Since pUL25 contains sequences that form a PDZ domain-binding motif and evidence indicates that pUL36 interacts with pUL25 (Coller et al., 2007, Pasdeloup et al., 2009), PROSITE was used to search the protein sequences of HSV-1 strain 17 syn<sup>+</sup> pUL36, and pUL37 for PDZ domains. However, no potential PDZ domain sequences were found in either tegument protein.

Intriguingly, a sequence alignment of alphaherpesviruses pUL25 homologues showed that 75% contained potential Class I or II PDZ binding motifs at the C-terminus (Table 6.2). In addition, across the alpha-, beta- and gammaherpesviruses subfamilies, approximately 73% of the C-terminal sequences of the UL25 homologues analysed also contained either Class I or II potential PDZ binding motifs. The other L6 construct generated, pFB-UL25-L6sub, consisted of substitutions S579A and V580A that, together with A579, formed a potential Class II PDZ-binding motif at the C-terminus of UL25 (L-A-A-A-COOH). The mutant protein expressed by pFB-UL25-L6sub during complementation analysis retained the ability to support the growth of  $\Delta$ UL25MO, producing complementation yields of 80% in comparison to the wt positive control (Figure 4.14). Although the wt pUL25 contains a Class I PDZ binding motif there is evidence that single PDZ domains may recognise and bind to more than one class of PDZ binding motif (Ham & Hendriks, 2003, Sheng & Sala, 2001). However, a mutant pUL25 containing sequences that do not form a PDZ domain-binding motif at the C-terminal L6 region would need to be generated and analysed in order to clarify the relevance of such a motif during HSV-1 replication.

<b>Alphaherpesviruses</b>	<b>C-terminal sequence</b>	<b>PDZ binding motif</b>
HSV-1	L-S-A-V-COOH	Class I
HSV-2	L-S-V-A-COOH	Class I
HHV-3	A-S-T-P-COOH	-
SuHV-1	F-A-A-A-COOH	Class II
CeHV-1	L-S-A-A-COOH	Class I
CeHV-2	L-S-T-A-COOH	Class I
CeHV-9	T-S-V-A-COOH	Class I
CeHV-16	L-S-T-A-COOH	Class I
BoHV-1	T-S-A-V-COOH	Class I
BoHV-5	T-S-A-V-COOH	Class I
EHV-1	T-S-A-M-COOH	Class I
EHV-4	T-S-A-M-COOH	Class I
GaHV-1	Q-R-G-V-COOH	-
GaHV-2	I-S-T-L-COOH	Class I
MeHV-1	V-S-A-P-COOH	-
PsHV-1	V-T-I-A-COOH	Class I

**Table 6.2 Potential PDZ binding-domains at the C-terminus of alphaherpesvirus UL25 homologues**

## 7 Interaction of mutant pUL25s with the capsid-binding domain of pUL36

### 7.1 Introduction

The aim of the experiments described in this section was to determine the ability of the UL25 mutant proteins, pUL25-C4A, L3, -L5 and -L6 to interact with the CBD of HSV-1 pUL36 (pUL36cbd) identified by Collier et al. (2007). These workers showed that the carboxyl terminus of the UL36 tegument protein is functionally conserved in HSV-1 and PrV and is a capsid-binding domain. Using a mutant virus screen they found that pUL25 was essential for association of the pUL36cbd with nuclear capsids. The results from co-immunoprecipitation experiments confirmed that pUL25 interacted directly with the CBD and the full length pUL36 (Collier et al., 2007, Padeloup et al., 2009). To investigate whether any of the mutant UL25 proteins failed to interact with pUL36cbd, which consists of the 62 carboxyl-terminal residues of the tegument protein, a GST pull-down assay was set up. An outline of the GST-gene fusion system and the GST pull-down assay is described in Section 2.2.19.

#### 7.1.1 Construction of GST-UL36cbd expression plasmid

A DNA fragment specifying the HSV-1 pUL36cbd (amino acids 3104-3164) was cloned into the plasmid pGEX-2TNMCR in frame with the GST gene, enabling the GST tag to become fused to the N-terminal region of the expressed pUL36cbd (Everett et al., 1997). The DNA fragment encoding the pUL36cbd was generated by PCR using the HSV-1 cosmid Cos14, which contained the entire UL36 ORF, as a DNA template, and the primers 36cbd-F and 36cbd-R that incorporated the cloning sites *EcoRI* and *BamHI*, respectively, (Table 7.1) (Cunningham & Davison, 1993). In addition, an internal *NruI* site was introduced by silent mutagenesis into the nucleotide sequence of 36cbd-F. The 198 bp PCR fragment, which was amplified using the PCR-cycle1 (Section 2.2.1.2), was purified and ligated to pGEM-T Easy. The ligated DNA was electroporated into DH5 $\alpha$  and plasmid DNA was prepared from the isolates obtained. Since *NruI* does not digest pGEM-T Easy sequences, the recombinant pGEM-T Easy plasmids were identified by the

presence of the single *Nru*I site located in the sequences encoding pUL36cbd. DNA samples from these plasmids were sequenced using the M13 sequencing primers (Table 4.1), and one was identified that contained the desired PCR product. The HSV-1 insert was released from the pGEM-T Easy recombinant by digestion with *Eco*RI plus *Bam*HI, and the purified HSV-1 fragment was then ligated to the 4921 bp pGEX-2TNMCR *Eco*RI-*Bam*HI fragment. The ligated DNA was electroporated into electrocompetent DH5 $\alpha$  and plasmid DNA was prepared from the isolates obtained. Since *Nru*I does not cut pGEX-2TNMCR, only recombinant plasmid DNAs containing the HSV-1 insert (pGEX-UL36cbd) were linearised with *Nru*I. One plasmid isolate containing a single *Nru*I site was selected and used in protein expression experiments.

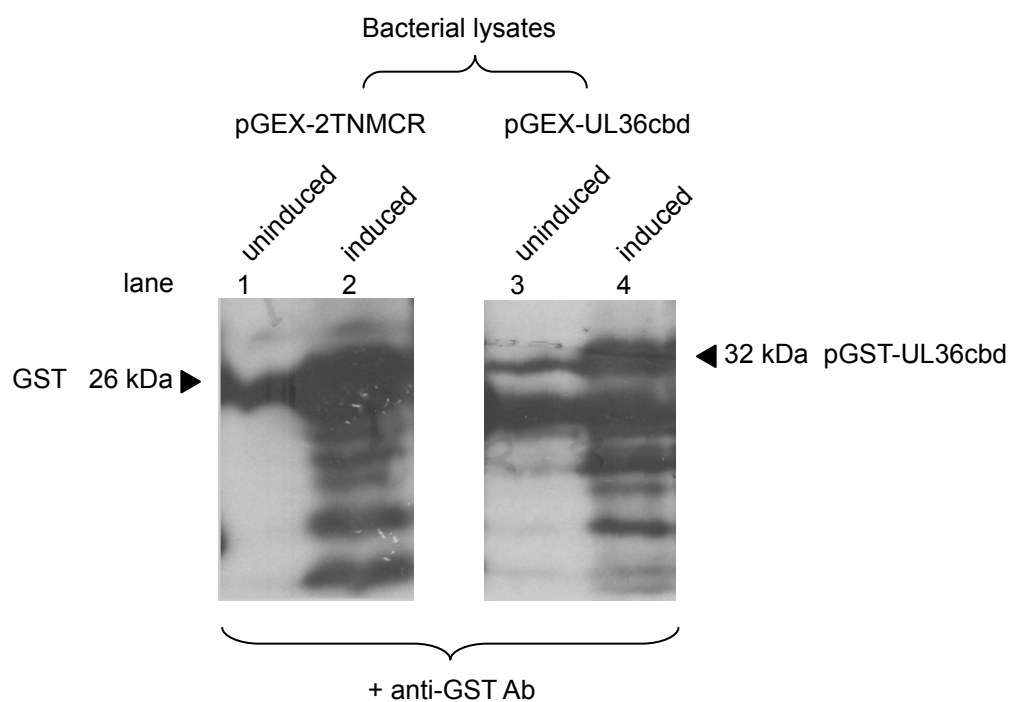
Primer ID	pUL36cbd Primers
36cbd-F	5'-TGGAATTC <sup><i>Eco</i>RI</sup> CGTATCGGCAAACGCAGTTCTGT <sup><i>Nru</i>I</sup> CGCGACGCTACGTGC-3'
36cbd-R	5'-TAGGATCC <sup><i>Bam</i>HI</sup> GCCCAGTAACATGCGCACGTGATGTAGGCTGGTCAGCACG-3'

Table 7.1 The primers used to generate the PCR fragment encoding pUL36cbd

### 7.1.2 GST pull-down assay

To express the desired proteins, electrocompetent *E. coli* BL21 were electroporated with either pGEX-UL36cbd, which encoded the GST tagged pUL36cbd, or pGEX-2TNMCR, which encoded the GST protein alone, as described in Section 2.2.19.1. Initially, the expression of GST and pGST-UL36cbd in the transformed *E. coli* BL21 cells was poor, but by increasing the IPTG concentration from 0.1mM to 0.2 mM and by extending the incubation period for IPTG induction from 2 h to 3 h at 37°C, both proteins were detected at levels sufficient for analysis (Figure 7.1).

The GST pull-down assays were carried out according to the method described in Section 2.2.19.3. Essentially, the soluble extracts containing bacterially expressed GST or pGST-UL36cbd (bait proteins) were mixed with Glutathione-Sepharose 4B beads. The GST protein bound beads served as a control to



**Figure 7.1 Expression of GST and pGST-UL36cbd in *E. coli***

Western blot analysis of *E. coli* BL21 lysates expressing GST (lanes 1 and 2) or pGST-UL36cbd (lanes 3 and 4). *E. coli* BL21 transformed with pGEX2TNMCR or pGEX-UL36cbd were grown at 37°C to an O.D of 0.4-0.6 and either harvested (uninduced samples) or treated with 0.2mM IPTG for 3 h at 37°C (induced samples). Bacterial lysates were prepared, the proteins were separated by SDS-PAGE and analysed by Western blotting using anti-GST antibody. The arrow head indicates the protein band that corresponds to the predicted size of GST (26 kDa) in lane 2 or pGST-UL36cbd (32 kDa) in lane 4.

confirm that there was no non-specific binding of the target protein lysates to the GST tag during the assay. The beads with the bound bait proteins were concentrated and washed extensively to remove any non-specifically bound proteins. Duplicate samples of pre-cleared baculovirus-infected Sf21 cell lysates, containing expressed wt pUL25, pUL25-C4A, -L3, -L5, or -L6, were subsequently mixed with the GST or the pGST-UL36cbd charged beads. A negative control lysate sample, derived from AcpCI-infected Sf21 cells, was included. After the samples had been incubated at 4°C for 1.5 h, the beads were washed extensively. The proteins were eluted from the beads, separated by SDS-PAGE and analysed by Western blotting, using anti-GST antibody or anti-pUL25 MAb166 as primary antibodies followed by secondary anti-goat hrp-conjugated antibody and anti-mouse hrp-conjugated antibody, respectively. Since the detergent concentration and the concentration of fusion and target proteins applied can affect the proteins pulled down during the assay, these conditions were optimised prior to experimental analysis. Aliquots of the baculovirus-infected cell extracts were mixed with Glutathione-Sepharose beads, the beads were removed and the extracts were analysed by SDS-PAGE to estimate the amount of pUL25 present in each of the extracts so that equivalent concentrations of each target protein could be used in the assay (data not shown). Similarly, aliquots of the bacterial extracts were mixed with Glutathione-Sepharose beads, the beads were washed and the eluted proteins were analysed by SDS-PAGE to determine the amount of bait protein in the extract.

A control experiment was performed to ensure that the expressed wt pUL25 specifically bound to pGST-UL36cbd beads and not to GST charged glutathione beads. AcWTUL25-infected and AcpCI-infected Sf21 protein samples were each incubated with beads charged with GST or pGST-UL36cbd, and the results of the protein interaction assays are shown in Figure 7.2. The appropriate bait protein was detected in all samples (Figure 7.2 blot A, lanes 1-4). In the GST pull-down assay using target protein samples with, or without, pUL25, no pUL25 band was detected in the protein blot probed with anti-pUL25 MAb166 (Figure 7.2 blot B, lanes 2 and 4), confirming that pUL25 did not bind to GST. Similarly, in a pGST-UL36cbd pull-down assay using target protein samples with no pUL25 probed with MAb166, no band of the expected size of pUL25 was observed in the blot

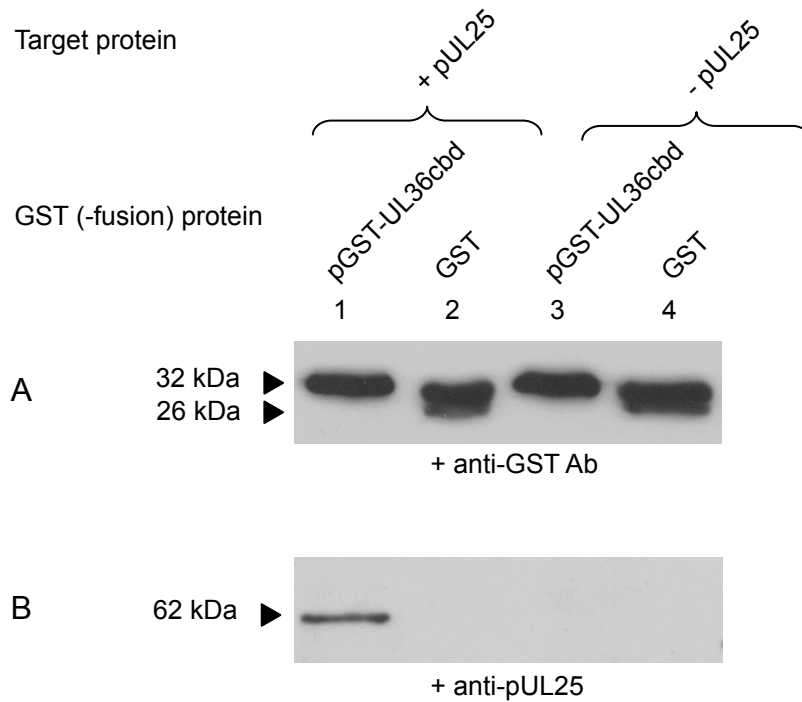


**Figure 7.2 GST pull-down assay to determine the specificity of binding of wt pUL25 to pGST-UL36cbd**

The GST pull-down assay was carried out according the method described in Section 2.2.19.3. AcWTUL25-infected U2OS cell extracts containing wt pUL25 (lanes 1 and 2) and AcpCI-infected U2OS cell extracts (lanes 3 and 4) were incubated with Glutathione beads charged with pGST-UL36cbd (lanes 1 and 3) or GST (lanes 2 and 4). The beads were washed and the co-precipitated proteins were analysed by SDS-PAGE followed by Western blotting. Blot A was stained with anti-GST antibody at a concentration of 1:2000 followed by the secondary anti-goat hrp-conjugated antibody diluted at 1:80,000. Blot B was stained with anti-pUL25 MAb166 at a concentration of 1:1000 followed by secondary anti-mouse hrp-conjugated antibody diluted at 1:1000.

(Figure 7.2 blot B, lane 3). However, a protein with a molecular weight of approximately 62 KDa was present when the AcWTUL25-infected cell sample was used in a pGST-UL36cbd pull assay (Figure 7.2 blot B, lane 1), confirming that the CBD of pUL36 interacted with wt pUL25.

The results of the GST pull-down assay to determine whether pGST-UL36cbd formed stable interactions with the target mutant proteins, pUL25-C4A, -L3, -L5 or -L6, are shown in Figure 7.3. The pGST-UL36cbd was detected in the pGST-UL36cbd pull-down assay protein samples eluted from the beads and analysed by Western blotting using anti-GST antibody, confirming the presence of the fusion protein (Figure 7.3 blot A). Similarly, the GST protein was present in GST pull-down assay protein samples eluted from the beads (Figure 7.3 blot B). To determine the ability of the mutant UL25 proteins to form stable interactions with the GST fusion protein, duplicate pGST-UL36cbd and GST pull-down protein samples eluted from the beads were separated by SDS PAGE, and analysed by Western blotting using anti-pUL25 MAb166 antibody. As expected, in the pGST-UL36cbd pull-down assay a band of the predicted size for pUL25 (62 KDa) was present in the wt pUL25 protein extract but not in the negative control extract lacking pUL25, confirming that the UL25 MAb166 reacted specifically with pUL25 (Figure 7.3 blot C, lanes 1 and 2). In addition, a band of approximately 62 KDa was also detected in each of the mutant protein extracts eluted from the beads in the pGST-UL36cbd pull-down assay (Figure 7.3 blot C, lanes 3-6). No protein bands of the size of pUL25, however, were observed in the GST blot. The results indicate that wt and mutant UL25 proteins formed stable interactions with pGST-UL36cbd.

## 7.2 Discussion

The data presented here indicate that the mutations present in pUL25-C4A, -L3, -L5 and -L6 do not disrupt the interaction of UL25 with the CBD of pUL36. Although the GST pull-down assay is an important instrument for determining protein interactions, the results have to be interpreted carefully. The presence of the GST tag may alter the conformation of the fusion protein in a manner that exposes or conceals potential interaction sites. In addition, the amounts of fusion and target protein applied in the assay may not reflect physiological

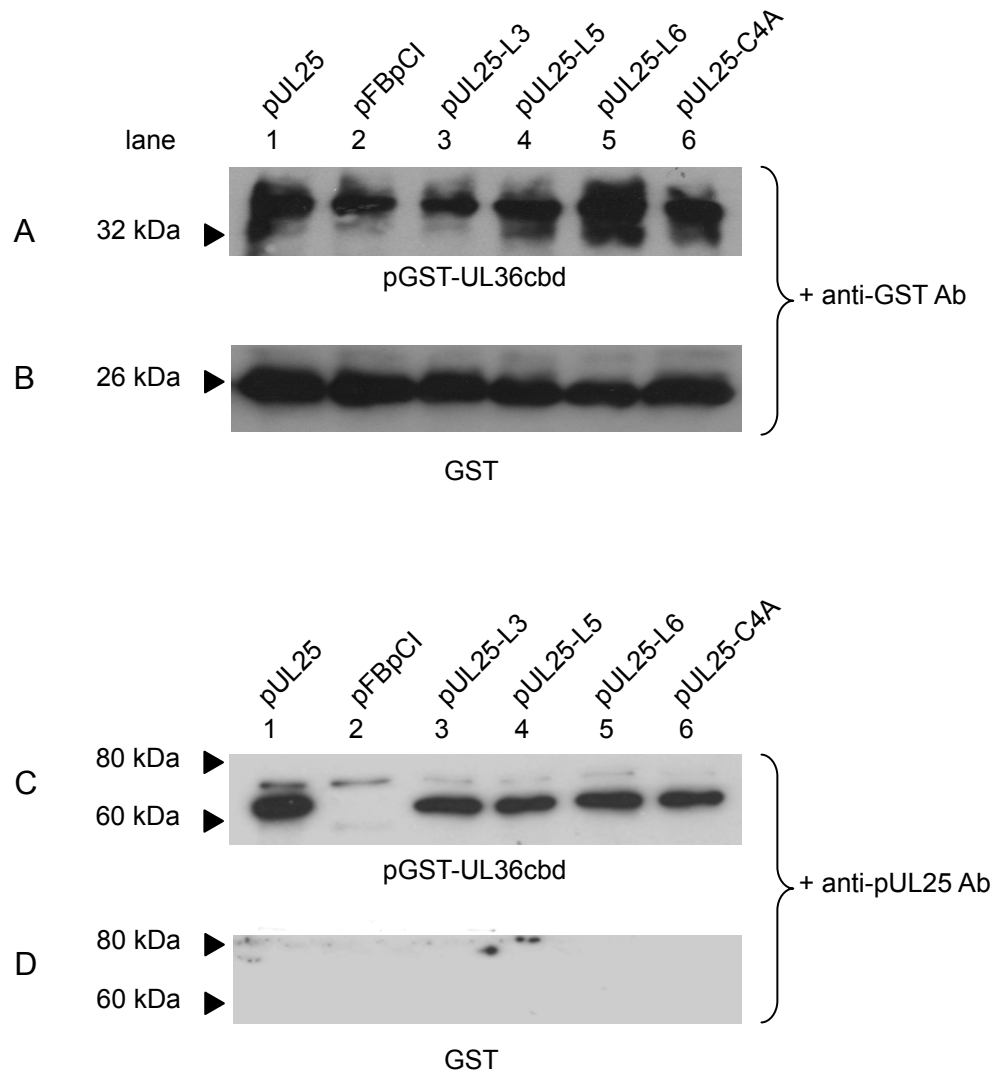


**Figure 7.3 GST pull-down assay to determine the interaction of pUL25-L3, -L5, -L6 and -C4A with pGST-UL36cbd**

The GST pull-down assay was carried out according to the method described in Section 2.2.19.3. Pre-cleared baculovirus-infected U2OS cell extracts containing either wt pUL25, no pUL25, pUL25-L3, -L5, -L6 or -C4A (lanes 1, 2, 3, 4, 5 or 6, respectively in blots A, B, C or D) were incubated with Glutathione beads charged with pGST-UL36cbd (blots A and C) or GST (blots B and D). The beads were washed and the co-precipitated proteins were analysed by SDS-PAGE followed by Western blotting. Blots A and B were incubated with anti-GST antibody and blots C and D were incubated with anti-pUL25 MAb166 and subsequently with secondary hrp-conjugated antibody as described in Figure 7.2.

concentrations of the proteins found *in vivo*. Both of these factors may produce aberrant results that lead to incorrect conclusions about the absence or presence of an interaction.

The wt residues mutated in pUL25-L5 are essential during packaging of full-length viral DNA (Section 5.3). Perhaps it is not surprising that pUL25-L5 and pUL36cbd interact, since the pUL25-L5 mutation would be predicted to affect a functional interface that interacts with the capsid. The presence of pUL25 on capsids is required for efficient binding of the pUL36cbd onto capsids (Coller et al 2007), therefore, the pUL25 functional interface involved in capsid interactions and pUL36cbd-binding may be distinct. The packaging assays performed during this study identified three distinct regions essential for encapsidation, the N-terminal portion of UL25 (residues 1-45), C3B and L5 (Section 5.3). Recent work has demonstrated that the N-terminal portion of pUL25, amino acids 1-50, contains a capsid-binding domain (Cockrell et al., 2009). In addition, the CCSC identified on C-capsids using cryo-electron microscopy and image reconstruction techniques was predicted to be a complex of pUL25 and pUL17, with additional contact points for pUL25 calculated to be on the triplexes and hexons (Trus et al., 2007). Since pUL25 has been shown to interact directly with all three proteins, it is possible that the protein incorporates more than one capsid-binding interface, one of which could be associated with the L5 region (Ogasawara et al., 2001; Thurlow et al., 2006). Clearly, characterisation of a mutant HSV-1 expressing pUL25-L5 would resolve this.

The post-packaging mutants pUL25-C4A, -L3 and -L6 would be expected to bind to capsids during encapsidation, since  $\Delta$ UL25MO-infected cells expressing these proteins produced mature C-capsids (Section 5.3). The wt residues mutated in pUL25-C4A and pUL25-L3 are essential for nuclear egress of C-capsids, while the pUL25-L6 mutation disrupts viral replication once the C-capsids have been released into the cytoplasm (Section 6.2). Although each of these post-packaging UL25 mutant proteins still interacted with pUL36cbd during the GST pull-down assay, an alternative pUL25 binding domain (pUL25 BD II) has recently been identified in HSV-1 pUL36 between residues 2037-2353 (Pasdeloup et al., 2009). In addition, the N-terminal portion of the protein has been reported to associate with capsids in virus-infected cells (Roberts et al., 2009). It is possible

that either pUL25-C4A, -L3 or -L6 failed to bind to pUL36 at an alternative site. Certainly, the EM observations suggested that secondary envelopment was disrupted in  $\Delta$ UL25MO-infected cells expressing pUL25-L6, since fewer enveloped viral particles were seen in the cytoplasm of these cells (Section 6.2), which may indicate a disruption during the earlier stage of tegumentation.

## 8 General Discussion

The overall aim of the work carried out in this thesis was to relate the function of pUL25 to the 3D structural information available for the protein. Fourteen UL25 constructs were generated and a total of 17 UL25 mutant proteins were characterised to determine the effect of the mutations on the function of pUL25 (Table 4.2). The results of this study are summarised in Table 8.1 and show that there were three different classes of pUL25 mutants that failed to complement the growth of the UL25 null mutant  $\Delta$ UL25MO. One category of mutant had lesions that affected the role of pUL25 during DNA packaging, whereas the mutants in the two other groups had no effect on the DNA packaging function of the protein. Interestingly, the post-packaging mutants disrupted a pUL25 function required either for the exit of C-capsids from infected nuclei or during virus assembly after C-capsids were released into the cytoplasm. The two novel phenotypes displayed by  $\Delta$ UL25MO in non-permissive cells expressing the post-packaging mutant proteins demonstrates for the first time that pUL25 is not only important for DNA encapsidation but also has essential roles at later stages of virus maturation.

Three regions of pUL25, C3, L5 and the N-terminal domain from residues 1-45, were identified as critical for the encapsidation of full-length viral genomes. The UL25 encoded gene product is predicted to stabilise the maturing capsid by attaching to binding sites that become available during DNA packaging, and recent work by Trus et al. (2007) suggested that pUL25 attaches to C-capsids by interacting with different proteins, VP5 present in the peripentonal hexon, the triplex subunit, Ta, and pUL17. Studies using mutant viruses or immunological assays have provided further evidence that pUL25 interacts with VP5, VP19C and pUL17 (Newcomb et al., 2006, Ogasawara et al., 2001, Padeloup et al., 2009, Thurlow et al., 2006). While additional work is necessary to confirm that C3, L5 and the N-terminal domain represent distinct functional interfaces, it is possible that the three regions identified here represent each of the potential UL25 capsid-binding sites proposed by Trus et al. (2007). Indeed, Cockrell et al. (2009) recently confirmed that the N-terminal portion of UL25 (residues 1-50) constitutes a capsid-binding domain. To determine if any of the mutant UL25 proteins disrupted the interaction with wt pUL17, the proteins were expressed in

UL25 protein	Complement $\Delta$ UL25MO	Full-length DNA Packaging	Virus location (EM)	Viral DNA location (FISH)	Interaction with UL36 CBD
pUL25	+	+	cytoplasm	cytoplasm	+
pUL25-C1	+				
pUL25-C2	+				
pUL25-C3A	+				
pUL25-C3B	+				
pUL25-C4A	-	+	nucleus	nucleus	+
pUL25-C4B	-				
pUL25-L6sub	+				
pUL25-L1	+				
pUL25-L2	+				
pUL25-L3	-	+	nucleus	nucleus	+
pUL25-L4	+				
pUL25-L5	-	-			+
pUL25-L6	-	+	cytoplasm	cytoplasm	+
pUL25 $\Delta$ 1-45	-	-			
pUL25 $\Delta$ 1-59	-	-			
pUL25 $\Delta$ 1-133	-	-			
pUL25-C1L2	+				

**Table 8.1 Summary of the characteristics of the UL25 proteins**

U2OS cells co-infected with AcWTUL25 or individual mutant AcUL25 recombinant baculoviruses and AcUL17 or were singly infected with each virus and immunoprecipitation assays were performed. Although acceptable amounts of the wt and mutant UL25 proteins were generated by the recombinant baculovirus in these cells, the levels of pUL17 expressed were substantially less than those of pUL25 and an interaction between the two wt proteins could not be demonstrated with UL17 MAb (data not shown). It was unclear why the levels of pUL17 under the control of the HCMV IE promoter were low, although this was a reproducible finding. Unfortunately, there was insufficient time to investigate this further and complete the experiments. Mutant HSV-1 viruses encoding the C3B or L5 mutant proteins are currently being constructed in the laboratory. The availability of these mutant viruses will allow the levels of mutant pUL25 present on purified capsids from mutant virus-infected cells to be compared with purified wt B-capsids and help to determine if the mutant pUL25s bind to capsids. In addition, immunoprecipitation assays can be carried out on the mutant virus-infected cells to establish whether the mutant pUL25s interact with pUL17.

Recent immunoprecipitation experiments have shown that pUL25 binds to pUL6, which is the structural unit that comprises the dodecameric portal and where the viral DNA is inserted during packaging (Pasdeloup et al., 2009). Although pUL25 has been demonstrated to lie adjacent to the pentons, its association with pUL6 indicates that protein may also be located at the unique vertex occupied by the portal, which is consistent with pUL25's function during DNA packaging (Newcomb et al., 2006, Pasdeloup et al., 2009). In addition to its predicted indirect role of stabilising the maturing capsid during DNA packaging, pUL25 may also bind directly with packaging machinery at the portal to ensure full-length viral genomes are encapsidated. It is therefore possible that C3, L5, the N-terminal region of pUL25, or a combination of these regions, is required for the interaction of the protein with pUL6.

Although the UL25 mutant ts1249 has an uncoating defect at the NPT, the mutant also displays a packaging defect if ts1249-infected cells are grown at the PT to allow uncoating of the viral genome prior to incubation at the NPT. The ts1249 phenotype is the result of the replacement of the negatively charged glutamic acid at position 233 in pUL25 with a positively charged lysine residue.

To determine if this mutation was structurally linked to the functional interfaces C3 and L5 involved in DNA packaging or to any of the other predicted functional clusters or unstructured portions of UL25, the ts1249 E233K mutation was located with respect to these regions on the UL25nt crystal structure using the Chimera structural imaging program (<http://www.cgl.ucsf.edu/chimera>). The glutamic acid residue, which is highly conserved among the alphaherpesvirus UL25 homologues, was found on the surface of pUL25 near a looped out region that is distinct from L1-L5. Since the glutamic acid residue does not lie close to any of the clusters identified by Bowman et al. (2006), it is unlikely that the ts1249 mutation affects the same functional interface as the ones identified here.

The residues mutated in pUL25-C4A and -L3 disrupted the function required for nuclear egress of C-capsids when the proteins were expressed in  $\Delta$ UL25MO-infected cells. As discussed in Chapter 6, the mutated regions of C4 and L3 may fail to interact with the transport machinery required to move C-capsids to the site of primary envelopment or affect the ability of the capsids to bud into the INM. The obvious binding partners for pUL25 at this point during virus assembly are the proteins that are essential during primary envelopment, pUL31 and pUL34. However, it is possible that other viral or cellular protein partners are required by pUL25 at this stage of the HSV-1 growth cycle, with a prime candidate viral protein being pUL36, although the point at which pUL36 associates with the capsid is controversial. Collier et al. (2007) showed that the transiently expressed pUL36cbd-GFP fusion protein bound to capsids in the nuclei of virus-infected cells. The small size of the CBD (62 amino acids), however, enabled the fusion protein to passively diffuse through nuclear pores. Whether full-length pUL36 enters the nucleus and binds to nuclear capsids during infection is debatable. In three separate studies it was reported that pUL36 was excluded from the nucleus, present in reduced levels in the nucleus relative to the cytoplasm, or evenly distributed throughout the nucleus and the cytoplasm (Klupp et al., 2002, Klupp et al., 2006, McNab & Courtney, 1992). Experiments using cell fractionation and capsid purification suggested that full-length HSV-1 pUL36 was associated with intranuclear HSV-1 capsids (Bucks et al., 2007). However, a subsequent study reported that no large proteins indicative of pUL36 were detected in preparations of purified nuclear HSV-1 capsids (Trus et al.,

2007). The idea that pUL36 attaches to capsids in the cytoplasm is supported by observations using UL36 null mutants. Ultrastructural analysis of non-permissive cells infected with an HSV-1 pUL36 deletion mutant, K $\Delta$ UL36, revealed an accumulation of unenveloped nucleocapsids in the cytoplasm, with no obvious defects in DNA packaging or nuclear egress (Desai, 2000). In addition, a similar phenotype has been described for the PrV pUL36 deletion mutant PrV- $\Delta$ UL36F (Fuchs et al., 2004). Consistent with these findings, a recent study demonstrated that removal of the entire HSV-1 UL36 ORF did not prevent efficient egress of capsids from the nucleus (Roberts et al., 2009). Electron microscopic analysis of UL36 null mutant AR $\Delta$ UL36-infected U2OS cells confirmed that this mutant had the same phenotype in these cells as reported previously (data not shown) (Roberts et al., 2009). Therefore, in the light of the phenotype displayed by the UL36 null mutants, it is unlikely that expression of the mutant C4 or L3 proteins in  $\Delta$ UL25MO-infected cells affects pUL25's interaction with pUL36 in the nucleus and at a stage that would influence nuclear egress of C-capsids. This conclusion is supported by the results of an interaction assay using the pGST-UL36cbd fusion protein showing that these two UL25 mutant proteins retained the capacity to interact with the C-terminal end of pUL36.

An alternative explanation for the phenotypes observed in  $\Delta$ UL25MO-infected cells expressing C4 and L3 mutant proteins, is that there may be additional capsid-binding sites for pUL25 that are distinct from those required during DNA packaging. Consistent with this idea is the suggestion by Trus et al. (2007) that there is a 'hidden' population of pUL25 present on C-capsids, in addition to the pUL25 associated with CCSC at the pentons. It is possible that binding of this alternative UL25 protein population to C-capsids, for example at the portal, triggers the appropriate exit machinery necessary for the mature capsids to leave the nucleus. Since HSV-1-UL25-C4A and -L3 mutants have subsequently been generated, it is now feasible to determine the amounts of pUL25 present on the C-capsids purified from mutant virus-infected cells in comparison to the level of the protein on C-capsids from wt HSV-1 infected cells.

Characterisation of pUL26-L6, which is the sole member of the third class of pUL25 mutants, led to the identification of unstructured wt residues that are essential for virus assembly following nuclear egress of C-capsids. In thin

sections of  $\Delta$ UL25MO-infected cells expressing pUL25-L6 examined under the electron microscope, more naked capsids were seen in the cytoplasm and fewer enveloped virus particles were observed in comparison to mutant-infected cells expressing the wt pUL25. These results suggest that the wt residues mutated in L6 are important for virus assembly at some point between tegumentation and secondary envelopment. One possibility is that the unstructured residues in the L6 region of pUL25 may be required for the interaction of pUL25 with pUL36. However, the results of a GST pull-down assay using the fusion protein pGST-UL36cbd indicated that the pUL25-L6 mutant protein interacted with the C-terminal end of pUL36 (Chapter 7). Since there is another pUL25 binding site available on pUL36 (BD II), it is possible that the L6 protein fails to bind to this site or potentially a third site at the N-terminus (Pasdeloup et al., 2009, Roberts et al., 2009). If this were the case, it would suggest that the large UL36 tegument protein (335.8 KDa) requires more than one attachment site in order for it to function properly. As a consequence of this partial binding of the pUL36 to capsids, reduced amounts of the protein may be present on the capsid or pUL36 may be incorrectly folded on the capsid. This in turn could lead to a reduced number of enveloped virus particles as a result of slower transport of capsids to the site of secondary envelopment in comparison to  $\Delta$ UL25MO-infected cells expressing wt pUL25, and/or inefficient envelopment (Desai, 2000, Fuchs et al., 2002a). Further studies of the interactions of the other pUL25 binding domains of pUL36, BD II and the predicted domain at the N-terminus, with the packaging competent mutant proteins (pUL25-C4A, -L3 and -L6) identified here may help to clarify when and where pUL36 attaches to the capsid in infected cells, and whether these mutant proteins have impaired interaction with pUL36.

The functional screens used in the current study did not investigate whether any of the mutant proteins generated affected the release of the virus genome from the capsid and it is possible that the L6 mutation, like ts1249, disrupts two different functions of pUL25. Although the L6 residues do not lie near the ts1249 mutation, they could affect the same function but not necessarily the same interface. There are several possible explanations for the uncoating phenotype of ts1249. The ts1249 E233K mutation could destabilise a critical interaction site of pUL25 with, for example, the nucleoporins CAN/Nup214 or hCG1. Support for this idea has come from observations that ts1249 capsids

produced at the PT fail to bind to isolated nuclei at the NPT but associate with them at the PT (Dr. D. Padeloup, personal communication). An alternative explanation for the phenotype of ts1249, which is similar to the pUL36 mutant tsB7 phenotype (Section 1.3.1.2), is that the interaction between pUL25 and pUL36 is altered in the ts1249-infected or tsB7-infected cells, leading to failure to release virus DNA from the capsid or the inability to expose UL25-NPC binding sites. The UL36 protein is a large protein and it is possible that it could interact with several functional interfaces of pUL25. Experiments are underway in the lab to determine if the HSV-1-UL25-L6 mutant virus has an uncoating defect using the same approach that was used to investigate whether capsids lacking pUL36 were able to initiate infection (Roberts et al., 2009).

The ET analysis used by Bowman et al. (2006) has proved to be an extremely powerful tool for identifying important functional interfaces on the pUL25 structure. Two of the four predicted functional ET clusters (C3 and C4) were found to be essential for the function of the protein, with the mutational analysis of selected residues in C4 identifying a novel function for pUL25 during the egress of capsids from the nucleus. Further mutagenesis of the two other ET clusters, C1 and C2, is necessary in order to investigate the functions of these predicted interfaces. SIFT analysis of the potentially functional amino acids in the C1 and C2 constructs generated here, calculated that two of the alanine substitutions in each of the C1 and C2 mutant proteins may be tolerated and, therefore, are unlikely to disrupt the function of the mutant proteins they expressed. In addition, only three of the nine possible functional residues were mutated in the C1 construct created. The tactical approach used to determine the functional significance of the unstructured amino acids in L1-L6 by creating deletion mutants was validated following analysis of the two L6 proteins, one of which encoded a deletion while the other contained missense mutations. The deletion of the wt residues in pUL25-L6 altered the function of the protein significantly, whereas the substitution of the same wt residues in pUL25-L6sub produced no major defect when expressed in  $\Delta$ UL25MO-infected cells. By deleting unstructured residues, three of the six disordered regions targeted were shown to be essential for the protein's function, enabling two new important roles to be identified for pUL25 in addition to DNA packaging.

Further analysis of the mutant viruses that have either been generated, HSV-1-UL25-C4A, -L3 and -L6, or is in progress, HSV-1-UL25-C3B and -L5, will help to confirm and extend the phenotypes identified during this study.

## References

- Abbotts, A. P., Preston, V. G., Hughes, M., Patel, A. H. & Stow, N. D. (2000). Interaction of the herpes simplex virus type 1 packaging protein UL15 with full-length and deleted forms of the UL28 protein. *J Gen Virol* 81, 2999-3009.
- Addison, C., Rixon, F. J., Palfreyman, J. W., O'Hara, M. & Preston, V. G. (1984). Characterisation of a herpes simplex virus type-1 mutant which has a temperature-sensitive defect in penetration of cells and assembly of capsids. *Virology* 138, 246-259.
- Addison, C., Rixon, F. J. & Preston, V. G. (1990). Herpes simplex virus type-1 UL28 gene product is important for the formation of mature capsids. *J Gen Virol* 71, 2377-2384.
- Adelman, K., Salmon, B. & Baines, J. D. (2001). Herpes simplex virus DNA packaging sequences adopt novel structures that are specifically recognized by a component of the cleavage and packaging machinery. *Proc Natl Acad Sci USA* 98, 3086-3091.
- Albrecht, J. C., Nicholas, J., Biller, D., Cameron, K. R., Biesinger, B., Newman, C., Wittmann, S., Craxton, M. A., Coleman, H., Fleckenstein, B. & Honess, R. W. (1992). Primary structure of the herpesvirus saimiri genome. *J Virol* 66, 5047-5058.
- Al-Kobaisi, M. F., Rixon, F. J., McDougall, I. & Preston, V. G. (1991). The herpes simplex virus UL33 gene- product is required for the assembly of full capsids. *Virology* 180, 380-388.
- Antinone, S. E. & Smith, G. A. (2006). Two modes of herpesvirus trafficking in neurons: membrane acquisition directs motion. *J. Virol.* 80, 11235-11240.
- Baer, R., Bankier, A. T., Biggin, M. D., Deininger, P. L., Farrell, P. J., Gibson, T. J., Hatfull, G., Hudson, G. S., Satchwell, S. C., Seguin, C., Tuffnell, P. S. & Barrell, B. G. (1984). DNA sequence and expression of the B95-8 Epstein-Barr virus genome. *Nature* 310, 207-211.
- Baines, J. D., Cunningham, C., Nalwanga, D. & Davison, A. (1997). The UL15 gene of herpes simplex virus type 1 contains within its second exon a novel open reading frame that is translated in frame with the UL15 product. *J. Virol.* 71, 2666-2673.
- Baines, J. D. & Roizman, B. (1992). The UL11 gene of herpes simplex virus 1 encodes a function that facilitates nucleocapsid envelopment and egress from cells. *J. Virol.* 66, 5168-5174.
- Baines, J. D. & Weller, S. K. (2005). Cleavage and packaging of herpes simplex virus 1 DNA. In *Viral genome packaging machines: Genetics, structure and mechanism.*, pp. 135-150. Edited by C. E. Catalano.: Eureka.com and Kluwer Academic/Plenum Publishers.
- Baird, N. L., Yeh, P.-C., Courtney, R. J. & Wills, J. W. (2008). Sequences in the UL11 tegument protein of herpes simplex virus that control association with detergent-resistant membranes. *Virology* 374, 315-321.
- Baker, M. L., Jiang, W., Rixon, F. J. & Chiu, W. (2005). Common ancestry of herpesviruses and tailed DNA bacteriophages. *J. Virol.* 79, 14967-14970.
- Baker, T. S., Newcomb, W. W., Booy, F. P., Brown, J. C. & C, S. A. (1990). Three-dimensional structures of maturable and abortive capsids of equine herpesvirus 1 from cryoelectron microscopy. *J. Virol.* 64, 563-573.

- Barry, G. F. (1988). A broad-host-range shuttle system for gene insertion into the chromosomes of Gram-negative bacteria. *Gene* 71, 75-84.
- Batterson, W., Furlong, D. & Roizman, B. (1983). Molecular genetics of herpes simplex virus VIII. Further characterisation of a temperature-sensitive mutant defective in the release of viral DNA and in other stages of the viral reproductive cycle. *J. Virol.* 45, 397-407.
- Batterson, W. & Roizman, B. (1983). Characterisation of the herpes simplex virion-associated factor responsible for the induction of  $\alpha$  genes. *J. Virol.* 46, 371-377.
- Bazinet, C. & King, J. (1985). The DNA translocating vertex of dsDNA bacteriophage. *Ann Rev Microbiol* 39, 109-129.
- Beard, P. M. & Baines, J. D. (2004). The DNA cleavage and packaging protein encoded by the UL33 gene of Herpes simplex virus 1 associates with capsids. *Virology* 324, 475-82.
- Beard, P. M., Duffy, C. & Baines, J. D. (2004). Quantification of the DNA cleavage and packaging proteins UL15 and UL28 in A and B capsids of Herpes simplex virus type 1. *J Virol* 78, 1367-74.
- Beard, P. M., Taus, N. S. & Baines, J. D. (2002). DNA cleavage and packaging proteins encoded by the genes UL15, UL28 and UL33 of Herpes simplex virus type 1 form a complex in infected cells. *J. Virol.* 76, 4785-91.
- Beitia Ortiz de Zarate, I., Kaelin, K. & Rozenberg, F. (2004). Effects of mutations in the cytoplasmic domain of herpes simplex virus type 1 glycoprotein B on intracellular transport and infectivity. *J Virol* 78, 1540-1551.
- Bender, F. C., Whitbeck, J. C., Lou, H., Cohen, G. H. & Eisenberg, R. J. (2005). Herpes simplex virus glycoprotein B binds to cell surfaces independently of heparan sulfate and blocks virus entry. *J Virol* 79, 11588-11597.
- Booy, F. P., Newcomb, W. W., Trus, B. L., Brown, J. C., Baker, T. S. & Steven, A. C. (1991). Liquid-crystalline, phage-like packing of encapsidated DNA in herpes simplex virus. *Cell* 64, 1007-1015.
- Bowman, B. R., Welschhans, R. L., Jayaram, H., Stow, N. D., Preston, V. G. & Quioco, F. A. (2006). Structural characterisation of the UL25 DNA-packaging protein from herpes simplex virus type 1. *J Virol* 80, 2309-2317.
- Bowzard, J. B., Visalli, R. J., Wilson, C. B., Loomis, J. S., Callahan, E. M., Courtney, R. J. & Wills, J. W. (2000). Membrane targeting properties of a herpesvirus tegument protein-retrovirus gag chimera. *J Virol* 74, 8692-8699.
- Brack, A. R., Dijkstra, J. M., Granzow, H., Klupp, B. G. & Mettenleiter, T. C. (1999). Inhibition of virion maturation by simultaneous deletion of glycoproteins E, I, and M of pseudorabies virus. *J Virol* 73, 5364-5372.
- Bucks, M. A., O'Regan, K. J., Murphy, M. A., Wills, J. W. & Courtney, R. J. (2007). Herpes simplex virus type 1 tegument proteins VP1/2 and UL37 are associated with intranuclear capsids. *Virology* 361, 316-324.
- Cai, W., Gu, B. & Person, S. (1988). Role of glycoprotein B of herpes simplex virus type 1 in viral entry and cell fusion. *J Virol* 8, 2596-2604.
- Cambell, M. E. M., Palfreyman, J. W. & Preston, C. M. (1984). Identification of Herpes simplex virus DNA sequences which encode a *trans*-acting polypeptide responsible for stimulation of immediate early transcription. *J Mol Biol* 180, 1-19.
- Campadelli-Fiume, G., Cocchi, F., Menotti, L. & Lopez, M. (2000). The novel receptors that mediate the entry of herpes simplex viruses and animal herpesviruses into cells. *Rev Med Virol* 10, 305-319.

- Caspar, D. L. D. & Klug, A. (1962). Physical principles in the construction of regular viruses. *Cold Spring Harbor Symp. Quant. Biol.* 27, 1-22.
- Cebrian, J., Berthelot, N. & Laithier, M. (1989). Genome structure of cottontail rabbit herpesvirus. *J Virol* 63 523-531.
- Cerritelli, M. E., Cheng, N., Rosenberg, A. H., McPherson, C. E., Booy, F. P. & Steven, A. C. (1997). Encapsidated conformation of bacteriophage T7 DNA. *Cell* 91, 271-280.
- Chakravarty, S., Hutson, A. M., Estes, M. K. & Prasad, B. V. V. (2005). Evolutionary trace residues in noroviruses: Importance in receptor binding, antigenicity, virion Assembly, and strain Diversity. *J Virol* 79, 554-568.
- Chang, J. T., Schmid, M. F., Rixon, F. J. & Chiu, W. (2007). Electron cryotomography reveals the portal in the herpesvirus capsid. *J Virol* 81, 2065-2068.
- Chang, J. T., Weigele, P., King, J., Chui, W. & Jiang, W. (2006). Cryo-EM asymmetric reconstruction of bacteriophage P22 reveals organisation of its DNA packaging and infecting machinery. *Structure* 14, 1073-1082.
- Chang, Y. E., Poon, A. W. P. & Roizman, A. (1996). Properties of the protein encoded by the UL32 open reading frame of Herpes simplex virus type 1. *J Virol* 70, 3938-46.
- Church, G. A. & Wilson, D. W. (1997). Study of Herpes simplex virus maturation during a synchronous wave of assembly. *J Virol* 71, 3603-3612.
- Coller, K. E., Lee, J. I.-H., Ueda, A. & Smith, G. A. (2007). The capsid and tegument of the alphaherpesviruses are linked by an interaction between the UL25 and VP1/2 proteins. *J Virol* 81, 11790-11797.
- Condreay, J. P., Witherspoon, S. M., Clay, W. C. & Kost, T. A. (1999). Transient and stable gene expression in mammalian cells transduced with a recombinant baculovirus vector. *Proc Natl Acad Sci USA* 96, 127-132.
- Conway, J. F., Wikoff, W. R., Cheng, N., Duda, R. L., Hendrix, R. W., Johnson, J. E. & Steven, A. C. (2001). Virus maturation involving large subunit rotations and local refolding. *Science* 292, 744-748.
- Crick, F. H. C. & Watson, J. D. (1956). Structure of small viruses. *Nature* 177, 473-475.
- Cunningham, C. & Davison, A. J. (1993). A cosmid-based system for constructing mutants of herpes simplex virus type 1. *Virology* 197, 116-124.
- Dargan, D., Patel, A. & Subak-Sharpe, J. (1995). PREPs: herpes simplex virus type 1-specific particles produced by infected cells when viral DNA replication is blocked. *J Virol* 69, 4924-4932.
- Das, S., Vasanji, A. & Pellett, P. E. (2007). Three-dimensional structure of the human cytomegalovirus cytoplasmic virion assembly complex includes a reoriented secretory apparatus. *J Virol* 81, 11861-11869.
- Dasgupta, A. & Wilson, D. W. (1999). ATP depletion blocks herpes simplex virus DNA packaging and capsid maturation. *J Virol* 73, 2006-2015.
- Davison, A. J. (1992). Channel catfish virus: a new type of herpesvirus. *Virology* 186, 9-14.
- Davison, A. J. (2002). Evolution of Herpesviruses. *Vet Microbiol* 86, 69-88.
- Davison, A. J., Dolan, A., Akter, P., Addison, C., Dargan, D. J., Alcendor, D. J., McGeoch, D. J. & Hayward, G. S. (2003). The human cytomegalovirus genome revisited: comparison with the chimpanzee cytomegalovirus genome. *J Gen Virol* 84, 17-28.
- Davison, A. J., Eberle, R., Ehlers, B., Hayward, G. S., McGeoch, D. J., Minson, A. C., Pellet, P. E., Roizman, B., Studdert, M. J. & Thiry, E. (2009). The order *Herpesvirales*. *Archiv Virol* 154, 171-177.

- Davison, A. J. & McGeoch, D. J. (1995). Herpesviridae. In *Molecular Basis of Viral Evolution.*, pp. 290-309: Cambridge University Press.
- Davison, A. J., Trus, B. L., Cheng, N., Steven, A. C., Watson, M. S., Cunningham, C., Deuff, R.-M. L. & Renault, T. (2005). A novel class of herpesvirus with bivalve hosts. *J Gen Virol* 86, 41-53.
- Davison, M. D., Rixon, F. J. & Davison, A. J. (1992). Identification of genes encoding 2 capsid proteins (VP24 and VP26) of herpes simplex virus type-1. *J Gen Virol* 73, 2709-2713.
- Davison, A. J. & Scott, J. E. (1986). The complete DNA sequence of varicella-zoster virus. *J Gen Virol* 67 1759-1816.
- Davison, A. J. & Wilkie, N. M. (1981). Nucleotide sequences of the joint between the L and S segments of herpes simplex virus types 1 and 2. *J Gen Virol* 55, 315-331.
- de Bruyn Kops, A., Uprichard, S. L., Chen, M. & Knipe, D. M. (1998). Comparison of the intranuclear distributions of herpes simplex virus proteins involved in various viral functions. *Virology* 252, 162-178.
- Deckman, I. C., Hagen, M. & McCann, P. J., III. (1992). Herpes simplex virus type 1 protease expressed in *Eschericia coli* exhibits autoprocessing and specific cleavage of the ICP35 assembly protein. *J Virol* 66, 7362-7367.
- Deiss, L. P., Chou, J. & Frenkel, N. (1986). Functional domains within the a sequence involved in the cleavage-packaging of herpes simplex virus DNA. *J Virol* 59, 605-618.
- Del Rio, T., Ch'ng, T. H., Flood, E. A., Gross, S. P. & Enquist, L. W. (2005). Heterogeneity of a fluorescent tegument component in single pseudorabies virus virions and enveloped axonal assemblies. *J Virol* 79, 3903-3919.
- DeLuca, N. A., McCarthy, A. M. & Schaffer, P. A. (1985). Isolation and characterisation of deletion mutants of herpes simplex virus type 1 in the gene encoding immediate-early regulatory protein ICP4. *J Virol* 56, 558-570.
- DeLuca, N. A. & Schaffer, P. A. (1988). Physical and functional domains of the herpes simplex virus transcriptional regulatory protein ICP4. *J Virol* 62, 732-743.
- Deng, B., O'Connor, C. M., Kedes, D. H. & Zhou, Z. H. (2007). Direct visualisation of the putative portal in the Kaposi's Sarcoma-associated herpesvirus capsid by cryoelectron tomography. *J Virol* 81, 3640-3644.
- Desai, P. (2000). A null mutation in the UL36 gene of herpes simplex virus type 1 results in accumulation of unenveloped DNA-filled capsids in the cytoplasm of infected cells. *J Virol* 74, 11608-11618.
- Desai, P., DeLuca, N. A. & Person, S. (1998). Herpes simplex virus type 1 VP26 is not essential for replication in cell culture but influences production of infectious virus in the nervous system of infected mice. *Virology* 247, 115-124.
- Desai, P. & Person, S. (1996). Molecular interactions between the HSV-1 capsid proteins as measured by the yeast two-hybrid system. *Virology* 220, 516-521.
- Desloges, N. & Simard, C. (2003). Implication of the product of the bovine herpesvirus type 1 UL25 gene in capsid assembly. *J Gen Virol* 84, 2485-2490.
- Dohner, K., Wolfstein, A., Prank, U., Echeverri, C., Dujardin, D., Vallee, R. & Sodeik, B. (2002). Function of dynein and dynactin in herpes simplex virus capsid transport. *Mol Biol Cell* 13, 2795-2809.

- Drolet, B. S., Perng, G. C., Cohen, J., Sianina, S. M., Yukht, A., Nesburn, A. B. & Wechsler, S. L. (1997). The region of the herpes simplex virus type 1 LAT gene involved in spontaneous reactivation does not encode a functional protein. *Virology* 242, 221-232.
- Everett, R. D. (2000). ICP0, a regulator of herpes simplex virus during lytic and latent infection. *Bioessays* 22, 761-770.
- Everett, R. D. (2006). Interactions between DNA viruses, ND10 and the DNA damage response. *Cell Microbiol* 8, 365-374.
- Everett, R. D., Meredith, M., Orr, A., Cross, A., Kathoria, M. & Parkison, J. (1997). A novel ubiquitin-specific protease is dynamically associated with the PML nuclear domain and binds to a herpesvirus regulatory protein. *Embo J* 16, 566-577.
- Everett, R. D. & Murray, J. (2005). ND10 components relocate to sites associated with herpes simplex virus type 1 nucleoprotein complexes during virus infection. *J Virol* 79, 5078-5089.
- Everett, R. D., Murray, J., Orr, A. & Preston, C. M. (2007). Herpes simplex virus type 1 genomes are associated with ND10 nuclear substructures in quiescently infected human fibroblasts. *J Virol* 81, 10991-11004.
- Everett, R. D., Rechter, S., Papior, P., Tavalai, N., Stamminger, T. & Orr, A. (2006). PML contributes to a cellular mechanism of repression of herpes simplex virus type 1 infection that is inactivated by . *J Virol* 80, 7995-8005.
- Faber, S. W. & Wilcox, K. W. (1986). Association of the herpes simplex virus regulatory protein ICP4 with specific nucleotide sequences in DNA. *Nucl Acids Res* 14, 6067-6083.
- Farnsworth, A. & Johnson, D. C. (2006). Herpes simplex virus gE/gI must accumulate in the trans-Golgi network at early times and then redistribute to cell junctions to promote cell-cell spread. *J Virol* 80, 3167-3179.
- Farnsworth, A., Wisner, T. W. & Johnson, D. C. (2007). Cytoplasmic residues of herpes simplex virus glycoprotein gE required for secondary envelopment and binding of tegument proteins VP22 and UL11 to gE and gD. *J Virol* 81, 319-331.
- Forrester, A. J., Sullivan, V., Simmons, A., Blacklaws, B. A., Smith, G. L., Nash, A. A. & Minson, A. C. (1991). *J Gen Virol* 72, 369-375.
- Fuchs, W., Granzow, H., Klupp, B. G., Kopp, M. & Mettenleiter, T. C. (2002b). The UL48 tegument protein of pseudorabies virus is critical for intracytoplasmic assembly of infectious virions. *J Virol* 76, 6729-6742.
- Fuchs, W., Klupp, B. G., Granzow, H. & Mettenleiter, T. C. (2004). Essential function of the pseudorabies virus UL36 gene product is independent of its interaction with the UL37 protein. *J Virol* 78, 11879-11889.
- Fuchs, W., Klupp, B. G., Granzow, H., Osterrieder, N. & Mettenleiter, T. C. (2002a). The interacting UL31 and UL34 gene products of pseudorabies virus are involved in egress from the host-cell nucleus and represent components of primary enveloped but not mature virions. *J Virol* 76, 364-378.
- Fulmer, P. A., Melancon, J. M., Baines, J. D. & Kousoulas, K. G. (2007). UL20 protein functions precede and are required for the UL11 functions of herpes simplex virus type 1 cytoplasmic virion envelopment. *J Virol* 81, 3097-3108.
- Gaffney, D. F., McLauchlan, J., Whitton, J. L. & Clements, J. B. (1985). A modular system for the assay of transcription regulatory signals: the

- sequence TAATGARAT is required for herpes simplex virus immediate early gene activation. *Nucl Acids Res* 13, 7847-7863.
- Gao, M., Matusick-Kumar, L., Hurlburt, W., DiTusa, S. F., Newcomb, W. W., Brown, J. C., McCann, P. J., III, Deckman, I. & Colonno, R. J. (1994). The protease of herpes simplex virus type 1 is essential for functional capsid formation and viral growth. *J Virol* 68, 3703-3712.
- Gerner, C. S., Dolan, A. & McGeoch, D. J. (2004). Phylogenetic relationships in the *Lymphocryptovirus* genus of the *Gammaherpesvirinae*. *Virus Res* 99, 187-192.
- Gibson, W. & Roizman, B. (1972). Proteins specified by herpes simplex virus VIII. Characterisation of and composition of multiple capsid forms of subtypes 1 and 2. *J Virol* 10, 1044-1052.
- Goshima, F., Watanabe, D., Takakuwa, H., Wada, K., Daikoku, T., Yamada, M. & Nishiyama, Y. (2000). Herpes simplex virus UL17 protein is associated with B capsids and colocalises with ICP35 and VP5 in infected cells. *Archiv Virol* 145, 417-426.
- Granzow, H., Klupp, B. G. & Mettenleiter, T. C. (2004). The pseudorabies virus US3 protein is a component of primary and of mature virions. *J Virol* 78, 1314-1323.
- Granzow, H., Klupp, B. G. & Mettenleiter, T. C. (2005). Entry of pseudorabies virus: an immunogold-labelling study. *J Virol* 79, 3200-3205.
- Grondin, B. & DeLuca, N. (2000). Herpes simplex virus type 1 ICP4 promotes transcription preinitiation complex formation by enhancing the binding of TFIID to DNA. *J Virol* 74, 11504-11510.
- Grünwald, K., Desai, P., Winkler, D. C., Heymann, J. B., Belnap, D. M., Baumeister, W. & Steven, A. C. (2003). Three-dimensional structure of herpes simplex virus from cryo-electron tomography. *Science* 302, 1396-1398.
- Hagglund, R. & Roizman, B. (2004). Role of in the strategy of conquest of the host cell by herpes simplex virus 1. *J Virol* 78, 2169-2178.
- Halford, W. P., Kemp, C. K., Isler, J. A., Davido, D. J. & Schaffer, P. A. (2001). ICP0, ICP4, or VP16 expressed from adenovirus vectors induces reactivation of latent herpes simplex virus type 1 in primary cultures of latently infected trigeminal ganglion cells. *J Virol* 75, 6143-6153.
- Ham, M. V. & Hendriks, W. (2003). PDZ domains - glue and guide. *Mol Biol Reports* 30, 69-82.
- Hammarsten, O., Yao, X. & Elias, P. (1996). Inhibition of topoisomerase II by ICRF-193 prevents efficient replication of herpes simplex virus type 1. *J Virol* 70, 4523-4529.
- Harley, C. A., Dasgupta, A. & Wilson, D. W. (2001). Characterisation of herpes simplex virus-containing organelles by subcellular fractionation: Role for organelle acidification in assembly of infectious particles. *J Virol* 75, 1236-1251.
- Harrison, S. C. (1983). Packaging of DNA into bacteriophage heads: a model. *J Mol Biol* 171, 577-580.
- Hendrix, R. (2005). Bacteriophage HK97: assembly of the capsid and evolutionary connections. *Adv Virus Res* 64, 1-14.
- Herold, B. C., WuDunn, D., Soltys, N. & Spear, P. G. (1991). Glycoprotein C of herpes simplex virus type 1 plays a principal role in the adsorption of virus to cells and in infectivity. *J Virol* 65, 1090-1098.
- Heymann, J. B., Cheng, N., Newcomb, W. W., Trus, B. L., Brown, J. C., & Steven, A. C. (2003). Dynamics of herpes simplex virus capsid maturation by time-lapse cryo-electron microscopy. *Nat Struct Biol* 10, 334-341.

- Ho, S. N., H.D. Hunt, R.M. Horton, J.K. Pullen, L.R/ Pease (1989). Site-directed mutagenesis by overlap extension using the polymerase chain reaction. *Gene* 77, 51-59.
- Hodge, P. D. & Stow, N. D. (2001). Effects of mutations within the Herpes simplex virus type 1 DNA encapsidation signal on packaging efficiency. *J Virol* 75, 8977-86.
- Hofemeister, H. & O'Hare, P. (2008). Nuclear pore composition and gating in herpes simplex virus-infected cells. *J Virol* 82, 8392-8399.
- Homa, F. L. & Brown, J. C. (1997). Capsid assembly and DNA packaging in herpes simplex virus. *Rev Med Virol* 7, 107-122.
- Hong, Z., Beaudet-Miller, M., Durkin, J., Zhang, R. & Kwong, A. (1996). Identification of a minimal hydrophobic domain in the herpes simplex virus type 1 scaffolding protein which is required for interaction with the major capsid protein. *J Virol* 70, 533-540.
- Hughes, T. A., Boissiere, S. L. & O'Hare, P. (1999). Analysis of functional domains of the host cell factor involved in VP16 complex formation. *J Biol Chem* 274, 16437-16443.
- Hung, A. Y. & Sheng, M. (2002). PDZ domains: structural modules for protein complex assembly. *J Biol Chem* 277, 5699-5702.
- Imber, R., Tsugita, A., Wurtz, M. & Hohn, T. (1980). Outer surface protein of bacteriophage lambda. *J Mol Biol* 139, 277-295.
- Jacob, R. J., Morse, L. S. & Roizman, B. (1979). Anatomy of herpes simplex virus DNA XII. Accumulation of head-to-tail concatemers in nuclei of infected cells and their role in the generation of the four isomeric arrangements of viral DNA. *J Virol* 29, 448-457.
- Jacobson, J. G., Yang, K., Baines, J. D. & Homa, F. L. (2006). Linker insertion mutations in the herpes simplex virus type 1 UL28 gene: Effects on UL28 interaction with UL15 and UL33 and identification of a second-site mutation in the UL15 gene that suppresses a lethal UL28 mutation. *J Virol* 80, 12312-12323.
- Jiang, W., Chang, J., Jakana, J., Weigele, P., King, J. & Chiu, W. (2006). Structure of epsilon15 bacteriophage reveals genome organisation and DNA packaging/injection apparatus. *Nature* 439, 612-616.
- Johnson, D. C. & Spear, P. G. (1982). Monensin inhibits the processing of herpes simplex virus glycoproteins, their transport to the cell surface, and the egress of virions from infected cells. *J Virol* 43, 102-1112.
- Johnson, J. E. & Chiu, W. (2007). DNA packaging and delivery machnines in tailed bacteriophages. *Curr Opin Struct Biol* 17, 237-243.
- Jovasevic, V., Liang, L. & Roizman, B. (2008). Proteolytic cleavage of VP1-2 is required for release of herpes simplex virus 1 DNA into the nucleus. *J Virol* 82, 3311-3319.
- Kaelin, K., Dez  lee, S., Masse, M. J., Bras, F. & Flamand, A. (2000). The UL25 protein of pseudorabies virus associates with capsids and localises to the nucleus and to microtubules. *J Virol* 74, 474-482.
- Kamen, D. E., Gross, S. T., Girvin, M. E. & Wilson, D. W. (2005). Structural basis for the physiological temperature dependence of the association of VP16 with the cytoplasmic tail of herpes simplex virus glycoprotein H. *J Virol* 79, 6134-6141.
- Klupp, B. G., Bottcher, S., Granzow, H., Kopp, M. & Mettenleiter, T. C. (2005). Complex formation between the UL16 and UL21 tegument proteins of pseudorabies virus. *J Virol* 79, 1510-1522.

- Klupp, B. G., Fuchs, W., Granzow, H., Nixdorf, R. & Mettenleiter, T. C. (2002). Pseudorabies virus UL36 tegument protein physically interacts with the UL37 protein. *J Virol* 76, 3065-3071.
- Klupp, B. G., Granzow, H., Fuchs, W., Keil, G. M., Finke, S. & Mettenleiter, T. C. (2007). Vesicle formation from the nuclear membrane is induced by coexpression of two conserved herpesvirus proteins. *Proc Natl Acad Sci USA* 104, 7241-7246.
- Klupp, B. G., Granzow, H., Keil, G. M. & Mettenleiter, T. C. (2006). The capsid-associated UL25 protein of the alphaherpesvirus pseudorabies virus is nonessential for cleavage and encapsidation of genomic DNA but is required for nuclear egress of capsids. *J Virol* 80, 6235-6246.
- Klupp, B. G., Granzow, H. & Mettenleiter, T. C. (2000). Primary envelopment of pseudorabies virus at the nuclear membrane requires the UL34 gene product. *J Virol* 74, 10063-10073.
- Knipe, D. M., Batterson, W., Nosal, C., Roizman, B. & Buchan, A. (1981). Molecular genetics of herpes simplex virus VI. Characterisation of a temperature-sensitive mutant defective in the expression of all early viral gene products. *J Virol* 38, 539-547.
- Koch, H. G., Delius, H., Matz, B., Flugel, R. M., Clarke, J. & Darai, G. (1985). Molecular cloning and physical mapping of the tupaia herpesvirus genome. *J Virol* 55, 86-95.
- Koshizuka, T., Kawaguchi, Y., Nozawa, N., Mori, I. & Nishiyama, Y. (2007). Herpes simplex virus protein UL11 but not UL51 is associated with lipid rafts. *Virus Genes* 35, 571-575.
- Koslowski, K. M., Shaver, P. R., Casey II, J. T., Wilson, T., Yamanaka, G. Y., Sheaffer, A. K., Tenney, D. J. & Pederson, N. E. (1999). Physical and functional interactions between the herpes simplex virus UL15 and UL 28 DNA cleavage and packaging proteins. *J Virol* 73, 1704-1707.
- Koslowski, K. M., Shaver, P. R., Wang, X.-Y., Tenney, D. J. & Pederson, N. E. (1997). The pseudorabies virus UL28 protein enters the nucleus after coexpression with the herpes simplex virus UL15 protein. *J Virol* 71, 9118-9123.
- Kost, T. A., Condreay, J. P. & Jarvis, D. L. (2005). Baculovirus as versatile vectors for protein expression in insect and mammalian cells. *Nat Biotech* 23, 567-575.
- Krautwald, M., Fuchs, W., Klupp, B. G. & Mettenleiter, T. C. (2009). Translocation of incoming pseudorabies virus capsids to the cell nucleus is delayed in the absence of tegument protein pUL37. *J Virol* 83, 3389-3396.
- Kuhn, J., Leege, T., Klupp, B. G., Granzow, H., Fuchs, W. & Mettenleiter, T. C. (2008). Partial functional complementation of a pseudorabies virus UL25 deletion mutant by herpes simplex virus type 1 pUL25 indicates overlapping functions of alphaherpesvirus pUL25 proteins. *J Virol* 82, 5725-5734.
- Ladin, B. F., Blankenship, M. L. & Ben-Porat, T. (1980). Replication of herpesvirus DNA V. Maturation of concatemeric DNA of pseudorabies virus to genome length is related to capsid formation. *J Virol* 33, 1151-1164.
- Ladin, B. F., Ihara, S., Hampl, H. & Ben-Porat, T. (1982). Pathway of assembly of herpesvirus capsids: an analysis using DNA+ temperature-sensitive mutants of pseudorabies virus. *Virology* 116, 544-561.
- Lake, C. M. & Hutt-Fletcher, L. M. (2004). The Epstein-Barr virus BFRF1 and BFLF2 proteins interact and coexpression alters their cellular localization. *Virology* 320, 99-106.

- Lamberti, C. & Weller, S. K. (1996). The herpes simplex virus type 1 UL6 protein is essential for cleavage and packaging but not for genomic inversion. *Virology* 226, 403-407.
- Lamberti, C. & Weller, S. K. (1998). The herpes simplex virus type 1 cleavage/packaging protein, UL32, is involved in efficient localization of capsids to replication compartments. *J Virol* 72, 2463-2473.
- Lander, G. C., Tang, L., R.C., S., Gilcrease, E. B., Prevelige, P., Poliakov, A., Potter, C. S., Carragher, B. & Johnson, J. E. (2006). The structure of an infectious P22 virion shows the signal for headful DNA packaging. *Science* 312, 1791-1795.
- Lee, J. I.-H., Luxton, G. W. G. & Smith, G. A. (2006). Identification of an essential domain in the herpesvirus VP1/2 tegument protein: The carboxy terminus directs incorporation into capsid assemblons. *J Virol* 80, 12086-12094.
- Leege, T., Granzow, H., Fuchs, W., Klupp, B. G. & Mettenleiter, T. C. (2009). Phenotypic similarities and differences between UL37-deleted pseudorabies virus and herpes simplex virus type 1. *J Gen Virol* 90, 1560-1568.
- Lehman, I. R. & Boehmer, P. E. (1999). Replication of herpes simplex virus DNA. *J Biol Chem* 274, 28059-28062.
- Leuzinger, H., Ziegler, U., Schraner, E. M., Fraefel, C., Glauser, D. L., Heid, I., Ackermann, M., Mueller, M. & Wild, P. (2005). Herpes simplex virus 1 envelopment follows two diverse pathways. *J Virol* 79, 13047-13059.
- Lichtarge, O., Bourne, H. R. & Cohen, F. E. (1996). An evolutionary trace method defines binding surfaces common to protein families. *J Mol Biol* 257, 342-358.
- Lichtartge, O. & Sowa, M. E. (2002). Evolutionary predictions of binding surfaces and interactions. *Curr Opin Struct Biol* 12, 21-27.
- Ligas, M. W. & Johnson, D. C. (1988). A herpes simplex virus mutant in which glycoprotein D sequences are replaced by  $\beta$ -galactosidase sequences binds to but is unable to penetrate into cells. *J Virol* 62, 1486-1494.
- Lim, Y. H. & Fahrenkrog, B. (2006). The nuclear pore complex up close. *Curr Opin Struct Biol* 18, 342-347.
- Liu, F. & Roizman, B. (1991). The promoter, transcriptional unit, and coding sequences of herpes simplex virus 1 family 35 proteins are contained within and in frame with the UL26 open reading frame. *J Virol* 65, 206-212.
- Liu, F. & Roizman, B. (1992). Differentiation of multiple domains in the herpes simplex virus 1 protease encoded by the UL26 gene. *Proc Natl Acad Sci USA* 89, 2076-2080.
- Liu, F. & Roizman, B. (1993). Characterisation of the protease and other products of amino-terminus proximal cleavage of the herpes simplex virus UL26 protein. *J Virol* 67, 1300-1309.
- Loomis, J. S., Courtney, R. J. & Wills, J. W. (2003). Binding partners for the UL11 tegument protein of herpes simplex virus type 1. *J Virol* 77, 11417-11424.
- Loomis, J. S., Courtney, R. J. & Wills, J. W. (2006). Packaging determinants in the UL11 tegument protein of herpes simplex virus type 1. *J Virol* 80, 10534-10541.
- Luckow, V. A., Lee, S. C., Barry, G. F. & Olins, P. O. (1993). Efficient generation of infectious recombinant baculoviruses by site-specific transposon-mediated insertion of foreign genes into a baculovirus genome propagated in *Escherichia coli*. *J Virol* 67, 4566-4579.

- Luxton, G. W. G., Haverlock, K. E., Coller, S. E., Antinone, S. E., Pincetic, A. & Smith, G. A. (2005). Targeting of herpesvirus capsid transport in axons is coupled to association with specific sets of tegument proteins. *Proc Natl Acad Sci USA* 102, 5832-5837.
- Luxton, G. W. G., Lee, J. I.-H., Haverlock-Moyns, S., Schober, J. M. & Smith, G. A. (2006). The pseudorabies virus VP1/2 tegument protein is required for intracellular capsid transport. *J Virol* 80, 201-209.
- Lyman, M.G., & Enquist, L.W. (2009). Herpesvirus interactions with the host cytoskeleton. *J Virol* 83, 2058-2066.
- Maxwell, K. L., Davidson, A. R., Murialdo, H. & Gold, M. (2000). Thermodynamic and functional characterisation of protein W from bacteriophage lambda. The three C-terminal residues are critical for activity. *J Biol Chem* 275, 18879-18886.
- McCarthy, A. M., McMahan, L. & Schaffer, P. A. (1989). Herpes simplex virus type 1 ICP27 deletion mutants exhibit altered patterns of transcription and are DNA deficient. *J Virol* 63, 18-27.
- McClelland, D. A., Aitken, J. D., Bhella, D., McNab, D., Mitchell, J., Kelly, S. M., Price, N. C. & Rixon, F. J. (2002). pH reduction as a trigger for dissociation of herpes simplex virus type 1 scaffolds. *J Virol* 76, 7407-7417.
- McGeoch, D. J., Barnett, D. J. C. & MacLean, C. A. (1993). Emerging functions of alphaherpesvirus genes. *Sem Virol* 4, 125-134.
- McGeoch, D. J., Dalrymple, M. A., Davison, A. J., Dolan, A., Frame, M. C., McNab, D., Perry, L. J., Scott, J. E. & Taylor, P. (1988). The complete DNA sequence of the long unique region in the genome of herpes simplex virus type 1. *J Gen Virol* 69, 1531-1574.
- McGeoch, D. J., Davison, A. J. & Rixon, F. J. (2006). Topics in herpesvirus genomics and evolution. *Virus Res* 117, 90-104.
- McGeoch, D. J., Gatherer, D. & Dolan, A. (2005). On phylogenetic relationships among major lineages of the *Gammaherpesvirinae*. *J Gen Virol* 86, 307-316.
- McLauchlan, J., Addison, C., Craigie, M. C. & Rixon, F. J. (1992). Noninfectious L-particles supply functions which can facilitate infection by HSV-1. *Virology* 190, 682-688.
- McLauchlan, J. & Rixon, F. J. (1992). Characterisation of enveloped tegument structures (L particles) produced by alphaherpesviruses: integrity of the tegument does not depend on the presence of capsid or envelope. *J Gen Virol* 73, 269-276.
- McNab, A. R. & Courtney, R. J. (1992). Characterisation of the large tegument protein (ICP 1/2) of herpes simplex virus type 1. *Virology* 190, 221-232.
- McNab, A. R., Desai, P., Person, S., Roof, L. L., Thomsen, D. R., Newcomb, W. W., Brown, J. C. & Homa, F. L. (1998). The product of the herpes simplex virus type 1 UL25 gene is required for encapsidation but not for cleavage of replicated viral DNA. *J Virol* 72, 1060-1070.
- McVoy, M. A., Nixon, D. E., Hur, J. K. & Adler, S. P. (2000). The ends on herpesvirus DNA replicative concatemers contain pac2 cis cleavage/packaging elements and their formation is controlled by terminal cis sequences. *J Virol* 74, 1587-1592.
- Mettenleiter, T. C. (2002). Herpesvirus assembly and egress. *J Virol* 76, 1537-1547.
- Mettenleiter, T. C. (2004). Budding events in herpesvirus morphogenesis. *Virus Res* 106, 167-180.

- Mettenleiter, T. C. (2006). Intriguing interplay between viral proteins during herpesvirus assembly or: The herpesvirus assembly puzzle. *Vet Microbiol* 113, 163-169.
- Mettenleiter, T. C., Minson, T. & Wild, P. (2006). Egress of alphaherpesviruses. *J Virol* 80, 1610-1612.
- Michael, K., Klupp, B. G., Mettenleiter, T. C. & Karger, A. (2006). Composition of pseudorabies virus particles lacking tegument protein US3, UL47, or UL49 or envelope glycoprotein E. *J Virol* 80, 1332-1339.
- Mikalek, I., Yao, R. I. & Lichtarge, O. (2003). Combining inference from evolution and geometric probability in protein structure evaluation. *J Mol Biol* 331, 263-279.
- Mocarski, E. S. & Roizman, B. (1981). Site-specific inversion sequence of the herpes simplex virus genome: Domain and structural features. *Proc Natl Acad Sci USA* 78, 7047-7051.
- Mocarski, E. S. & Roizman, B. (1982). Structure and role of the herpes simplex virus DNA termini in inversion circularisation and generation of virion DNA. *Cell* 31, 89-97.
- Mossman, K. L., Sherburne, R., Lavery, C., Duncan, J. & Smiley, J. R. (2000). Evidence that herpes simplex virus VP16 is required for viral egress downstream of the initial envelopment event. *J Virol* 74, 6287-6299.
- Mou, F., Wills, E. G., Park, R. & Baines, J. D. (2008). Effects of lamin A/C, lamin B1, and viral US3 kinase activity on viral infectivity, virion egress, and the targeting of herpes simplex virus UL34-encoded protein to the inner nuclear membrane. *J Virol* 82, 8094-8104.
- Muranyi, W., Hass, J., Wagner, M., Krohne, G. & Koszinowski, U. H. (2002). Cytomegalovirus recruitment of cellular kinases to dissolve the nuclear lamina. *Science* 297, 854-857.
- Nagel, C.-H., Dohner, K., Fathollahy, M., Strive, T., Borst, E. M., Messerle, M. & Sodeik, B. (2008). Nuclear egress and envelopment of herpes simplex virus capsids analysed with dual-colour fluorescence HSV1(17+). *J Virol* 82, 3109-3124.
- Nasseri, M. & Mocarski, E. S. (1988). The cleavage recognition signal is contained within sequences surrounding an aa junction. *Virology* 167, 25-30.
- Newcomb, W. W., Booy, F. P. & Brown, J. C. (2007). Uncoating the herpes simplex virus genome. *J Mol Biol* 370, 633-642.
- Newcomb, W. W., Homa, F. L. & Brown, J. C. (2005). Involvement of the portal at an early step in herpes simplex virus capsid assembly. *J Virol* 79, 10540-10546.
- Newcomb, W. W., Homa, F. L. & Brown, J. C. (2006). Herpes simplex virus capsid structure: DNA packaging protein UL25 is located on the external surface of the capsid near the vertices. *J Virol* 80, 6286-6294.
- Newcomb, W. W., Homa, F. L., Thomsen, D. R., Booy, F. P., Trus, B. L., Steven, A. C., Spencer, J. V. & Brown, J. C. (1996). Assembly of the herpes simplex virus capsid: characterisation of intermediates observed during cell-free capsid formation. *J Mol Biol* 263, 432-446.
- Newcomb, W. W., Homa, F. L., Thomsen, D. R., Trus, B. L., Cheng, N., Steven, A., Booy, F. & Brown, J. C. (1999). Assembly of the herpes simplex virus procapsid from purified components and identification of small complexes containing the major capsid and scaffolding proteins. *J Virol* 73, 4239-4250.
- Newcomb, W. W., Homa, F. L., Thomsen, D. R., Ye, Z. & Brown, J. C. (1994). Cell-free assembly of the herpes simplex virus capsid. *J Virol* 68, 6059-6063.

- Newcomb, W. W., Juhas, R. M., Thomsen, D. R., Homa, F. L., Burch, A. D., Weller, S. K. & Brown, J. C. (2001). The UL6 gene product forms the portal for entry of DNA into the herpes simplex virus capsid. *J Virol* 75, 10923-10932.
- Newcomb, W. W., Trus, B. L., Booy, F. P., Steven, A. C., Wall, J. S. & Brown, J. C. (1993). Structure of the herpes simplex virus capsid molecular composition of the pentons and the triplexes. *J Mol Biol* 232, 499-511.
- Newcomb, W. W., Trus, B. L., Cheng, N., Steven, A. C., Sheaffer, A. K., Tenney, D. J., Weller, S. K. & Brown, J. C. (2000). Isolation of herpes simplex virus procapsids from cells infected with a protease-deficient mutant virus. *J Virol* 74, 1663-1673.
- Nicholson, P., Addison, C., Cross, A. M., Kennard, J., Preston, V. G. & Rixon, F. J. (1994). Localisation of the herpes simplex virus type 1 major capsid protein VP5 to the cell nucleus requires the abundant scaffolding protein VP22a. *J Gen Virol* 75, 1091-1099.
- Ogasawara, M., Suzutani, T., Yoshida, I. & Azuma, M. (2001). Role of the UL25 gene product in packaging DNA into the herpes simplex virus capsid: location of UL25 product in the capsid and demonstration that it binds DNA. *J Virol* 75, 1427-1436.
- O'Hare, P., Goding, C. R. & Haigh, A. (1988). Direct combinatorial interaction between a herpes simplex virus regulatory protein and a cellular octamer-binding factor mediates specific induction of virus immediate-early gene expression. *Embo J* 7.
- Panagiotidis, C., Lium, E. & Silverstein, S. (1997). Physical and functional interactions between herpes simplex virus immediate-early proteins ICP4 and ICP27. *J Virol* 71, 1547-1557.
- Park, R. & Baines, J. D. (2006). Herpes simplex virus type 1 infection induces activation and recruitment of protein kinase C to the nuclear membrane and increased phosphorylation of lamin B. *J Virol* 80, 494-504.
- Pasdeloup, D., Blondel, D., Isidro, A. L. & Rixon, F. J. (2009). Herpesvirus capsid association with the nuclear pore complex and viral DNA release involve the nucleoporin CAN/Nup214 and the capsid protein pUL25. *J Virol* 83, 6610-6623.
- Patel, A. H., Rixon, F. J., Cunningham, C. & Davison, A. J. (1996). Isolation and characterisation of herpes simplex virus type 1 mutants defective in the UL6 gene. *Virology* 217, 111-123.
- Pellet, P. E. & Roizman, B. (2007). The Family *Herpesviridae*: A Brief Introduction. In *Fields Virology*, pp. 2479-2512.
- Perucchetti, R., Parris, W., Becker, A. & Gold, M. (1988). Late stages in bacteriophage lambda head morphogenesis: in vitro studies on the action of the bacteriophage lambda D-gene and W-gene products. *Virology* 165, 103-114.
- Polvino-Bodnar, M., Orberg, P. K. & Schaffer, P. A. (1987). Herpes simplex virus type 1 oriL is not required for virus replication or for the establishment and reactivation of latent infection in mice. *J Virol* 61, 3528-3535.
- Ponten, J., Saksela, E. (1967). Two established *in vitro* cell lines from human mesenchymal tumors. *Int J Cancer* 2, 434-447
- Ponting, C. P. (1997). Evidence for PDZ domains in bacteria, yeast and plants. *Prot Sci* 6, 464-468.
- Poon, A. P. W., Benetti, L. & Roizman, B. (2006). US3 and US3.5 protein kinases of herpes simplex virus 1 differ with respect to their functions in blocking apoptosis and in virion maturation and egress. *J Virol* 80, 3752-3764.

- Preston, C. & Nicholl, M. (1997). Repression of gene expression upon infection of cells with herpes simplex virus type 1 mutants impaired for immediate-early protein synthesis. *J Virol* 71, 7807-7813.
- Preston, V. G., Al-Kobaisi, M. F., McDougall, I. M. & Rixon, F. J. (1994). The herpes simplex virus gene UL26 proteinase in the presence of the UL26.5 gene product promotes the formation of scaffold-like structures. *J Gen Virol* 75, 2355-2366.
- Preston, V. G., Coates, J. A. & Rixon, F. J. (1983). Identification and characterisation of a herpes simplex virus gene product required for encapsidation of viral DNA. *Virology* 45, 1056-1064.
- Preston, V. G., Murray, J., Preston, C. M., McDougall, I. M. & Stow, N. D. (2008). The UL25 gene product of herpes simplex virus type 1 is involved in uncoating of the viral genome. *J Virol* 82, 6654-6666.
- Preston, V. G. a. M., Iris, M. (2002). Regions of the herpes simplex virus scaffolding protein that are important for intermolecular self-interaction. *J Virol* 76.
- Przech, A. J., Yu, D. & Weller, S. K. (2003). Point mutations in exon I of the herpes simplex virus putative terminase subunit, UL15, indicate that the most conserved residues are essential for cleavage and packaging. *J Virol* 77, 9613-9621.
- Qinlan, M. P., Chen, L. B. & Knipe, D. M. (1984). The intranuclear location of a herpes simplex virus DNA-binding protein is determined by the status of viral DNA replication. *Cell* 36, 857-868.
- Reynolds, A. E., Fan, Y. & Baines, J. D. (2000). Characterisation of the UL33 gene product of herpes simplex virus 1. *Virology* 266, 310-318.
- Reynolds, A. E., Liang, L. & Baines, J. D. (2004). Conformational changes in the nuclear lamina induced by herpes simplex virus type 1 require genes UL31 and UL34. *J Virol* 78, 5564-5575.
- Reynolds, A. E., Ryckman, B. J., Baines, J. D., Zhou, Y., Liang, L. & Roller, R. J. (2001). UL31 and UL34 proteins of herpes simplex virus type 1 form a complex that accumulates at the nuclear rim and is required for envelopment of nucleocapsids. *J Virol* 75, 8803-8817.
- Reynolds, A. E., Wills, E. G., Roller, R. J., Ryckman, B. J. & Baines, J. D. (2002). Ultrastructural localization of the herpes simplex virus type 1 UL31, UL34, and UL33 proteins suggests specific roles in primary envelopment and egress of nucleocapsids. *J Virol* 76, 8939-8952.
- Rhim, J. & Schell, K. (1967). Cytopathic and plaque assay of rubella virus in a line of african green monkey kidney cells (Vero). *Proc Soc Exp Biol & Med* 125, 475-488.
- Rixon, F. J. (2008). A good catch: packaging the virus genome. *Cell Host Microbe* 3, 120-122.
- Rixon, F. J., Addison, C., McGregor, A., Macnab, S. J., Nicholson, P., Preston, V. G. & Tatman, J. D. (1996). Multiple interactions control the intracellular localization of the herpes simplex virus type 1 capsid proteins. *J Gen Virol* 77, 2251-2260.
- Rixon, F. J., Addison, C. & McLauchlan, J. (1992). Assembly of enveloped tegument structures (L particles) can occur independently of virion maturation in herpes simplex virus type 1-infected cells. *J Gen Virol* 73, 277-284.
- Rixon, F. J., Cross, A. M., Addison, C. & Preston, V. G. (1988). The products of herpes simplex virus type-1 gene UL26 which are involved in DNA packaging are strongly associated with empty but not with full capsids. *J Gen Virol* 69, 2879-2891.

- Rixon, F. J. & McNab, D. (1999). Packaging-competent capsids of a herpes simplex virus temperature-sensitive mutant have properties similar to those of in vitro-assembled procapsids. *J Virol* 73, 5714-5721.
- Roberts, A. P. E., Abaitua, F., O'Hare, P., McNab, D., Rixon, F. J. & Pasmeloup, D. (2009). Differing roles of inner tegument proteins pUL36 and pUL37 during entry of herpes simplex virus type 1. *J Virol* 83, 105-116.
- Robertson, B., McCann, P., 3rd, Matusick-Kumar, L., Newcomb, W., Brown, J., Colonna, R. & Gao, M. (1996). Separate functional domains of the herpes simplex virus type 1 protease: evidence for cleavage inside capsids. *J Virol* 70, 4317-4328.
- Rock, D. L. (1993). The molecular basis of latent infections by alphaherpesviruses. *Semin Virol* 4, 157-165.
- Roizman, B. (1979). The structure and isomerisation of herpes simplex virus genomes. *Cell* 16, 481-494.
- Roizman, B., Knipe, D. M. & Whitley, R. J. (2007). Herpes simplex viruses. In *Fields Virology*, pp. 2502-2698.
- Saeki, Y., Ichikawa, T., Saeki, A., Chiocca, E. A., Tobler, K., Achermann, M., Breakefield, X. O. & Fraefel, C. (1998). Herpes simplex virus type 1 DNA amplified as bacterial artificial chromosome in *Escherichia Coli*: rescue of replication-competent virus progeny and packaging of amplicon vectors. *Human Gene Therapy* 9, 2787-2794.
- Salmon, B. & Baines, J. D. (1998). Herpes simplex virus DNA cleavage and packaging: association of multiple forms of UL15-encoded proteins with B capsids requires at least the UL6, UL17 and UL28 genes. *J Virol* 72, 3045-3050.
- Salmon, B., Cunningham, C., Davison, A. J., Harris, W. J. & Baines, J. D. (1998). The herpes simplex virus type 1 UL17 gene encodes virion tegument proteins that are required for cleavage and packaging of viral DNA. *J Virol* 72, 3779-3788.
- Salmon, B., Nalwanga, D., Fan, Y. & Baines, J. D. (1999). Proteolytic cleavage of the amino terminus of the UL15 gene product of herpes simplex virus type 1 is coupled with maturation of viral DNA into unit-length genomes. *J Virol* 73, 8338-8348.
- Samaniego, L. A., Neiderhiser, L. & DeLuca, N. A. (1998). Persistence and expression of the herpes simplex virus genome in the absence of immediate-early proteins. *J Virol* 72, 3307-3320.
- Sanchez, V., Greis, K. D., Sztul, E. & Britt, W. J. (2000). Accumulation of virion tegument and envelope proteins in a stable cytoplasmic compartment during human cytomegalovirus replication: Characterisation of a potential site of virus assembly. *J Virol* 74, 975-986.
- Sanchez, V. & Spector, D. H. (2002). CMV makes a timely exit. *Science* 297, 778-779.
- Schaffer, P. A., Aron, G. M., Biswal, N. & Benyesh-Melnick, M. (1973). Temperature-sensitive mutants of herpes simplex virus type 1: isolation, complementation and partial characterisation. *Virology* 52, 57-71.
- Schildgen, O., Graper, S., Blumel, J. & Matz, B. (2005). Genome replication and progeny virion production of herpes simplex virus type 1 mutants with temperature-sensitive lesions in the origin-binding protein. *J Virol* 79, 7273-7278.
- Shahin, V., Hafezi, W., Oberleithner, H., Ludwig, Y., Windoffer, B., Schillers, H. & Kuhn, J. E. (2006). The genome of HSV-1 translocates through the nuclear pore as a condensed rod-like structure. *J Cell Sci* 119, 23-30.

- Sheaffer, A. K., Newcomb, W. W., Brown, J. C., Gao, M., Weller, S. K. & Tenney, D. J. (2000). Evidence for controlled incorporation of herpes simplex virus type 1 UL26 protease into capsids. *J Virol* 74, 6838-6848.
- Sheaffer, A. K., Newcomb, W. W., Gao, M., Yu, D., Weller, S. K., Brown, J. C. & Tenney, D. J. (2001). Herpes simplex virus DNA cleavage and packaging proteins associate with the procapsid prior to its maturation. *J Virol* 75, 687-698.
- Sheng, M. & Sala, C. (2001). PDZ domains and the organisation of supramolecular complexes. *Ann Rev Neurosci* 24, 1-29.
- Sherman, G. & Bachenheimer, S. L. (1988). Characterisation of intranuclear capsids made by ts morphogenic mutants of hsv-1. *Virology* 163, 471-480.
- Shieh, M., WuDunn, D., Montgomery, R., Esko, J. & Spear, P. (1992). Cell surface receptors for herpes simplex virus are heparan sulfate proteoglycans. *J Cell Biol* 116, 1273-1281.
- Simpson-Holley, M., Colgrove, R. C., Nalepa, G., Harper, J. W. & Knipe, D. M. (2005). Identification and functional evaluation of cellular and viral factors involved in the alteration of nuclear architecture during herpes simplex virus 1 infection. *J Virol* 79, 12840-12851.
- Skepper, J. N., Whiteley, A., Browne, H. & Minson, A. (2001). Herpes simplex virus nucleocapsids mature to progeny virions by an envelopment, deenvelopment, reenvelopment pathway. *J Virol* 75, 5697-5702.
- Smith, D. E., Tans, S. J., Smith, S. B., Grimes, S., Anderson, D. L. & Bustamante, C. (2001). The bacteriophage  $\phi$ 29 portal motor can package DNA against a large internal force. *Nature* 413, 748-752.
- Sodeik, B., Ebersold, M. W. & Helenius, A. (1997). Microtubule-mediated transport of incoming herpes simplex virus 1 capsids to the nucleus. *J Cell Biol* 136, 1007-1021.
- Song, S. U., Shin, S.-H., Kim, S.-K., Choi, G.-S., Kim, W.-C., Lee, M.-H., Kim, S.-J., Kim, I.-H., Choi, M.-S., Hong, Y.-J. & Lee, K.-H. (2003). Effective transduction of osteogenic sarcoma cells by a baculovirus vector. *J Gen Virol* 84, 697-703.
- Sourvinos, G. & Everett, R. D. (2002). Visualization of parental HSV-1 genomes and replication compartments in association with ND10 in live infected cells. *EMBO J* 21, 4989 - 4997.
- Sowa, M. E., He, W., Slep, K. C., Kercher, M. A., Lichtarge, O. & Wensel, T. G. (2001). Prediction and confirmation of a site critical for effector regulation of RGS domain activity. *Nat Struct Biol* 8, 234-237.
- Spear, P. G. & Longnecker, R. (2003). Herpesvirus entry: an update. *J Virol* 77, 10179-10185.
- Stackpole, C. W. (1969). Herpes-type virus of the frog renal adenocarcinoma: I. Virus development in tumor transplants maintained at low temperature. *J Virol* 4, 75-93.
- Sternberg, N. & Weisberg, R. (1977a). Packaging of coliphage lambda DNA: 1. The role of the cohesive end site and the gene A protein. *J Mol Biol* 117, 733-759.
- Sternberg, N. & Weisberg, R. (1977b). Packaging of coliphage lambda DNA. II. The role of the gene D protein. *J Mol Biol* 117, 733-759.
- Steven, A. C., Heymann, J. B., Cheng, N., Trus, B. L. & Conway, J. F. (2005). Virus maturation: dynamics and mechanism of a stabilizing structural transition that leads to infectivity. *Curr Opin Struct Biol* 15, 227-236.
- Steven, A. C. & Spear, P. G. (1997). Herpesvirus capsid assembly and envelopment. In *Structural Biology of Viruses*, pp. 312-351. Edited by W.

- Chiu, R. M. Burnett & R. Garcea. New York and Oxford: Oxford University Press.
- Stow, N. D. (2001). Packaging of genomic and amplicon DNA by the herpes simplex virus type 1 UL25-null mutant KUL25NS. *J Virol* 75, 10755-10765.
- Strang, B. L. & Stow, N. D. (2005). Circularisation of the herpes simplex virus type 1 genome upon lytic infection. *J Virol* 79, 12487-12494.
- Strang, B. L. & Stow, N. D. (2007). Blocks to herpes simplex virus type 1 replication in a cell line, tsBN2, encoding a temperature-sensitive RCC1 protein. *J Gen Virol* 88, 376-383.
- Szilágyi, J. F. & Cunningham, C. (1991). Identification and characterisation of a novel non-infectious herpes simplex virus-related particle. *J Gen Virol* 72, 661-668.
- Taddeo, B., Zhang, W. & Roizman, B. (2006). The UL41 protein of herpes simplex virus 1 degrades RNA by endonucleolytic cleavage in absence of other cellular or viral proteins. *Proc Natl Acad Sci USA* 103, 2827-2832.
- Tatman, J. D., Preston, V. G., Nicholson, P., Elliott, R. M. & Rixon, F. J. (1994). Assembly of herpes simplex virus type 1 capsids using a panel of recombinant baculoviruses. *J Gen Virol* 75, 1101-1113.
- Taus, N. S., Salmon, B. & Baines, J. D. (1998). The Herpes simplex virus 1 UL17 gene is required for localisation of capsids and major and minor capsid proteins to intranuclear sites where viral DNA is cleaved and packaged. *Virology* 252, 115-25.
- Tengelsen, L. A., Pederson, N. E., Shaver, P. R., Wathen, M. W. & Homa, F. L. (1993). Herpes simplex virus type 1 DNA cleavage and encapsidation require the product of the UL28 gene: isolation and characterisation of two UL28 deletion mutants. *J Virol* 67, 3470-3480.
- Thomsen, D. R., Newcomb, W. W., Brown, J. C. & Homa, F. L. (1995). Assembly of the herpes simplex virus capsid: requirement for the carboxyl-terminal twenty-five amino acids of the proteins encoded by the UL26 and UL26.5 genes. *J Virol* 69, 3690-3703.
- Thomsen, D. R., Roof, L. L. & Homa, F. L. (1994). Assembly of herpes simplex virus (HSV) intermediate capsids in insect cells infected with recombinant baculoviruses expressing HSV capsid proteins. *J Virol* 68, 2442-2457.
- Thurlow, J. K., Murphy, M., Stow, N. D. & Preston, V. G. (2006). Herpes simplex virus type 1 DNA-packaging protein UL17 is required for efficient binding of UL25 to capsids. *J Virol* 80, 2118-2126.
- Thurlow, J. K., Rixon, F. J., Murphy, M., Targett-Adams, P., Hughes, M., White, C. A., McDougall, I. M. & Preston, V. G. (2005). The herpes simplex virus type 1 DNA packing protein UL17 is a virion protein, present in both the capsid and tegument compartments. *J Virol* 79, 150-158.
- Tischer, B. K., von Einem, J., Kaufer, B., & Osterrieder, N., (2006). Two-step Red-mediated recombination for versatile high-efficiency markerless DNA manipulation of *Escherichia coli*. *BioTechniques* 40, 191-197.
- Trus, B. L., Booy, F. P., Newcomb, W. W., Brown, J. C., Homa, F. L., Thomsen, D. R. & Steven, A. C. (1996). The herpes simplex virus procapsid: structure, conformational changes upon maturation, and roles of the triplex proteins VP19c and VP23 in assembly. *J Mol Biol* 263, 447-462.
- Trus, B. L., Cheng, N., Newcomb, W. W., Homa, F. L., Brown, J. C. & Steven, A. C. (2004). Structure and polymorphism of the UL6 portal protein of herpes simplex virus type 1. *J Virol* 78, 12668-12671.
- Trus, B. L., Homa, F. L., Booy, F. P., Newcomb, W. W., Thomsen, D. R., Cheng, N., Brown, J. C. & Steven, A. C. (1995). Herpes simplex virus capsids

- assembled in insect cells infected with recombinant baculoviruses: structural authenticity and localization of VP26. *J Virol* 69, 7362-7366.
- Trus, B. L., Newcomb, W. W., Cheng, N., Giovanni, C., Marekov, L., Homa, F. L., Brown, J. C. & Steven, A. C. (2007). Allosteric signaling and a nuclear exit strategy: binding of UL25/UL27 heterodimers to DNA-filled HSV-1 capsids. *Mol Cell* 26, 479-489.
- Turner, A., Brunn, B., Minson, T. & Browne, H. (1998). Glycoproteins gB, gD, and gHgL of herpes simplex virus type 1 are necessary and sufficient to mediate membrane fusion in a Cos cell transfection system. *J Virol* 72, 873-875.
- Tzliil, S., Kindt, J. T., Gelbart, W. M. & Ben-Shaul, A. (2003). Forces and pressures in DNA packaging and release from viral capsids. *Biophysical J* 84, 1616-1627.
- Umbach, J. L., Kramer, M. F., Jurak, I., Karnowski, H. W., Coen, D. M. & Cullen, B. R. (2008). MicroRNAs expressed by herpes simplex virus 1 during latent infection regulate viral mRNAs. *Nature* 454, 780-783.
- Valpuesta, J. M. & Carrascosa, J. L. (1994). Structure of viral connectors and their function in bacteriophage assembly and DNA packaging. *Quart Rev Biophysics* 27.
- Van Genderen, I. L., Brandimarti, R., Torrisi, M. R., Campadelli, G. & Van Meer, G. (1994). The phospholipid composition of extracellular herpes simplex virions differs from that of host cell nuclei. *Virology* 200, 831-836.
- Varmuza, S. L. & Smiley, J. R. (1985). Signals for site-specific cleavage of HSV DNA: maturation involves two separate cleavage events at sites distal to the recognition sequences. *Cell* 41, 793-802.
- Vaughn, J.C., Goodwin, R.H., Tompkins, G.J., McCawley, P. (1977). The establishment of two cell lines from the insect *Spodoptera fugiperda* (Lepidoptera: Noctuidae). *In Vitro* 13, 213-217.
- Wagenaar, F., Pol, J. M. A., Peeters, B., Gielkens, A. L. J., de Wind, N. & Kimman, T. G. (1995). The US3-encoded protein kinase from pseudorabies virus affects egress of virions from the nucleus. *J Gen Virol* 76, 1851-1859.
- Wagner, E. K., Devi-Rao, G., Feldman, L. T., Dobson, A. T., Zhang, Y. F., Flanagan, W. M. & Stevens, J. G. (1988). Physical characterization of the herpes simplex virus latency-associated transcript in neurons. *J Virol* 62, 1194-1202.
- Wagner, E. K., Guzowski, J. F. & Singh, J. (1995). Transcription of the herpes simplex virus genome during productive and latent infection. *Prog Nucl Acid Res Mol Biol* 51, 123-165.
- Ward, P. L., Ogle, W. O. & Roizman, B. (1996). Assemblons: nuclear structures defined by aggregation of immature capsids and some tegument proteins of herpes simplex virus 1. *J Virol* 70, 4623-4631.
- White, C., Stow, N. D., Patel, A. H., Hughes, M. & Preston, V. (2003). The herpes simplex virus type 1 portal protein UL6 interacts with the putative terminase subunits UL15 and UL28. *J Virol* 77, 6351-6358.
- Wikoff, W. R., Liljas, L., Duda, R. L., Tsuruta, H., Hendrix, R. W. & Johnson, J. E. (2000). Topologically linked protein rings in the bacteriophage HK97 capsid. *Science* 289, 2129-2133.
- Wild, P., Engels, M., Senn, C., Tobler, K., Ziegler, U., Schraner, E. M., Loepfe, E., Ackermann, M., Mueller, M. & Walther, P. (2005). Impairment of nuclear pores in bovine herpesvirus 1-infected MDBK cells. *J Virol* 79, 1071-1083.

- Wildy, P., Russell, W. C. & Horne, R. W. (1960). The morphology of herpes virus. *Virology* 12, 204-222.
- Wolfstein, A., Nagel, C. H., Radtke, K., Dohner, K., Allan, V. J. & Sodeik, B. (2006). The inner tegument promotes herpes simplex virus capsid motility along microtubules in vitro. *Traffic* 7, 227-237.
- WuDunn, D. & Spear, P. G. (1989). Initial interaction of herpes simplex virus with cells is binding to heparan sulfate. *J Virol* 63, 52-58.
- Yang, K. & Baines, J. D. (2006). The putative terminase subunit of herpes simplex virus 1 encoded by UL28 is necessary and sufficient to mediate interaction between pUL15 and pUL33. *J Virol* 80, 5733-5739.
- Yang, K., Homa, F. & Baines, J. D. (2007). Putative terminase subunits of herpes simplex virus 1 form a complex in the cytoplasm and interact with portal protein in the nucleus. *J Virol* 81, 6419-6433.
- Yeh, P.-C., Meckes, D. G., Jr. & Wills, J. W. (2008). Analysis of the interaction between the UL11 and UL16 tegument proteins of herpes simplex virus. *J Virol* 82, 10693-10700.
- Yu, D., Sheaffer, A. K., Tenney, D. J. & Weller, S. K. (1997). Characterisation of ICP6:lacZ insertion mutants of the UL15 gene of herpes simplex virus type 1 reveals the translation of two proteins. *J Virol* 71, 2656-2665.
- Yu, D. & Weller, S. K. (1998a). Herpes simplex virus type 1 cleavage and packaging proteins UL15 and UL28 are associated with B but not C capsids during packaging. *J Virol* 72, 7428-7439.
- Yu, D. & Weller, S. K. (1998b). Genetic analysis of the UL15 gene locus for the putative terminase of herpes simplex virus type 1. *Virology* 243, 32-44.
- Zhou, Z. H., Chen, D. H., Jakana, J., Rixon, F. J. & Chiu, W. (1999). Visualization of tegument-capsid interactions and DNA in intact herpes simplex virus type 1 virions. *J Virol* 73, 3210-3218.
- Zhou, Z. H., Dougherty, M., Jakana, J., He, H., Rixon, F. J. & Chiu, W. (2000). Seeing the herpesvirus capsid at 8.5 Å. *Science* 288, 877-880.
- Zhou, Z. H., Prasad, B. V. V., Jakana, J., Rixon, F. J. & Chiu, W. (1994). Protein subunit structures in the herpes simplex virus A-capsid determined from 400 kV spot-scan electron cryomicroscopy. *J Mol Biol* 242, 456-469.